



VNIVERSITATIS VALÈNCIA

***PROGRAMA DE DOCTORADO EN BIOTECNOLOGÍA Y
BIOMEDICINA***

DEPARTAMENTO DE BIOQUÍMICA Y BIOLOGÍA MOLECULAR.

FACULTAD DE CIENCIAS BIOLÓGICAS.

**Maternal-fetal cross-talk. Elucidating the role of mir-30d
in endometrial receptivity and pregnancy outcome**

TESIS DOCTORAL

Presentada por:

Nuria Balaguer Cuenca

Dirigida por:

Dr. Carlos Simón Vallés

Dr. Felipe Vilella Mitjana

Valencia, Octubre 2018



El Dr. Carlos Simón Vallés, catedrático de Pediatría, Obstetricia y Ginecología de la Universidad de Valencia y director Científico de Igenomix; el Dr. Felipe Vilella Mitjana, director del departamento de investigación de Igenomix Foundation e investigador Miguel Servet del Incliva; y el Dr. Antonio Pellicer Martínez, Catedrático de Pediatría, Obstetricia y Ginecología de la Universidad de Valencia y presidente del grupo IVI

CERTIFICAN:

Que el trabajo de investigación titulado: “Maternal-fetal cross-talk. Elucidating the role of mir-30d in endometrial receptivity and pregnancy outcome” ha sido realizado íntegramente por Dña. Nuria Balaguer Cuenca bajo su dirección. Dicha memoria está concluida y reúne todos los requisitos para su presentación y defensa como **TESIS DOCTORAL** ante un tribunal.

Y para que así conste a los efectos oportunos, firman la presente certificación en:

Valencia, a 30 de Octubre de 2018

Fdo: Carlos Simón Vallés (Director)

Fdo: Felipe Vilella Mitana (Director)

Fdo: Antonio Pellicer Martínez (Tutor)

The work presented in this doctoral thesis has been carried out in the laboratories of Fundació IVI and Igenomix Foundation thanks to the financial support of the Grant “Atracció del talent” given by the University of Valencia (Ref: Predoc14-178329). During the thesis, a brief three-month predoctoral stay was carried out in the National Institute of Health Sciences (NIEHS), under the supervision of Francesco Demayo (PhD). The generated results have been presented in the following international congresses:

Congress 1

Title of the work: MicroRNAs secreted by the human endometrium act as transcriptomic regulators of the pre-implantation embryos.

Name of the conference: 2014 Mammalian Reproduction Conference GRC

Date of event: 10/08/2014

Type of presentation: Poster

Authors: Felipe Vilella, Juan Manuel Moreno Moya, Nuria Balaguer Cuenca, Antonio Pellicer, Carlos Simón Vallés.

Congress 2

Title of the work: Hsa-miR-30d is transported by exosomes from human endometrial epithelium to the trophectoderm of preimplantation embryos and modulates embryo adhesion.

Name of the conference: SRI 2015 Society for Reproductive Meicine 62nd Annual Scientific Meeting.

Date of event: 25/03/2015.

Type of presentation: Oral

Authors: Nuria Balaguer Cuenca, Felipe Vilella Mitjana, Juan Manuel Moreno Moya, María Herrero Baena, Carlos Simón Vallés.

Award: New Investigator plenary award (SRI-Pfizer President's Presenter's Award).

Congress 3

Title of the work: Maternal endometrial hsa-miR-30d is internalized and secreted in exosomes by binding with hnRNPC1.

Name of the conference: SRI 2016 Society for Reproductive Medicine 63rd Annual meeting.

Date of event: 16/03/2016

Type of presentation: Oral

Authors: Nuria Balaguer Cuenca, Inmaculada Moreno Gimeno, Maria Herrero Baena, Felipe Vilella Mitjana, Carlos Simón Vallés.

Award: Best abstract (SRI-Pfizer President's Presenter's Award).

Congress 4

Title of the work: Maternal endometrial has-miR-30d is necessary for embryo implantation.

Name of the conference: 2016 Mammalian Reproduction Conference GRC

Date of event: 21/08/2016

Type of presentation: Poster

Authors: Felipe Vilella, Nuria Balaguer Cuenca, Inmaculada Moreno, Carlos Simón Vallés.

Congress 5

Title of the work: Maternal miR-30d deficiency is associated with defects in endometrial receptivity, embryonic implantation and fetal development.

Name of the conference: SRI 2015 Society for Reproductive Medicine 63rd Annual Scientific Meeting.

Date of event: 16/03/2017.

Type of presentation: Oral

Authors: Nuria Balaguer Cuenca, Inmaculada Moreno, María Herrero, Marta González-Monfort, Carlos Simón, Felipe Vilella Mitjana.

Also, the following publications have emerged from the results presented in the thesis.

Publications

Vilella, F., Moreno-Moya, J. M., Balaguer, N., Grasso, A., Herrero, M., Martínez, S., Marcilla, A. and Simón, C. (2015) 'Hsa-miR-30d, secreted by the human endometrium, is taken up by the pre-implantation embryo and might modify its transcriptome', *Development*, 142(18), pp. 3210-21.

Balaguer, N., Moreno, I., Herrero, M., González, M., Simón, C. and Vilella, F. (2018) 'Heterogeneous nuclear ribonucleoprotein C1 may control miR-30d levels in endometrial exosomes affecting early embryo implantation', *Mol Hum Reprod*, pp. 1-15.

Balaguer, N., Moreno, I., Herrero, M., González, M., Simón, C. and Vilella, F. (2018). 'Reproductive and fetal outcome of miR-30d deficiency at the maternal embryonic interface'. *Ajog*. **(Under review)**.

Balaguer, N., Domínguez, F., Simón, C. and Vilella, F. (2017) 'Embryo/fetal maternal cross-talk', in Simón, C. & Giudice, L.C. (eds.) *The endometrial factor. A reproductive precision medicine approach*: CRC Press, pp. 241-255.

AGRADECIMIENTOS

A Carlos por haberme dado la oportunidad de unirme a su equipo de investigación y enseñarme la valiosa lección de que muchas veces los árboles no te dejan ver el bosque.

A Felip, por su plena confianza y ver cosas en mí que ni yo misma soy capaz de ver. Gracias por todo el apoyo incondicional que me has dado.

A Inma, por todos los consejos que me has dado durante todo este tiempo. Siempre sentiré que parte de esta tesis es tuya.

A mis compañeros y amigos que comenzaron conmigo Iolin, Irene, Martuki, Melito, Alessia, María, Paty y David. Todos y cada uno de vosotros sois especiales para mí, me habéis dado el regalo más grande que puedo tener y es vuestra amistad. Gracias por sufrirme durante todo este tiempo, por los buenos y no tan buenos momentos, el camino ha sido duro, pero no me imagino mejor compañía con la que poder haberlo hecho. Os quiero. Me gustaría con permiso de todos ellos, agradecerse a María, durante 4 años ha sido mi compañera de batallas, hemos reído, gritado y llorado, pero sobre hemos superado todas las dificultades juntas. Tu ausencia se nota y no hay día que no te eche de menos. Más que una amiga, eres mi hermana.

A las nuevas incorporaciones: Anita, Fany y Tere. Lleváis poco tiempo, pero ya no me imagino el día a día sin vosotras, en especial sin mi

Anita, para mi has sido todo un gran descubrimiento. Estoy segura de que vamos a hacer grandes cosas juntas, te quiero baby.

A mis antiguas compañeras de FIVI, Silvia y Nuria. Sin duda, lo más bonito que me llevo de mi paso por la fundación sois vosotras dos.

A toda la familia de Igenomix, por acogerme y hacerme sentirme una más, en especial a mi Laurita y mi Lu, sin las cuales los jueves dejarían de ser uno de mis días favoritos de la semana. Por muchas más!!

A Eulogio, por haber sido amigo y mentor al mismo tiempo, de no ser por ti no estaría escribiendo estas palabras. Gracias por tus sabios consejos y sobre todo gracias por quererme como si fuera una hija.

A mi Valentina preferida (con permiso de Isabel), por ser como es, única e irreplicable. No conozco a nadie a quien tu paso le haya sido indiferente. Eres grande amiga.

A Juanita y a Richard, por darme todo a cambio de nada. Sin vosotros mi estancia en USA no hubiese sido lo mismo.

To Francesco DeMayo, PhD., thank you for giving me the opportunity to be in your laboratory and learn from you. I will always remember with great affection my colleagues from there.

A la familia que se escoge, en especial a Delia, Pau, MH, Vic, Encar y Magda. Sois pilares fundamentales en mi vida. Gracias por estar incondicionalmente a mi lado.

A Pedro y a Marta, por quererme y apoyarme siempre. Ha sido un honor formar parte de la gran familia de dieléctricas. Grandes amigos, pero sobre todo grandes personas.

A mis padres y hermanas, por no dejarme caer cuando no tenía ganas de seguir caminando.

A Amparo y Enrique, por todo el esfuerzo que han hecho para que pueda estar donde estoy ahora. Gracias por toda vuestra ayuda y sobre todo por vuestra infinita paciencia.

A Pablo, mi compañero de viaje. Sin ti esta tesis no hubiese sido posible. Gracias por todos los sacrificios que has tenido que hacer para que yo pudiese volar.

A ella, por regalarme su sonrisa todos los días a pesar de las ausencias.

Reciprocal communication between the endometrium and the preimplantation embryo is required for pregnancy. Our previous work described a novel cell-to-cell communication mechanism involving the delivery of endometrial microRNAs from the maternal endometrium to the trophectoderm cells of preimplantation embryos. More specifically, *in vitro* transfer of hsa-miR-30d supported mouse embryo adhesion by increasing expression of the adhesion molecules *Cdh5*, *Itβ3*, *Itα5* in trophectoderm cells. The present doctoral thesis uses a miR-30d KO model to give answer two well-defined objectives: determine the mechanism by which miR-30d is incorporated into the maternal-derived extracellular vesicles and to investigate the impact of maternal or embryonic-origin miR-30d deficiency on implantation and subsequent fetal development. Regarding the first objective, mass spectrometry carried out after performing a co-immunoprecipitation with a biotinylated miR-30d in lysates from human endometrial epithelial cells (hEECs) and their derived exosomes allowed us to identify several proteins that could exert this role within cells. Among them, we found hnRNPC1, a ribonucleoprotein traditionally involved in directing the transfer of mRNAs from the nucleus to the cytoplasm. Co-localization studies of hnRNPC1 with the exosome marker CD63 and FACS analyses demonstrated the presence of hnRNPC1 inside exosomes. Silencing of hnRNPC1 in an Ishikawa endometrial adenocarcinoma cell line resulted in a sharp decrease of the levels of miR-30d in both epithelial-like cells and exosomes, suggesting its pivotal role in miR-30d biogenesis and transfer. Co-culture assays of miR-30d knock out (KO) embryos with sihnRNPC1 hEECs revealed a decrease in embryo-miR-30d acquisition in the adhesion and invasion stages. The lower adhesion levels observed are evidence that hnRNPC1 is an important player in the maternal-fetal communication

established in the early stages of implantation. On the other hand, the endometrial receptivity markers COX2, LIF, MSX1, MSX2, ESR, and PGR were used to examine the impact of miR-30d deficiency, being LIF significantly downregulated in the endometrium of KO mothers. Next, different maternal-embryonic crosstalk scenarios were tested by controlling the origin of miR-30d or its deficiency by transferring WT, miR-30d KO, or KO embryos pre-treated with miR-30d into WT or KO recipients. When transferred into WT recipients, KO embryos had poorer implantation rates (IR) than WT embryos ($p = 0.0061$). Even lower implantation rates were seen when comparing KO and WT embryos transferred into KO dams ($p = 0.0059$). Interestingly, a positive correlation ($r = 0.9978$) was observed for maternal LIF expression and the IR, suggesting dysregulation of LIF associated with the miR-30d knockdown. Also, the course of gestation appeared compromised in KO females as evidenced by smaller implantation sites, higher rates of resorption, and fetuses with smaller crown rump-lengths and FW:PW ratios.

Introducción

En el proceso de implantación embrionaria se produce una relación sincrónica entre el endometrio y el embrión que resulta fundamental para su correcta consecución; dicha sincronía se mantiene durante la gestación gracias a la existencia de una comunicación bidireccional entre la madre y el feto basada en la secreción de señales específicas que permiten regular un desarrollo cooperativo. Efectivamente, se ha observado como el embrión libera moléculas específicas del estado gestacional (ej.: gonadotropina coriónica humana o interferón tau en rumiantes), para prevenir la luteólisis inducida por la prostaglandina F₂α, posibilitando la secreción continua de progesterona durante la gestación. Del mismo modo, las secreciones uterinas regulan el estado de desarrollo embrionario y promueven la proliferación del trofotodermo, la migración, o la unión al epitelio luminal endometrial.

Debido a la relevancia de este proceso de comunicación entre la madre y el embrión, el estudio del microambiente en el que se produce dicha comunicación bidireccional ha suscitado un gran interés recientemente. Entre las publicaciones más destacadas en este campo, se encuentran aquellas que se focalizan en el papel que ejerce el líquido endometrial (LE), tanto en el proceso de implantación como en el desarrollo embrionario posterior. El LE está constituido principalmente por el trasudado plasmático y las secreciones del epitelio luminal y glandular, que aportan toda una batería de compuestos como aminoácidos, iones, carbohidratos, lípidos y proteínas (incluyendo citoquinas, enzimas, hormonas, factores de crecimiento, transportadores, proteasas y factores inmunomoduladores) encargados de suministrar una nutrición temprana al *conceptus* (embrión junto con sus membranas asociadas) durante el periodo previo a la formación de las estructuras placentarias.

La presencia de microARNs (miARNs) en el LE ha suscitado gran interés debido a su función en la regulación de la expresión génica. Los miARNs son moléculas de ARN no codificante de aproximadamente 22-25 nt de longitud capaces de regular hasta cientos de ARN mensajeros (mRNA) diana mediante complementación perfecta o imperfecta con las regiones 3' no traducidas (UTR) de sus transcritos diana. Normalmente participan en procesos de degradación o inhibición de la traducción, aunque también se han descrito casos de miARNs capaces de inducir expresión proteica (Mehta y Baltimore, 2016).

Los miARNs regulan la expresión génica en tejidos fetales y maternos a lo largo de todo el curso gestacional. Inicialmente, se describió la existencia de patrones de expresión diferencial de miARNs en células epiteliales endometriales a lo largo del ciclo menstrual, sugiriendo que su presencia podría estar sujeta a regulación hormonal en el endometrio humano (Kuokannen et al., 2010). Más tarde, se identificó un perfil específico de miARNs en pacientes con fallo recurrente de implantación que inhibían a genes implicados en rutas de señalización cruciales para la implantación embrionaria (ej.: vía de uniones adherentes, señalización WNT, ruta p53, ciclo celular, adhesión celular o cáncer) (Revel et al., 2011). Asimismo, se ha podido identificar un perfil diferencial entre la ventana de implantación y estadios pre-receptivos, tanto en ciclos naturales como estimulados, lo cual se podría emplear como potencial biomarcador de receptividad endometrial (Sha et al., 2011; Altmäe et al., 2012).

Actualmente, los miARNs se consideran uno de los mejores reguladores de comunicación celular, ya que pueden transferirse intercelularmente desempeñando papeles fundamentales en múltiples procesos celulares. Su estructura y tamaño, así como sus mecanismos de transporte asociados, les confieren una gran estabilidad en múltiples fluidos biológicos (Larrea et al., 2016; Turchinovich et al., 2013), pudiendo persistir de esta forma a condiciones adversas como: bajos niveles de pH, elevadas temperaturas o procesos de congelación

(Pieters et al., 2015). Los miARNs extracelulares pueden transportarse asociados a proteínas como Argonauta 2, nucleophosmina 1 o lipoproteínas. Sin embargo, uno de los métodos de transporte más importante es el mediado por vesículas extracelulares (cuerpos apoptóticos, microvesículas y/o exosomas) ya que protegen a los miARNs de la degradación y contribuyen a su vez a incrementar su estabilidad dentro de los fluidos biológicos.

Nuestro grupo de investigación ha descrito un mecanismo de comunicación materno-embionario donde los miARNs de origen materno eran internalizados por el trofoectodermo de embriones murinos, bien de forma libre o en el interior de vesículas (Vilella et al., 2015). Concretamente, este trabajo mostró que la transferencia del miARN miR-30d favorecía la sobreexpresión de moléculas implicadas en procesos de adhesión celular (IT α 7, IT β 3 y CDH5) en células del trofoectodermo. Asimismo, se demostró que el pretratamiento de embriones murinos con un análogo del miR-30d incrementaba significativamente las tasas de adhesión embrionaria, sugiriendo que los miARNs extracelulares podrían actuar como modificadores transcriptómicos de embriones pre-implantatorios. De forma análoga, se ha descrito que las células epiteliales endometriales liberan exosomas en el interior de la cavidad uterina a lo largo de las diferentes fases del ciclo menstrual, siendo la firma de miARNs en el interior de vesículas claramente distinta a la identificada en las células epiteliales endometriales de origen. Dicha firma diferencial tiene como dianas genes que participan de forma activa en diversas rutas relacionadas con la implantación (ej. uniones adherentes, interacciones receptor-matriz extracelular, factor de crecimiento endotelial vascular, JAK-STAT o receptores tipo Toll) (Ng et al., 2013).

Actualmente, los miARNs están adquiriendo relevancia como potenciales biomarcadores de enfermedades, perfilándose de esta manera como nuevas herramientas de cribado genético no invasivo (Barcigitta et al., 2017). De hecho, ya existen indicios de la existencia de una estrecha relación entre perfiles anómalos de

miARNs y complicaciones gestaciones tales como el fallo de implantación (Revel et al., 2011, Sha et al., 2011), preeclampsia (Choi et al., 2013, Li et al., 2013, Munaut et al., 2016), parto prematuro (Elovitz et al., 2014, Elovitz et al., 2015, Sanders et al., 2015) o restricción del crecimiento intrauterino (Song et al., 2013, Hromadnikova et al., 2017, Hu et al., 2014).

Hipótesis

La hipótesis del presente trabajo es que la comunicación bidireccional establecida entre el endometrio materno y el embrión a través del miR-30d afecta tanto a la implantación del embrión, así como el desarrollo fetal posterior dependiendo de si su origen es materno o embrionario.

Objetivos

- Determinar el mecanismo de incorporación del miR-30d al interior de las vesículas extracelulares secretadas por el endometrio materno.
- Investigar el impacto de la deficiencia del miR-30d de origen materno o embrionario sobre la implantación embrionaria y el desarrollo fetal.

Metodología

Inicialmente, se realizó un cribado preliminar de aquellas proteínas que podían dirigir el transporte de miR-30d al interior de la cavidad exosomal mediante espectrometría de masas utilizando extractos de células epiteliales endometriales (hEECs), así como exosomas derivados de las mismas. Del conjunto de las proteínas identificadas, se seleccionaron aquellas que estaban relacionadas con el transporte de ARN en el interior celular. Posteriormente, para discernir si dichas proteínas se localizaban en el interior de exosomas y no adheridas a la superficie de estos, se realizaron ensayos de western blot (WB), estudios de co-localización con el marcador exosomal CD63 y citometría de flujo con exosomas previamente acoplados a bolas aldehído sulfato. La validación de la interacción proteína-ARNm se efectuó mediante una inmunoprecipitación con extractos de células Ishikawa y

exosomas obtenidos a partir de las mismas. Finalmente, con el fin de determinar la relevancia funcional de la proteína identificada en los primeros estadios de la implantación se llevó a cabo su silenciamiento mediante mecanismos de silenciamiento mediados por ARNs pequeños de interferencia (ARNspi). En este sentido, se realizaron ensayos de adhesión embrionaria con embriones procedentes de una cepa *knock out* (KO) para el miR-30d sobre células Ishikawa doblemente transfectadas con ARNspi y sondas *molecular beacon* (MB) diseñadas específicamente para el reconocimiento del miR-30d en células vivas.

Tras confirmar en un modelo heterólogo *in vitro* que el bloqueo del transporte del miR-30d ocasionaba un fenotipo de implantación deficiente, se realizaron ensayos *in vivo* en los que se estudiaron los marcadores de receptividad endometrial. Con este fin, se generaron ratonas pseudogestantes en las que en día 4 y 5 se analizó la expresión de *Cox2*, *Lif*, *Msx1*, *Msx2*, *Esr* y *Pgr* mediante PCR cuantitativa, ensayos de inmunofluorescencia y WB. A continuación, se evaluó el impacto del bloqueo de la transferencia bidireccional del miR-30d en el fenotipo de implantación en distintos contextos de comunicación materno-fetal. Para ello, se realizaron transferencias de embriones *wild type* (WT), KO y KO pretratados con un análogo del miR30d en úteros de ratonas pseudogestantes WT y KO, registrándose tanto la expresión de los marcadores de receptividad, como las tasas de implantación embrionaria alcanzadas. Finalmente, se evaluaron ciertos parámetros de desarrollo fetal y placentario tanto en el genotipo WT como el KO, realizándose en última instancia análisis morfológico de las crías de ambos genotipos, una vez destetadas.

Resultados y discusión

Las vesículas secretadas por el endometrio materno participan en la comunicación materno-fetal en las primeras etapas del proceso de implantación. En este contexto, nuestro grupo de investigación observó que la transferencia del miR-30d a través de exosomas favorecía la implantación embrionaria regulando la

expresión de moléculas de adhesión en células del trofotodermo. Sin embargo, se desconocía el mecanismo por el cual, el miARN se incorporaba al interior de exosomas y el efecto que este producía una vez internalizado *in vivo*.

Con este fin, se realizó un cribado preliminar de aquellas proteínas que podían dirigir el transporte del miR-30d a la cavidad interna de los exosomas de origen materno. Los resultados obtenidos mediante espectrometría de masas revelaron la presencia de proteínas implicadas en cambios transcripcionales, post-transcripcionales, adhesión celular o morfogénesis embrionaria (**Tabla 5.1**). Del conjunto de proteínas detectadas, se seleccionó la ribonucleoproteína hnRNP1, ya que una de sus principales funciones biológicas está relacionada con el transporte de ARNm desde el citosol al citoplasma. Los estudios de co-localización de hnRNP1 con el marcador exosomal CD63 (**Figura 5.3**) y los ensayos de citometría de flujo (**Figura 5.4**) demostraron que dicha proteína estaba presente en el interior de los exosomas y no adherida a la superficie de la membrana de estos.

HnRNP1 fue una de las primeras ribonucleoproteínas descritas en la participación de procesos de *splicing* del ARN (Han et al., 2010). Regula la estabilización, transporte y biogénesis del ARNm (Rajagopalan et al., 1998; Shetty, 2005), así como la traducción dependiente del sitio interno de entrada al ribosoma (IRES) de proteínas implicadas en la división celular y apoptosis (Holcík et al., 2003; Kim et al., 2003). HnRNP realiza estas funciones a través de heterotetrámeros estables (Dreyfuss et al., 1993; McAfee et al., 1996) constituidos por tres moléculas de la isoforma más abundante, hnRNP1 y una molécula de una variante ligeramente más grande, hnRNP2 (Burd et al., 1989). Normalmente, hnRNP1/C2 reside principalmente en el núcleo (Lee et al., 2004), pero ciertas condiciones celulares (ej: apoptosis, mitosis e infección viral) inducen la translocación de hnRNP1/C2 del núcleo al citoplasma (Nakielny y Dreyfuss, 1996; Gustin y Sarnow, 2001; 2002; Kim y col., 2003; Lee y col., 2004; Pettit Kneller y col., 2009). De hecho, los resultados derivados del estudio de localización intracelular/subcelular de las

proteínas mediante In-cell analyzer permitieron determinar que una cierta proporción de hnRNPC1 se podía detectar en el compartimento citoplasmático (**Figura 5.5**).

La validación de la unión hnRNPC1-miR-30d mediante inmunoprecipitación y los ensayos de silenciamiento, donde se bloqueaba de manera transitoria la expresión de hnRNPC1 en células Ishikawa, constituyen evidencias tangibles del posible papel de hnRNPC1 como transportador del miR-30d. De hecho, tras el bloqueo de hnRNPC1 se pudo observar una disminución significativa de los niveles de miR-30d tanto en las células (**Figura 5.7C**), como en los exosomas secretados de las mismas (**Figura 5.7D**). Sin embargo, dicha reducción podría estar asociada también con una deficiencia en la maquinaria de biogénesis de miARNs ligada al silenciamiento de hnRNPC1.

Finalmente, la prueba de concepto sobre la relevancia de la proteína hnRNPC1 en la transferencia del miR-30d proviene del co-cultivo de embriones WT o miR-30dKO con células sihnRNPC1 (**Figuras 5.9, 5.10, 5.11**). Se observó que el silenciamiento de hnRNPC1 compromete la detección de la señal miR-30d CY3 en toda la estructura del embrión en dos de las etapas principales de la implantación: adhesión e invasión (**Figura 5.9, 5.10**). Independientemente de que el embrión fuese WT o KO, los niveles de miR-30d se redujeron significativamente. A su vez, los ensayos de adhesión mostraron que el silenciamiento transitorio de hnRNPC1 produjo una disminución significativa de las tasas de adhesión en ambos genotipos, siendo esta reducción más pronunciada en los embriones KO para el miR-30d (**Figura 5.11**). Este efecto adverso al comienzo del proceso de implantación puede estar asociado con un efecto aditivo derivado de la ausencia del miR-30d y el silenciamiento de hnRNPC1. Teniendo en cuenta estos resultados, hnRNPC1 podría desempeñar un papel relevante en la comunicación materno-fetal mediante su participación en la biogénesis del miR-30d y su transporte posterior a las células del trofotodermo.

El siguiente objetivo fue investigar el impacto de la transferencia del miR-30d, procedente de la madre o del embrión en la implantación embrionaria y desarrollo fetal. Primeramente, se caracterizó la expresión de determinados marcadores de receptividad (*Cox2*, *Lif*, *Msx1*, *Msx2*, *Esr*, *Pgr*) en úteros de ratonas no gestantes y pseudogestantes, a día 4 y 5 de pseudogestación. Los análisis mediante qPCR e inmunofluorescencia revelaron una reducción de estos marcadores en úteros de ratonas KO al comienzo del periodo de receptividad (día 4), pero no así al final del mismo (día 5) (**Figura 5.12**). No obstante, se demostró una reducción significativa de LIF en úteros de ratonas KO durante todo el periodo de receptividad (**Figura 5.14**); esta disminución de la expresión de LIF como consecuencia de la ausencia del miR-30d, resulta a priori contradictorio teniendo en cuenta que los miARNs normalmente regulan negativamente la expresión de ARNm. Sin embargo, no es la primera vez que la familia del miR-30d participa en contextos fisiológicos donde la ausencia de alguno de sus miembros da lugar a una disminución de los niveles de proteína. En este sentido, la inhibición de miR-30d en células epiteliales genera una reducción de los niveles de SOX9, a pesar de incrementar los niveles de ARNm tras alterar el mecanismo ubiquitina-proteasoma (Peck et al., 2016). Del mismo modo, se ha observado que la familia del miR-30d incrementa la síntesis proteica en células ováricas de hámster chino (CHO) al afectar la expresión de la proteína “Ubiquitin E3 ligase S-phase kinase-associated protein 2” de la ruta ubiquitina-proteasoma (Fisher et al, 2015). Por tanto, estas observaciones sugieren que el miR-30d podría regular el balance proteico en función de estímulos externos o internos, comprometiendo de esta forma procesos celulares fundamentales como la regulación del ciclo celular, expresión génica, apoptosis y/o la transducción de señales (Sadowski et al., 2012; Wang y Maldonado, 2016).

A continuación, se evaluó como podía afectar la no transferencia del miR-30d, bien desde de la madre o del embrión, en el transcurso de la implantación. Para ello, se realizaron diferentes combinaciones de transferencia embrionaria en

hembras WT y KO para cubrir todos los posibles escenarios de comunicación materno-fetal. Los resultados obtenidos sugieren que la deficiencia en la transferencia del miR-30d, ya sea desde la madre o desde el embrión disminuye significativamente los porcentajes de implantación alcanzados. Sin embargo, éstos se restauran significativamente en el genotipo KO tras realizar una transferencia de embriones KO pretratados con un análogo del miR-30d (**Figura 5.15**). El análisis de los marcadores de receptividad mediante microscopía de fluorescencia muestra una afectación significativa de LIF, especialmente en aquellos casos donde la transferencia del miR-30d está comprometida. Más aún, el patrón de variación de los porcentajes de implantación en las diferentes condiciones de transferencia coincide con el observado para los valores medios de intensidad de fluorescencia (VIF) de LIF (**Figura 5.17B**). En este sentido, se ha logrado identificar una correlación positiva entre el VIF medio de LIF y el porcentaje de implantación alcanzando (**Figura 5.18B**), sugiriendo que LIF podría ser una potencial diana indirecta del miR-30d.

LIF es un regulador esencial de la implantación embrionaria en modelos murinos y un marcador de receptividad crucial en varias especies de mamíferos, incluida la humana, donde, la desregulación de la expresión de LIF se ha asociado con varios casos de infertilidad femenina debido a fallos en el proceso de implantación (Hambartsoumian et al., 1998; Mikolajczyk et al., 2007; Frasiak et al., 2014). LIF alcanza su máxima expresión en el epitelio glandular endometrial momentos antes de que la implantación tenga lugar, promoviendo la activación de vías de señalización cruciales para este proceso [ej.: JAK/STAT3, MAPK y fosfatidilinositol-3 quinasa (PI3K)] (Aghajova, 2010). En la literatura, se han descrito casos en los que la regulación de LIF es controlada por medio de miARNs. En este sentido, existen evidencias de que la expresión del ARNm de LIF es prácticamente opuesta a la del miR-181a y miR-181b durante el embarazo (Chu et al., 2015). Del mismo modo, se ha visto que miR-223-39 afecta a la implantación embrionaria

suprimiendo la expresión de LIF y la generación de pinópodos en el endometrio de ratonas gestantes (Dong et al., 2016).

Es importante tener en cuenta que la mayoría de las investigaciones que se centran en el estudio del papel de los miARNs sobre la receptividad endometrial destacan el efecto ejercido por el endometrio sobre el embrión, pero no la posible influencia de este último en la adquisición de un endometrio receptivo. El enfoque más cercano hasta la fecha describe que las células epiteliales endometriales humanas (hEECs) son capaces de adquirir miR-661, un miARN presente en el medio condicionado de blastocistos no implantados, dando como resultado una disminución de la tasa de adhesión de trofoblastos (Cuman et al. 2016). De forma similar, la infusión de vesículas extracelulares fluorescentes de origen embrionario en cuernos uterinos de ovejas permitió la detección de fluorescencia en el citoplasma del epitelio luminal y glandular. Por lo tanto, estos estudios establecen que los miARNs extracelulares originarios del embrión son internalizados por las células uterinas y modulan la expresión génica materna, hecho que indica un papel funcional de la señalización entre el blastocisto y el endometrio materno durante la ventana de implantación. En este contexto, los resultados de esta tesis evidencian que los miARNs transferidos desde los embriones en las primeras etapas de desarrollo tienen un impacto en la función endometrial. De hecho, como se ha indicado anteriormente, el pretratamiento de embriones KO con un análogo del miR-30d no sólo aumentó los valores de intensidad de fluorescencia de LIF en receptoras KO, sino también el porcentaje de implantación registrado (**Figura 5.15, 5.16 y 5.17**).

Hasta la fecha, el fallo de implantación se ha asociado con determinados efectos adversos durante el embarazo, incluidos el retraso de crecimiento feto-placentario y la existencia de elevadas tasas de reabsorción (Song et al., 2002; Ye et al., 2005). Estas características fueron evaluadas en los genotipos WT y KO en los días 5, 6, 8 y 12 de embarazo. Los sitios de implantación son significativamente más

pequeños en hembras KO a lo largo de los diferentes tiempos de gestación analizados (**Figura 5.19A**). Además, los sitios de reabsorción son más evidentes en el genotipo KO (**Figura 5.19B**). Sin embargo, el rasgo fenotípico más relevante es el retraso en el crecimiento feto-placentario en los fetos KO evaluado a través de los parámetros de longitud céfalo-caudal y los ratios peso feto/peso placenta (**Figura 5.20**). Estos resultados sugieren una leve afectación del desarrollo placentario, asociada a la disminución de los niveles de miR-30d.

Este fenotipo deficiente de implantación puede tener su origen en una posible alteración de las transiciones epitelio-mesenquimales (EMT). Durante el desarrollo normal de la placenta, el citotrofoblasto vellosos se diferencia en trofoblasto extraveloso (EVT) más invasivo, un proceso marcado por la existencia de una transición epitelial-mesenquimal (Dasilva-Arnold et al., 2014). Su desregulación está asociada con metástasis tumorales y progresión del cáncer (Kalluri et al., 2009; Davies et al., 2016), así como con trastornos en el embarazo, incluyendo la preeclampsia, la restricción del crecimiento fetal (FGR) (Du et al., 2017) o la endometriosis (Mari-Alexandre et al, 2016). Estudios recientes sugieren que la EMT durante la implantación está parcialmente regulada por los niveles de miR-30d (Cai et al., 2016); específicamente, la expresión reducida de miR-30d promueve la EMT y la invasividad que afectan la receptividad endometrial. Teniendo eso en cuenta, es factible que la EMT pueda verse afectada en el modelo murino KO debido a la desregulación del miR-30d. Como resultado, el desarrollo de la vascularización fetal y materna responsable del intercambio de nutrientes podría estar comprometido, lo que podría explicar porque los ratones miR-30d KO presentan pesos, anchuras y longitudes significativamente inferiores que el genotipo WT (**Figura 5.20 F, G, H**).

Es importante tener en cuenta que la disfuncionalidad de la transición epitelio-mesenquimal en trastornos del embarazo tiene su origen en una decidualización defectuosa. LIF es un regulador esencial de este proceso, ya que los

úteros de ratones *Lif*^{-/-} no son capaces de decidularizar, incluso bajo los efectos de los estímulos inductores de dicho proceso. Por lo tanto, el defecto en el desarrollo en el modelo KO podría tener su origen en toda la sucesión de eventos desencadenados por LIF, aunque hay que tener en cuenta que, dado que los miARNs afectan a la expresión de miles de ARNm (Mehta et al., 2016), los defectos observados podrían deberse a efectos pleiotrópicos del miR-30d. De hecho, puesto que los experimentos realizados solo evidencian parte del potencial de este miARN, sería necesario continuar la investigación para dilucidar por completo la regulación de la receptividad endometrial mediada por el miR-30d. Sin embargo, la hipótesis inicial en la que se planteaba un posible papel del miR-30d en la interfaz materno-fetal se cumple dados los efectos observados en la adquisición de un endometrio receptivo y el posterior desarrollo del embrión. Por otro lado, con respecto al modo de internalización del miR-30d en el interior de exosomas, se precisan más experimentos para determinar de qué manera se establece un enlace entre la proteína hnRNPC1 y el miARN antes de su liberación al ambiente intrauterino.

Conclusiones

- Los ensayos de espectrometría de masas identificaron hnRNPC1 como la proteína responsable, al menos en parte, del transporte del miR-30d al interior de la cavidad exosomal de células epiteliales endometriales humanas. Asimismo, análisis posteriores verificaron tanto la presencia de hnRNPC1 en exosomas, así como la interacción miR-30d-hnRNPC1 en el interior de los mismos.
- El silenciamiento de hnRNPC1 en células Ishikawa redujo los niveles de miR-30d tanto en dichas células como en los exosomas derivados de las mismas, sugiriendo un posible papel de hnRNPC1 en la biogénesis del miR-30d. A su vez, el bloqueo transitorio de hnRNPC1, dio lugar a una disminución significativa de las tasas de adhesión de embriones WT y KO

para el miR-30d, siendo dicha disminución más significativa en el genotipo KO.

- El análisis de los marcadores de receptividad en el modelo animal demuestra que la ausencia del miR-30d afecta a la expresión de LIF durante toda la ventana de implantación tanto en condiciones de pseudogestación como en diferentes contextos de comunicación materno-fetal. En este último caso, la transferencia de embriones KO pretratados con un análogo del miR-30d permite reestablecer los niveles basales de fluorescencia de LIF tanto en úteros WT como KO.
- El análisis del fenotipo de implantación en diferentes contextos de comunicación materno-fetal reveló que el bloqueo de la transferencia del miR-30d, ya sea desde la madre o el embrión, reduce significativamente las tasas de implantación alcanzadas.
- El patrón de variación de las tasas de implantación en las diferentes condiciones de transferencia coincide con el observado para los valores de fluorescencia de LIF, dándose una correlación positiva entre ambos parámetros. Estos resultados sugieren, por tanto, que LIF constituye una potencial diana indirecta del miR-30d.
- La ausencia del miR-30d en hembras gestantes afecta al crecimiento intrauterino, hecho reflejado en la existencia de sitios de implantación más pequeños, aumento de las tasas de reabsorción y una disminución significativa de los parámetros: longitud céfalo caudal y ratio peso feto/peso placenta. Como resultado, la descendencia en el genotipo KO presenta unas dimensiones inferiores en comparación con el genotipo WT.
- Estos análisis sugieren que el miR-30d desempeña un papel importante en la regulación de la implantación y posterior desarrollo fetal a través de LIF.

1. INTRODUCTION	4
1.1	Hormonal communication 4
1.2	Cell-to cell communication via adhesion and anti-adhesion molecules 11
1.3	Cytokines and growth factors 13
1.3.1	Signaling via cytokines 14
1.3.2	Signaling via growth factors 17
1.4	Homeobox genes in implantation 19
1.5	Prostaglandins 21
1.6	Non-coding sequences in maternal-fetal crosstalk: special insights into the role of microRNAs in implantation 22
1.6.1	MicroRNA biogenesis 22
1.6.2	MicroRNAs as regulatory elements of endometrial receptivity 24
1.6.3	Models of extracellular microRNA transport 26
1.6.4	Embryo-maternal crosstalk: the role exerted by microRNAs 30
2. HYPOTHESIS	41
3. OBJECTIVES	45
3.1	General objectives 45
3.2	Specific objectives 45
4. MATERIALS AND METHODS	49
4.1	Murine model and housing conditions 49
4.2	Recovery of preimplantation embryos 49
4.3	Isolation and primary culture of human endometrial epithelial cells 50
4.3.1	Collection of endometrial biopsies 50
4.3.2	Isolation and primary culture of human endometrial epithelial cells 50

4.4	Endometrial sample collection in wild-type and miR-30d knockout mice	51
4.5	Exosome isolation from hEECs	52
4.6	MicroRNA pull-down	52
4.7	Protein identification by tandem mass spectrometry	54
4.7.1	In-gel digestion proteins	54
4.7.2	Nano liquid-chromatography tandem mass-spectrometry analysis	54
4.7.3	Protein identification	55
4.8	Protein extraction	56
4.8.1	Endometrial epithelial cell lysate protein extraction	56
4.8.2	Human endometrial epithelial cell-derived exosome protein extraction	56
4.8.3	Uteri sample protein extraction	57
4.9	Subcellular fractioning	57
4.10	Western blots	58
4.11	Immunofluorescence	60
4.11.1	Co-localization studies	60
4.11.2	Study of key receptivity markers	60
4.12	Flow cytometry analysis of exosome-coupled beads	61
4.13	Validation of the microRNA pull-down assay	62
4.13.1	Sample preparation	62
4.13.2	Immunoprecipitation	62
4.13.3	MicroRNA extraction and quantitative PCR	63
4.14	Silencing hnRNPC1 in the Ishikawa cell line	63
4.15	Retro-transcription quantitative PCR	64
4.16	Molecular-beacon probe design and characterization	66
4.17	Co-culture of murine embryos with siRNA hnRNPC1-transfected cells	66
4.18	Embryo adhesion assay	67
4.19	Transfer assays	67
4.20	Characterization of the implantation-phenotype and pregnancy-outcome associated with miR-30d deficiency	69
4.21	Statistical analysis	70

5. RESULTS		73
5.1	Screening for the miR-30d transporter protein in exosomes	73
5.2	Silencing hnRNPC1 in human endometrial epithelial cells confirms their involvement in sorting miR-30d into endometrial exosomes	81
5.3	Impact of miR-30d deficiency on endometrial receptivity	86
5.4	Reproductive impact of maternal and/or embryonic-origin of miR-30d	90
5.5	Impaired fetal development linked to miR-30d deficiency	97
6. DISCUSSION		103
7. CONCLUSIONS		117
8. REFERENCES		121
9. ANNEXES		155
9.1	Supplementary files	155
9.2	Supplementary videos	157
9.3	Publications	158
9.3.1	Publication 1. Hsa-miR-30d secreted by the human endometrium is taken up by the pre-implantation embryo and might modify its transcriptome	161
9.3.2	Publication 2. Heterogeneous nuclear ribonucleoprotein C1 may control miR-30d levels in endometrial exosomes affecting early embryo implantation	175
9.3.3	Publication 3. Reproductive and fetal outcome of miR-30d deficiency at the maternal-embryonic interface	193
9.3.4	Publication 4. Embryo/fetal maternal crosstalk	227

FIGURE 1.1	Schematic representation of the maternal-fetal crosstalk	4
FIGURE 1.2	Schematic representation of the hormone-regulated menstrual cycle	6
FIGURE 1.3	Regulation of the endometrial proliferation and receptivity by estrogen receptor (ESR) signaling	8
FIGURE 1.4	Regulation of endometrial receptivity by progesterone receptor (PR) signaling	10
FIGURE 1.5	MUC-1 as an anti-adhesion molecule acting as a barrier to embryo attachment onto the apical surface of the uterine epithelium	13
FIGURE 1.6	Schematic representation of the canonical miRNA processing pathway	24
FIGURE 1.7	Schematic of a novel maternal-fetal crosstalk mechanism promoted by hsa-miR-30d	28
FIGURE 4.1	Schematic representation of the process followed to identify specific miR-30d-protein linkage	53
FIGURE 4.2	Schematic representation of the procedure for the different transfer combinations	69
FIGURE 5.1	Screening for proteins that direct miR-30d loading into exosomes (I)	76
FIGURE 5.2	Screening for proteins that direct miR-30d loading into exosomes (II)	77
FIGURE 5.3	Identification of hnRNPC1 inside exosomes (I)	78
FIGURE 5.4	Identification of hnRNPC1 inside exosomes (II)	79
FIGURE 5.5	Identification of hnRNPC1 inside exosomes (III)	80
FIGURE 5.6	Validation of miR-30d-hnRNPC1 linkage in whole lysates and exosomes	81
FIGURE 5.7	Silencing hnRNPC1 in hEECs confirms its involvement in sorting hsa-miR-30d into endometrial exosomes (I)	82
FIGURE 5.8	Characterization of the molecular beacon probe	83
FIGURE 5.9	Silencing hnRNPC1 in hEECs confirms its involvement in sorting hsa-miR-30d into endometrial exosomes (II)	84

FIGURE 5.10	Silencing hnRNPC1 in hEECs confirms its involvement in sorting hsa-miR-30d into endometrial exosomes (III)	85
FIGURE 5.11	Silencing hnRNPC1 in hEECs confirms its involvement in sorting hsa-miR-30d into endometrial exosomes (IV)	86
FIGURE 5.12	Analysis of essential receptivity markers in WT and miR-30d KO uteri throughout the implantation period (I)	87
FIGURE 5.13	Analysis of essential receptivity markers in WT and miR-30d KO uteri throughout the implantation period (II)	89
FIGURE 5.14	Analysis of essential receptivity markers in WT and miR-30d KO uteri throughout the implantation period (III)	90
FIGURE 5.15	Characterization of the implantation phenotype associated with miR-30d deficiency (I)	91
FIGURE 5.16	Analysis of receptivity marker expression (COX2, LIF, MSX1, MSX2, ESR, and PGR) in different maternal-fetal crosstalk scenarios (I)	93
FIGURE 5.17	Analysis of receptivity marker expression (COX2, LIF, MSX1, MSX2, ESR, and PGR) in different maternal-fetal crosstalk scenarios (II)	95
FIGURE 5.18	Correlation between LIF expression and implantation rates in different maternal-fetal crosstalk scenarios	96
FIGURE 5.19	Characterization of the implantation phenotype associated with miR-30d deficiency (II)	97
FIGURE 5.20	Characterization of the pregnancy outcome associated with miR-30d deficiency	99

TABLE 1.1	Maternal-origin intracellular miRNAs reported in the scientific literature	32
TABLE 1.2	Extracellular and circulating miRNAs reported in the scientific literature	34
TABLE 1.3	Embryo-derived miRNAs reported in the scientific literature	36
TABLE 4.1	Antibodies used for western blot analysis	59
TABLE 4.2	Primers for quantitative PCR assays	65
TABLE 5.1	Proteins specifically identified in exosomes and their main biological functions	74

V

ABBREVIATIONS

A: area

AA: arachidonic Acid

ABC: ammonium bicarbonate

ACN: acetonitrile

AGO2: argonaute

ART: assisted reproductive technology

BMP: bone morphogenetic protein

BSA: bovine serum albumin

C: negative control

C-: non-transfected cells

CaL: calnexin

Cdh5: cadherin 5

CHO: chinese hamster ovarian

CL: corpus luteum

CM: culture media

CO₂: carbon dioxide

COUP-TFII (Nr2f2): chicken ovalbumin upstream promoter transcription factor II

COX: cyclooxygenase

COX1: cyclooxygenase 1 [human]

COX2: cyclooxygenase 2 [human]

Cox2: cyclooxygenase 2 [mouse]

Cps: counts per seconds

CRL: crown-rump length

CSF: colony-stimulating factor

CYR61: cysteine-rich angiogenic inducer 61

CYT: cytoplasm

d: day

D: donor

DAPI: 4', 6-diamidino-2-phenylindole

DC: dendritic cell

DGCR8: diGeorge syndrome critical region 8

DMEM: dulbecco modified eagle medium

DNA: deoxyribonucleic acid

DROSHA: drosha ribonuclease III

DTT: dithiothreitol

D_x: diameter

E: embryonic day

E0: non-pregnant mouse endometrium condition

E₂: estrogen

E4: embryonic day 4, beginning of mouse embryo implantation

E5: embryonic day 5, moment when the implantation becomes effective

ECM: extracellular matrix

EDTA: ethylenediamine tetra-acetic acid

EEC: endometrial epithelial cell

EF: endometrial fluid

EGF: epidermal growth factor

EGFR: epidermal growth factor receptor

EGF-R: ErbB1

EMT: epithelial-to-mesenchymal transition

EP: prostaglandin E receptors

EP1, EP2, EP3, and EP4: PGE2 receptors subtypes

EREG: epiregulin

ERK1/2: extracellular signal-regulated kinase

ESCRT: endosomal sorting complex

ESC: endometrial stromal cell

ESR: estrogen receptor [human]

Esr: estrogen receptor [mouse]

ESR α : estrogen receptor alpha

ESR β : estrogen receptor beta

EVs: extracellular vesicles

EVT: extravillous cytotrophoblast

EXO: exosomes

FA: formic acid

FACS: fluorescent-activated cell sorting

FBS: fetal bovine serum

FC: fold change

FDR: false discovery rate

FGF: fibroblast growth factor

FGFR: fibroblast growth factors receptor

FGR: fetal growth restriction

FIV: fluorescence intensity value

FSH: follicle-stimulating hormone

FW: fetal weight

Fw: forward primer

GDF: growth and differentiation factor

GE: glandular epithelium

GM-CSF: granulocyte-macrophage colony-stimulating factor

GP130: glycoprotein 130 [human]

gp130: glycoprotein 130 [mouse]

GPCRs: G protein-coupled receptors

h: hour

HAND2: heart and neural crest derivatives expressed 2

HB-EGF: heparin-binding epidermal growth factor

hCG: human chorionic gonadotropin

HDL: high density lipoprotein

hEECs: human endometrial epithelial cells

HEK293: human embryonic kidney cell line 293

HIS: histone

HLA-G: human leukocyte antigen G

Hmx3: H6 homeobox 3

hnRNP: heterogeneous nuclear ribonucleoproteins

HNRNPC1: heterogeneous ribonucleoprotein C1 [human]

hnRNP1: heterogeneous ribonucleoprotein C1 [mouse]

Hoxa: homeobox A genes

HSP: heat shock protein

IAM: iodoacetamide

IF: immunofluorescence

IFN: Interferon

Ig: Immunoglobulin

IGF1: insulin-like growth factor 1

IHH: Indian hedgehog

IL: interleukin

Ip: immunoprecipitation

IR: Implantation rate

IRES: internal ribosome entry site

IS: Implantation site

Itg α 7: integrin alpha 7

It β 3: integrin β 3

IU: international units

IUGR: intrauterine growth restriction

IVF: in vitro fertilization

IVI: *Instituto Valenciano de Infertilidad*

JAK/STAT: janus kinase/ signal transducer and activator of transcription

JEM: jeol electron microscope

KEGG: kyoto Encyclopedia of Genes and Genomes

KLF15: krüppel-like factor 15

KO: knock out

KOE-KOR: KO embryos transferred into KO recipients

KOE-WTR: KO embryos transferred into WT recipients

KRT: keratin [family]

KSRP: KH-type splicing regulatory protein

LC-MS/MS: liquid chromatography tandem-mass spectrometry

LDL: low-density lipoprotein

LE: luminal epithelium

LH + 2: pre-receptive [state]

LH + 7: receptive [state]

LH: luteinizing hormone

LIF: leukemia inhibitory factor [human]

Lif: leukemia inhibitory factor [mouse]

LIFR: leukemia inhibitory factor receptor

LNA: locked nucleic acid

MAPK: mitogen-activated protein kinase

MB: molecular beacon

MCDB-105: MCDB-105 medium

MCL1: myeloid cell leukemia sequence 1

MCM2: minichromosome maintenance complex component 2

MECA-79: high endothelial venule marker

MEM: modified eagle medium

mg: milligram

MgCl₂: magnesium chloride

MIC: major histocompatibility complex class I chain related molecules

min: minutes

miRNA: microRNA

MIS: mullerian inhibiting substance

MMP: matrix metalloproteinase

mRNA: messenger ribonucleic acid

MS/MS: tandem mass spectrometry

Msx1: msh homeobox 1

Msx2: msh homeobox 2

MUC1: mucin 1

MVB: multivesicular body

MVs: microvesicles

n: number size

Na-DOC: sodium deoxycholic acid

NEAA: non-Essential amino acid

NIH: National Institutes of Health

NK: natural killer

NKG2D: natural-killer group2, member D

NP-40: nonyl phenoxy polyethoxy ethanol

NPM1: nucleophosmin 1

NPN: neuropilin [proteins]

NR: nucleus receptor [superfamily]

NSET: non-surgical embryo transfer

nt: nucleotides

NTA: nanoparticle tracking analysis

NUC: nucleus

o/n: overnight

P₄: progesterone

PAGE: polyacrylamide gel electrophoresis

PBS: phosphate buffered saline

PBST: phosphate buffered saline tween

PDGF: platelet-derived growth factor

PDZ: primary decidual zone

PFA: paraformaldehyde

PGD: preimplantation genetic diagnosis

PGD2: prostaglandin D2

PGE2: prostaglandin E2

PGF2 α : prostaglandin F2 alpha

PGI2: prostacyclin

PGR: progesterone receptor [human]

Pgr: progesterone receptor [mouse]

PGs: prostaglandins

PI-3: phosphatidylinositol-3

PI3K: phosphatidylinositol-3 kinase

PLA2: phospholipase A2

pMSC: placenta mesenchymal cell

PMSF: phenylmethanesulfonyl fluoride

PPAR γ : peroxisome proliferator-activated receptor- γ

PPAR- δ : peroxisome proliferator-activated receptor- δ

PGR: progesterone receptor

PGRA: progesterone receptor isoform A

PGRB: progesterone receptor isoform B

pre-miRNA: precursor miRNA

Pri-miRNA: primary miRNA

PRKO: progesterone receptor Knock-out [mouse model]

PTCH: patched

Ptgs1: prostaglandin-endoperoxide synthase 1 (cyclooxygenases 1) [mouse]

Ptgs2: prostaglandin-endoperoxide synthase 2 (cyclooxygenases 2) [mouse]

PTKOE-KOR: miR-30d pretreated KO embryos transferred into KO recipients

PTKOE-WTR: miR-30d pretreated KO embryos transferred into WT recipients

p-value: probability value

PVDF: polyvinylidene difluoride

PW: placental weight

qPCR: quantitative polymerase chain reaction

R: receptor

RBP: RNA binding protein

RCL: rostral-caudal length

rhLIF: recombinant human leukemia inhibitory factor

rhVEGF: recombinant human vascular endothelial growth factor

RIPA: radioimmunoprecipitation assay [buffer]

RISC: RNA-induced silencing complex

RNA: ribonucleic Acid

ROI: region of interest

Rpm: revolutions per minute

RT: room temperature

RT-qPCR: retro transcription-quantitative polymerase chain reaction

Rv: reverse primer

RYK: receptor-like tyrosine kinase

SA: spiral artery

SBCM: spent blastocyst culture media

SC: stromal cell

SCR: scramble

SDS: sodium dodecyl sulfate

SGA: 'small for gestational age'

sihnRNPC1: small interfered hnRNPC1

siRNA: small interfering RNA

SMO: smoothened

SOX9: sex determining region Y box 9

STAT3: signal transducer and activator of transcription 3

TBS: tris buffered saline

TBST: tris buffered saline-tween20

TEM: transmission electron microscopy

TFA: trifluoroacetic acid

TGF: transforming growth factor

TIMP: tissue inhibitor of matrix metalloproteinase

TLR: toll-like receptor

TNF: tumor necrosis factor

ULBP: uL binding protein

UTR: untranslated region

VEGF: vascular endothelial growth factor

VEGFR: vascular endothelial growth factor receptor

VEGF-R1 (FLT-1): vascular endothelial growth factor receptor 1

VEGF-R1 (FLK-2): vascular endothelial growth factor receptor 2

VSMC: vascular smooth muscle cell

WB: western blot

Wcl: whole cell lysate

WGA: wheat germ agglutinin

WNTs: wingless-type MMTV integration site [family members]

WOI: window of implantation

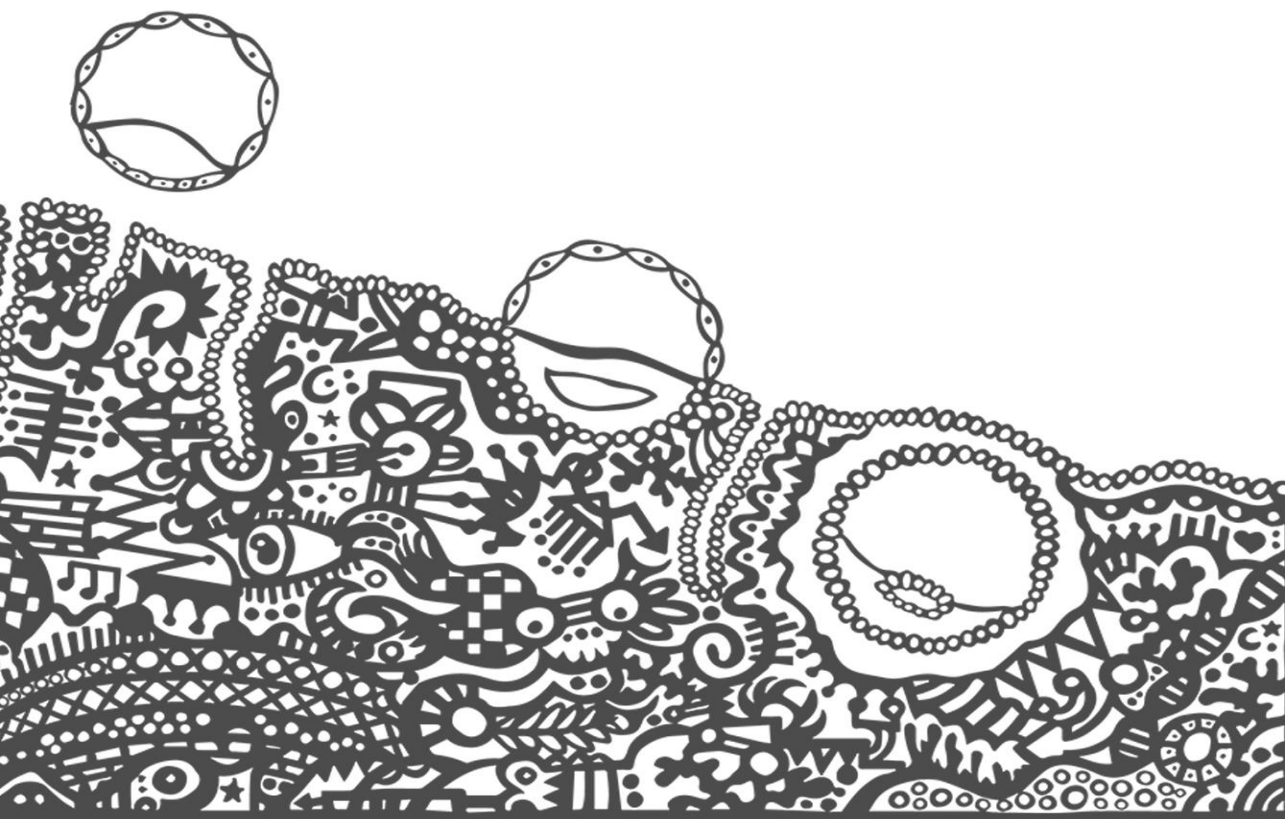
WT: wild type

WTE-KOR: WT embryos transferred into KO recipients

WTE-WTR: WT embryos transferred into WT recipients

Zo: zonula Occludens

INTRODUCTION



01 | INTRODUCTION

The gestational period is a time when a profound and direct relationship between the mother and offspring occurs during a baby's initial development, first as an embryo, then as a fetus, and finally as a newborn. The importance of the intrauterine environment encountered during fetal development is key and any dysregulation negatively affects the baby's subsequent life outside the womb by increasing its risk of suffering non-communicable diseases in adulthood (Barker, 2004). This communication is reciprocal because embryo-derived factors (Thouas et al., 2015, Simon et al., 2018) profoundly affect maternal physiology during and after pregnancy. Therefore, the nature of this relationship is complex, and thus, proper bidirectional communication is the primary key that contributes towards a pregnancy's success (Douglas, 2011).

Recent advances in gene expression studies and genetically engineered mouse models have provided valuable clues to understanding embryo-uterine crosstalk and have highlighted steroid hormones, growth factors, cytokines, lipid mediators, adhesion molecules, transcription factors, and miRNAs as the primary regulators of the implantation process and subsequent fetal development (Salamonsen et al., 2016, Atwood and Vadakkadath Meethal, 2016, Bazer et al., 2010, Robertson and Moldenhauer, 2014; **Figure 1.1**). Thus, a comprehensive understanding of the role exerted by each of these players is essential, not only to improve implantation rates, but also to pregnancy outcomes.

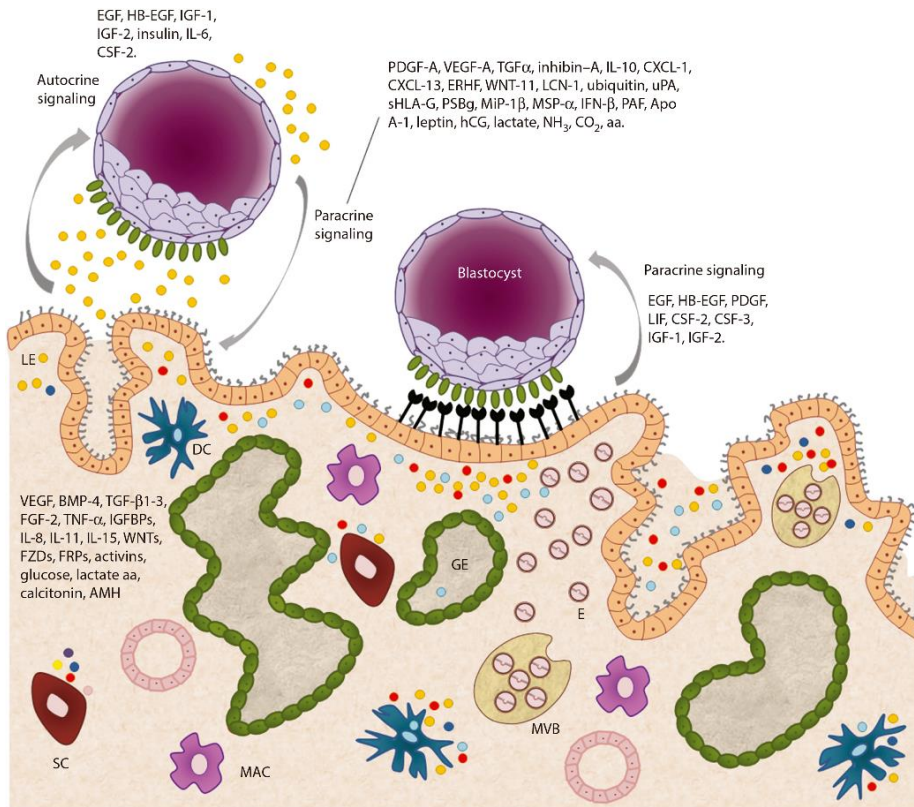


Figure 1.1 Schematic representation of maternal-fetal crosstalk. LE, luminal epithelium; GE, glandular epithelium; SC, stromal cells; DC, dendritic cells; MBV, multivesicular bodies.

1.1 Hormonal communication

The ovarian steroids, estrogen (E $_2$) and progesterone (P $_4$), and their receptors, the estrogen receptor (ESR) and progesterone receptor (PGR) orchestrate the complex sequence of events required for the development of uterine receptivity and the establishment of pregnancy (Adams and DeMayo, 2015). E $_2$ is the predominant hormone driving the proliferation of the luminal and glandular epithelium. In humans, the proliferative phase is influenced by rising E $_2$ levels generated by growing ovarian follicles. It results in the proliferation of the epithelium, stroma, and vascular endothelium to regenerate the endometrium.

Numerous developing glands assume a tortuous morphology during the late proliferative phase. Increasing pituitary gonadotropin levels during this phase lead to folliculogenesis and the subsequent selection of a dominant follicle.

At mid-cycle, there is a surge of gonadotropins, follicle-stimulating hormone (FSH), and luteinizing hormone (LH) which trigger ovulation at around day 14 (Cha et al., 2012, Ramathal et al., 2010; **Figure 1.2**). The early secretory phase is characterized by the formation of the corpus luteum (CL) from the ruptured follicle and subsequent P_4 secretion in preparation for implantation. Concurrently, glands become secretory as stromal cells differentiate (pre-decidualization) and this is accompanied by endometrial edema (Hess et al., 2006). Rising E_2 levels superimposed onto P_4 define the window of implantation (WOI) during the mid-luteal phase. This transition to a receptive status involves structural and functional remodeling of the uterine epithelium. In this sense, epithelial cells lose polarity via downregulation of the cell-cell adhesion molecule E-cadherin, exhibit inhibition of the cell surface glycoprotein mucin 1 (MUC1), and develop protrusions along the apical surface (Thie et al., 1995, Surveyor et al., 1995, Nikas and Psychoyos, 1997). In the absence of a viable embryo, the receptive window transits into a refractory phase, thus leading to luteolysis, hormone withdrawal, and menstruation. On the contrary, embryo attachment triggers proliferation and differentiation of the surrounding stroma into decidual secretory cells (Cha et al., 2012, Ramathal et al., 2010). Thus, the implanting blastocyst secretes human chorionic gonadotropin (hCG) to maintain the CL, thereby supporting pregnancy.

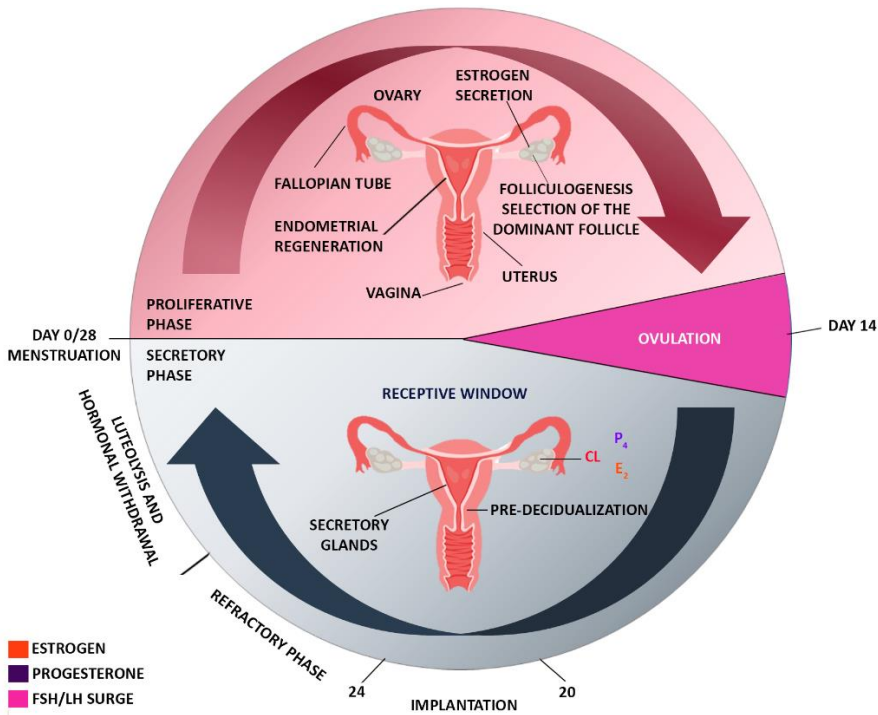


Figure 1.2. Schematic representation of the hormone-regulated menstrual cycle. (Adapted from Cha et al., 2012).

E_2 and P_4 are synthesized from cholesterol in the ovaries and can diffuse into target cells where they act upon their cognate receptors. Estrogen receptors, $ESR\alpha$ and $ESR\beta$, and the progesterone receptors A and B (PRA and PRB) are transcription factors which, in the absence of their respective hormones, are mainly found in the cytoplasm. Hormone binding favors receptor activation, resulting in its dimerization and subsequent translocation into the nucleus. Once activated, they can bind to specific genomic sites to enable or repress the expression of their target genes (Hewitt et al., 2012, Rubel et al., 2012).

E_2 regulates proliferation in a biphasic manner, directing both early and late proliferative events in the endometrium by modifications in the transcription of cell cycle genes, DNA synthesis, epithelial mitosis, hyperemia, stromal edema,

and the infiltration of immune cells. Estrogen-driven proliferation is mediated by paracrine signaling involving fibroblast growth factor (FGF) ligands, and ESR signaling induces FGF expression in stromal cells (Fujimoto et al., 1997, Tsai et al., 2002). Stromal FGF ligands activate epithelial FGF receptors (FGFRs), which drive the proliferative response by activating the downstream extracellular signal-regulated kinase (ERK1/2) or phosphoinositide 3-kinase (PI3K) pathways (**Figure 1.3**). ESR α is considered the predominant ESR isoform because its loss results in female infertility and insensitivity to the mitogenic effects of E₂ (Hewitt and Korach, 2003). In contrast, ER β ablation does not seem to affect uterine functionality but does negatively impact fertility by causing an ovarian defect (Krege et al., 1998). Surprisingly, loss of epithelial ESR α does not prevent estrogen-induced epithelial cell proliferation, suggesting that the action of ESR α upon the stroma is critical for mediating this event.

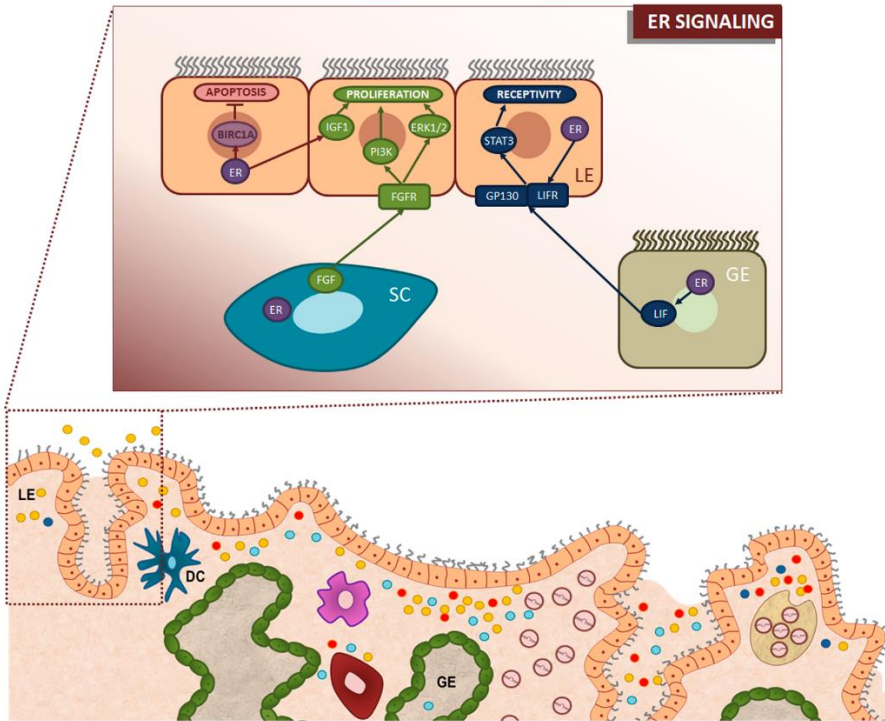


Figure 1.3. Regulation of endometrial proliferation and receptivity by estrogen receptor (ESR) signaling. In mice, stromal ESR induces proliferation of the endometrial epithelium via a paracrine signaling network. ERs activate FGF expression in stromal cells which act on FGFR expressed on the surface of epithelial cells. FGFR drives the proliferation of epithelial cells by activating downstream signaling via PI3K and ERK1/2. In addition, IGF1 is induced by ERs to further enhance proliferation. Concurrently, epithelial ESR stimulates the activation of antiapoptotic targets like BIRC1A. Likewise, uterine receptivity is mediated by ESR-induced leukemia inhibitory factor (LIF) signaling. Thus, ESR induces expression of both LIF and its receptor, LIFR. LIF is produced via glandular epithelium signaling to LIFR and its co-receptor, GP130, which are expressed in the LE. LIFR/GP130 activation results in activation of STAT3 and transition of the LE to the receptive state (Adapted from Adam & Demayo, 2015).

The roles of PR in mouse uteri have been explored by examining the main downstream pathways involved in progesterone signaling. The expression of epithelial PR appears to increase in the days preceding implantation, suggesting its relevance in establishing uterine receptivity. Specifically, PR expression decreases in the uterine epithelium at the time of attachment but simultaneously increases in

the endometrial stroma surrounding the implantation site. One of the leading functions driven by endometrial PR is the induction of Indian hedgehog (IHH) in the epithelium during the pre-receptive phase (Takamoto et al., 2002). As a result, IHH exerts its effects on its receptors, Patched and Smoothed (PTCH/SMO), which are mainly located on the surface of endometrial stromal cells. This paracrine signaling pathway drives the proliferation and differentiation of stromal cells in a PR-dependent manner. Thus, the induction of IHH in the epithelium is critical to both embryo implantation and stromal cell decidualization. In subepithelial stromal cells, IHH signaling stimulates the production of chicken ovalbumin upstream promoter transcription factor II (COUP-TFII, Nr2f2), an orphan member of the nucleus receptor (NR) superfamily (Lee et al., 2006). Although COUP-TFII is expressed exclusively in the stromal compartment, it performs functions that are critical both to implantation and decidualization (Takamoto et al., 2005). COUP-TFII drives the latter by coordinating several growth-factor signaling pathways, including epidermal growth factor receptor (EGFR), bone morphogenetic protein (BMP), and wingless-type MMTV integration site family members (WNTs; **Figure 1.4**).

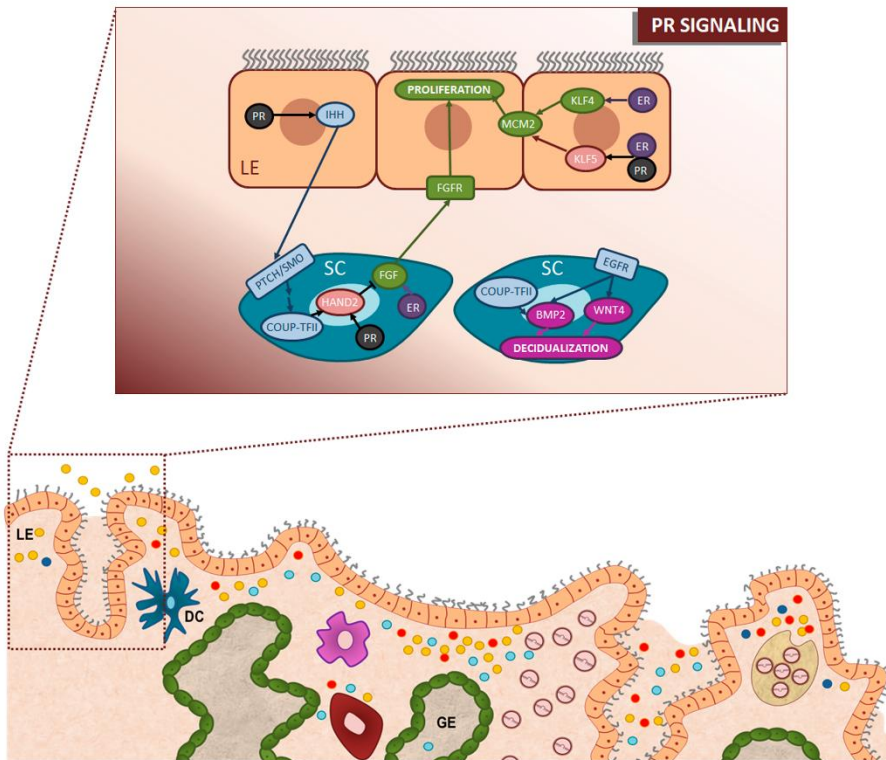


Figure 1.4. Regulation of endometrial receptivity by progesterone receptor (PR) signaling. PR regulates multiple signaling pathways in the endometrium and coordinates the functions of the endometrial epithelium and stroma via paracrine signaling networks. In mice, epithelial PR induces IHH expression, which then acts on its receptors, Patched and Smoothed (PTCH/SMO) expressed on stromal cells. This results in the induction of COUP-TFII in endometrial stromal cells. HAND2 is induced directly by PR, downstream of COUP-TFII signaling. HAND2 inhibits production of FGF ligands, thereby abrogating proliferative signaling to the epithelium. PR also inhibits epithelial proliferation directly, by favoring KLF15 production, resulting in downregulation of the proliferative target, MCM2. PR signaling also drives the decidualization of stromal cells. COUP-TFII, a downstream PR signaling target, induces expression of BMP2 and WNT4 but their induction also requires EGFR signaling. BMP2 and WNT4 are required for optimal PR signaling and decidualization of endometrial stromal cells (Adapted from Adam e DeMayo, 2015).

Mouse models lacking functional PR (PRKO) are characterized by their infertility which is caused by an ovulation defect (Lydon et al., 1995). Specifically, their uteri are hyperplastic and non-receptive to implanting embryos. Interestingly,

these mutant mice also fail to trigger a decidual response following artificial stimulation of their hormone-primed uteri. In addition, mice lacking PR exclusively in the epithelium show clear signs of infertility associated with the existence of persistent proliferation of the luminal epithelium (LE; Wetendorf and DeMayo, 2014).

1.2 Cell-to-cell communication via adhesion and anti-adhesion molecules

Endometrial cells can be characterized by the wide range of integrins they host; these are implicated in cellular processes, including adhesion, migration, and invasion, activated in response to both intracellular and extracellular signals (Lessey et al., 1992, Singh and Aplin, 2009). Specific integrins are constitutively expressed on the LE, while others, located in the stroma are regulated during the menstrual cycle, both spatially and temporally (Bowen and Hunt, 2000, Singh and Aplin, 2009). The integrins whose levels are increased the most during the mid-luteal phase of the cycle are currently used as uterine receptivity markers. Integrins are actually formed by the interaction of two different non-covalently linked α and β subunits (Achache and Revel, 2006). These proteins are receptors for extracellular matrix (ECM) ligands such as collagen, laminin, and fibronectin, as well as for transducing signals from soluble ligands such as osteopontin (Aplin, 2006). In humans, $\alpha 2\beta 1$, $\alpha 3\beta 1$, $\alpha 6\beta 1$, $\alpha 9\beta 1$, $\alpha \nu\beta 1$, $\alpha \nu\beta 3$, $\alpha \nu\beta 5$, and $\alpha \nu\beta 6$ are localized on the LE. The glandular epithelium (GE) expresses the same proteins, except for $\alpha \nu\beta 5$ and $\alpha \nu\beta 6$, and it additionally expresses $\alpha 1\beta 1$ and $\alpha 4\beta 1$ (Hoozemans et al., 2004, Minas et al., 2005).

In the murine model, $\beta 1^{-/-}$ knockout mouse embryos develop until up to the blastocyst stage but they show defects in cell lineage allocation and fail to implant (Fässler and Meyer, 1995). $\alpha 5\beta 1$, $\alpha \nu\beta 3$, $\alpha \nu\beta 5$, and $\alpha \nu\beta 6$ are expressed by the trophoctoderm during early apposition and adhesion (Sutherland et al., 1993,

Bloor et al., 2002), while $\alpha 1\beta 1$, $\alpha 6\beta 1$, and $\alpha 7\beta 1$ tend to dominate during embryonic invasion (Bowen and Hunt, 2000). In early blastocysts, $\alpha 5\beta 1$ is initially expressed by cells located between the inner cell mass and the blastocoele cavity. However, as the trophoblast differentiates, $\alpha 5\beta 1$ translocates to the apical surface of trophoblast cells, the first cells to come into contact with the uterus (Clark et al., 2005). Specific evidence indicates that integrin $\alpha 4\beta 1$ is strongly related with implantation success because its reduced presence in endometrial stroma is associated with recurrent miscarriage. Likewise, blocking intrauterine $\alpha 4\beta 1$ with a specific antibody led directly to implantation failure or delayed implantation (Basak et al., 2002). In addition, integrin $\alpha v\beta 3$ is of particular interest because its deficiency has been related to infertility, endometriosis (Lessey et al., 1994), and polycystic ovarian syndrome. In fact, it has been suggested that the expression levels of this integrin could be indicators for successful pregnancy after an assisted reproductive technology (ART) intervention is performed.

Selectins, the lectin-like proteins that include E-, L-, and P-selectins, are responsible for the endothelial surface tether and roll mechanism (Torry et al., 2007). At the time of implantation, carbohydrate ligands (e.g., MECA-79) that bind L-selectin are present on the LE, and this event coincides with stable L-selectin expression by the trophoblast after hatching. Human studies have revealed that a lack of MECA-79 expression in mid-luteal endometrial biopsies is indicative of low or no probability of pregnancy (Fouk et al., 2007). Expression of anti-adhesion molecules in the endometrium is regulated by the signals secreted by the blastocyst during the first stages of conception. One of the most important in the maternal-conceptus dialogue is that of anti-cellular adhesion molecule MUC1, an integral membrane glycoprotein expressed on the apical surface of secretory epithelial cells. MUC-1 constitutes a major component of interest in the glycocalyx and is likely to sterically block E-cadherin-based cell-to-cell interactions (**Figure 1.5**; Komatsu et al., 1997). In humans, the MUC-1 concentration increases during the WOI and decreases in the late secretory phase. However, despite the existence of a

general steroid-mediated rise in MUC-1 during the WOI, in vitro experiments have shown that paracrine effects from the blastocyst may cause local clearance of MUC-1 at the attachment site (Meseguer et al., 2001).

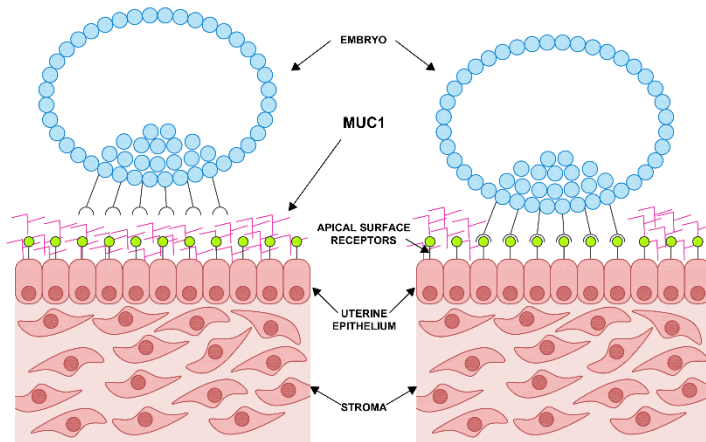


Figure 1.5. MUC-1 acts as an anti-adhesion molecule by creating a barrier to embryo attachment to the apical surface of the uterine epithelium. MUC-1 clearance allows access to the apical cell surface receptors for implantation. (Adapted from (Davidson and Coward, 2016).

1.3 Cytokines and growth factors

Factors released by the maternal tract, especially cytokines, exert paracrine cell-to-cell signaling influencing embryo physiology and developmental potential (Kaye, 1997, Hardy and Spanos, 2002, Richter, 2008). In turn, these factors act in synergy with autocrine growth factors and cytokines produced by the embryo itself to modulate gene expression and physiological function. As a result, the acquisition of implantation competence and post-implantation developmental ability may be profoundly affected, both in physiological and pathological conditions (Bromfield et al., 2014, O'Neill, 2008).

1.3.1 Signaling via cytokines

Cytokines are a family of several hundred small, diffusible glycoproteins that act as soluble intercellular signaling agents (Robertson et al., 2008) which play a major role in the regulation of immune-related events. Cytokine binding to specific, high-affinity receptors located on target cells, triggers the activation of a broad range of tyrosine kinases belonging to the Janus kinase/signal transducers and activators of transcription (JAK/STAT) family (Ihle, 1995, Ihle, 2001, Gadina et al., 2001). The production of endometrial cytokines is primarily regulated by ovarian steroid hormones, but paracrine factors can also be secreted by adjacent endometrial cells or emanate from microorganisms or the trophoctoderm itself. Dysregulation of cytokine production, especially those in the interleukin (IL)-6 family, is associated with implantation failure and miscarriage, even for euploid embryos. The IL-6 family includes leukemia inhibitory factor (LIF), IL-6, and IL-11 (Cork et al., 2002). LIF is a pro-inflammatory factor that regulates proliferation, differentiation, and cell survival (Stewart, 1994), whose expression appears to be maternally controlled and becomes considerably increased during the WOI. LIF acts by binding to its receptor, LIFR, and co-receptor, gp130; this binding triggers several signaling pathways, including the JAK/STAT, mitogen-activated protein kinase (MAPK), and phosphatidylinositol-3 (PI-3) kinase pathways (Cha et al., 2013).

The phenotype of Lif knockout mice demonstrates the importance of LIF in reproduction: females are fertile, but their blastocysts fail to implant (Song et al., 2000). These discoveries prompted the implementation of clinical trials investigating the effect of recombinant human LIF (rhLIF) administration during the luteal phase in women with implantation failure; however, no noticeable improvements in pregnancy rates were achieved (Brinsden et al., 2009). IL-6 is a multifunctional cytokine that regulates several aspects of the immune response, acute-phase reaction, and hematopoiesis (Robertson et al., 2000). IL-6 is minimally expressed during the proliferative phase of the menstrual cycle, but its highly

expressed during the mid-secretory phase, predominantly in the glandular and luminal epithelial cells (Tabibzadeh and Babaknia, 1995). Aberrant IL-6 expression is associated with recurrent miscarriage (Von Wolff et al., 2000), suggesting that it plays an autocrine or paracrine role in implantation (Vandermolen and Gu, 1996). Moreover, higher levels of IL-6 appear to be linked with lower implantation rates in patients with endometriosis by impairing oocyte and embryo quality (Pellicer et al., 1998). Embryo viability is, in turn, related to IL-6 consumption. Our group validated this finding in an investigation into the secretome profile of implanted blastocysts grown in sequential media versus those co-cultured with endometrial epithelial cells (EECs; Dominguez et al., 2010). There was a differential protein pattern between these two culture conditions, and interestingly, IL-6 was the most abundantly secreted protein in the EEC co-culture and may have been consumed or metabolized by the blastocysts. Furthermore, compared with the sequential media from blastocysts that did not implant, the media from the culture of blastocysts that later successfully implanted was nearly devoid of IL-6 (Dominguez et al., 2010), thus reinforcing the hypothesis that IL-6 consumption or metabolism may be necessary for proper blastocyst development and implantation.

IL-11 exerts critical pleiotropic effects (Dimitriadis et al., 2005): both IL-11 and its receptor IL-11R α localize to decidualized stromal cells in mid-secretory phase endometrium (Dimitriadis et al., 2000, Cork et al., 2001, von Rango et al., 2004). The functional relevance of IL-11 is demonstrated by the fact that mice lacking IL-11 have a phenotype of impaired fertility and small litter sizes (Makrigiannakis et al., 2006). Incidentally, relative to fertile women, IL-11 deficiency has been observed in patients suffering from recurrent miscarriage (Linjawi et al., 2004). Very large amounts of cytokines are synthesized in the placental–decidual interface postimplantation, of which, colony-stimulating factor (CSF) 1, transforming growth factor (TGF) β , tumor necrosis factor (TNF) α , granulocyte-macrophage (GM)-CSF, LIF, interferon (IFN) γ , IL-6, and IL-10 are the most functionally relevant in trophoblast differentiation and invasion (Robertson et

al., 1994). The patterns of receptor expression in specific trophoblast cell populations, combined with data from in vitro models, suggest that individual cytokines have specific roles in the regulation of the invasive, adhesive, secretory, and antigenic properties of different trophoblast lineages (Robertson et al., 2008). Some cytokines, such as IL-1, IL-6, IL-15, and TNF α , enhance matrix metalloproteinase (MMP) activity, while others, like IL-10, LIF, and TGF β , inhibit MMP secretion or stimulate the expression of tissue inhibitors of matrix metalloproteinases (TIMPs; Saeki et al., 1998).

Among the wide array of cytokines, chemokines stand out because they have chemotactic properties that allow them to regulate leukocyte recruitment from the blood, they show directional movement within tissues, and they can disperse via the lymphatic system (Du et al., 2014). Chemokines can be classified into different subfamilies based on their structural motifs: the CXC, CC, CX3C, and C groups, or the α , β , γ , and δ subfamilies (Carvalho-Gaspar et al., 2005). To assess the paracrine effect that embryos have on the expression of chemokine receptors in the endometrium, human embryos were co-cultured with EECs. The chemokine receptors CXCR1, CXCR4, and CCR5 were barely detectable in the EEC monolayer, but in the presence of a human blastocyst, EEC expression of CXCR1, CXCR4, and CCR5 increased, and moreover, these receptors polarized to one of the poles of these cells. In another study using the same co-culture model, the embryonic regulation of IL-8 was examined (Dominguez et al., 2003), showing that this cytokine was significantly upregulated in EECs in the presence of blastocysts compared to controls without embryos (Caballero-Campo et al., 2002). Taken together, these results show that embryos exert a paracrine effect on cytokines and chemokines in the maternal endometrium.

The in vivo study of human implantation sites is impracticable for ethical reasons. Therefore, animal models, mainly gene knockouts (Dey et al., 2004), and in vitro studies using human co-culture models of decidualizing endometrial

stromal cells (ESCs) and single hatched blastocysts are of great interest for identifying the soluble factors involved in implantation (Teklenburg et al., 2010). Over a 3-day co-culture period, the development of approximately 75% of embryos arrested, while the remainder continued normal development. Multiplex immunoassays were used to determine the levels of 14 factors secreted by the ESCs; the presence of a normal blastocyst had no significant effect on decidual secretions, but a response, characterized by selective inhibition of IL-1 β , IL-6, IL-10, IL-17, IL-18, eotaxin, and heparin binding epidermal growth factor (HB-EGF) secretion was triggered in the presence of arrested embryos. The authors concluded that this response to developmentally-impaired embryos might represent a mechanism for controlled embryo disposal, mediated by the induction of menstruation-like tissue breakdown and shedding (Teklenburg et al., 2010).

1.3.2 Signaling via growth factors

Growth factors comprise a group of peptides and polypeptides that are usually divided into families based primarily on their structural characteristics (Sporn et al., 1986). They interact with specific cell membrane receptors, thus initiating intracellular signaling pathways (Giudice and Saleh, 1995). The major families include epidermal growth factors (EGFs), TGF β , fibroblast growth factors (FGFs), insulin-like growth factors (IGFs), and platelet-derived growth factors (PDGFs). The EGF family encompasses EGF itself, TGF α , HB-EGF, amphiregulin, β -cellulin, epiregulin (EPRG), and neuregulins (Dey et al., 2004). Specifically, they interact with the receptor subtypes of the ErbB family, which comprise four receptor tyrosine kinases: ErbB1 (EGF-R), ErbB2, ErbB3, and ErbB4 (Olayioye et al., 2000). Spatiotemporal expression patterns of EGF gene family members and ErbB in the uterus during the peri-implantation period suggest that EGF-like growth factors have compartmentalized functions during implantation (Bass et al., 1994, Dakour et al., 1999, Li and Zhuang, 1997, Maruo et al., 1995, Staun-Ram et al., 2004).

HB-EGF appears to play a critical role in this process, as well as in embryo development because its expression peaks in the late secretory phase, a period of maximum receptivity (Rathjen et al., 1990). Moreover, decreasing HB-EGF levels lead to pregnancy complications, such as preeclampsia and small-for-gestational-age (SGA), caused by aberrant trophoblast invasion and intrauterine growth restriction (IUGR) resulting from increased apoptosis (Ozbilgin et al., 2015). Concurrently, cells expressing the transmembrane form of HB-EGF adhere to human blastocysts expressing cell surface ErbB4 (Chobotova et al., 2002). Day-4 blastocysts express ErbB4 at both the protein and mRNA levels (Paria et al., 1999), while it is primarily located in the sub-myometrial stroma and connective tissues and is expressed at basal levels throughout the stroma (Lim et al., 1998).

Besides HB-EGF, the LE also expresses β -cellulin and EPRG ligands at the site of implantation and these can interact with ErbB1 and ErbB4. Thus, the contribution of these different ligands to implantation may be redundant. In general, the expression of multiple ligands and multiple ErbB family receptors might be a protective mechanism to ensure a high probability of blastocyst development and implantation. Notably, Wnt proteins may behave as growth factors in the uterus; they are reported to be involved in cell specification and epithelial-mesenchymal interactions (Dunlap et al., 2011, Bui et al., 1997, Tulac et al., 2003). Wnt signaling can occur through the canonical pathway, mediated by a family of receptors that induce β -catenin stabilization, or through an unrelated receptor tyrosine kinase, RYK (Ben-Shlomo, 2005). Wnt signaling also regulates vascular endothelial growth factors (VEGFs), which are angiogenesis effectors. VEGF splicing variants differentially interact with the two VEGF receptors (VEGF-R1 and VEGF-R2, also known as FLT-1 and FLK-2). Moreover, one VEGF isoform (VEGF165) binds to neuropilin proteins (NPN-1 and NPN-2), transmembrane proteins which are unrelated to VEGF-R. The interaction between VEGF165 and NPN-2 promotes VEGF165 binding to VEGF-R (Pavelock et al., 2001). Pathway redundancy and cross-talk between them increases the complexity of biological

responses, making it very difficult to elucidate the molecular mechanisms involved in the paracrine mediation of hormone action (Biggsby and Bethin, 2008)

Hannan et al. were the first to detect high levels of VEGF165 in the uterine fluid during the WOI and that these levels are significantly lower in women with unexplained infertility (Hannan et al., 2011). In mice, rhVEGF administration substantially improves preimplantation embryo development and in vitro embryo outgrowth, as well as the implantation rates and appearance of fetal growth in vivo. These findings further support the existence of a precise paracrine and autocrine dialogue between the blastocyst and endometrial epithelium during the WOI and highlight the importance of the changing microenvironment as embryos develop (Binder et al., 2014). TGF β superfamily members are associated with tissue remodeling events and reproductive processes. They include at least 42 different mammalian dimeric proteins which share a similar structure (Kingsley, 1994, Piek et al., 1999); these are divided into two subfamilies, the TGF β /activating/nodal subfamily and the bone morphogenetic protein (BMP)/Mullerian inhibiting substance (MIS)/growth and differentiation factor (GDF) subfamily (Chimote, 2010). The roles of these proteins in preparation for implantation have been previously detailed, particularly in promoting endometrial stroma decidualization (Jones et al., 2006). However, given the complexity of these mechanisms, it is not surprising that disruption of individual members of this family does not produce alterations in implantation.

1.4 Homeobox genes in implantation

Homeobox genes are evolutionally conserved transcriptional regulators involved in the control of embryonic morphogenesis and differentiation (Krumlauf, 1994). In mice, homeobox A (Hoxa) genes, *Hoxa10*, and *Hoxa11* are expressed in uterine stromal cells during receptivity and they are upregulated upon decidualization in a steroid hormone-responsive manner. Both *Hoxa10*^{-/-} and *Hoxa11*^{-/-} mice show characteristic signs of impaired infertility associated with

defective decidualization events, with the *Hoxa11*^{-/-} knockout showing the stronger phenotype of the two. Defective decidualization in *Hoxa10*^{-/-} mice is linked to downregulation of a cell-cycle regulatory axis involving cyclinD3, cdk4/6, and p21 (Lim et al., 1999b, Tan et al., 2002). Likewise, the absence of LIF expression in *Hoxa11*^{-/-} uteri reinforces its role as a key player in uterine receptivity and subsequent implantation events (Gendron et al., 1997). During a regular menstrual cycle, HOXA10 and HOXA11 are maximally expressed during the mid-secretory phase and their expression remains elevated thereafter. However, in infertility-related disorders including endometriosis, polycystic ovarian syndrome, leiomyoma, and hydrosalpinx, these genes are markedly downregulated during the secretory phase (Eun Kwon and Taylor, 2004, Fischer et al., 2011, Matsuzaki et al., 2009, Taylor, 2000).

It is also important to consider that non-classical Hox genes may also play a significant role during implantation. Ablation of H6 homeobox 3 (*Hmx3*) in mice results in implantation failure (Wang et al., 1998). Muscle segment homeobox gene family members *Msx1* and *Msx2* are known tissue morphogenesis regulators, and play critical roles in uterine stromal-epithelial interactions (Alappat et al., 2003). During pregnancy, *Msx1* and *Msx2* expression is confined to the LE and GE on day 3 and 4, but are markedly downregulated on the evening of day 4, coinciding with blastocyst attachment. Conditional deletion of either *Msx1* or *Msx2* results in subfertility, whereas double knockout of both *Msx1* and *Msx2* (*Msx1*^{d/d} *Msx2*^{d/d}) causes infertility, suggesting that a compensatory mechanism exists between MSX1 and MSX2 (Daikoku et al., 2011, Nallasamy et al., 2012). In double knockouts, the LE fails to transition from a highly polarized, columnar state with tight cellular adherence, to a less polar, cuboidal state conducive to blastocyst attachment. Moreover, this enhanced polarity in *Msx1*^{d/d}/*Msx2*^{d/d} uteri correlates with increased Wnt5a-mediated E-cadherin/ β -catenin complex formation at adherens junctions during the receptive state.

1.5 Prostaglandins

Prostaglandins (PGs), together with other factors produced by the conceptus and the endometrium, prepare a pro-inflammatory environment during embryo implantation (Waclawik, 2011). Moreover, roles for PGs in vascular permeability, stromal decidualization, blastocyst growth and development, leukocyte recruitment, embryo transport, trophoblast invasion, and ECM remodeling during implantation have also been described (Salleh, 2014). PGs are eicosanoid family bioactive lipid compounds which are derived from the essential fatty acid arachidonic acid (AA; Irvine, 1982). The participation of specific terminal PG synthases enables the formation of a set of well-known PGs: PGD₂, PGE₂, PGF₂α, and PGI₂ (Hara et al., 2010) with PGE₂ and PGF₂α being the most relevant in acquiring endometrial receptivity (Vilella et al., 2013). The action of PGs is mediated by their binding to various G protein-coupled receptors (GPCRs), which include four PGE₂ subtypes (EP1, EP2, EP3, and EP4) and one PGF₂α subtype (FP; Gu et al., 2012). Our group demonstrated that PGE₂ and PGF₂α concentrations in endometrial fluid (EF) 24 hours before embryo transfer can predict pregnancy outcome (Vilella et al., 2013). Moreover, we showed that blocking PG receptors on the trophectoderm membrane of mouse embryos considerably reduces embryo adhesion rates, thus suggesting that transport of PGs from mother to embryo is essential for acquiring a proper adhesion phenotype.

PG production can be inhibited in female mice lacking PLA₂ and cyclooxygenase (COX) enzymes, resulting in significant implantation defects (Song et al., 2002). COX1 and COX2, the most common COX-derived prostaglandins, are spatiotemporally expressed during pregnancy (Lim et al., 1997). In mice, *Cox1* (*Ptgs1*) is expressed in the epithelium early on day 4, suggesting that it has a role in generalized uterine edema and may participate in luminal closure for blastocyst apposition. *Cox2* (*Ptgs2*) is induced in the LE and underlying stroma at embryonic attachment sites, signifying that it likely has roles in attachment and localized endometrial vascular permeability. Moreover, *Ptgs2*^{-/-} mice show implantation

failure although genetic background-dependent compensation by *Ptgs1* can partially rescue implantation (Lim et al., 1997). A role for Cox2 in implantation, by activating uterine peroxisome proliferator-activated receptor- δ (PPAR- δ) and retinoid X receptor, has also been described (Lim et al., 1999a). While maternal PPAR- δ is crucial for implantation and decidualization, embryonic PPAR- δ is required for placentation (Wang et al., 2007). Upon attachment, *Ptgs2* localizes to the antimesometrial decidua, but by day 6 of pregnancy, it displaces to the opposite (mesometrial) side (Lim et al., 1997, Lim et al., 1999a). *Ptgs2*^{-/-} females also show defective ovulation, fertilization, decidualization, and placentation, thus highlighting the roles of Cox2-derived prostaglandin signaling at several stages of pregnancy. In addition, epithelial sodium channels must be activated to induce Cox2 at the implantation stage (Ruan et al., 2012).

1.6 Non-coding sequences in maternal-fetal crosstalk: special insights into the role of microRNAs in implantation

Regulation of numerous key biological processes depends not only on classic transcriptional mechanisms, but also on other regulatory phenomena such as epigenetic mechanisms (Wilkins-Haug, 2009). These mechanisms include DNA methylation and post-translational histone modifications, as well as regulation by small noncoding RNAs. The latter includes microRNAs (miRNAs), small RNA fragments that do not encode proteins but rather, post-transcriptionally regulate many gene targets (Ambros, 2001, Maccani and Marsit, 2009, Wilkins-Haug, 2009, Morales Prieto and Markert, 2011).

1.6.1 MicroRNA biogenesis

Mature miRNAs are non-coding RNA molecules about 22-25 nucleotides (nt) long that regulate up to hundreds of mRNA targets through perfect or imperfect complementation with the 3' untranslated regions (UTRs) of their target transcripts. They usually promote degradation or translation-inhibition events,

although instances of miRNAs inducing mRNA or protein expression have also been documented (Mehta and Baltimore, 2016). miRNA function can be influenced by interactions with RNA-binding proteins or sequestration by endogenous sponges, such as competing RNAs (Mehta and Baltimore, 2016). miRNA transcription normally occurs in the cell nucleus via the action of RNA polymerase II (Lee et al., 2004b) or RNA polymerase III (Borchert et al., 2006). These pri-miRNAs can then be processed by canonical or non-canonical pathways.

In the canonical pathway, pri-miRNAs are recognized and cleaved by the microprocessor complex comprising DROSHA (Drosha Ribonuclease III) and its cofactor DGCR8 (DiGeorge syndrome critical region 8) to produce a 70-nt hairpin molecule referred to as precursor miRNA (pre-miRNA). The non-canonical pathway acts in a DROSHA/DGCR8-independent manner: pri-miRNAs are processed via other endonucleases or by direct transcription into short hairpins in the nucleus, to form their respective pre-miRNAs (Abdelfattah et al., 2014, Liu et al., 2016). Both the canonical and non-canonical pathways merge with the production of these pre-miRNAs, which are then transported into the cytoplasm by Exportin 5 (Winter et al., 2009) where it is cleaved into a double-stranded RNA duplex by the enzyme DICER (Ha and Kim, 2014). A single strand of this duplex is subsequently incorporated into the RNA-induced silencing complex (RISC; He and Hannon, 2004) where it serves as a template for binding to mRNA targets. Thus, throughout an interaction with the RISC, each miRNA can pair with several 3'UTR targets and this is usually mediated by a 6–8 nt seed sequence at the 5' end of the miRNA (Friedman et al., 2009, Agarwal et al., 2015; **Figure 1.6**).

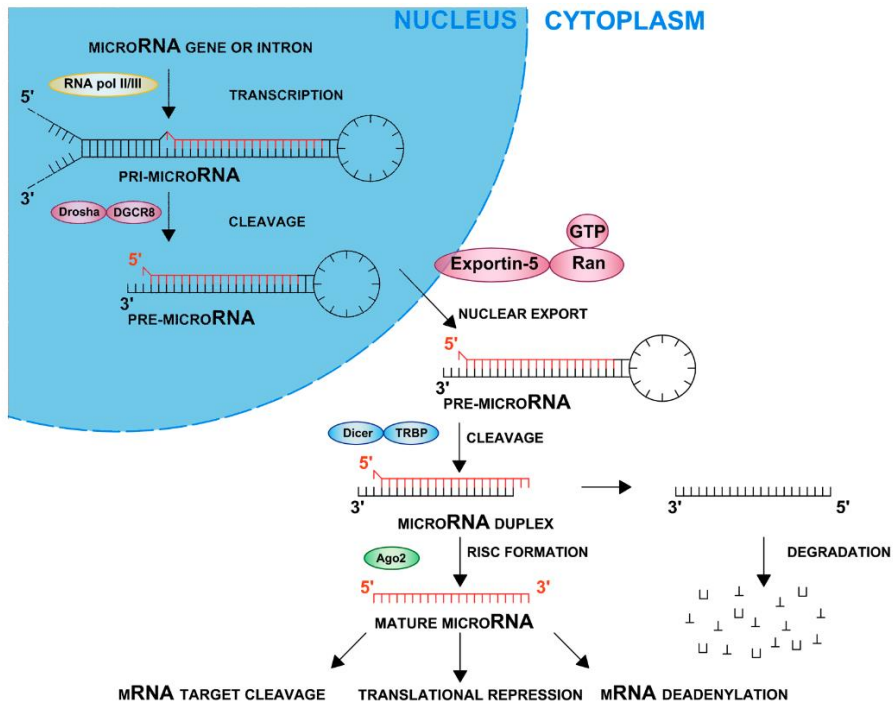


Figure 1.6. Schematic representation of the canonical miRNA processing pathway (Adapted from (Winter et al., 2009).

1.6.2 MicroRNAs as regulatory elements of endometrial receptivity

miRNAs are essential regulators of gene expression in fetal and maternal tissues following conception and over the course of pregnancy. Moreover, a broad range of miRNAs appear to be linked with endometrial receptivity, implantation, placental function, and parturition in both mice and humans (Bidarimath et al., 2014). The existence of differential miRNA expression patterns in EECs throughout the menstrual cycle has been described (Kuokkanen et al., 2010), suggesting that some miRNAs could be hormonally regulated in the human endometrium. Furthermore, 13 differentially-expressed miRNAs (including miR-23b, miR-145, miR-27b, and miR-195) were identified in endometrial samples from patients with recurrent implantation failure (RIF) when compared with women with normal fertility (Revel et al., 2011). This allowed the identification of a set of 23

downregulated genes with biological functions in adherens junctions, Wnt signaling, p53 signaling, the cell cycle, cell adhesion molecules, and cancer pathways, all of which are considered crucial in the implantation process.

Additionally, they observed a link between the downregulation of ER α expression in vitro and the upregulation of miR-145, an event that led them to consider targeting miR-145 as a therapeutic option for these patients. Following the same line of research, Sha and co-workers (Sha et al., 2011) designed a clinical study in which proposed miRNAs as potential biomarkers for human endometrial receptivity. Using a deep sequencing approach, they compared miRNA expression profiles between a pre-receptive (LH + 2) and a receptive (LH + 7) state in both natural and stimulated cycles. In natural cycles, they found 8 upregulated miRNAs and 12 downregulated miRNAs in LH + 7 compared to LH + 2. Bioinformatic analysis revealed that these miRNAs target a set of genes that are differentially-expressed during the WOI. Most recently, Altmäe et al. identified 4 miRNAs (miR-30b, miR-30d, miR-494, and miR-923) that are specifically regulated in receptive endometrium at the time of implantation (Altmäe et al., 2013): miR-30b and miR-30d were upregulated while miR-494 and miR-923 were downregulated in receptive endometrium. These results are consistent with those of Sha et al., who found that miR-30b and miR-30d are upregulated in non-stimulated LH + 7 versus LH + 2 in the endometria of infertile women (Sha et al., 2011). Another study highlighted the importance of miR-30d, after demonstrating that it is downregulated in decidualized stromal cells versus non-decidualized cells (Qian et al., 2009). Finally, bioinformatic analyses revealed that several signaling pathways, including WNT, axon guidance, ERK/MAPK, *TGF β* , *p53*, and leukocyte extravasation, are regulated by these microRNAs, confirming their indispensable role in successful blastocyst implantation.

1.6.3 Models of extracellular microRNA transport

Because they can be easily transferred between cells and they execute essential roles in many cellular processes, miRNAs are extremely useful for studying the regulation of cell-cell communication (Valadi et al., 2007). Their structure, size, and transportability allow them to remain stable in multiple biological fluids (Larrea et al., 2016, Turchinovich et al., 2013) and to survive some extremely adverse biological conditions including low pH, boiling, and freezing (Pieters et al., 2015). Thus, miRNAs have been identified in most body fluids, including saliva (Park et al., 2009), urine (Hanke et al., 2010), plasma (Mitchell et al., 2008, Chen et al., 2008), serum (Chen et al., 2008), blood, tears, amniotic fluid, colostrum, breast milk, bronchial lavage, cerebrospinal fluid, peritoneal fluid, pleural fluid, and seminal, follicular (Santonocito et al., 2014, Sohel et al., 2013), and uterine fluids (Burns et al., 2014). The presence of miRNAs in these latter reproductive fluids demonstrates that they are present as circulating factors capable of relocation throughout reproductive systems.

Extracellular miRNAs can be transported by both high and low-density lipoproteins (HDLs and LDLs; Vickers et al., 2011, Michell and Vickers, 2016) or bound to other proteins such as argonaute2 (AGO2; Turchinovich et al., 2011, Arroyo et al., 2011) and nucleophosmin1 (NPM1; Wang et al., 2010). However, one of their most novel distribution methods is mediated by extracellular vesicles (EVs) such as apoptotic bodies (Zernecke et al., 2009), microvesicles (MVs; Hunter et al., 2008), and exosome-like vesicles (Raposo and Stoorvogel, 2013) which protect them from degradation and contribute to their stability within fluids (Pieters et al., 2015); thus, these miRNAs have been extensively studied. EV is considered a generic term because it includes MVs (50–1,000 nm in diameter), exosomes (40–100 nm in diameter), and apoptotic bodies (50–5,000 nm in diameter; Simpson et al., 2012). It appears that EVs can transport a wide range of selectively-packaged components. For instance, one study in macrophages and endothelial cells showed

that miRNA sorting into EVs for heterotrophic cell communication is altered by the presence of both the miRNAs themselves, and of their respective miRNA target transcripts (Squadrito et al., 2014). In addition, the miRNA signature found in exosomes significantly differs from that detected in parent cells (Koppers-Lalic et al., 2014). It is also worth noting that miRNAs contain well-defined motifs, EXOmotifs, that direct miRNA allocation into exosomes prior to their delivery into recipient cells (Villarroya-Beltri et al., 2013).

A lot of published research has so far focused on elucidating the interplay between the miRNAs loaded into exosomes and the implantation success. In this regard, our group recently described a novel cell-to-cell communication mechanism involving delivery of endometrial miRNAs from the maternal endometrium to preimplantation embryo trophectoderm cells. We observed that both EV-associated and free miR-30d could be observed in B6C3-derived mouse embryos, found specific evidence that this results in the overexpression of genes involved in adhesion processes, including *Itga7* and *Cdh5* (**Figure 1.7**; Vilella et al., 2015). Furthermore, supplementation of murine embryos with miR-30d significantly improved embryo adhesion, suggesting that external miRNAs may play a functional role as transcriptomic modifiers in preimplantation embryos. Profiling miRNA expression in endometrial fluid revealed that maternally-derived miRNAs are present in EVs in the uterine microenvironment. However, although the internalization of maternally-derived exosomes was visualized, the mechanism(s) by which embryos take external miRNAs in remain unknown.

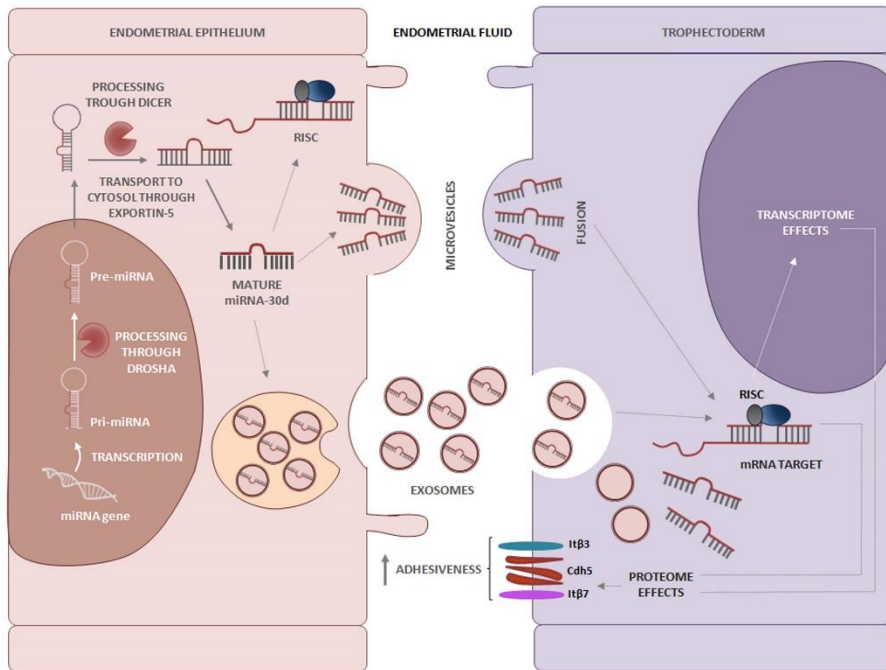


Figure 1.7: Schematic of a novel maternal-fetal cross-talk mechanism promoted by hsa-miR-30d. Hsa-miR-30d is delivered to the EF from the maternal endometrium, modifying the embryo transcriptome and its adhesive phenotype.

Likewise, Ng et al. examined the release of exosomes from endometrial epithelial cells (EECs) into the uterine cavity throughout the different stages of the menstrual cycle (Ng et al., 2013). Interestingly, they identified specific miRNA profiles within vesicles which were clearly distinct from those of EEC origin. Bioinformatic analyses showed that this unique miRNA signature has potential target genes that contribute to many Kyoto Encyclopedia of Genes and Genomes (KEGG) pathways, many of which are relevant to implantation; these included adherents junctions, ECM-receptor interactions, and VEGF, JAK-STAT, and toll-like receptor (TLR) signaling pathways. Another recent study describes how exosomes released from first-trimester placental mesenchymal stem cells (pMSCs) promote endothelial cell migration and vascular tube formation in vitro (Salomon et al., 2013b). Similarly, more cytotrophoblast-derived exosomes were found in the

presence of increased extravillous trophoblasts (EVTs) in vitro (Salomon et al., 2013a). This group also demonstrated that exosomes released from EVT's might play a role in remodeling spiral arteries by inducing vascular smooth muscle cell (VSMC) migration (Salomon et al., 2014).

Related to this, molecular characterization of trophoblast-derived exosomes highlighted the presence of immunomodulatory proteins such as fibronectin and syncytin, Wnt/ β -catenin-related molecules, galectin-3, HLA-G, bioactive lipid compounds (immunosuppressive PGE2 and the PPAR γ ligand, 15d-PGJ2), and miRNAs (Record et al., 2014). This molecular profile suggests that exosomes may promote intercellular fusion and syncytiotrophoblast formation. On the other hand, syncytiotrophoblast-derived microvesicles have pro-inflammatory, anti-endothelial, and procoagulant effects that appear to be involved in preeclampsia (Redman et al., 2012). Specifically, isolated human placental exosomes carry NKG2D ligands, ULBPs (ULBP1-5), and MIC proteins on their surface which allows them to induce NKG2D (natural-killer group 2, member D) receptor downregulation on natural killer (NK), CD8(+), and gamma delta T cells (Hedlund et al., 2009). Moreover, bioactive FasL- and TRAIL-carrying exosomes capable of triggering apoptosis are secreted by the placenta and are responsible for its immunomodulatory and protective role in humans (Stenqvist et al., 2013).

Embryo-derived exosomes may also be important biomarkers. A study examining the embryo-culture supernatant from 239 embryos (from 18 couples; on day 3 [n = 148] and day 5 [n = 91]) by nanoparticle tracking analysis (NTA) following routine clinical morphological grading showed a strong correlation between median-sized EVs and the embryo development stage at days 3 and 5 ($r_{1/4}$ 0.50, $p = 0.0001$). In addition, there was a reduction in the embryo quality attained as the median EV-size increased (202 nm = good, 218 nm = average, 222 nm = poor, and 227 nm = slow development; $p = 0.004$). Moreover, DNA was detected inside the EVs, which could soon allow the implementation of a non-invasive method for

assessing embryo quality and implantation ability, and thus, offer an alternative to current invasive prenatal diagnosis techniques such as preimplantation genetic testing for aneuploidies (PGT-A; Saadeldin et al., 2015). Given these promising results, elucidating the regulation and function of exosomes in the uterine cavity will improve our understanding of the early embryo-maternal dialogue and could potentially impact our perception of infertility and IVF success rates.

Saadeldin et al. showed that the addition of exosomes isolated from conditioned medium from parthenogenetic embryos could increase the developmental competence of cloned embryos (Saadeldin et al., 2014). However, whether this influence is attributable to the proteins, lipids, or miRNAs present in these exosomes remains to be clarified. Nonetheless, this study provides evidence that a dynamic microenvironment or niche exists among cultured embryos and highlights the advantages of continuous miRNA transfer via exosomes over the 'bulk' transfer via conditioned medium. In any case, it would be interesting to exosome-encapsulate proteins with possible autocrine functions and add these to the culture medium of preimplantation embryos and compare these results with the addition of these proteins alone. This approach may contribute to the development of new synthetic media for embryo production and may improve embryo development and viability rates (Calkins and Devaskar, 2011).

1.6.4 Embryo-maternal crosstalk: the role exerted by microRNAs

As previously stated, implantation is a complex process requiring the synchronous development of a viable embryo and a receptive endometrium. miRNAs act as important gene expression regulators, modulating important events during the gestation period such as embryo development, endometrial function, and maternal-embryo communication. Recent verification of several functional extracellular miRNAs may help to improve implantation outcomes in terms of (1) improving our knowledge of mechanisms of intercellular communication mediated by extracellular miRNAs; (2) using extracellular miRNAs as effective biomarkers in

IVF embryo transfers for detecting embryo quality, endometrium receptivity, and the implantation prognosis. The following tables summarize the publications that describe the maternal-fetal communication roles exerted by several miRNAs and recapitulate our current knowledge of maternal-origin and embryonic-origin intracellular, extracellular, or freely-circulating miRNAs.

Table 1.1. Maternal-origin intracellular miRNAs reported in the scientific literature.

MATERNAL-ORIGIN INTRACELLULAR miRNAs				
miRNA	Population	Expression	Described Functions	References
miR-30b	Human	LH+7 ▲	Cyclic remodeling of the endometrium. The level of the endometrial miR-30b on the day of hCG administration in assisted reproduction treatment is low in women with elevated progesterone levels: a situation associated with a poor prognosis.	<i>Altmae et al., 2013; Li et al., 2011</i>
miR-30d	Human	LH+7 ▲	Promotes the overexpression of the adhesion molecules CDH5, ITA7, and ITB3 in the trophoctoderm of murine embryos during the WOI, thus favouring the initial stages of implantation.	<i>Vilella et al., 2015; Altmae et al; 2013</i>
miR-494	Human	LH+7 ▲	Cyclic remodeling of the endometrium.	<i>Altmae et al; 2013</i>
miR-181	Mouse	Day 4 ▼	Impairs implantation by lowering LIF expression.	<i>Chu et al; 2015</i>
miR-223-3p	Mouse	Day 4 ▲	Reduces the formation of pinopodes on the surface of the epithelium where the embryo will attach.	<i>Dong et al., 2016</i>
miR-199a	Mouse	Day 4,5 ▲	Downregulates the expression of <i>Muc-1</i> during the WOI.	<i>Inyawilert et al., 2014</i>
let-7a	Mouse	Day 4 ▲	Decreases the expression of <i>Muc-1</i> during the WOI.	<i>Inyawilert et al., 2015</i>
let 7b	Mouse	Day 4 ▲	Decreases the expression of <i>Muc-1</i> during the WOI.	<i>Inyawilert et al., 2015</i>
miR-145	In vitro/Human	WOI ▲	Supresses embryo-epithelial juxtacrine communication at implantation by modulating maternal IGF1R. Elevation of miR-145 has been shown in the endometrium of RIF patients.	<i>Li et al., 2015</i>
miR-200 family	In vitro and human studies	▲	Plays a critical role in the supression of epithelial-mesenchimal transition (EMT).	<i>O'Brien et al., 2018</i>
miR-429	Mouse	Day 4 ▲	Mediates the supression of the migratory and invasive capacities of cells, probably by targeting protocadherin 8 (Pcdh8), leading to reduced implantation site size.	<i>Li et al., 2015</i>

Table 1.1 (Cont). Maternal-origin intracellular miRNAs reported in the scientific literature.

MATERNAL-ORIGIN INTRACELLULAR miRNAs				
miRNA	Population	Expression	Described Functions	References
miR-126-3p	Mouse	Day 4 ▲	Promotes cell migratory and invasive capacity by regulating the expression of ITA11. Loss of function of miR-126-3p results in a significant reduction in the implantation sites in vivo.	Zhengyu et al., 2015
miR-125b	Human /Mouse	WOI ▲	Inhibits the cell movement and impedes implantation by targeting MMP26, which is involved in cellular matrix degradation.	Chen et al., 2016
miR-96	Mouse	Day 4 ▲	Promotes the apoptosis of stromal and decidual cells by regulating the anti-apoptotic factor Bcl-2.	Yang et al., 2017
miR-181-a	Mouse	Day 4 ▲	Stimulates the expression of hESC decidualization-related genes (i.e. <i>FOXO1A</i> , <i>PRL</i> , <i>IGFBP-1</i> , <i>DCN</i> , <i>TIMP3</i>) and induces morphological transformation.	Zhang et al., 2015
miR-222	Human	In vitro Decidualization ▼	Participates in ESC differentiation by regulating ESCs, terminally withdrawing from the cell cycle, partly by permitting <i>CDKN1C/p57</i> expression.	Qian et al., 2009
miR-200a	Mouse	Day 4 ▼	Facilitates the expression of PTEN, which in turn influences cell proliferation and apoptosis during decidualization.	Shen et al., 2013
miR-141	Mouse	Day 4 ▼	Might influence cell proliferation and apoptosis in the endometrium by negatively regulating PTEN expression; could also influence the number of embryo implantation sites.	Liu et al., 2013
miR29b, miR-29c, miR-30b, miR-30d, miR-31; miR-193a-3p, miR-203, miR-204, miR-200c, miR-210, miR-582-5p, miR-345	Human	LH+7 ▲	Bioinformatic analysis reveals that the conjunction of these miRNAs target many genes involved in the cell cycle, thereby suppressing cell proliferation.	Kuokannen et al., 2010
miR-145; miR-23b, miR-99	Human	Secretory phase ▲	Appears to be overexpressed in RIF patients. Predicted analysis relates these miRNAs with biological functions in adherens junctions, Wnt signaling, p53, the cell cycle, cell adhesion molecules, and cancer pathways.	Revel et al., 2011

Table 1.2. Extracellular and circulating miRNAs reported in the scientific literature.

EXTRACELLULAR AND CIRCULATING miRNAs				
	Population	Location	Described Functions	References
miR-200c, miR-17, miR-106 (and more)	Human	Endometrial Evs (EF)	Bioinformatic analysis showed that exosome/MVs-specific miRNAs have potential targets in biological pathways which are highly relevant for embryo implantation, including adherens junctions, ECM-receptor interactions, VEGF, JAK-STAT, and TLR signaling pathways.	<i>Ng et al., 2013</i>
miR-423	Ewes	Endometrial Evs (EF)	Present specifically in the Evs secreted from pregnant ewes. Thought to target genes associated with metabolism, immune system, cell cycle, and apoptosis.	<i>Burns et al., 2014</i>
miR-30d	Human	Endometrial Evs (EF)	Promotes the overexpression of the adhesion molecules CDH5, ITA7, and ITB3 in the trophoctoderm of murine embryos during the WOI, thus favouring the initial stages of implantation.	<i>Vilella et al., 2015</i>
miR-517a, miR-21	Human	Placenta EVs (serum plasma)	Strong evidence that placenta-derived miRNAs are transferred into maternal circulation in an exosome-mediated manner. Proteins regulated by miR517a overexpression may be involved in TNF-signaling mediated events.	<i>Luo et al., 2009</i>
miR-515-3p, miR-517a, miR-517c, miR-518b, miR-526b and miR-323-3p.	Human	Placenta EVs (serum plasma)	21 of 24 genes encoding pregnancy-associated miRNAs present in plasma were clustered on 19q13.42 or 14q3, critical regions for placental growth and embryonic development.	<i>Miura et al., 2010</i>
miR-517a, miR-519b, miR-525-3p.	Human	Serum plasma	Patients with ectopic pregnancies or spontaneous abortions had lower serum concentrations of these miRNAs than women with viable intrauterine pregnancies.	<i>Zhao et al., 2012</i>
miR-31	Human	Serum plasma ▲	Downregulation of immune related genes such as FOXP3 and CXCL12, suggesting this miRNA could play a role in regulating the immune system during implantation.	<i>Kresowski et al., 2014</i>

Table 1.2 (Cont). Extracellular and circulating miRNAs reported in the scientific literature.

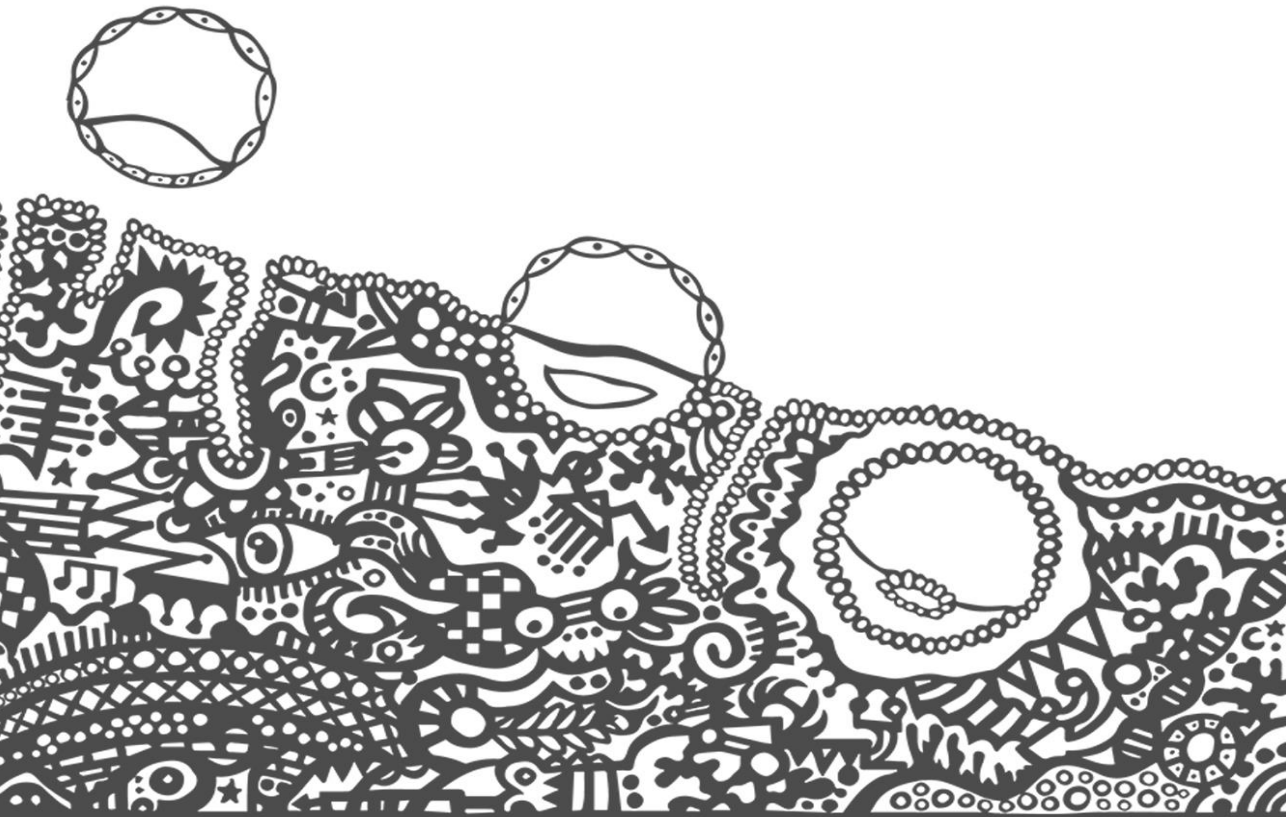
EXTRACELLULAR AND CIRCULATING miRNAs				
	Population	Location	Described Functions	References
miR-26	Cow	Serum Plasma ▲	Concentration of miR-26 was higher in the serum plasma from pregnant heifers on day 16 of pregnancy and the concentration of this miRNA increased from day 16 to day 24, suggesting that miR-26 is a potential marker for early pregnancy in cows.	<i>Ioannidis et al., 2016</i>
miR-25, miR-16a/b and miR-3596	Cow	Circulating EV	These miRNAs differentiate between successful implantation and embryonic mortality at the early stage of pregnancy: their expression is higher in the embryo mortality group compared to pregnant and control groups and thus, can potentially differentiate pregnancy status.	<i>Pohler et al., 2017</i>
miR-767-5p, miR-30c, miR-323-5p	Mare	Circulating EV	Main miRNAs identified in targeted focal adhesion molecules. Evidence suggesting that serum exosomes contain different miRNAs depending on pregnancy status, and may affect mRNA expression related to the endometrial focal adhesion pathway, with a potential role in maternal pregnancy recognition.	<i>Klöhnatz et al., 2016</i>
miR-181a2; miR-196a2; miR-302c; miR-25	Bovine	Embryo culture media	These miRNAs were present in higher levels in degenerate embryos.	<i>Kropp et al., 2014</i>
miR-24	Bovine	Embryo culture media	Using a deep sequencing approach, this miRNA was confirmed to be present in the culture media of degenerate embryos. Adding miR-24 to the culture media of normal morulas significantly reduced the embryo development rate, partly by inhibiting <i>CDKN1b</i> , a cell cycle inhibitor.	<i>Kropp and Khatib; 2015</i>
miR-372, miR-191	Human	Embryo culture media	The expression of these miRNAs in human embryo culture media is associated with IVF implantation failure. Interestingly, miR-191 was present in the culture media of aneuploid embryos, indicating the possible role of this miRNA as a biomarker of embryo aneuploidy.	<i>Rosenbluth et al., 2014</i>
miR-20a, miR-30c	Human	Embryo culture media	The presence of these miRNAs was significantly higher in the culture media of implanted blastocysts compared to those that lead to implantation failure. The target genes of these miRNAs (<i>PTEN, NRAS, MAPK1, APC, KRAS, PIK3CD, SOS1</i>) have predicted roles in endometrial cell proliferation, hence, embryo-derived miRNAs may modulate uterine functions.	<i>Capalbo et al., 2016</i>

Table 1.3 Embryo-derived miRNAs reported in the scientific literature.

EMBRYO-DERIVED miRNAs				
miRNA	Population	Expression	Described Functions	References
miR-661	Human	Secreted from human blastocysts	miR-661 is present in significantly higher amounts in culture media from blastocysts that failed to implant than those that implanted successfully. Elevated miR-661 expression inhibited trophoblast cell spheroid attachment to human EECs, partly via PVRL1, a membrane-bound immunoglobulin-like cell adhesion molecule.	<i>Cuman et al., 2015</i>
miR-22, miR-320a	Bovine	Supplemented to EEC	Induces overexpression of the progesterone receptor transcript in EECs, suggesting that these miRNAs can positively upregulate expression via direct or indirect mechanisms.	<i>Gross et al., 2017</i>
miR-125, miR-16	Sow	Embryo-derived Evs	Present in the uterine fluid of pregnant sows; their predicted mRNA targets play roles in pathways regulating pregnancy-related growth factors, receptors, and cytokines, and so they may influence the molecular mechanisms of implantation.	<i>Krawczynsky et al., 2015</i>
Broad range of miRNAs	Sheep	Embryo-derived Evs	Fluorescently-labelled embryo-derived Evs infused into the uterine horns were present in the cytoplasm of the uterine LE and GE suggesting that these miRNAs originated from embryos and can be acquired by uterine cells, thus modulating maternal gene expression.	<i>Burns et al., 2016</i>

Given the pleiotropic effects of miRNAs, defining the specific role of any miRNA entails certain difficulties. Most experiments of this type are performed at the cellular level *in vitro*, although some researchers have made attempts to study miRNAs *in vivo* by injecting miRNA mimics or inhibitors. However, because these experiments only provide limited data on specific miRNAs, additional investigation will be required to gain a comprehensive understanding of miRNA regulation. Furthermore, extracellular miRNAs represent a promising line of future investigation for developing high-quality non-invasive biomarkers because they are stable, sensitive to their bio-environment, can be accessed non-invasively, and are specifically associated with physiological and pathological conditions.

HYPOTHESIS



02 | HYPOTHESIS

Blocking maternal miR-30d transfer in vitro reduces the implantation rates of B6C3F1/CrI murine embryos by downregulating certain trophoctoderm cell adhesion molecules. Here, we propose that the in vivo bi-directional communication established between the mother and embryo in a miR-30d KO murine model impacts implantation and/or fetal development depending on its maternal or embryonic origin.

OBJECTIVES



03 | OBJECTIVES

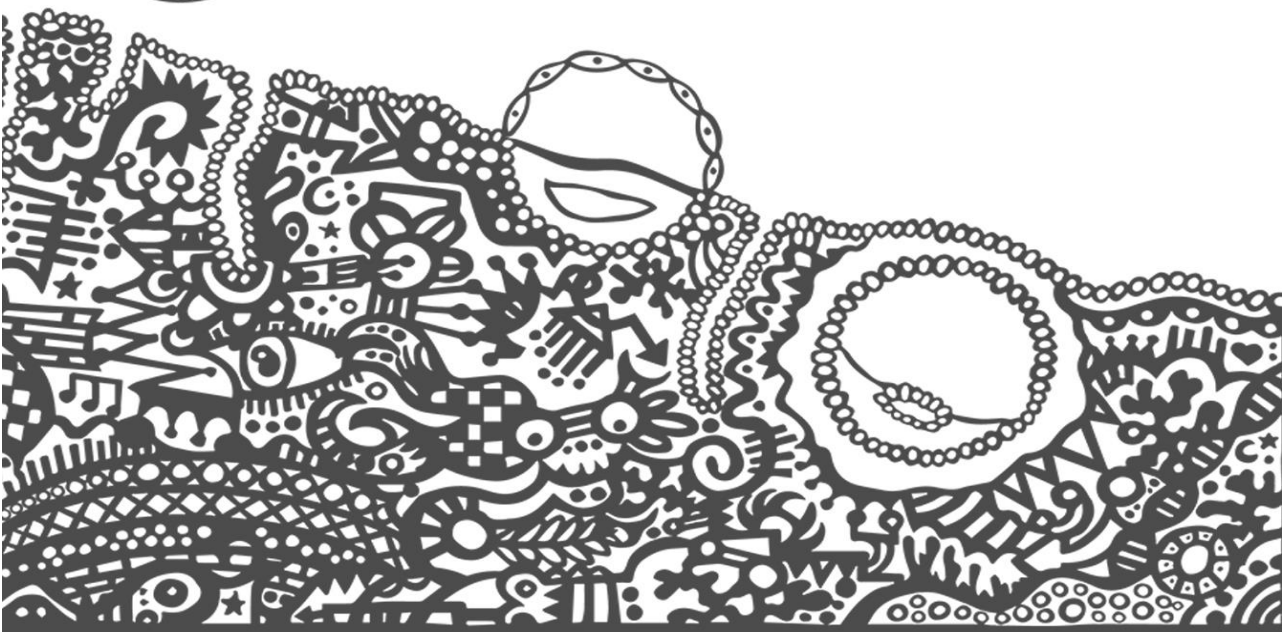
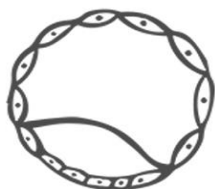
3.1 General objectives

- To determine the mechanism by which miR-30d is incorporated into the extracellular vesicles secreted by the maternal endometrium.
- To investigate the impact of maternal or embryonic-origin miR-30d deficiency on implantation and subsequent fetal development.

3.2 Specific objectives

- To identify the protein responsible for directing miR-30d upload from the cytosol to the inner cavity of exosomes before their transfer to preimplantation embryos.
- To determine how the maternal-fetal crosstalk established in the wild-type (WT) and miR-30d knockout (KO) genotypes affects implantation success rates and thus, define the extent to which the maternal niche and the embryo influence the acquisition of a favorable implantation phenotype.
- To study the impact of miR-30d deficiency on the implantation phenotype and pregnancy outcome in physiological conditions.

MATERIALS AND METHODS



04 | MATERIALS AND METHODS

4.1. Murine model and housing conditions

Mice lacking miR-30d were produced at the Jackson laboratories from the MirC26tm1Mtm/Mmjax strain using C57BL/6, Fvb, and 192P2 as a background. Matured mice were caged in a controlled environment with a 14L:10D cycle. All animal procedures were revised by the Ethics Commission on Experimental Research at the University of Valencia and approved by the Spanish Government Ministry of Agriculture, Livestock, and Fisheries. Research from two projects involving animal research is described in this thesis: (1) “Role of miR-30d in embryo adhesion” (Code: 2016/VSC/PEA/00140); (2) “Analysis of miR-30d in endometrial receptivity” (Code:2017/VSC/PEA/00005). To confirm the reproducibility of the results, at least three mice per group were used in each stage of treatment in this study.

4.2 Recovery of preimplantation mouse embryos

Female mice aged 6–8 weeks, were primed to ovulate by administering 10 IU of pregnant mare serum gonadotropin (Sigma-Aldrich, St. Louis, Mi, USA), followed by 10 IU of human chorionic gonadotropin 48 h later (Sigma-Aldrich, St. Louis, Mi, USA). Females were housed overnight (o/n) with male studs and examined the following morning for the presence of a vaginal plug (this was considered day 1 of pregnancy). On embryonic day (E) E1.5 of pregnancy, the mice were euthanized by cervical dislocation and the embryos were flushed from the oviduct with PBS (Life Technologies, Waltham, MA, USA) using a 30-gauge blunt needle. Embryos were then washed three times with fresh G2™ Plus medium (Vitrolife, Göteborg, Sweden). After washing, the embryos were incubated at 37°C with 5% CO₂ in G2™ Plus medium for 72 h until they reached a blastocyst stage.

4.3 Human endometrial epithelial cell isolation and primary culture

4.3.1 Endometrial biopsy collection

Endometrial biopsies were obtained at day LH+0 from healthy donors (aged 18–35 y). Patients diagnosed with endometriosis and endometritis were excluded. All patients signed their informed consent before sample collection; the procedures were approved by the local Ethical Committee at IVI Valencia, Spain (code: 138-FIVI-127-FV).

4.3.2. Isolation and primary culture of human endometrial epithelial cells

Endometrial samples were processed to separate the epithelial and stromal fractions by collagenase digestion and gravity sedimentation, as previously described (Simón et al., 1997). Briefly, endometrial biopsies were initially cleansed of blood and mucus in a 60 mm Petri dishes containing 1 mL of PBS (Sigma-Aldrich, Madrid, Spain). Next, the tissue was mechanically disaggregated with blades to obtain smaller fragments approximately 1 mm³. The resulting pieces were subjected to mild collagenase digestion with type IA-collagenase (Sigma-Aldrich, St Louis, Mi, USA) diluted in 10 mL DMEM (Gibco®, Thermo Fisher Scientific, Waltham, Ma, USA) to reach a final concentration of 10 mg/mL and the mixture was incubated o/n at 4°C. After this digestion, the tissue was allowed to settle by gravity at room temperature (RT) for 10 min. The supernatant containing the stromal fraction was removed and the remaining pellet, holding the epithelial fraction, was washed three times with 10 mL of DMEM (Gibco®, Thermo Fisher Scientific, Waltham, Ma, USA) for 10 min. Following these washes, the pelleted cells were diluted with 5 mL of DMEM (Gibco®, Thermo Fisher Scientific, Waltham, Ma, USA) and added to a 25 cm² flask for 20 min at 37°C with 5% CO₂. After this, 3 mL of DMEM (Gibco®, Thermo Fisher Scientific, Waltham, Ma, USA) was added to the cell suspension and it was transferred to a new 25cm² flask which was incubated again for 20 min at 37°C with 5% CO₂. These incubations allowed us to

remove any stromal cells that persisted in the cell suspension. The cells were then centrifuged at 300 xg for 5 min and the resulting pellet was resuspended in EEC medium (75% DMEM [Gibco®, Thermo Fisher Scientific, Waltham, Ma, USA], 25% MCDB-105 [Gibco®, Thermo Fisher Scientific, Waltham, Ma, USA], 10% fetal bovine serum [FBS; Gibco®, Thermo Fisher Scientific, Waltham, Ma, USA], 220 µL insulin and 0.1% fungizone and gentamicin).

4.4 Endometrial sample collection in wild-type and miR-30d knockout mice

Uterine tissues were isolated from non-pregnant (day 0 [E0]) pseudopregnant (day 4 [E4]; 22:00 h and day 5 [E5]; 9:00 h), and pregnant (day 4 [E4]; 22:00 h and day 5 [E5] 9:00 h) WT and miR-30d KO females in which estrus had previously been synchronized (achieved by introducing sawdust from the males' cages into the females' cages). Three days after exposure to the males' sawdust, some females were euthanized by cervical dislocation to obtain the 'non-pregnancy' condition, while the others were housed o/n with male studs in a ratio of two females per male. Females who presented a vaginal plug (classified as day 1 of pregnancy or pseudopregnancy) were separated and sacrificed at day 4 or 5 of pseudopregnancy/pregnancy, as appropriate, to obtain uteri for RT-qPCR (n = 6 uteri per condition tested and per genotype analyzed; total uteri, WT: n = 18; KO: n = 18), immunofluorescence (n = 3 uteri per condition tested and per genotype analyzed; total uteri, WT: n = 9; KO: n = 9), and western blot (n = 6 uteri per condition tested and per genotype analyzed; total uteri, WT: n = 18; KO: n = 18) analyses. Uteri for RNA extraction were stored in 1.5 mL Eppendorf tubes containing an RNA stabilization reagent, RNALater (Qiagen, Hilden, Germany) until they were processed. Uteri for protein extraction were directly frozen at -80°C.

4.5 Exosome isolation from hEECs

Endometrial biopsies were obtained at day LH+0 from healthy 18 to 35-year old donors. Patients diagnosed with endometriosis and/or endometritis were excluded. All patients signed their informed consent prior to sample collection and these procedures were approved by the local Ethics Committee at IVI Valencia, Spain (code: 1308-FIVI-127-FV). Endometrial samples were processed to separate the epithelial and stromal fractions by collagenase digestion and gravity sedimentation, as previously described (Simón et al., 1997). When the cultures reached confluence, they were washed with DMEM (Gibco®, Thermo Fisher Scientific, Waltham, Ma, USA) to remove FBS-contaminated exosomes and then cultured in serum-depleted EEC medium (75% DMEM, 25% MCDB-105, 10%, 220 µL insulin, and 0.1% of fungizone and gentamicin). After 24 h, the conditioned medium was collected, and cells were incubated with hEEC medium without serum for a further 24 h. All the collected conditioned media were subjected to a series of differential centrifugations: (1) media were centrifuged at 300 xg for 10 min to pellet the residual cells; (2) the supernatants were centrifuged at 2,000 xg for 10 min; (3) the supernatants from step 2 were centrifuged at 10,000 xg for 30 min; (4) the supernatants from step 3 were passed through 0.22 µm-diameter filters (Acrodisc® syringe filters, Pall Corporation, Newquay Cornwall, UK) and the filtrate was then ultracentrifuged at 120,000 xg for 70 min using a P50AT4 Hitachi rotor. The resulting supernatants were kept as EV-negative controls; the step-4 pellets were washed by resuspending them in 1 mL PBS and centrifuging them again under the same conditions (120,000 xg for 70 min). The final pellet obtained contained the exosome-enriched fraction.

4.6 MicroRNA pull-down

Two biological samples of hEECs and a pool of exosomes obtained from the spent media of 4 hEEC primary cultures were subjected to a pull-down assay with biotinylated miR-30d. Briefly, the samples were isolated, resuspended in

400 μL of buffer 1 (TBS; pH 7.5, 0.5% NP-40, 2.5 mM MgCl_2 , 40 U/mL RNase inhibitor [Invitrogen, Carlsbad, CA, USA], and protease inhibitors [Complete, {Roche, Basel, Switzerland}]) and precleared by incubation with streptavidin-sepharose beads (GE Healthcare, Little Chalfont, UK) for 1.5 h at 4°C. Biotinylated (miR-30d)-[Biotin-CCCUCUUA-UGU AAA CAU CCC CGA CUG GAA G] or (poly-A)-[Biotin-CCCUCUU-AAA AAA AAA AAA AAA AAA AAA AA] (20 nmol; Thermo Fisher Scientific, Waltham, MA, USA) were resuspended in TBS with RNase inhibitor (40 U/mL; Invitrogen, Carlsbad, CA, USA,) and incubated with 40 μL streptavidin-sepharose beads for 4 h at 4°C. The beads were then washed twice with TBS and incubated with the protein lysates o/n at 4°C. Following this, the beads were washed 6 times in buffer 2 (TBS, 0.05% NP-40, RNase inhibitor, and protease inhibitors). Protein loading buffer (Fermentas, Waltham, MA, USA) was added and beads were heated at 90°C for 10 min before proteomics analysis. Figure 4.1 shows a schematic representation of the experimental procedure.

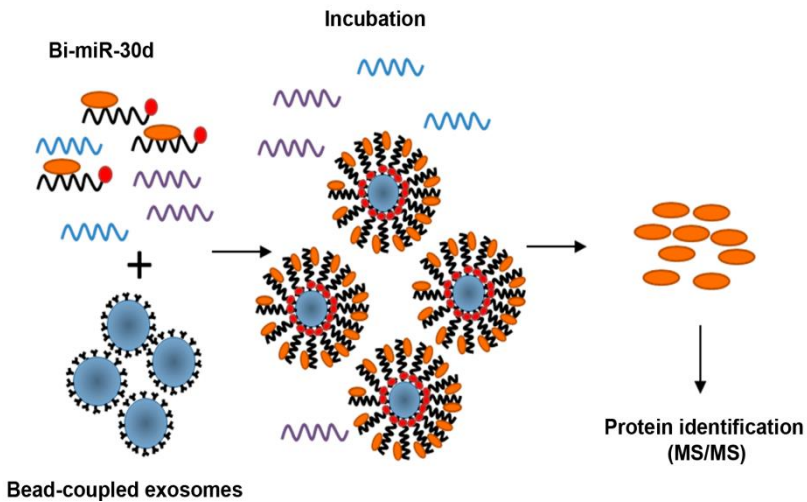


Figure 4.1. Schematic representation of the process followed to identify specific miR-30d-protein linkage. Exosome extracts and hEEC lysates were incubated with streptavidin beads coated with a biotinylated miR-30d. The proteins recovered were identified by tandem mass spectrometry (MS/MS).

4.7 Protein identification by tandem mass spectrometry

4.7.1 *In-gel protein digestion*

Samples were digested with 500 ng sequencing-grade trypsin (Promega, Madison, WI, USA), as described elsewhere (Shevchenko et al., 1996). Briefly, each slide was cut and small pieces approximately 1 mm² were transferred into 1.5 mL Eppendorf tubes. After washing them in 50 mM ammonium bicarbonate (ABC) diluted in water (pH 8; Sigma Aldrich, Madrid, Spain) the gel was dehydrated in acetonitrile (ACN; Fisher Scientific, Waltham, MA, USA), reduced with dithiothreitol (DTT; 10 mM in 50 mM ABC; 20 min at 60°C) and alkylated with iodoacetamide (IAM; 50 mM in 50 mM ABC; 30 min at RT in the dark). For protein digestion, 500 ng of trypsin in 200 µl of 50 mM ABC were added to each dried gel piece and digestion was set at 37°C o/n. The trypsin digestion was stopped with 10% trifluoroacetic acid (TFA) to 1% final concentration, and the supernatant, containing the extracted digests, was carefully removed, leaving behind the sliced gels in the Eppendorf tube. For additional peptide extraction, 200 µl of pure ACN were added to each tube and these were incubated for 15 min at 37°C in a shaker. The new supernatant containing the new peptide mixture was carefully withdrawn. Both supernatants were mixed in a tube and dried in a speed vacuum (ISS 110 SpeedVac System, Thermo Savant, Thermo Scientific, Langenselbold, Germany) for 20 min and re-suspended in 15 µl of 2% ACN and 0.1% TFA prior to liquid chromatography (LC) coupled with tandem mass spectrometry (MS/MS) analysis (LC-MS).

4.7.2 *Nano liquid-chromatography tandem mass-spectrometry analysis*

The peptides recovered from in-gel digestion processing were analyzed by LC using NanoLC Ultra 1-D plus Eksigent® equipment (Eksigent Technologies, Dublin, CA, USA) directly connected to an SCIEX TripleTOF 5600 mass spectrometer (SCIEX, Framingham, MA, USA) operated in direct-injection mode. Briefly, 5 µl from each digested sample were trapped on a NanoLC pre-column (3 µm particle-size C18-CL, 350 µm-diameter, 0.5 mm long; Eksigent) and desalted with 0.1% TFA at

3 $\mu\text{l}/\text{min}$ for 5 min. The digested peptides present in the samples were then separated using an analytical LC column (3 μm particle-size C18-CL, 75 μm -diameter, 12 cm long, Nikkyo Technos Co[®], Tokyo, Japan) equilibrated in 5% ACN and 0.1% formic acid (FA; Fisher Scientific, Waltham, MA, USA). The peptides were eluted from the column with a linear gradient of solvent B (from 5% to 40%) at a constant flow rate of 300 nL/min over 120 min. Solvent A was 0.1% FA in water and solvent B was 0.1% FA in ACN.

Eluted peptides were ionized by applying 2.8 kV to the spray emitter on an ESI NanoSpray III (SCIEX). The analysis was carried out in a data-dependent mode. Survey MS1 scans were acquired from 350–1250 m/z for 250 ms; the quadrupole resolution was set to 'UNIT' for MS2 experiments, which were acquired from 100–1500 m/z for 50 ms in 'high sensitivity' mode. The following dynamic selection criteria were used: charge: 2+ to 5+; minimum intensity; 70 counts per second (cps). Up to 50 ions were selected for fragmentation after each survey scan; the dynamic exclusion time was set to 15 s and the instrument automatically set the collision energy according to its rolling collision energy equations. The mass spectrometry proteomics data were deposited in the ProteomeXchange Consortium via the PRIDE (Vizcaíno et al., 2016) partner repository, with the dataset identifiers PXD008773 and 10.6019/PXD008773.

4.7.3 Protein identification

The MS/MS information was processed with a PARAGON algorithm via the Protein Pilot (v4.5) software (AB Sciex). Protein Pilot default parameters were used to generate the peak list directly from a TripleTOF 5600+ system. The algorithm was used to search ExPASy protein database according to the following parameters: 'trypsin specificity', 'Cys-alkylation', 'no taxonomy restriction', and a 'through search effort'. To avoid using the same spectral evidence for more than one protein, the identified proteins were grouped based on the MS/MS spectra produced by the Protein-Pilot Pro Group algorithm. A protein group in a Pro Group

report is a set of proteins that share some spectral evidence; unobserved regions of protein sequences play no role in explaining the data. False discovery rate (FDR) was calculated with the PSPEP algorithm in Protein Pilot (**see Supplementary files 1 to 6**).

4.8 Protein extraction

4.8.1 Protein extraction from endometrial epithelial cell lysates

hEECs used for exosome collection served as positive controls for western blot analysis. To obtain cellular lysates, cells were washed with PBS and frozen at -80°C for at least 1 h. They were then incubated with 1.5 mL of RIPA buffer (150 mM NaCl, 1% IGEPAL CA 630, 0.5% Na-DOC, 0.1% SDS, 0.5 M EDTA, 50 mM Tris-HCl; pH 8) with protease inhibitors (1% PMSF 0.1 M [Sigma-Aldrich, Madrid, Spain], 10% Roche mini complete [Roche, Basel, Switzerland]) for 10–15 min. Once lysis was completed, the supernatant was centrifuged at 13,000 $\times g$ for 15 min. The pellet obtained was discarded and the resulting supernatant frozen until use. The proteins were quantified using a Bradford assay. Briefly, 5 μL of protein extract was mixed with 200 μL of a Bradford solution (150 μL distilled water + 50 μL Bradford reagent [QuickStart™ Bradford 1 \times dye reagent; Bio-Rad, Hercules, CA, USA]) in a 96-well microplate. As a standard curve, 7 concentrations (2, 1.5, 1, 0.75, 0.5, 0.25, and 0.125 mg/mL) of bovine serum albumin (BSA; Sigma-Aldrich, St Louis, Mi, USA) were used. The resultant mixture was incubated at RT for at least 5 min. Absorbance reads were performed at 595 nm in a Multiskan Go plate reader (ThermoFisher Scientific, Waltham, Ma, USA); 6 \times reducing Laemmli SDS sample buffer (Alfa Aesar, Haverhill, MA, USA) was used as a loading buffer.

4.8.2. Protein extraction from human endometrial epithelial cell-derived exosomes

hEEC-derived exosomes were lysed in 200 μL of RIPA buffer containing protease inhibitors (1% PMSF 0.1 M [Sigma-Aldrich, Madrid, Spain], 10% Roche mini complete [Roche, Basel, Switzerland]) at 4°C for 30 min. Once lysis was

completed, the supernatant was centrifuged at 13,000 xg for 15 min. The pellet obtained was discarded and the resulting supernatant frozen until use; protein quantification was performed using a Bradford assay.

4.8.3. Protein extraction from uterine samples

Uteri were flash-frozen, cut into pieces, and disintegrated in 1 mL of lysis buffer (150 mM NaCl, 1% IGEPAL CA 630, 0.5% Na-DOC, 0.1% SDS, 0.5 M EDTA, 50 mM Tris-HCl; pH 8) with protease inhibitors (1% PMSF 0.1 M [Sigma-Aldrich, Madrid, Spain], 10% Roche mini complete [Roche, Basel, Switzerland]) in a TissueLyser LT device (Qiagen, Hilden, Germany). Samples were ground at 30 s intervals until complete disruption was accomplished (n = 6 uteri per condition tested and per genotype analyzed; total uteri, WT: n = 18, KO: n = 18). The supernatant and the remaining tissue was transferred into a clean 1.5 mL Eppendorf tube and allowed to incubate at 4°C for 1 h. The samples were then centrifuged at 10,000 xg for 30 min. The supernatant was recovered, and the protein extract was quantified using a Bradford assay.

4.9 Subcellular fractioning

hEEC subcellular compartments were fractionated with a Subcellular Proteome Extraction kit (Calbiochem, Burlington, MA, USA). The cytosol, membranous organelles, and nuclear fractions were blotted with hnRNPC1 (ab10294, Abcam, Cambridge, UK), the cytosolic marker, HSP70 (System biosciences, Palo Alto, CA, USA), the tetraspanin markers, CD81, CD63, and CD9 (System biosciences, Palo Alto, CA, USA), the membrane organelle marker, Calnexin (Enzo Life Sciences, Farmingdale, NY, USA), the nuclear marker, Histone 4 (ab10158, Abcam, Cambridge, UK), and the cytoskeletal marker, Actin (ab8227, Abcam, Cambridge, UK). Western blots of these subcellular fractions were performed twice, and representative images have been used in this thesis.

4.10 Western blot

The samples were first denatured by heating them at 95°C for 5 min. They were further analyzed by SDS-PAGE, followed by electroblotting onto PVDF membranes (Bio-Rad Laboratories, Hercules, CA, USA) that had been previously activated with methanol for 2 min. Transfer quality was checked by Ponceau red staining. The membranes were blocked by incubation with 5% skimmed milk diluted in 1% PBS with Tween (PBST) for 1 h at RT. The membranes were then incubated o/n with specific primary antibodies (1:1,000) diluted in 3% skimmed milk dissolved in 1% PBST according to the manufacturers' specifications; a list of the primary antibodies is summarized in table 4.1. After incubation, the membranes were washed 3 times with 1% PBST and then incubated with the secondary antibodies (Santa Cruz Biotechnology, Dallas, TX, USA) in 1% PBST (1:10,000). Finally, the target proteins were detected using a SuperSignal West Femto Chemiluminescent kit (Thermo Fisher Scientific, Waltham, MA, USA). Western blots of the whole lysates and exosomes were performed in triplicate; representative images are shown in this thesis.

Table 4.1. Antibodies used for western blot analysis, including details of the host, supplier, and dilutions used.

	ANTIGEN	NAME	HOST	REF	COMPANY	DILUTION
Primary antibodies	HNRNPC1	Heterogeneous Ribonucleoprotein C1	Mouse	ab10294	Abcam	1:1,000
	CYR61	Cysteine-Rich Angiogenic Inducer 61	Rabbit	ab24448	Abcam	1:1,000
	CD63	CD63 molecule	Rabbit	EXOAB-KIT-1	Systems Biosciences	1:1,000
	CD9	CD9 molecule	Rabbit	EXOAB-KIT-1	Systems Biosciences	1:1,000
	CD81	CD81 molecule	Rabbit	EXOAB-KIT-1	Systems Biosciences	1:1,000
	HSP70	Heat shock protein 70	Rabbit	EXOAB-KIT-1	Systems Biosciences	1:1,000
	HIS4	Histone 4	Rabbit	ab10158	Abcam	1:1,000
	ACTIN	Actin	Rabbit	ab82227	Abcam	1:1,000
	CALNEXIN	Calnexin	Rabbit	ADI-SPA-860D	Enzo Life Sciences	1:1,000
	COX2	Cytochrome C Oxidase Subunit II	Rabbit	ab1519	Abcam	1:1,000
	LIF	Leukemia Inhibitory factor	Rabbit	ab11362	Abcam	1:1,000
	MSX1	Msh homeobox 1	Rabbit	ab174207	Abcam	1:1,000
	MSX2	Msh homeobox 2	Rabbit	HPA005652	Sigma Aldrich	1:1,000
	ESR	Estrogen receptor	Rabbit	ab32063	Abcam	1:1,000
	PGR	Progesterone receptor	Mouse	8757	Cell signaling	1:1,000
Secondary antibodies	Anti-Mouse	Goat anti-mouse IgG-HRP	Goat	sc-2005	Santa Cruz Biotechnology	1:10,000
	Anti-rabbit	Goat anti-rabbit IgG-HRP	Goat	sc-2357	Santa Cruz Biotechnology	1:10,000

4.11 Immunofluorescence

4.11.1 Co-localization studies

hEECs were grown on μ -Slide 8-Well ibiTreat plates (ibidi GmbH, Planegg/Martinsried, Germany) until 50–70% confluent; they were then fixed with 4% paraformaldehyde for 15–20 min at RT. Two washes were performed with 1 \times TBST (20 mM Tris-HCl; pH 7.4, 0.15 mM NaCl, 0.05% Tween 20), permeabilized with 0.1% Triton X-100/PBS (Ca_2^+ , Mg_2^+) for 10 min at RT, and blocked with 4% normal goat serum for 30 min at RT; following this they were incubated o/n with a 1:50 dilution of primary antibodies against hnRNPC1 (ab10294, Abcam, Cambridge, UK) or CYR61 (ab24448, Abcam, Cambridge, UK) according to the manufacturers' instructions. The cells were washed 3 times before incubating them for 60 min with secondary antibodies; Alexa 488 and Alexa 555-labeled antibodies (5 $\mu\text{g}/\text{mL}$; Life Technologies, Molecular Probes, Eugene, OR, USA) were used to identify the proteins of interest, and exosomes were identified using CD63. The labeled cells were washed 3 times and then protein co-localization was visualized with a 60 \times water-immersion confocal microscope (FV1000, Olympus). Finally, the images were processed and assembled using Imaris software (Bitplane, Zurich, Switzerland). All co-localization studies were performed in triplicate, and representative images are presented in this thesis. For internal cellular immunofluorescence hnRNPC1 analysis, Nunc 146485 24-well plates (Waltham, MA, USA) were used with an IN-Cell Analyzer 2000; these IN-Cell analyses were performed in triplicate.

4.11.2 Study of key receptivity markers

Uterine tissues were isolated from non-pregnant (day 0 [E0]) pseudopregnant (day 4 [E4]; 22:00 h and day 5 [E5]; 9:00 h), and pregnant (day 4 [E4]; 22:00 h and day 5 [E5] 9:00 h) WT and miR-30d KO females ($n = 3$ uteri per condition tested and per genotype analyzed; total uteri, WT: $n = 9$; KO: $n = 9$), flash frozen, and stored in cryovials at -80°C . Cryosections (7 μm) were cut onto poly-L-lysine-coated slides, rehydrated with PBS, and fixed with 4% paraformaldehyde

(PFA) for 10 min. Permeation was performed with PBS-1% Triton X-100 for 10 min. Sections were blocked with a solution of 5% BSA, 0.05% Triton X-100, and 4% FBS diluted in PBS. Next, the cryosections were incubated o/n at 4°C in a humidified chamber with the following primary antibodies (detailed in table 4.1) COX2 (1 µg/mL), LIF (20 µg/mL), MSX-1 (1:200), ESR (1:200; Abcam, Cambridge, United Kingdom), MSX-2 (1:200; Sigma-Aldrich, St. Louis, Mi, USA), PGR (1:200; Cell Signaling Technology, Danvers, Ma, USA). Sections were washed 3 times with PBS-0.05% Triton X-100, and 0.1% BSA and incubated with goat anti-rabbit IgG (H+L) Superclonal™ secondary antibody with Alexa Fluor 555® (Thermo Fisher Scientific, Waltham, MA, USA) or goat anti-mouse IgG (H+L) Superclonal™ secondary antibody with Alexa Fluor 488® (Thermo Fisher Scientific, Waltham, MA, USA), as appropriate. Nuclei were stained with 4',6-diamidino-2-phenylindole (DAPI) solution (Thermo Fisher Scientific, Waltham, MA, USA). Aquatex® (Merck-Millipore, Billerica, MA, USA) was used as a mounting agent. Tissues from WT control and experimental KO uteri were processed on the same slide. Images were acquired with a 60× water immersion confocal microscope (FV1000, Olympus) and imaging processing was conducted by using Imaris software (Bitplane, Zurich, Switzerland). The fluorescence-intensity values (integrated density/area) were measured with ImageJ software (National Institute of Health [NIH], Bethesda, MD).

4.12 Flow cytometry analysis of exosome-coupled beads

Exosomes were obtained by ultracentrifugation, were resuspended in PBS, and coupled with 4 µm aldehyde-sulfate beads (Invitrogen, Carlsbad, CA, USA) o/n at RT with rotation. The exosome-coupled beads were then washed and blocked for 60 min at RT in 4% BSA diluted in PBS. For intracellular staining, bead-bound exosomes were permeabilized and fixed for 5 min at RT with 0.2% Triton X-100 and 2% formaldehyde diluted in PBS. These were then incubated with anti-hnRNPC1 (Abcam, Cambridge, UK) or anti-CD9 (System Biosciences, Palo Alto, CA, USA) for 1 h at 4°C, washed, and incubated with Alexa 488-goat-anti-mouse IgG (Invitrogen,

Carlsbad, CA, USA) for 30 min. Bead signals were acquired on a FACSCalibur flow cytometer (BD Biosciences, USA) and data were analyzed with FlowJo software (Tree Star). The negative controls were exosome-coupled beads incubated with the secondary antibody only. Fluorescent-activated cell sorting (FACS) was performed twice and a representative experiment is presented in this thesis.

4.13 Validation of the microRNA pull-down assay

4.13.1 Sample preparation

The Ishikawa endometrial carcinoma cell line purchased from Sigma Aldrich (Ref: 99040201) was used to validate the results obtained from the miRNA pull-down assay. Cells were grown in T-175 flasks until they reached confluence, using the following culture media: modified Eagle's medium (MEM; Sigma Aldrich, Madrid, Spain), 2 mM Glutamine, 1% non-essential amino acids (NEAAs), 5% FBS, 0.2% gentamycin, and 0.2% fungizone. Next, they were washed with DMEM (Gibco®, Thermo Fisher Scientific, Waltham, Ma, USA) to remove FBS-contaminated exosomes and then cultured in serum-depleted medium. After 24 h, the conditioned media from 5 T-175 flasks were collected and pooled, and the exosomes were isolated from it, as already described in section 4.5. Once the isolation was finished, exosomes were lysed in a buffer comprising: 25 mM Tris; pH 8, 150 mM NaCl, 2 mM MgCl₂, 0.5% NP-40, 5 mM DTT, protease inhibitors, and 40 U/mL RNase inhibitor (Invitrogen). The cell lysate was collected in the same way as described for obtaining the hEEC extract.

4.13.2 Immunoprecipitation

Protein G Dynabeads (50 µl per condition; Invitrogen, Carlsbad, CA, USA) were washed twice in buffer 3 (PBS with 0.01% Tween) and resuspended in 200 µl of buffer 3 containing 10 µg mouse anti-hnRNPA2B1 (Santa Cruz biotechnology, Dallas, TX, USA) or mouse anti-IgG control (Santa Cruz biotechnology, Dallas, TX, USA) and incubated o/n at 4°C. Isolated exosomes and cell lysates were incubated for 1 h at 4°C with non-conjugated Dynabeads (50 µl per condition). The

precleared lysates were incubated with 50 μ l of Ab-conjugated Dynabeads for 1.5 h at 4°C, then washed twice with buffer 4 (25 mM Tris; pH 8, 150 mM NaCl, 2 mM MgCl₂, 0.5% NP-40, 5 mM DTT, protease inhibitors, and 40 U/mL RNase inhibitor [Invitrogen, Carlsbad, CA, USA]), 3 times with buffer 5 (25 mM Tris; pH 8, 900 mM NaCl, 2 mM MgCl₂, 1% NP-40, 5 mM DTT, protease inhibitors, and 40 U/mL RNase inhibitor), transferred to clean tubes, and finally, washed with buffer 6 (25 mM Tris; pH 8, 150 mM NaCl, 2 mM MgCl₂, 0.05% NP-40, 5 mM DTT, protease inhibitors, and 40 U/mL RNase inhibitor). For quantitative polymerase chain reaction (qPCR) analysis, 700 μ l of QIAzol lysis reagent (Qiagen) were added and samples were vortexed; the miRNAs were then extracted using a miRNeasy kit, according to the manufacturer's instructions (Qiagen, Hilden, Germany).

4.13.3 MicroRNA extraction and quantitative PCR

Retro transcription and qPCR for miR-30d and miR-450 (used in this experiment to test for unspecific binding) were performed with miScript reverse transcription and miScript SYBR Green PCR kits (Qiagen, Hilden, Germany), respectively. To quantify the miRNA recovered from the immunoprecipitation, standard curves were created for each miRNA; this was achieved by retro-transcribing miR-30d (Ref: MSY0000245, Qiagen, Hilden, Germany) and miR-450 (Ref: MSY0001545, Qiagen, Hilden, Germany) mimics using the following primers for the qPCRs: (miR-450a-5p)-[5'-UUU UGC GAU GUG UUC CUA AUA U]; and (miR-30d)-[5'-UGU AAA CAU CCC CGA CUG GAA G]; the resulting products were then diluted to 0, 5, 15, 20, 25, 50, and 75 pM concentrations and used to construct the curves.

4.14 Silencing hnRNPC1 in the Ishikawa cell line

The Ishikawa endometrial carcinoma cell line was purchased from Sigma Aldrich (Ref: 99040201). These cells were grown in 24-well plates until they reached 70% confluence, using culture media comprising: MEM (Sigma Aldrich, Madrid, Spain), 2 mM glutamine, 1% NEAAs, 5% FBS, 0.2% gentamycin, and 0.2%

fungizone. Silencing was performed using SMARTPool Accell HNRNPC siRNA (Dharmacon, Lafayette, CO, USA) which contains several siRNA sequences intended to target different regions of the target RNA. Invitrogen™ BLOCK-iT™ Alexa Fluor Red Fluorescent Control (Invitrogen, Carlsbad, CA, USA) was used to test the transfection efficiency, and Accell non-targeting control siRNA (Dharmacon, Lafayette, CO, USA) was used as a negative control. A time course experiment (24, 48, 72, 90, and 96 h) was designed to determine when the protein was maximally reduced. Transfections were performed using Lipofectamine™ (Thermo Fisher Scientific, Waltham, MA, USA) following the manufacturer's instructions; the final concentration of siRNAs in the cell cultures was 50 nM. Cells were recovered for both RNA and protein extraction at all the time points analyzed and spent media was also collected to isolate and test the exosomes in it for packaged miR-30d. For protein and RNA extraction, cells were trypsinized for 5 min, centrifuged at 300 xg for 5 min and washed twice with PBS before extraction. RNA was extracted using a RNeasy kit (Qiagen, Hilden, Germany) and was quantified using a NanoDrop spectrophotometer (Thermo Fisher Scientific Inc., MA, USA). Protein was isolated using RIPA buffer, as previously described. Western blotting for hnRNPC1 (ab10294, Abcam, Cambridge, UK) was performed as previously described, using Actin (ab8227, Abcam, Cambridge, UK) as a housekeeping control. All experiments were performed in triplicate.

4.15 Retro-transcription quantitative PCR

Retro-transcription-qPCR (RT-qPCR) was performed to determine the levels of hnRNPC1 mRNA in hEECs, miR-30d in both hEECs and hEEC-derived exosomes (n = 3), and the presence of receptivity markers in non-pregnant and pseudopregnant females at days 4 and 5 of pseudopregnancy (n = 6 uteri per condition tested and per genotype analyzed; total uteri: WT, n = 18; KO: n = 18). RT and qPCR for miR-30d were performed with miScript reverse transcription and miScript SYBR Green PCR kits (Qiagen, Hilden, Germany), respectively. To

determine the relative quantity of these mRNAs, a PrimeScript™ RT ‘Perfect Real Time’ reagent kit (Clontech Laboratories, Mountain View, CA, USA) and the KAPA SYBR FAST qPCR universal 2× master mix (Sigma Aldrich, St. Louis, Mi, USA) were used. Fold changes were estimated using the $-2\Delta\Delta C_t$ formula. Actin and Snord96 were used as housekeeping controls for relative mRNA and miR-30d quantification, respectively; the primer sequences used are detailed in table 4.2.

Table 4.2. Primers used for qPCR assay. Fw: Forward; Rv: reverse.

	ID	PRIMERS
mRNAs	<i>HNRNPC1</i>	FW: 5'-AGACGAAGACTGAGCGGTTG-3' RV: 5'-AGCCGAAAACAAGAAGGGGA-3'
	<i>Cox2</i>	FW: 5'-AACCGAGTCGTTCTGCCAAT-3' RV: 5'-CTAGGGAGGGGACTGCTCAT-3'
	<i>Lif</i>	FW: 5'-TGTCGCCTAGATTACCC-3' RV: 5'-CACAAATCCCTGCATCTCATC-3'
	<i>Msx1</i>	FW: 5'-TCTCGGCCATTTCTCAGTTCG-3' RV: 5'-CCGATCTAGTTTCTCGGGGC-3'
	<i>Msx2</i>	FW: 5'-TCGTCAAGCCCTTCGAGACC-3' RV: 5'-TGGTGGGGCTCATATGTCTGGG-3'
	<i>Esr</i>	FW: 5'-TGCCAAGGAGACTCGCTACT-3' RV: 5'-CTCCGGTTCTGTCAATGGT-3'
	<i>Pgr</i>	FW: 5'-CACAAAGCCTGACACTTCCA-3' RV: 5'-AAACACCATCAGGCTCATCC-3'
miRNAs	<i>miR-30d</i>	FW: 5'-UGUAAACAUCCCGACUGGAAG-3'
Housekeeping controls	<i>ACTIN</i>	FW: 5'-GATCATTGCTCCTCTGAGC-3' RV: 5'-AGTCCGCCTAGAAGCACTTG-3'
	<i>Actin</i>	FW: 5'-GATCATTGCTCCTCTGAGC-3' RV: 5'-AGTCCGCCTAGAAGCACTTG-3'
	<i>Snord96</i>	FW: Hs_SNORD96A_11 miScript Primer Assay Ref: 218300 (Qiagen, Hilden, Germany)

4.16 Molecular-beacon probe design and characterization

Molecular beacon (MB) probes were designed to recognize miR-30d in living cells by Dharmacon (Lafayette, CO, USA). MBs are internally-quenched hairpin-shaped oligonucleotide probes that fluoresce upon hybridization with their target sequence. Target-bound probes fluoresce as much as 100 times more intensely than background levels of unbound probes, enabling their highly-sensitive detection. Because of their stem, MB target-recognition is so specific that if the target differs even by a single nucleotide, the probe will not bind (Bratu et al., 2011). The miR-30d MB and negative control sequences were: (miR-30d)-[5'-CAC UGC AGU CGG CGA UGU UUA CCA GUG-3] and (negative control)-[5'-CUC AGA AAA AAA AAA AAA AAC UGA C]. Thermal denaturation profiles were used to determine the specificity of the molecular beacon probe used in this study. The changes in fluorescence in a 10 μ L solution containing 0.2 μ M of the beacon probe with (miR-30d mimic)-[5'-UGU AAA CAU CCC CGA CUG GAA G] (Ref: MSY0000245; Qiagen, Hilden, Germany) or without 1 μ M of a complementary single-stranded oligonucleotide were measured. Solutions were analyzed using the Quantum Studio 5 Real time PCR system. Specifically, samples were initially heated to 95°C and held at this temperature for 10 min; then they were cooled to 25°C at a rate of 1.6°C/s; miR-190 (miR-190 mimic)- [5'-UGA UAU GUU UGA UAU AUU AGG U] (Ref: MS00008911) was used as a negative control.

4.17 Co-culture of murine embryos with siRNA HNRNPC1-transfected cells

Ishikawa endometrial carcinoma cells were seeded at a density of 80,000 cells/cm² in μ -Slide 8-Well ibiTreat plates (Ibidi GmbH, Planegg/Martinsried, Germany). At 70% confluency, the cells were simultaneously transfected with Smart Pool Accell HNRNPC siRNA (Dharmacon, Lafayette, CO, USA) and the miR-30d MB probe using HiPerFect (Qiagen, Hilden, Germany) transfection reagent, following the manufacturer's instructions. After 90 h of transfection, the cells were

washed with PBS and refreshed with new media. WT and KO blastocysts were transferred onto the seeded cells for 24 h at 37°C and with 5% CO₂. The co-culture was then incubated at 37°C for 30 min with 5 µg/mL Hoechst 33342 (Sigma-Aldrich, Madrid, Spain) and 10 µg/mL of WGA-Alexa 488 (Life Technologies, Molecular Probes, Eugene, OR, USA), for nuclear and the membrane staining, respectively. Once the labeling was completed, the co-cultures were visualized at 60× with a water immersion confocal microscope (FV1000, Olympus); 3D modeling was carried out using Imaris software (Bitplane, Zurich, Switzerland). Experiments were performed in duplicate, so that in each replicate we analyzed the signal distribution of 3–4 embryos per condition tested. A representative experiment is shown in this thesis.

4.18 Embryo adhesion assay

Ishikawa cell lines, either the non-transfected condition using BLOCK-iT or transfected with sihnRNPC1, were cultured until confluence in µ-Slide 8-Well ibiTreat plates (Ibidi GmbH, Planegg/Martinsried, Germany). The WT or miR-30d KO embryos were then added (14 embryos per condition, 6 conditions) in two independent experiments (n = 168, total embryos). The attachment of mouse blastocysts to the epithelial cell monolayer was measured after 24 h by a mechanical assay. Briefly, plates were moved on a rotation shaker for 10 s, and any blastocysts that were subsequently floating were deemed to be unattached.

4.19 Transfer assays

Embryos from WT and KO uteri were obtained, as described in section 4.2. Some miR-30d KO embryos were pretreated with 400 nM of a miR-30d analog (miScript miRNA Mimic [Qiagen, Cat No. MSY0000245]). Blastocyst-stage embryos were used to perform the embryo transfer in both WT and KO pseudopregnant females. Estrous synchronization in pseudopregnant females was achieved by introducing sawdust from the males' cages into the females' environments; after 2

days they were allowed to mate with vasectomized mice. Females who presented a vaginal plug (considered day 1 of pseudopregnancy) the day after mating or 48 h later were separated and underwent embryo transfer on day 4. Six different transfer conditions were implemented to analyze the influence of the maternal niche and embryo in the implantation process: (1) WT embryos transferred into WT recipients (WTE-WTR); (2) KO embryos transferred into WT recipients (KOE-WTR); (3) miR-30d-pretreated KO embryos transferred into WT recipients (PTKOE-WTR); (4) WT embryos transferred into KO recipients (WTE-KOR); (5) KO embryos transferred into KO recipients (KOE-KOR); and (6) miR-30d-pretreated KO embryos transferred into KO recipients (PTKOE-KOR).

A non-surgical embryo transfer (NSET™) device for mice (ParaTechs, Lexington, KY, USA) was used to perform these transfers. For every condition, an average of 10–15 embryos were transcervically introduced into the uterine cavity (see figure 4.2 for a schematic representation of the embryo-transfer strategy); there were 3 biological replicates for day 5 of pregnancy (~36 embryos transferred per condition; ~216 total embryos transferred in the six conditions) and 6 biological replicates for day 6.5–7 of pregnancy (~90 embryos transferred per condition; ~540 total embryos transferred in the six conditions). To visualize the implantation sites, Chicago Sky blue (Sigma-Aldrich, St. Louis, Mi, USA) was injected intravenously via the tail vein. Finally, the females were euthanized by cervical dislocation and the implantation sites obtained were used to calculate the implantation rates. Uteri obtained from the pseudopregnant females who were sacrificed on day 5 of pregnancy were flash-frozen and stored in cryovials at –80°C. Cryosections and immunofluorescence analyses were performed following the previously detailed protocol. In addition to the primary antibodies used to recognize the critical receptivity markers, a ZO-1 primary antibody (Abcam, Cambridge, United Kingdom) was used to detect the zona occludens. ZO-1 is a tight junction protein often expressed in the primary decidual zone (PDZ) after implantation, making it useful for detecting the region surrounding the implantation sites.

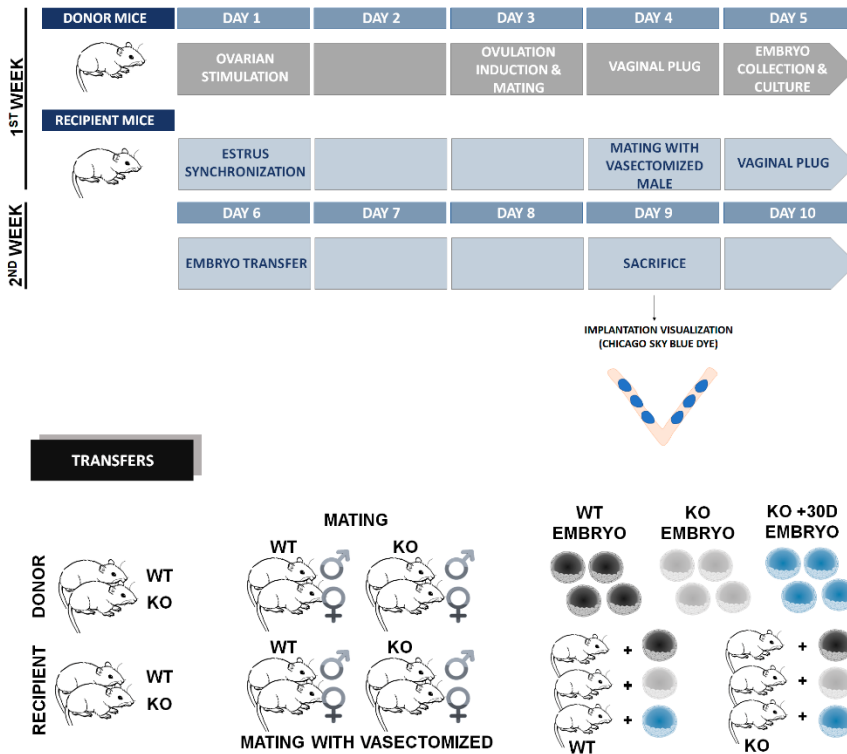


Figure 4.2. Schematic representation of the strategy performed to conduct the different transfer combinations.

4.20 Characterization of the implantation-phenotype and pregnancy-outcome associated with miR-30d deficiency

The gestation course was evaluated in pregnant females on days 5, 6, 8, and 12. Specifically, the implantation sites were visualized by intravenous injection of a Chicago Sky blue (Sigma-Aldrich, St. Louis, Mi, USA) solution on days 5 and 6, and the number of implantation sites — demarcated by distinct blue bands — was recorded (number of uteri evaluated: WT, n = 4; KO, n = 5). Resorption sites were identified and recorded on day 12 in both genotypes (number of uteri evaluated: WT, n = 5; KO, n = 5). Any abnormal embryo-spacing was recorded, and the implantation site sizes were evaluated, as determined by considering the characteristic ellipsoid area according to the following equation (Eqn.1).

$$A = \pi \cdot \frac{D_1}{2} \cdot \frac{D_2}{2} \quad (\text{Eqn.1})$$

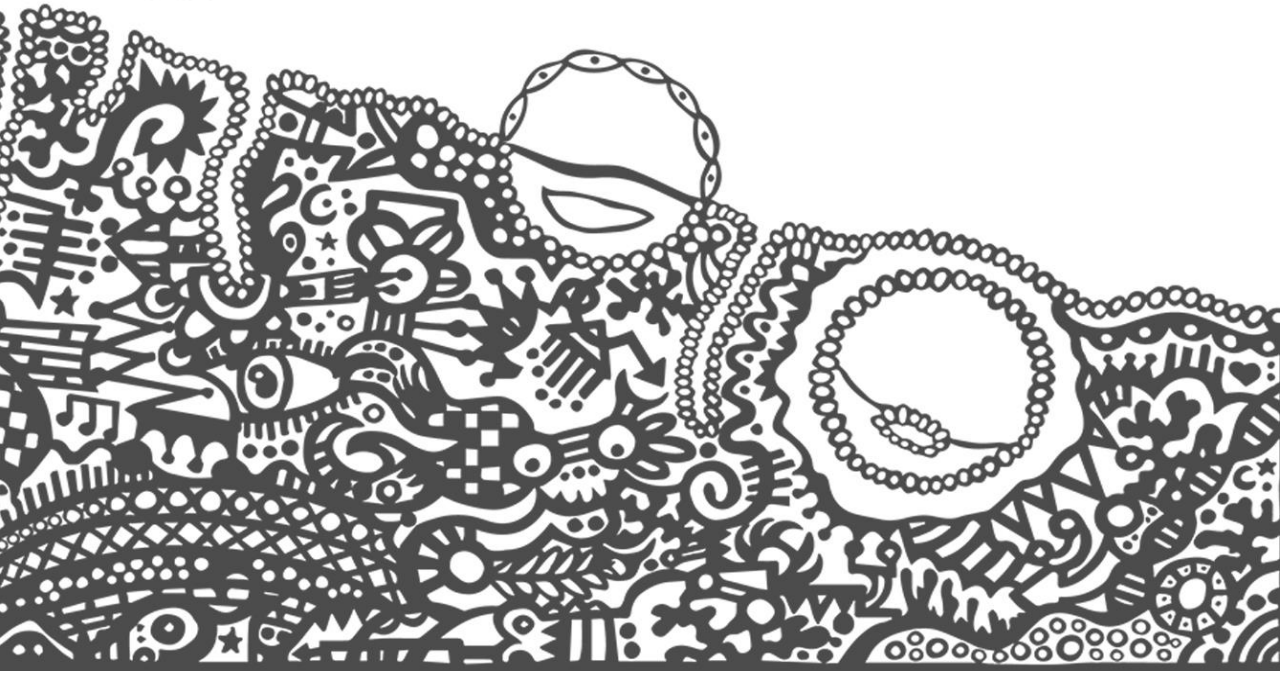
Where A is the area (cm²), D₁ is the smallest radius (cm) and D₂ the highest radius (cm).

These measurements were made by image analysis using Adobe Photoshop software (WT: E5 [n = 16]; E6 [n = 37]; E8 [n = 28]; E12 [n = 16]; KO: E5 [n = 23]; E6 [n = 15]; E8 [n = 20]; E12 [n = 17]). Intrauterine growth restriction (IUGR) was evaluated by analyzing the fetuses and placentas at day 12 and 16 of pregnancy (WT: E12 [n = 14]; E16 [n = 17]; KO: E12 [n = 12]; E16 [n = 5]). Two parameters were assessed in the fetuses, the crown-rump-length (CRL; cm) and the weight (mg) but only the weight was calculated for the placenta; these weights were used to estimate the fetal-to-placental weight ratio (FW:PW). Finally, parturition events were monitored from day 17 to 21 by daily observation (morning, noon, and evening). Pups were allowed to grow until weaning (WT: n = 40; KO: n = 37) and were then sacrificed by cervical dislocation and their weight (mg), the width (cm) and the length (cm) were recorded.

4.21 Statistical analysis

The Statgraphics Centurion software package (v.16.1.11) was used to study the significance of the results. One-way ANOVA was applied and a p-value of less than 0.05 was considered to indicate significance.

RESULTS



5.1 Screening for the hsa-miR-30d transporter protein in exosomes

Having phenotypically characterized the transfer of miR-30d in our previous work, we then wanted to elucidate the molecular mechanism responsible for sorting this miRNA into endometrial exosomes before its incorporation into trophectoderm cells. First, we screened for proteins present in the endometrium and endometrial exosomes that could exert this role in cells. To achieve this, extracts from hEECs (n = 2) and exosomes which were isolated by ultracentrifugation (of a pool of supernatants obtained from 4 T75 hEEC cultures) were incubated with streptavidin beads coated with several copies of a biotinylated miR-30d; poly-A-coated beads were used as a negative control. Once this pull-down assay was completed, we identified the proteins by mass spectrometry. Then, we pre-screened these results by discarding any proteins belonging to the keratin (KRT) gene family or that appeared to be linked to the poly-A beads. Finally, we selected proteins which were explicitly identified in exosomes and whose ProtScore (a measure of the confidence in a given detected protein) was 2 or more, or which had a confidence level exceeding 99% (**Supplementary file 7**). These functional analyses revealed that the proteins detected were mainly associated with transcriptional and post-transcriptional modifications, cell adhesion and embryonic morphogenesis (**Table 5.1**).

Table 5.1. Proteins specifically identified in exosomes and their main biological function (these functions were obtained from the UniProt database; <http://www.uniprot.org>).

IDENTIFIED PROTEIN	BIOLOGICAL PROCESSES
40S ribosomal protein S9	Nuclear-transcribed mRNA involved in catabolic processes and nonsense-mediated decay; positive regulation of cell proliferation and translational fidelity; rRNA processing, SRP-dependent co-translational protein targeting to membrane, translation, translational initiation, and viral transcription.
60S ribosomal protein L11	5S rRNA and RNA binding; structural constituent of ribosomes; involved in ubiquitin ligase inhibitor activity and ubiquitin protein ligase binding.
60S ribosomal protein L22	Heparin and RNA binding; structural constituent of ribosomes.
Agrin OS = <i>Homo sapiens</i>	Clustering of voltage-gated sodium channels; involved in extracellular matrix organization, glycosamin biosynthetic processes, glycosaminoglycan catabolic processes, glycosaminoglycan metabolic processes, and G-protein coupled acetylcholine receptor signaling pathway; positive regulation of filopodium assembly, synaptic growth at neuromuscular junctions, and transcription from RNA polymerase II promoter; receptor clustering, retinoid metabolic processes, signal transduction, and synapse organization.
Casein kinase II subunit alpha 3	Positive regulation of cell growth, cell proliferation, and protein catabolic processes; protein autophosphorylation and protein phosphorylation.
Gremlin-1	Regulation of organogenesis, body patterning, and tissue differentiation.
Heterogeneous nuclear ribonucleoproteins C1/C2	3'-UTR-mediated mRNA stabilization, ATP-dependent chromatin, mRNA splicing via spliceosome, negative regulation of telomere maintenance via telomerase osteoblast differentiation, RNA metabolic processes, and RNA splicing.
Hyaluronan-mediated motility receptor	Hyaluronan catabolic processes; regulation of G2/M transition of the mitotic cell cycle.
Interstitial collagenase	Cellular protein metabolic processes and collagen catabolic process; extracellular matrix disassembly, leukocyte migration, positive regulation of protein oligomerization, proteolysis, and viral processes.

Table 5.1 (Cont.) Proteins specifically identified in exosomes and their main biological function (Functions were obtained from the UniProt database; <http://www.uniprot.org>).

IDENTIFIED PROTEIN	BIOLOGICAL PROCESSES
KN motif and ankyrin repeat domain-containing protein 2	Apoptotic processes, negative regulation of cell proliferation, G1/S mitotic cell cycle transition, intracellular ER signaling pathways, programmed cell death, transcription from RNA pol II promoter, and vitamin D receptor signaling pathways; transcription and DNA templates.
Protein FAM110C	Positive regulation of cell migration and protein Kinase B signaling; regulation of cell projection assembly.
Protein GPR108	No annotated function.
Small nuclear ribonucleoprotein-associated protein N	mRNA splicing via spliceosome, hormone responses, and RNA splicing.
Stanniocalcin-1	Cellular response to cAMP, glucocorticoid stimulus, and hypoxia; decidualization, embryo implantation, ossification, and response to vitamin D.
Stromelysin-1	Enzyme which can degrade fibronectin, laminin, gelatins I, III, IV, and V, collagens III, IV, X, and IX, and cartilage proteoglycans; activates procollagenase.
Tubulin alpha-1C	Cell division, cytoskeleton-dependent intracellular transport, and microtubule-based processes.
Tubulin beta-2B chain	Microtubule based processes, neuron migration, positive regulation of axon guidance.

Next, we selected the proteins whose prevalence was higher in the pool of exosomes or whose biological function was related to intercellular mRNA transport. Thus, heterogeneous ribonucleoprotein C1 (hnRNPC1) was selected based on a previous report showing its role transporting mRNA from the nucleus to the cytosol (Villarroya-Beltri et al., 2013); CYR61 was used as an unspecific miR-30d binding protein because it was detected in high amounts in every condition (see **Supplemental file 7**). The presence of both these proteins in the endometrial exosomal fraction was confirmed by western blot analysis (n = 3; **Figure 5.1**); the supernatant from the ultracentrifugation process was used as the negative control.

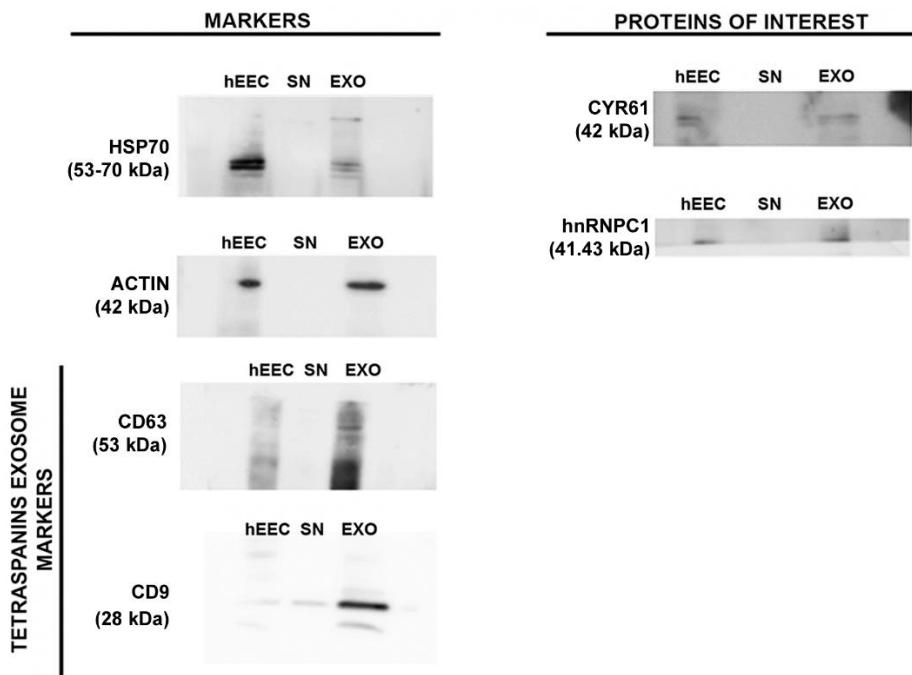
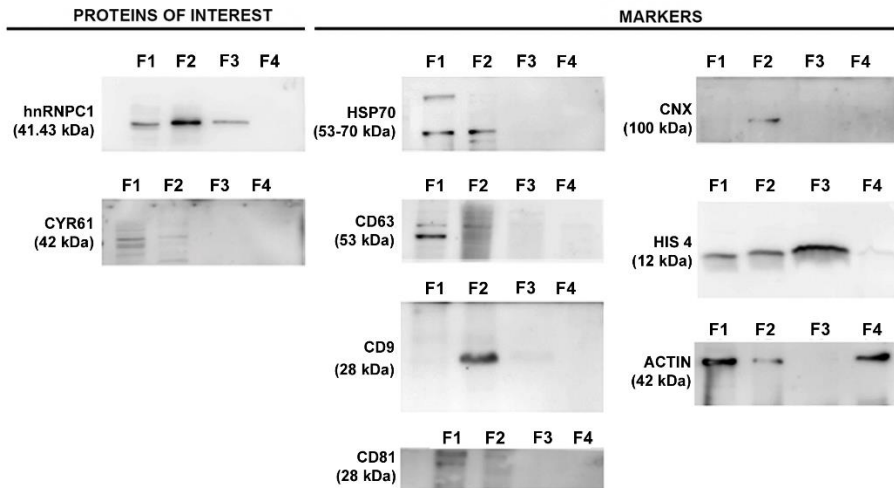


Figure 5.1. Screening for proteins that direct miR-30d loading into exosomes (I). Western blot analysis of CYR61 and hnRNPC1 in hEEC lysate exosomes and remaining supernatant. CD63, CD9, and HSP70 were used as exosome markers. As it can be observed, both CYR61 and hnRNPC1 were present in the exosomal fraction.

A western blot of subcellular fractions determined that hnRNPC1 was enriched in the protein fraction associated with membranous organelles; CYR61 was also detected in the membranous fraction, but its location was predominantly cytoplasmic (**Figure 5.2**).



F1: Cytosolic fraction; F2: Membrane protein fraction; F3: Nuclear fraction; F4: Cytoskeleton protein fraction

Figure 5.2. Screening for proteins that direct miR-30d loading into exosomes (II). Western blot of subcellular fractions to determine the presence of the main candidate proteins in the membrane organelle fraction. HSP70 and CD63 were used as cytosol and membrane markers; CD9, CD81, and Calnexin (Cal) were markers for the membrane organelle fraction, His4 was used as a reference for the nuclear fraction, and actin as a marker for the cytoskeletal fraction.

To confirm these western blot results, we used confocal microscopy to examine co-localization of these proteins with CD63 as a multivesicular body (MVB) marker (**Figure 5.3**). Because the subcellular structures analyzed are close to the microscope's resolution limit, we decided to manually identify the regions of interest (ROI) and subsequently measure their fluorescence intensity curves (Bolte and Cordelières, 2006). To achieve this, we drew vectors through these structures and plotted the fluorescence intensity for the green and red channels against the vector length (**Figure 5.3**). In the figure, the left panel shows the results for CYR61 (red) and the exosome marker CD63 (green). Of note, the fluorescence intensity

distributions for the randomly selected ROI do not coincide, suggesting that CYR61 and MVBs do not colocalize. This supports the previous observation that CYR61 is not an exosomal protein and so it is unlikely it is involved in miR-30d loading inside exosomes. The right panel of **Figure 5.3** shows hnRNPC1 (green) and CD63 (red) co-localization and indicates that hnRNPC1 is predominantly nuclear but is also present in considerable amounts in the cytoplasm. Unlike CYR61, the hnRNPC1 fluorescence intensity distribution overlapped with CD63 for certain regions of the vectors traced in the cytoplasmic compartment, suggesting partial hnRNPC1 and MVB co-localization.

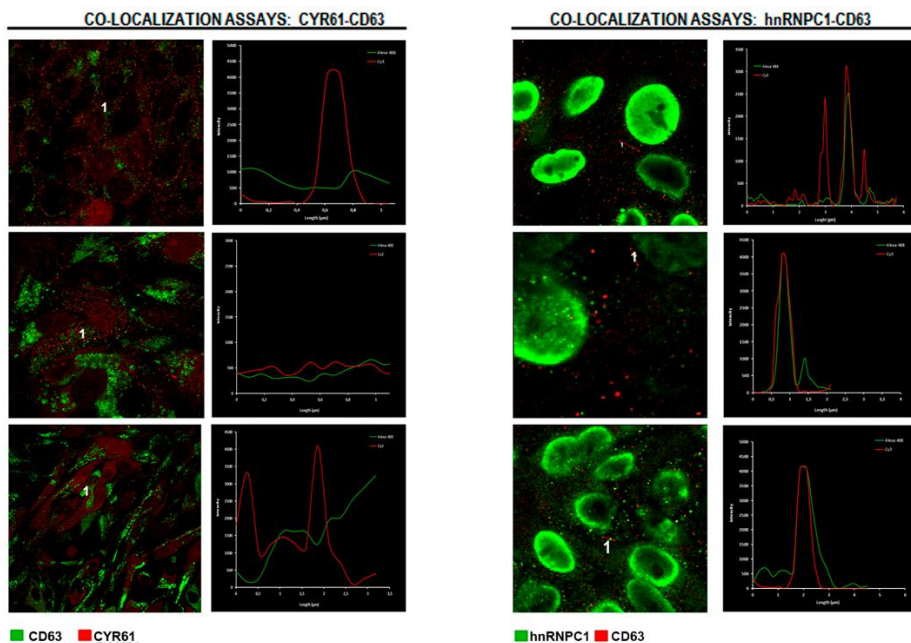


Figure 5.3. Identification of hnRNPC1 inside exosomes (I). Co-localization assays to determine if the proteins of interest were present in the inner cavity of the exosomes. The left panel shows CYR61 (red) and exosome marker CD63 (green) staining. The fluorescence intensity distributions for the defined region of interest do not coincide, indicating that CYR61 was not present inside the exosomes. The right panel shows the co-localization assay for hnRNPC1 (green) and CD63 (red). The overlap between the fluorescence intensity distributions suggests that it is possible that hnRNPC1 directs miR-30d loading into exosomes.

To eliminate the possibility that this protein might adhere to the exosome membranes, FACS analysis was performed (**Figure 5.4**). hnRNPC1 fluorescence was higher in permeabilized rather than non-permeabilized exosomes (**Figure 5.4**), suggesting that hnRNPC1 may be located inside multivesicular structures.

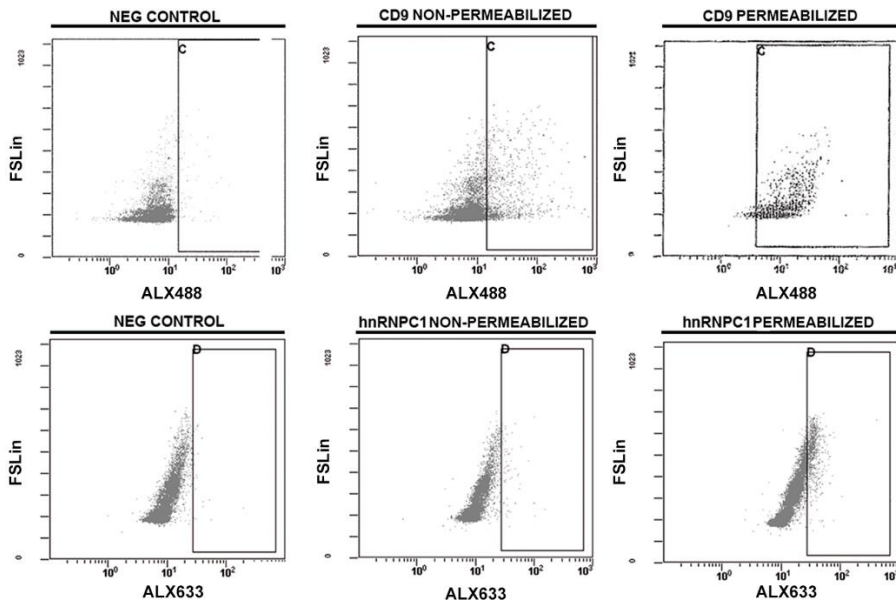


Figure 5.4. Identification of hnRNPC1 inside exosomes (II). FACS analysis of hnRNPC1 and CD9 in exosome-coupled beads. Exosomes coupled to aldehyde-sulfate beads, were permeabilized or left intact, and were incubated with antibodies to hnRNPC1 (bottom panels) or CD9 (top panels) and a secondary antibody. Exosome-coupled beads incubated only with the secondary antibody were used as negative controls (left panels).

Because hnRNPC1 is thought to be predominantly nuclear (Dreyfuss et al., 1993), we investigated whether this protein could be found in the cytoplasm of conventionally cultured hEECs by comparing the percentage fluorescence signal distribution of this protein by IN-Cell analysis (**Figure 5.5**). The signal from the cytoplasm was stronger than from the nucleus, which might be because of the relative surface area analyzed. However, these results seem to confirm the presence of hnRNPC1 in the cytoplasm of hEECs and agrees with findings by Kim et

al. (2003) that showed that this protein can migrate to the cytoplasm during different cell cycle phases (Kim et al., 2003).

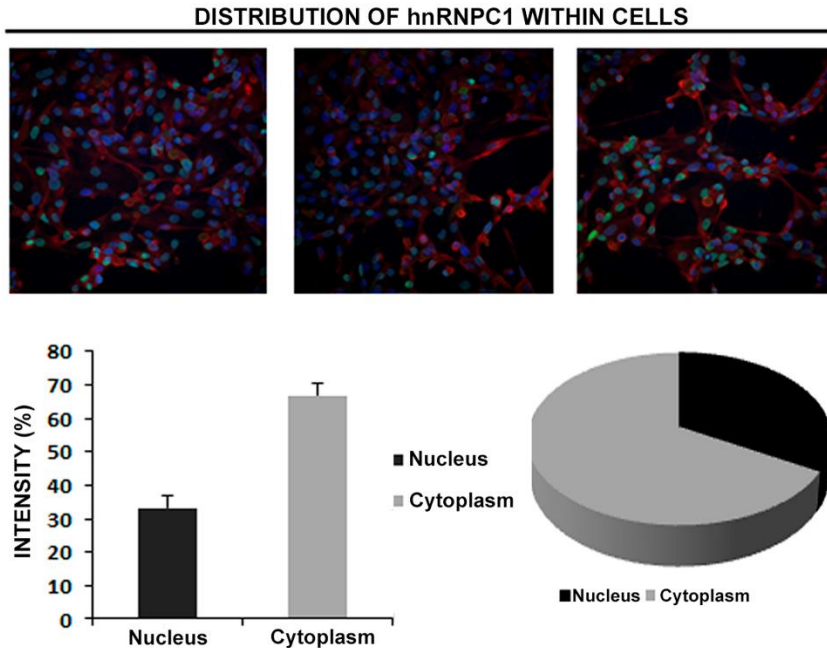


Figure 5.5. Identification of hnRNPC1 inside exosomes (III). *IN-Cell analysis of the distribution of hnRNPC1 throughout cells. The top panel shows three representative fluorescence images obtained: nucleus in blue (Hoescht 33382), hnRNPC1-Alexa 488 in green, and WGA-Texas red in red. The bottom panel shows the proportion of hnRNPC1 in either the cytoplasm or the nucleus.*

Finally, specific binding of hnRNPC1 to miR-30d was verified by immunoprecipitation of hnRNPC1 from exosome lysates followed by qPCR for these miRNAs (**Figure 5.6**). MiR-30d, but not miR-450, was amplified from hnRNPC1 immunoprecipitates, thus demonstrating specific binding of hnRNPC1 and miR-30d in exosomes *in vitro*. Therefore, from the results obtained, and given that hnRNPC1 has already been identified as a possible miRNA transporter (Villarroya-Beltri et al., 2013), it is feasible that an interaction between hnRNPC1 protein and miR-30d exists prior to the loading of this miRNA into the inner cavity of the exosomes.

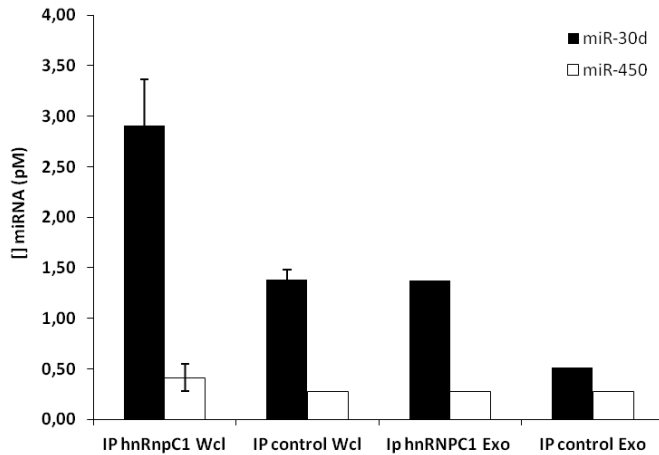


Figure 5.6. Validation of miR-30d-hnRNP1 linkage in whole lysates and exosomes. qPCR analysis of miRNAs in hnRNP1 immunoprecipitates from exosome and cell lysates, showing the specific binding of miR-30d to hnRNP1 both in exosomes and in the cellular cytoplasm. Immunoprecipitation was performed with magnetic beads coated with anti-hnRNP2B1 or anti-IgG1 control antibody. Error bars represent the s.d. (n = 2); Wcl, whole cell lysate; Exo, exosomes.

5.2 Silencing hnRNP1 in hEECs confirms their involvement in sorting hsa-miR-30d into endometrial exosomes

To investigate the function of hnRNP1 in packaging miR-30d into exosomes, we assessed the effect of silencing hnRNP1 in hEECs. Because the survival rate of primary hEECs after transfection is low, we tested hnRNP1 silencing in the Ishikawa endometrial cancer cell line. This is a good model for studying normal endometrium because it retains its capacity to maintain normal hormonal responsiveness to ovarian steroids (Nishida, 2002). A time-course experiment showed that maximal silencing efficiency was achieved 72 h post-transfection (**Figure 5.7A**). This is in accordance with the results obtained by western blotting, in which the lowest hnRNP1 protein yield was obtained 72–96 h post-transfection (**Figure 5.7B**). After 90 h of hnRNP1 knock-down, the level of

miR-30d in the cellular cytoplasm ($p = 0.0001$; $n = 3$; **Figure 5.7C**), as well as in the inner exosomal cavity ($p = 0.0152$; $n = 3$; **Figure 5.7D**), was reduced.

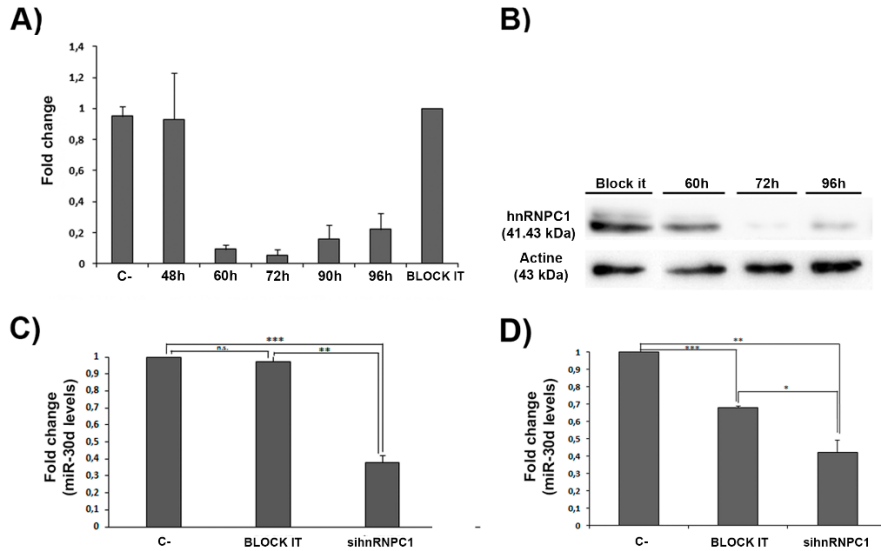


Figure 5.7. Silencing hnRNPC1 in hEECs confirms its involvement in sorting hsa-miR-30d into endometrial exosomes (A) RT-qPCR to detect mRNA levels of hnRNPC1 in Ishikawa cells previously transfected with sihnRNPC1 at different time points: 48, 60, 72, 90, and 96 h post-transfection. As a negative control for transfection, BLOCK-IT siRNA was transfected for 96 h. The levels of hnRNPC1 reached their minimum level at 72 h. (B) Western blot analyses to detect the best time frame for obtaining maximum silencing efficiency; Actin was used as a housekeeping control. After 72 h, hnRNPC1 levels dramatically decreased. (C) miR-30d levels detected in Ishikawa cells 90 h after hnRNPC1 silencing. (D) miR-30d levels detected in exosomes isolated from the spent media from Ishikawa cells 90 h after hnRNPC1 silencing.

Characterization of the specificity of the MB probes designed to detect miR-30d in living cells showed that the MB thermal denaturation fluorescence profiles were higher for miR-30d compared to the negative or mismatch target oligonucleotide controls (**Figure 5.8**)

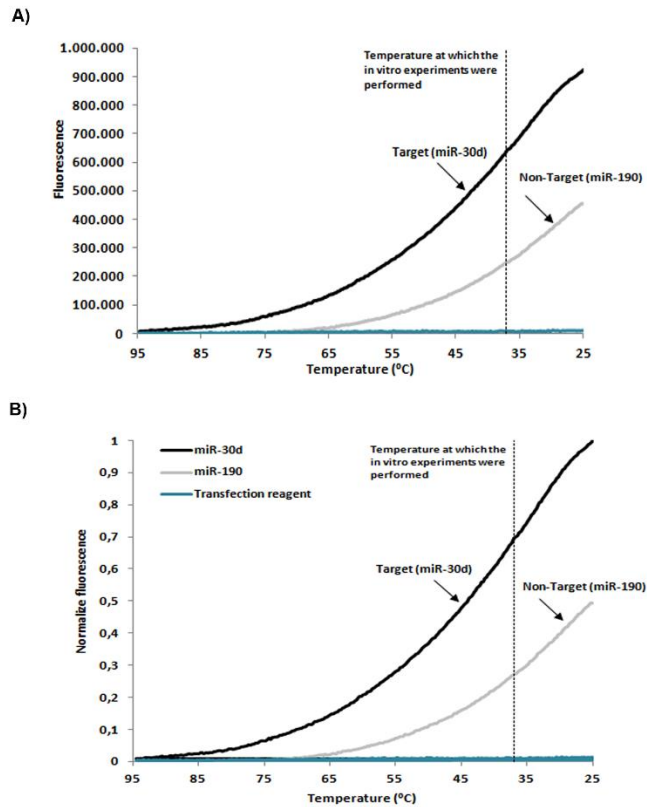


Figure 5.8. Characterization of the molecular beacon probe. (A) Thermal denaturation profiles of the molecular beacon probe in the presence of a miR-30d analog (black line) or a mismatch target—a miR-190 analog (grey line)—and the transfection reagent used to transfect the hEECs in vitro. The dotted line represents the temperature at which the in vitro experiments were conducted. (B) The results from the previous experiment, considering the normalized fluorescence.

WT or miR-30d KO embryos were then co-cultured with Ishikawa cells doubly-transfected with the hnRNPC1 siRNA and the MB-miR-30d probe ($n = 2$). Confocal microscopy images showed that the transfer of miR-30d between epithelial-like cells and trophoblast cells is reduced after hnRNPC1 silencing (**Figure 5.9**). Subsequent image analysis indicated that the transferred miR-30d signal considerably decreased in co-cultures where hnRNPC1 was silenced (**Figure 5.10**).

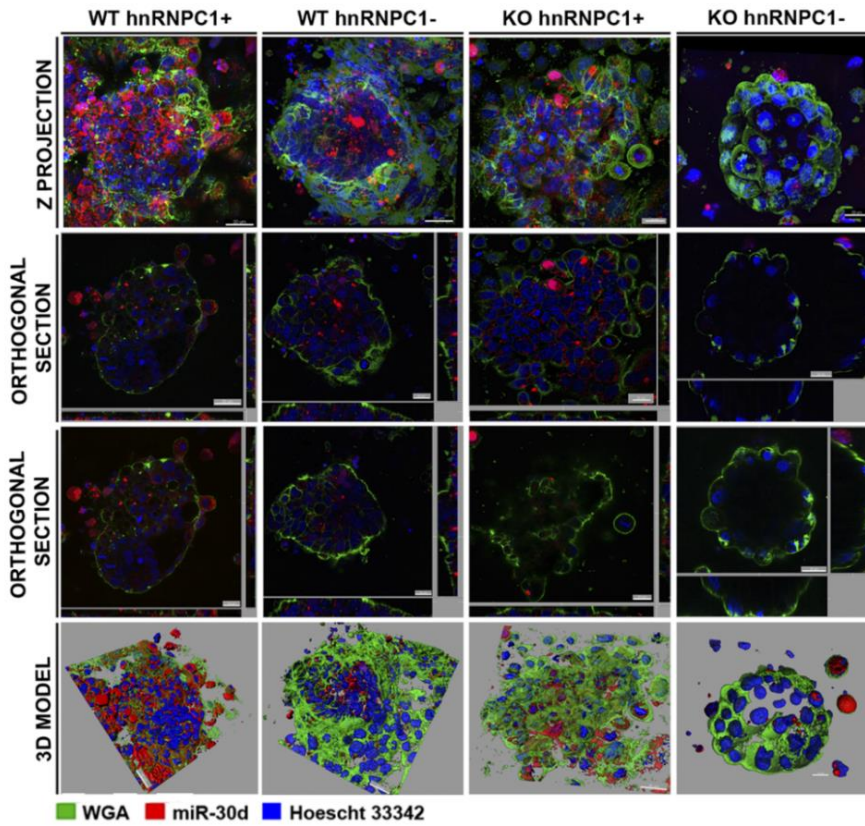


Figure 5.9. Silencing *hnRNP1* in hEECs cells confirms its involvement in sorting *hsa-miR-30d* into endometrial exosomes (II). Confocal images of the co-culture of WT or miR-30d KO embryos with Ishikawa cells previously simultaneously transfected with both the *sihnRNP1* and miR-30d MB probe. Cy3: miR-30d; WGA-Alexa 488: membrane labelling; Hoechst 33382: nuclear staining.

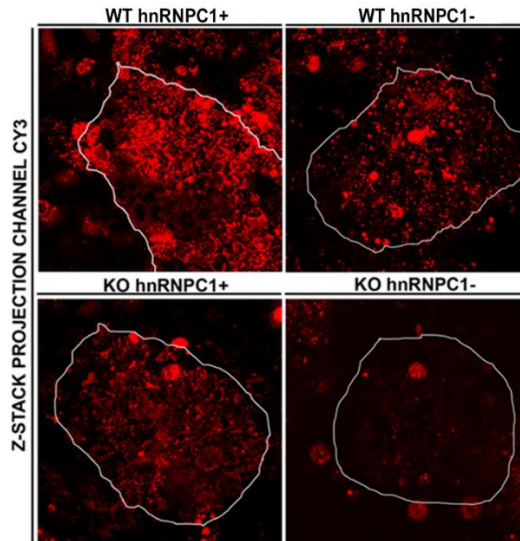


Figure 5.10. Silencing *hnRNP1* in hEECs confirms its involvement in sorting *hsa-miR-30d* into endometrial exosomes (III). Fluorescence intensity distribution for the Cy3 channel (*miR-30d*) in all the conditions tested.

Finally, to determine if a reduction in *hnRNP1* and *miR-30d* levels impairs blastocyst adhesion to hEECs, in vitro embryo adhesion assays were performed (**Figure 5.11**). Specifically, WT and *miR-30d* KO embryos were added to a monolayer of Ishikawa cells which had previously been transfected with either *sihnRNP1* or the negative control (BLOCK-iT). Adhesion assays showed that in non-transfected cells (C-) the adhesion rates for KO embryos were significantly lower than for WT embryos (WT: $78.75 \pm 2.50\%$ vs. KO: $60 \pm 0.00\%$; $p < 0.0001$). Likewise, transient silencing of *hnRNP1* significantly decreased blastocyst adhesion compared to mock transfection using BLOCK-iT, for both WT ($66.67 \pm 10.01\%$ vs. $38.33 \pm 8.45\%$; $p = 0.0006$) and *miR-30d* KO embryos ($50.00 \pm 11.50\%$ vs. $22.50 \pm 8.76\%$; $p = 0.0029$).

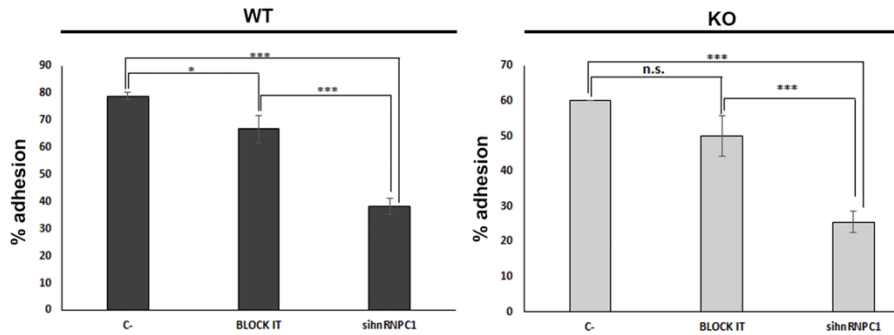


Figure 5.11. Silencing *hnRNPC1* in hEECs confirms its involvement in sorting *hsa-miR-30d* into endometrial exosomes (IV). Adhesion assays for WT (left graph) and KO embryos (right graph) cocultured with Ishikawa cells previously transfected with either a negative control (BLOCK-iT) or *sihnRNPC1*. The adhesion rates were significantly lower for KO embryos (WT: $78.75 \pm 2.50\%$ vs. KO: $60 \pm 0.00\%$; $p < 0.0001$) at baseline conditions. In both cases, there was a significant decrease in the percentage adhesion after transient *hnRNPC1* silencing both when compared with baseline conditions (WT: $78.75 \pm 2.50\%$ vs. $38.33 \pm 8.45\%$; $p = 0.0000$; KO: $60 \pm 0.00\%$ vs. $22.50 \pm 8.76\%$; $p = 0.0000$) and when transfected with the BLOCK iT negative control (WT: $66.67 \pm 10.01\%$ vs. $38.33 \pm 8.45\%$; $p = 0.0006$; KO: $50.00 \pm 11.50\%$ vs. $22.50 \pm 8.76\%$; $p = 0.0029$).

These results confirm that for KO embryos, the strongest decrease in adhesion was caused by the combined effect of the intrinsic reduction of endogenous miRNA miR-30d levels and the decrease linked with the drop in *hnRNPC1* levels.

5.3 Impact of miR-30d deficiency on endometrial receptivity

After confirming that the adhesion rates of miR-30d KO embryos are decreased in a heterologous model, we explored the molecular and phenotypic effects of miR-30d deficiency during the implantation process in an in vivo model, checking whether the absence of miR-30d directly impacts the acquisition of a receptive endometrium. We analyzed the expression of cyclooxygenase-2 (*Cox2*), leukemia inhibitory factor (*Lif*), msh homeobox 1 (*Msx1*), msh homeobox 2 (*Msx2*), estrogen receptor (*Esr*), and progesterone receptor (*Pgr*) in the mouse

endometrium at days 0, 4, and 5 of pseudopregnancy. Thus, in the non-pregnant endometrium condition (E0), *Lif* mRNA levels were significantly reduced ($p = 0.0355$) and *Msx1* mRNA levels were increased in KO compared to WT tissues ($p = 0.0014$; **Figure 5.12**). Of note, all the receptivity markers significantly reduced at the beginning of implantation (E4) in KO uteri, but once implantation was established (E5), these differences were no longer significant.

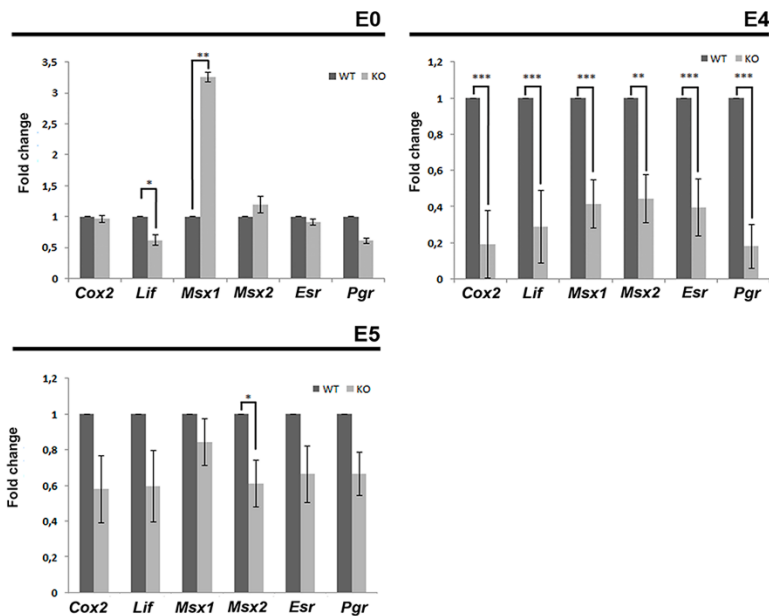


Figure 5.12. Analysis of essential receptivity markers in WT and miR-30d KO uteri throughout the implantation period (I). RT-qPCRs performed on WT and miR-30d KO uteri samples during a non-pregnancy state (E0) and at day 4 (E4) and 5 (E5) of pseudopregnancy ($n = 6$ uteri per condition tested and per genotype analyzed; total uteri: WT, $n = 18$; KO, $n = 18$). Fold-change (FC) values are presented for all the analyzed receptivity markers (*Cox2*, *Lif*, *Msx1*, *Msx2*, *Esr*, and *Pgr*). Significant differences were observed at E0 (*Lif* [$p = 0.0355$]; *Msx1* [$p = 0.0014$]), E4 (*Cox2* [$p = 0.0000$]; *Lif* [$p = 0.0000$]; *Msx1* [$p = 0.0002$]; *Msx2* [$p = 0.0036$]; *Esr* [$p = 0.0002$]; *Pgr* [$p = 0.0000$]), and E5 (*Msx2* [$p = 0.0355$]).

To determine if the mRNA expression changes were also reproduced at the protein level, immunofluorescence (IF) and western blot (WB) analyses were performed. The changes in the protein levels of COX2, LIF, and ESR were like those

detected for their respective mRNAs over the time course (E0, E4, and E5; **Figure 5.13**) and the expression of these markers was higher in WT than in KO uteri. WB analysis (**Figure 5.14**) revealed significant genotype-dependent differences between COX2, LIF, and Msx1 at E0, for LIF at E4, and for LIF and Msx1 at E5, while MSX2 was barely detectable in either genotype during implantation (**Figures 5.13, 5.14**). Finally, PGR levels were similar in WT and KO uteri at all the analyzed time points (**Figures 5.13, 5.14**).

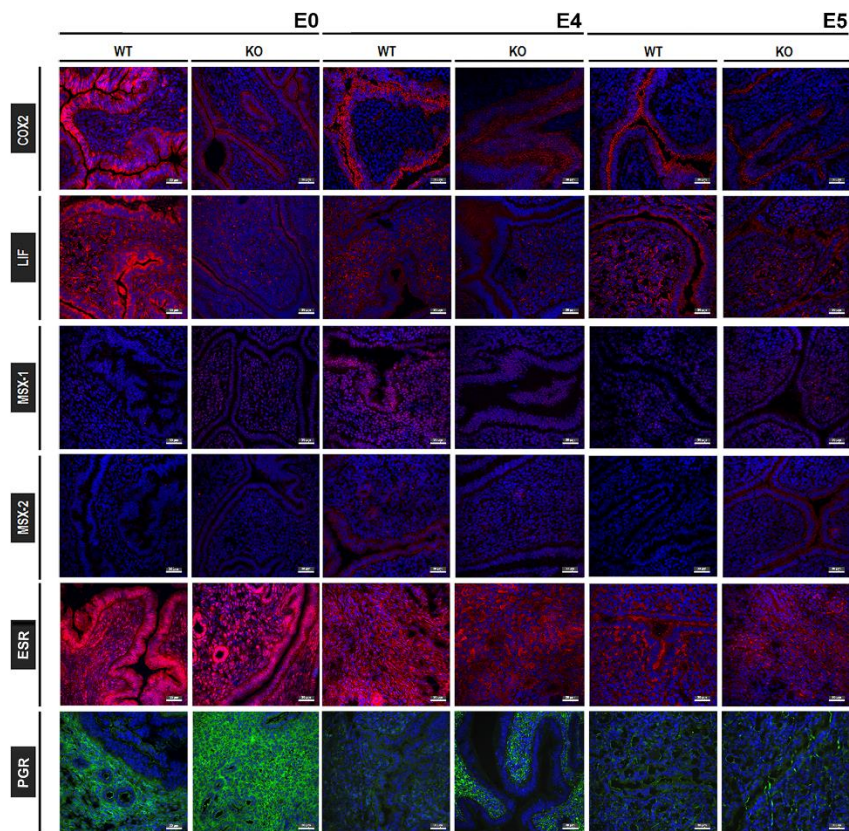


Figure 5.13. Analysis of essential receptivity markers in WT and miR-30d KO uteri throughout the implantation period (II). IF assays performed on WT and miR-30d KO uteri in a non-pregnancy state (E0) and on day 4 (E4) and day 5 (E5) of pseudopregnancy (n = 3 uteri per condition tested and per genotype analyzed; total uteri: WT, n = 9; KO, n = 9). Micrographs suggest that COX2, LIF, and ESR expression was higher in the WT genotype than in the KO at all the stages analyzed. Staining was with Hoechst 33382 (blue): nucleus; Alexa Fluor 555 dye (red): receptivity markers COX2, LIF, MSX1, MSX2, and ESR; Alexa Fluor 488 dye (green): receptivity marker PGR.

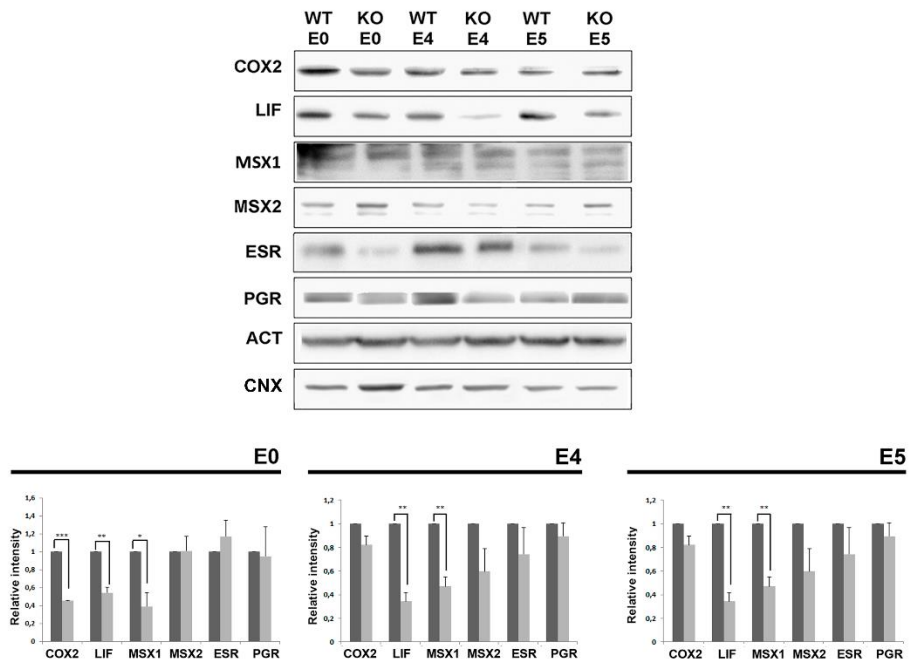


Figure 5.14. Analysis of essential receptivity markers on WT and miR-30d KO uteri through implantation period (III). WB analysis performed on WT and miR-30d KO uteri at a non-pregnancy state (E0) and at day 4 (E4) and 5 (E5) of pseudopregnancy ($n = 6$ uteri per condition tested and genotype analyzed; total uteri: WT, $n = 18$; KO, $n = 18$). Significant differences were detected for COX2 ($p = 0.0000$) at E0, LIF at E0 ($p = 0.002$), E4 ($p = 0.0011$) and E5 ($p = 0.0000$); and ESR ($p = 0.0000$) at E5.

5.4 Reproductive impact of maternal and/or embryonic-origin miR-30d

Next, we investigated the reproductive phenotype according to the maternal or embryonic origin of the miR-30d deficiency. Thus, WT, miR-30d KO, and miR-30d KO embryos pretreated with 400 nM of synthetic miR-30d (Vilella et al., 2015) were transferred into either WT or KO pseudopregnant mice in which estrus had been previously synchronized. The different conditions evaluated were: (1) WT embryos transferred into WT recipients (WTE-WTR); (2) KO embryos into WT recipients (KOE-WTR); (3) miR-30d-pretreated KO embryos into WT recipients (PTKOE-WTR); (4) WT embryos into KO recipients (WTE-KOR); (5), KO embryos into KO recipients (KOE-KOR); and (6) miR-30d-pretreated KO embryos into KO

recipients (PTKOE-KOR). **Figure 5.15** is a representative image of the implantation sites (IS) in uteri surgically removed after these transfers and the implantation rates (IR) achieved at day 6.5–7 of pregnancy. Note that average and standard deviations are calculated from 6 biological replicates, with a total of 12–15 embryos per condition transferred in each replicate (total of 463 embryos transferred in the six conditions tested).

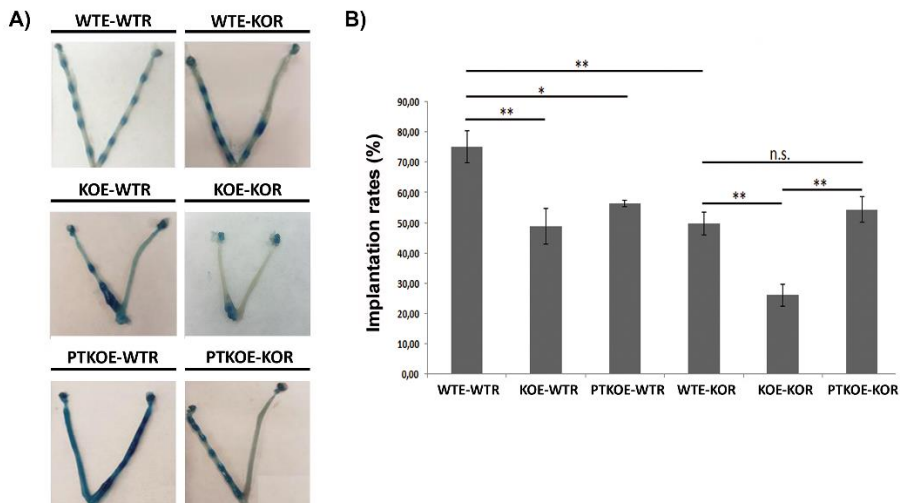


Figure 5.15. Characterization of the implantation phenotype associated with miR-30d deficiency (I). Left panel: representative images of the IS (demarcated by distinct blue bands) registered for the WT and KO uteri at days 6.5–7 of pregnancy. Six biological replicates were performed for day 6.5–7 of pregnancy (approximately 90 embryos transferred per condition; total of 463 embryos transferred in the six conditions tested). Right panel: implantation rate (IR) at day 6.5–7 of pregnancy. The IRs for KO embryos transferred into WT recipients was less than for the transfer of WT embryos into WT recipients ($48.86\% \pm 14.33$ vs. $75.00\% \pm 10.47$; $p = 0.0061$); transfer of KO embryos into KO recipients led to lower IRs compared to the transfer of WT embryos into KO recipients ($26.04\% \pm 7.15$ vs. $49.71\% \pm 8.59$; $p = 0.0059$); pretreating KO embryos with miR-30d significantly restored these IRs in KO uteri ($54.39\% \pm 10.13$ vs. $26.04\% \pm 7.15$; $p = 0.0025$).

KO embryos transferred into WT recipients had a lower IR than WT embryos transferred into WT recipients ($48.86 \pm 14.33\%$ and $75.00 \pm 10.47\%$,

respectively; $p = 0.0061$). Similarly, when transferred into KO recipients, KO embryos had a lower IR than WT embryos ($26.04 \pm 7.15\%$ and $49.71 \pm 8.59\%$; $p = 0.0059$). Interestingly, KO embryos pretreated with miR-30d and transferred into KO uteri had a higher implantation rate than untreated KO embryos ($54.39 \pm 10.13\%$ and $26.04 \pm 7.15\%$, respectively; $p = 0.0025$), but this rescue was not observed for WT uteri ($56.26 \pm 2.44\%$ and $48.86 \pm 14.33\%$; $p = 0.3288$; **Figure 5.15**), suggesting that the maternal and embryonic expression of miR-30d are equally important for achieving pregnancy.

To determine if the implantation rates observed in the different conditions were associated with deregulation of receptivity markers during gestation, we evaluated marker expression on days 4 (E4) and 5 (E5) of pregnancy under physiological conditions (i.e., with no transfer) as compared to expression in the different transfer conditions indicated (**Figure 5.16 and 5.17**). Under physiological conditions, the mean receptivity marker fluorescence intensity value (FIV) on day 4 was lower in KO than WT samples; however, this generalized trend was not significant when the complete panel of micrographs from all the biological replicates was considered (**Figure 5.17A**). In contrast, on day 5 of pregnancy (E5) the FIV of LIF was significantly lower in the KO relative to the WT uteri (64.73 ± 3.86 and 49.15 ± 9.05 , respectively; $p = 0.0336$; **Figure 5.17A**), although there were no statistically significant differences in expression for any other markers.

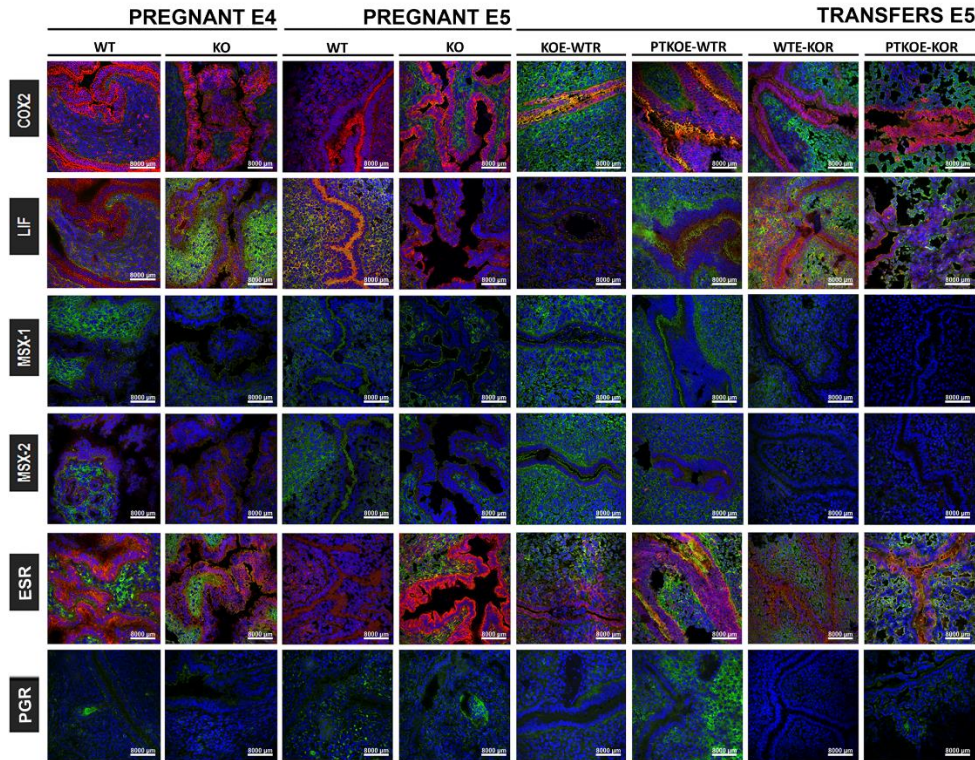


Figure 5.16. Analysis of receptivity marker (COX-2, LIF, MSX1, MSX2, ESR, and PGR) expression in different maternal-fetal crosstalk scenarios (I). Left panels: Micrographs of WT and KO uteri at day 4 (E4) and 5 (E5) of pregnancy. Representative images for every receptivity marker are presented ($n = 3$ uteri per condition tested and per genotype analyzed; total uteri: WT; $n = 9$; KO, $n = 9$). Staining was with Hoechst 33382 (blue): nucleus; Alexa Fluor 555 dye (red): receptivity markers COX2, LIF, MSX1, MSX2, and ESR; Alexa Fluor 488 dye (green): from rows 1–5, represents the ZO-1 location. In row 6, Alexa Fluor 488 demarcates PGR expression. Right panels: Micrographs of WT and KO uteri in the different transfer conditions tested. For every condition tested; an average of 10–15 embryos were introduced. Three biological replicates were performed for day 5 (E5; approximately 36 embryos transferred per condition tested). The staining was Hoechst 33382 (blue): nucleus; Alexa Fluor 555 dye (red): receptivity markers COX2, LIF, MSX1, MSX2, and ESR; Alexa Fluor 488 dye (green): from rows 1–5, represents the ZO-1

In any case, it is more interesting to consider what the mean FIV patterns indicate about endometrial-embryo communication in the different transfer conditions (**Figures 5.16 and 5.17B**). Although in some cases changes in the FIVs failed to reach significance, the expression levels of LIF were significantly different in practically all the conditions tested (**Figure 5.17B**). Thus, KO embryos transferred into either WT or KO mothers elicited considerably less LIF expression than WT embryos under the same conditions (WT uteri [42.82 ± 11.85 and 64.74 ± 8.63 , respectively; $p = 0.0381$] and KO uteri [66.25 ± 9.05 and 88.54 ± 7.18 , respectively; $p = 0.0061$]). Interestingly, treatment of KO embryos with a miR-30d analog prior to their transfer normalized, or even increased, the mean FIV for LIF, regardless of whether the recipient uterus was WT or KO (WT uteri [miR-30d treated: 81.83 ± 3.49 ; untreated: 42.82 ± 11.85 ; $p = 0.0467$ and KO uteri [miR-30d treated: 94.50 ± 9.31 ; untreated: 66.25 ± 9.05 ; $p = 0.0046$]). Finally, COX2 exhibited perhaps the most intriguing changes: miR-30d pretreatment of KO embryos significantly increased the COX2 FIVs in WT hosts (miR-30d treated: 34.52 ± 6.40 ; untreated 60.54 ± 1.24 , $p = 0.0299$), thus recovering or exceeding the find at the basal conditions (**Figure 5.17B**).

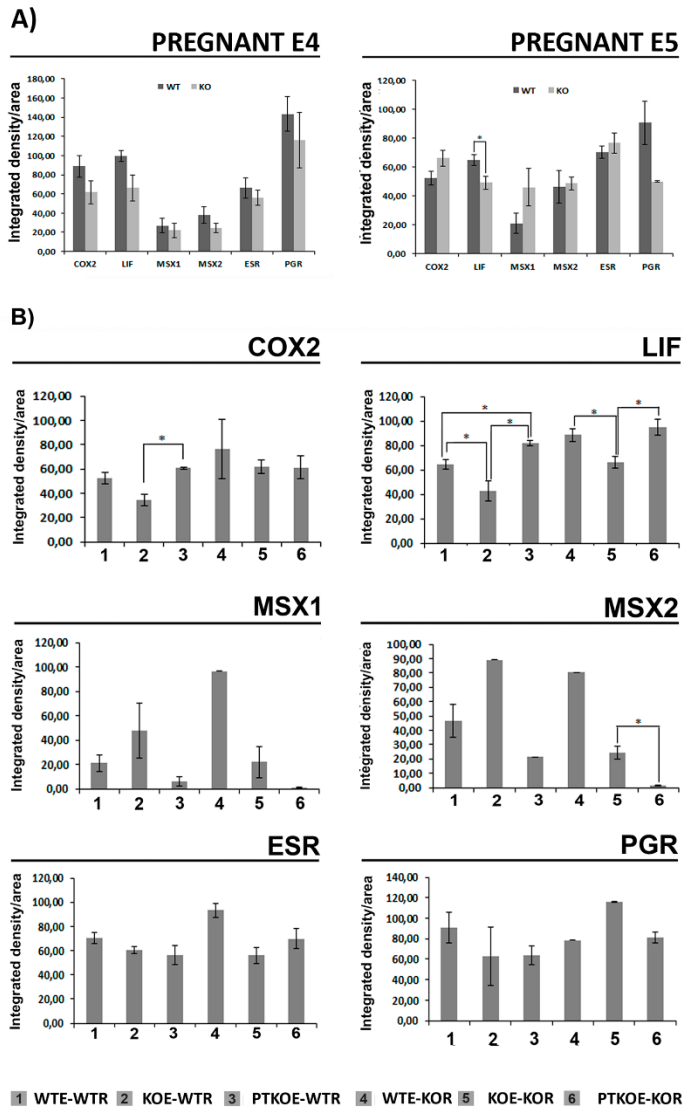


Figure 5.17. Analysis of receptivity marker expression (COX2, LIF, MSX1, MSX2, ESR, and PR) in different maternal-fetal crosstalk scenarios (II). (A) Right panel: integrated fluorescence value (FIV) density/area calculated for every receptivity marker at day 4 of pregnancy. In general, all the mean FIVs decreased for all the receptivity markers, but this decrease was not significant. Left graph: integrated density/area calculated for every receptivity marker at day 5 of pregnancy. The FIV of LIF was significantly downregulated in KO uteri (64.73 ± 3.86 vs. 49.15 ± 9.05 ; $p = 0.0336$). For the rest of the markers, the

differences were not significant. (B) Integrated fluorescence density/area calculated for every transfer condition tested: (1) WTE-WTR; (2) KOE-WTR; (3) PTKOE-WTR; (4) WTE-KOR; (5) KOE-KOR; (6) PTKOE-KOR. Compared to WT embryos, transfer of KO embryos significantly reduces the presence of LIF in both WT and KO uteri (WT uteri [42.82 ± 11.85 vs. 64.74 ± 8.63; $p = 0.0381$ and KO uteri [66.25 ± 9.05 vs. 88.54 ± 7.18; $p = 0.0061$]). Transfer of miR-30d-pretreated KO embryos results in an increase of the LIF mean FIV in both WT and KO recipients (WT uteri [81.83 ± 3.49 vs. 42.82 ± 11.85; $p = 0.0467$ and KO uteri [94.50 ± 9.31 vs. 66.25 ± 9.05; $p = 0.0046$]). Transfer of miR-30d-pretreated KO embryos increases the COX2 mean FIVs compared to transferring KO embryos to WT recipients (34.52 ± 6.40 vs. 60.54 ± 1.24, $p = 0.0299$).

Notably, the IR pattern of the different transfer conditions coincided with the LIF mean FIV pattern (**Figure 5.18A**) and there was a positive correlation ($r = 0.9978$) between the LIF mean FIV and the IR for KO recipients (**Figure 5.18B**).

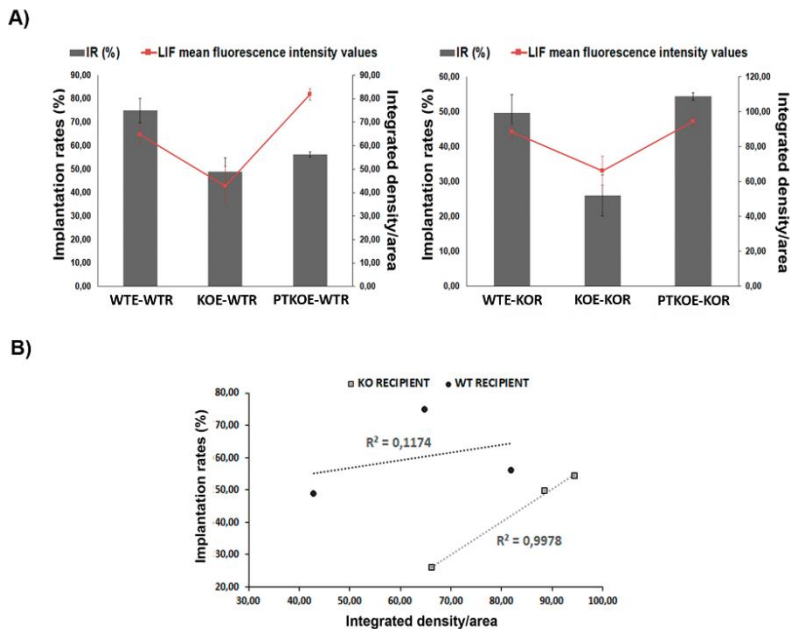


Figure 5.18. Correlation between LIF expression and implantation rates in different maternal-fetal crosstalk scenarios. (A) Graphs representing the overlapping tendency between the mean FIVs for LIF (red line) and the percentage IR (grey bars) observed for the WT (left graph) and KO (right graph) recipient. Primary axis: IR (%), secondary axis: integrated density/area. (B) Correlation between the LIF mean FIVs and the IR (%) observed in all the transfer conditions tested. A positive correlation was found for the KO recipients ($r = 0.9978$).

5.5 Impaired fetal development linked to miR-30d deficiency

Considering the changes in maternal-embryo communication described above, we hypothesized that mir-30d deficiency in the mother or embryo would also affect placentation and fetal development. IS size, embryo spacing, and the number of resorptions were first assessed on days 5, 6, 8, and 12 of pregnancy in both WT and KO genotypes under physiological conditions. The IS sizes were significantly smaller ($p < 0.001$) in KO mothers at all the time points analyzed (**Figure 5.19A**). Likewise, the number of resorptions identified by day 12 of pregnancy was slightly higher in KO females compared to the WTs (25% and 10%, respectively; **Figure 5.19B**).

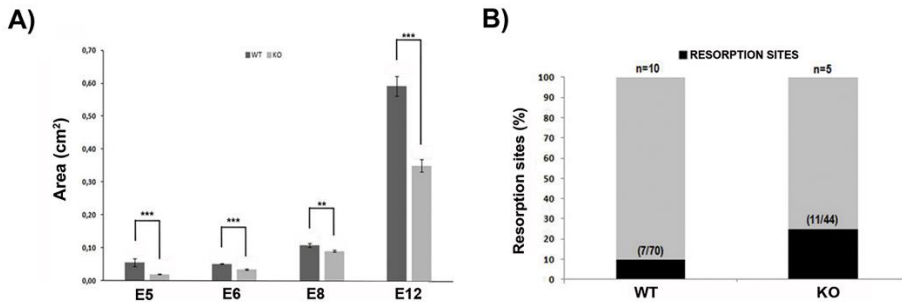


Figure 5.19. Characterization of the implantation phenotype associated with miR-30d deficiency (II). (A) IS size calculated throughout gestation (days 5, 6, 8, and 12) as measured by Adobe Photoshop image analysis software (WT: E5 [n = 16]; E6 [n = 37]; E8 [n = 28]; E12 [n = 16]; KO E5 [n = 23]; E6 [n = 15]; E8 [n = 20]; E12 [n = 17]). The IS sizes were significantly smaller (E5, E6, E8, E12; $p = 0.0000$) in the KO genotype on all the gestation days analyzed. (B) Resorption sites registered on day 12 (E12) of pregnancy.

To determine if these defects slow fetoplacental growth, we analyzed fetuses and placentas on day 12 (E12) and 16 (E16) of pregnancy (**Figure 5.20**). Placentas and fetuses obtained from KO females were significantly smaller ($p < 0.001$), in terms of the crump-rump length ($p < 0.001$) and fetal/placental weight ratio (FW:PW_E12 [$p = 0.0120$] and FW:PW_E16 [$p = 0.0011$]), compared to WT females (**Figures 5.20A–D**). The FW:PW is a proxy for placental efficiency (Hayward et al., 2016), defined as the grams of fetus produced per gram of

placenta. These results suggest that miR-30 deficiency might affect the nutrient supply, resulting in smaller offspring. This hypothesis is supported by the observation that the weight (**Figure 5.20F**), length (**Figure 5.20G**), and width (**Figure 5.20H**) of weaned offspring derived from KO dams were also significantly less than the controls ($p \leq 0.05$).

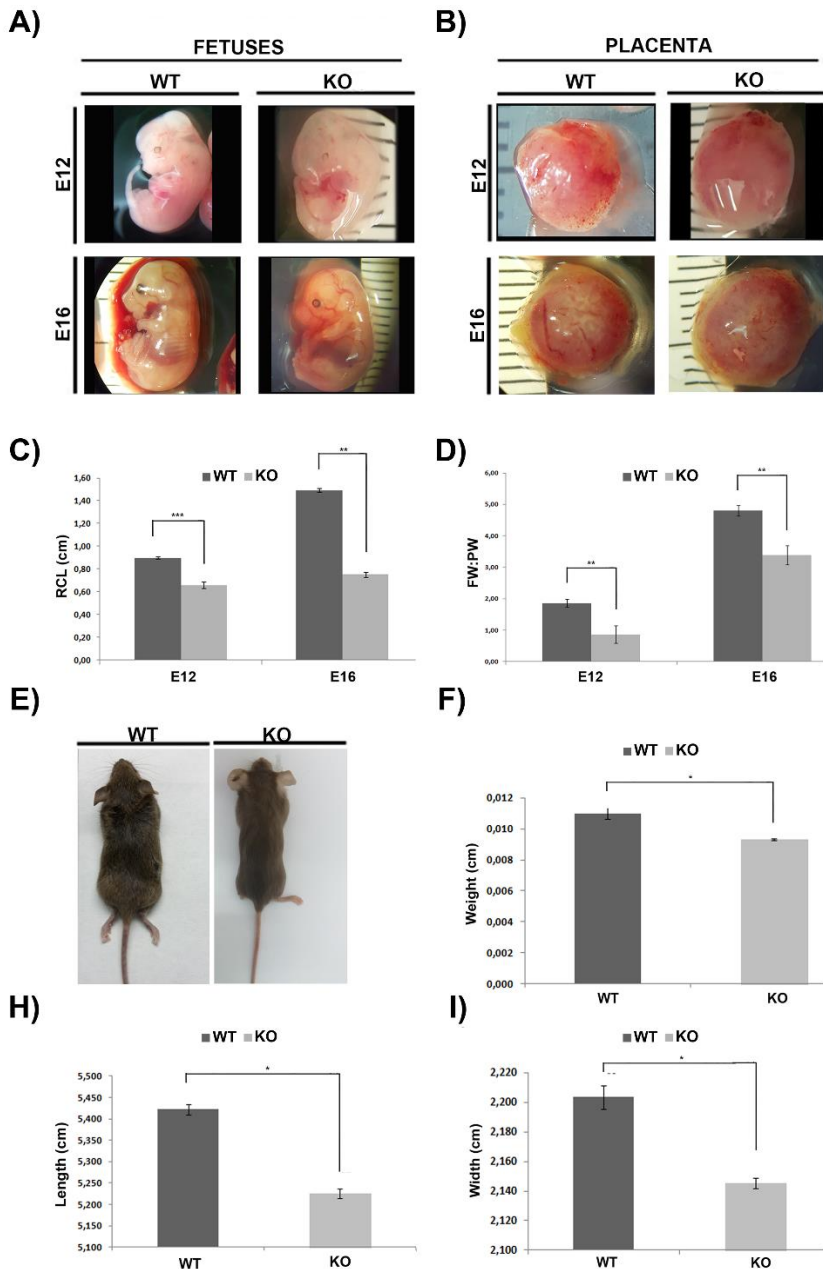
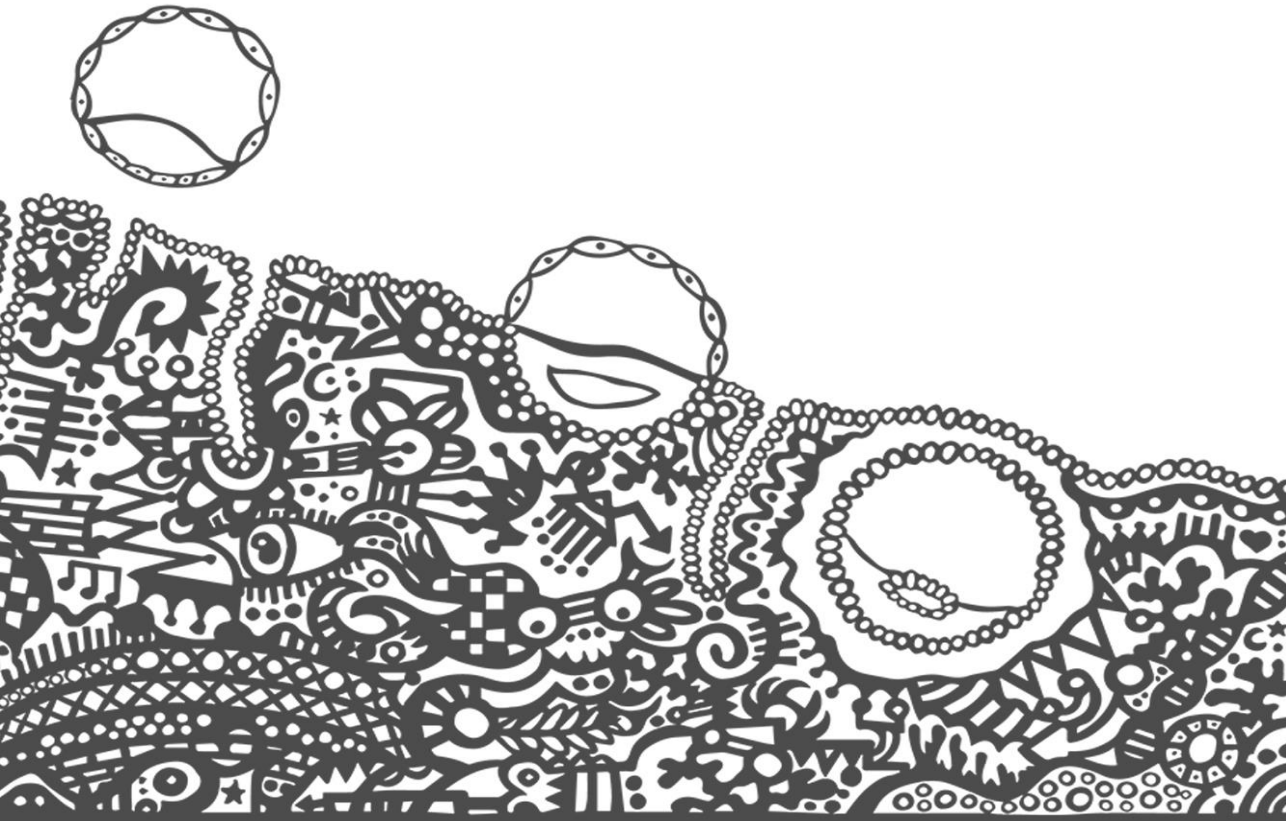


Figure 5.20. Characterization of the pregnancy outcome associated with miR-30d deficiency. Intrauterine growth restriction (IUGR) was evaluated by analyzing the fetuses and the placentas on day 12 (E12) and 16 (E16) of pregnancy (WT: E12 [n = 14]; E16 [n = 17]; KO: E12 [n = 12]; E16 [n = 5]). (A) Representative images of the fetuses obtained for the WT and

KO genotypes on day 12 and 16 of pregnancy. (B) Representative images of the placentas obtained for the WT and KO genotypes on day 12 (E12) and 16 (E16) of pregnancy. (C) Crump-rump length (CRL) determination for WT and KO genotype embryos on day 12 (E12) and 16 (E16) of pregnancy. There was a significant reduction in the RCL in the KO genotype on both days (RCL_E12 [$p = 0.0000$]; RCL_E16 [$p = 0.0000$]). (D) The FW:PW ratio estimated for the WT and KO genotypes on day 12 (E12) and 16 (E16) of pregnancy. A significant reduction in the FW:PW was observed in the KO genotype on both days (FW:PW_E12 [$p = 0.0120$]). (E) Representative images of weaned WT and KO mice (WT [$n = 40$]; KO [$n = 37$]). (F) Weight determination for WT and KO weaned mice after 4 weeks of delivery; there were significant differences between these genotypes ($p = 0.05$). (G) Length determination for weaned WT and KO mice 4 weeks after delivery; significant differences between these genotypes were detected ($p = 0.05$). (H) Width determination for WT and KO weaned mice 4 weeks after delivery; significant differences between these genotypes were detected ($p = 0.05$).

DISCUSSION



06 | **DISCUSSION**

Synchronized embryo and endometrium development is essential for successful pregnancy; in fact, the existence of embryo-endometrial asynchrony beyond a certain period results in defective implantation (Teh et al., 2016; Liang et al., 2017). To ensure synchronization, there must be intimate cross-talk between the embryo and the uterus. Besides regulating estrogen and progesterone, both the embryo and the endometrium can secrete unique signals directed towards the other which can adjust the pace of their development. For example, the embryo releases pregnancy recognition signals (e.g., chorionic gonadotropin in humans, interferon tau in ruminants) to prevent luteolysis by prostaglandin F₂ α and in so maintains an environment suitable for pregnancy. Likewise, uterine secretions regulate embryo developmental status and promote trophoctoderm proliferation, migration, and attachment to the endometrial LE. There is now growing interest in the study of this bidirectional communication microenvironment. In this context, the EF present in the uterine cavity is of special interest because of its incipient involvement in implantation and subsequent embryonic development. In fact, given the non-invasive nature of collecting this sample type, it is considered a promising source of endometrial receptivity biomarkers.

Substantial evidence for the presence of miRNAs in the exosomes and microvesicles found in EF has recently been uncovered. Our group demonstrated that differential miRNA expression profiles exist through the different phases of the menstrual cycle, and that miR-30d is the most overexpressed during the WOI. Further investigation showed that this miRNA could be transported through vesicles secreted by the maternal endometrium and can subsequently be internalized by murine embryos, and thus, modify their transcriptome. However, the mechanism by which this miRNA was incorporated into these vesicles remained unknown. Thus, the work presented here tried to identify proteins which may be

responsible for the incorporation of miR-30d into maternal-derived exosomes. MS/MS revealed the presence of proteins involved in several biological processes, including transcriptional changes, post-transcriptional modifications, cell adhesion, and embryonic morphogenesis (**Table 5.1**). Among these, hnRNPC1 was the most plausible candidate capable of such transportation because both co-localization (**Figure 5.3**) and FACS (**Figure 5.4**) analyses demonstrated its presence in the inner cavity of exosomes.

hnRNPC is the founding member of the heterogeneous nuclear ribonucleoproteins (hnRNP) family and was one of the first found to be involved in RNA splicing (Han et al., 2010). Apart from this function, it has been described to regulate the stabilization, transport, and biogenesis of mRNA (Rajagopalan et al., 1998, Shetty, 2005), and the internal ribosome entry site (IRES)-dependent translation of proteins implicated in cell division and apoptosis (Holcík et al., 2003, Kim et al., 2003). hnRNPC performs these functions as stable heterotetramers (Dreyfuss et al., 1993, McAfee et al., 1996) comprised of three molecules of the more abundant hnRNPC1 and one molecule of a slightly larger splice variant, hnRNPC2, which contains a 13 amino acid insertion (Burd et al., 1989). Both isoforms contain a basic leucine zipper-like RNA-binding motif, but the functional difference between the two variants remains unclear (McAfee et al., 1996). Normally, hnRNPC1/C2 resides mainly in the nucleus (Lee et al., 2004), but certain cellular conditions (e.g., apoptosis, mitosis, or viral infection) induce hnRNPC1/C2 to translocate from the nucleus to the cytoplasm (Nakielny and Dreyfuss, 1996, Gustin and Sarnow, 2001, Gustin and Sarnow, 2002, Kim et al., 2003, Lee et al., 2004a, Pettit Kneller et al., 2009). In fact, our results from the IN-Cell analyses allowed us to determine that some hnRNPC1 was detectable in the cytoplasmic compartment (**Figure 5.5**).

This is not the first time that hnRNPC1 has been identified as a candidate for miRNA transportation into the inner cavity of exosomes. Indeed, Villarrolla-

Beltri et al. identified two hnRNP families—hnRNPA1 and hnRNPC—that could potentially bind to exosomal miRNAs, suggesting that they might also be candidates for miRNA sorting (Villarroya-Beltri et al., 2013). However, their main discovery was that sumoylated hnRNPA2B1 can direct the loading of certain miRNAs into exosomes by recognizing specific short motifs (e.g., GGAG) located in the 3'-region of miRNAs. Moreover, they suggested that miRNAs destined for packaging and secretion in vesicles contained distinct sequence signatures that were perhaps cell or tissue-specific. In connection with this idea, a post-transcriptional modification process involving uridylation of miRNAs regulates sorting into MVBs and exosomes has been described (Koppers-Lalic et al., 2014). More specifically, it was discovered that the 3'-ends of uridylated endogenous miRNAs mainly present in urine or B-cell-derived exosomes, whereas the 3'-end of adenylated endogenous miRNAs was located in B cells. In any case, both selection modes indicate that the 3'-end of the miRNA sequence contains a critical sorting signal.

Apart from involvement of the hnRNP family in the miRNA cargo, alternative mechanisms which may be responsible for RNA packaging into exosomes have also been described (Guduric-Fuchs et al., 2012). However, despite the available information, it is unclear if these mechanisms are each specific to a given cell type or if they can act in a complementary way to direct miRNA packaging in cell-secreted vesicles. In any case, the evidence that hnRNPC1 represents a plausible mechanism of miR-30d transport into exosomes comes from our silencing assays in which the levels of miR-30d decreased in both hEECs (**Figure 5.7C**) and epithelial-derived exosomes (**Figure 5.7D**). This sharp reduction in miR-30d inside cells may be associated with a deficiency in the miRNA biogenesis machinery.

RNA binding proteins (RBPs) play pivotal roles in miRNA function by regulating their biogenesis, localization, and degradation (van Kouwenhove et al.,

2011). For instance, KH-type splicing regulatory protein (KSRP) promotes the biogenesis of a subset of miRNAs containing a GGG triplet motif in their terminal loop by enhancing Drosha-mediated microprocessing. More specifically, KSRP phosphorylation increases accessibility to pre-miRNAs thus, promoting miRNA biogenesis (Trabucchi et al., 2009). Similarly, hnRNPA1 binds to a conserved miRNA loop region which facilitates Drosha-mediated cleavage (Michlewski et al., 2009). However, hnRNPA1 negatively regulates let-7 miRNA biogenesis by interfering with KSRP binding at the terminal loop of pri-let-7-a. Therefore, although more exhaustive research is needed to determine exactly how hnRNPC1 interacts with miR-30d, its biological role in RNA splicing and mRNA stability appears to involve both miR-30d biogenesis and its subsequent transfer. Park et al. reached a similar conclusion and described that hnRNPC1 silencing is closely related to reduced levels of miR-21 in glioblastoma cells (Park et al., 2012).

Finally, proof-of-concept evidence in support the possible role of hnRNPC1 in miR-30d transfer comes from co-culturing WT or miR-30d KO embryos with sihnRNPC1 cells (**Figures 5.9, 5.10, and 5.11**). Knocking down hnRNPC1 compromises the detection of the miR-30d-CY3 signal throughout the embryo structure during two of the main stages of implantation: adhesion and invasion (**Figure 5.9 and 5.10**), and the miR-30d levels were significantly reduced regardless of whether the embryo was WT or KO. In turn, adhesion assays showed that transient silencing of hnRNPC1 resulted in a significant decrease in adhesion in both genotypes, although this reduction was more pronounced in miR-30d KO embryos (**Figure 5.11**). This adverse effect at the beginning of embryo implantation could be associated with an additive effect derived from the simultaneous absence of miR-30d miRNA and the protein hnRNPC1. Given these results, we posit that hnRNPC1 could play a role in mutual maternal-fetal communication, and in miR-30d biogenesis and its subsequent transport to trophectoderm cells. In any case, because we observed that impairing miR-30d transfer compromised embryo adhesion rates in an in vitro heterologous model, next we determined if these

results were comparable to a homologous in vivo miR-30d KO model and studied the impact this phenotype has on further embryonic development.

In mice, the uterus is non-responsive to blastocysts during the pre-receptive phase (days 1–3) but becomes receptive on day 4 of pregnancy or pseudopregnancy (Dey et al., 2004, Daikoku et al., 2011). The onset of receptivity entails critical structural alterations in the uterine LE, including a transition from high to low apicobasal polarity and loss of apical microvilli and the surface glycocalyx (Murphy, 2004; Sun et al., 2016). Thus, failure to acquire the physiological, cellular, and microstructural characteristics of uterine receptivity results in defective implantation (Cha et al., 2012).

To characterize the receptivity status of miR-30d KO mice, the expression of essential receptivity markers (Cox2, Lif, Msx1, Msx2, Esr, and Pgr) was evaluated by RT-qPCR, IF, and WB assays. There was a significant difference in marker mRNA levels in the early stages of receptivity in KO uteri, but surprisingly, this difference was not observed in the late stages (**Figure 5.12**). However, LIF protein levels were reduced in KO uteri throughout the WOI (**Figures 5.13 and 5.14**). It is generally assumed that miRNAs negatively regulate mRNA expression, however, this is not the first time that a member of the miR-30d family has been implicated in physiological contexts where the absence of one of its members causes protein downregulation. Inhibition of miR-30d using complementary locked nucleic acids (LNA30bcd) in epithelial-like cells resulted in significant SOX9 mRNA upregulation but substantial SOX9 protein downregulation, caused by a proteasome pathway alteration (Peck et al., 2016). Likewise, the miR-30d family enhanced protein production in Chinese hamster ovarian (CHO) cells by targeting Ubiquitin E3 ligase S-phase kinase-associated protein 2 from the ubiquitin pathway (Fischer et al., 2015). These observations suggest that miR-30d could be involved in managing the protein balance, depending on internal or external stimuli. As a result, fundamental cellular processes including cell cycle regulation, gene expression, apoptosis, and

signal transduction (Sadowski et al., 2012, Wang and Maldonado, 2006) could be compromised.

Hence, given the possible impairment of protein expression in the miR-30d KO model, variation in receptivity marker expression was evaluated in a maternal-fetal crosstalk context regulated by bi-directional miR-30d transfer. With that purpose, different embryo-transfer combinations were performed in both WT and KO females to cover all the possible maternal-embryo crosstalk scenarios. Interestingly, re-analysis of receptivity marker expression showed evidence of an intriguing modified fluorescence pattern for LIF (**Figures 5.16 and 5.17**). Thus, to determine if a defective implantation phenotype might accompany this dysregulation, we evaluated the IR at days 6.5–7 of pregnancy in the different transfer-conditions tested (**Figure 5.15**); the results suggest that a miR-30d-transfer deficiency between the mother and the embryo significantly decreased the IR. Of note, this impaired phenotype could be substantially recovered in the KO genotype after transferring KO embryos pretreated with a miR-30d analog (**Figure 5.15**). Interestingly, the variation in IR among the mice in the different transfer conditions coincided with that observed for the mean FIVs for LIF (**Figure 5.18A**). Furthermore, there was a positive correlation between the mean FIV for LIF and the IR registered, suggesting LIF as a potential indirect miR-30d target (**Figure 5.18B**).

LIF is an essential regulator of embryo implantation in mice and is a crucial receptivity marker in several mammalian species, including humans. Deregulation of LIF expression has been linked to several cases of female infertility associated with defective implantation (Hambartsumian, 1998, Mikołajczyk et al., 2007, Franasiak et al., 2014). In mice, LIF is maximally expressed in the endometrial GE just before implantation and LIF transcription increases in the GE within 1 h of E₂ administration and subsequently declines to basal levels (Chen et al., 2000). LIF produced in the GE is secreted into the uterine lumen where binding to the heterodimeric LIF receptor complex is stabilized. This complex comprises a LIF

receptor (LIFR) and glycoprotein 130 (gp130) and localizes to the apical membrane of the LE (Rosario et al., 2014). The stabilized LIF-LIFR-gp130 complex promotes activation of specific pathways crucial for the success of the implantation process, including the JAK/STAT3, MAPK, and PI3K signaling pathways (Aghajanova, 2010).

Other researchers have suggested that LIF is regulated by miRNAs, hence, the LIF mRNA expression pattern has been found to be virtually the inverse of miR-181a and miR-181b expression during pregnancy (Chu et al., 2015). In addition, administering miR-181a or miR-181b mimics to mice led to decreased LIF mRNA and protein levels in their uteri on day 4 of pregnancy. Likewise, miR-223-39 has been described to affect embryo implantation by suppressing the expression of LIF and pinopodes in the endometrium of pregnant mice (Dong et al., 2016).

It is important to consider that most researchers studying the role of miRNAs in endometrial receptivity highlight the effect exerted by the endometrium on the embryo, but not how this might influence the acquisition of endometrial receptivity. To date, the closest described in the literature is that of hEECs which were able to acquire fluorescently-tagged miR-661, a miRNA present in non-implanted blastocyst-conditioned medium (Cuman et al., 2015). Thus, extracellular miR-661 reduced trophoblast spheroid adhesion to hEECs, in so establishing a functional role for extracellular miRNAs in the maternal-fetal interface. Similarly, infusion of fluorescently-labeled embryo-derived EVs into the uterine horns of ewes near the time of implantation, resulted in the detection of fluorescence in the cytoplasm of the uterine LE and GE (Burns et al., 2016). These studies established that extracellular miRNAs originating from the embryo are internalized by uterine cells and modulate maternal gene expression, thus indicating the presence of a functional signaling role between the blastocyst and maternal endometrium during the WOI. In this context, here we show evidence that miRNAs transferred from early developmental-stage embryos impact endometrial function. In fact, as stated before, pretreatment of KO embryos with a miR-30d analog increased the mean

FIVs for LIF, as well as the percentage IR, in KO recipients (**Figure 5.15, 5.16, and 5.17**).

At this point, it is important to highlight the importance of evaluating the roles of extracellular miRNAs in improving our understanding of the fetal-maternal communication established during conception. In this sense, although many studies did not demonstrate bi-directional communication as such, they do reveal the functional relevance of miRNAs secreted by the embryo to the extracellular environment. In this sense, differential miRNA expression was identified in bovine embryos that developed to the blastocyst stage and those that were unable to progress past the morula stage (Kropp et al., 2014). Based on these observations, it was suggested for the first time that miRNAs present in culture media (CM) could be used as biological markers for selecting better quality embryos, thus improving the successful pregnancy rates obtained for in vitro fertilization (IVF) treatments. In another study, miR-24 was highly expressed in the CM from degenerate bovine embryos (Kropp and Khatib, 2015). In fact, supplementing the CM of normal morulas with miR-24 mimics impaired embryo development, inhibiting cell proliferation by targeting *CDKN1b*—a cell cycle inhibitor.

The presence of miRNAs in the CM from IVF human embryos was more recently confirmed (Rosenbluth et al., 2014). Specifically, this group reported that the expression levels of miR-191, miR-372, and miR-645 were higher in the media of failed IVF cycles compared to those resulting in a live birth. Similarly, a comprehensive analysis of the miRNA profiles present in the spent blastocyst culture media (SBCM) showed that miR-20a and miR-30c was overexpressed in SBCM from human blastocysts that implanted compared to those that did not, once again suggesting the importance of the miR-30d family as potential modulators of uterine functions (Capalbo et al., 2016). Likewise, the miRNAs in SBCM they analyzed were specific to the blastocyst stage, strengthening the idea that embryo sends signals into its environment to promote its subsequent

implantation process. Finally, miRNA secretion within EVs was identified in conditioned CM derived from the BeWo trophoblast cell line (Luo et al., 2009) and in primary human trophoblasts, suggesting their potential functional role in the maternal-fetal interface. Keeping this in mind, the miRNAs and protein cargo contained in porcine trophoblast cell-derived EVs were found to have a stimulatory effect on the proliferation of maternal endothelial cells, thus promoting angiogenesis (Bidarimath et al., 2017). Therefore, these findings support the idea that the content of EVs can elicit a biological response in recipient cells which leads to increased proliferation and is crucial to avoid implantation failure. In fact, extravillous trophoblast-derived exosomes may promote vascular smooth muscle cell migration, favoring the spiral uterine arterial remodeling observed in normal pregnancies (Salomon et al., 2014).

Defective implantation leads to adverse 'ripple' effects throughout pregnancy, including abnormal embryo spacing, retarded fetoplacental growth, and higher rates of resorption (Song et al., 2002, Ye et al., 2005). Consistent with this, the IS sizes in miR30d-KO females were significantly smaller at all the analyzed timepoints (**Figure 5.19A**) and, based on the CRL and FW:PW analysis, their fetuses exhibited retarded fetoplacental growth (**Figure 5.20**). These results suggest that miR-30d deficiency is associated with a modest effect on placental development.

The miR-30d-associated phenotypes observed, particularly those evident during implantation, might arise from altered epithelial-to-mesenchymal transition (EMT). EMT is the process by which an immotile, polarized, epithelial cell undergoes several biochemical changes to acquire mesenchymal cell characteristics, which include the ability to migrate and invade (Kalluri and Weinberg, 2009, E Davies et al., 2016). During normal placental development, villous cytotrophoblast differentiates into more invasive extravillous trophoblast (EVT), a process marked by an EMT (DaSilva-Arnold et al., 2015). Nevertheless, while EMT is tightly regulated and precisely orchestrated during normal

development, the dysregulation of EMT is associated with the pathological processes of tumor metastasis and cancer progression (Kalluri and Weinberg, 2009, E Davies et al., 2016) as well as with pregnancy disorders such as preeclampsia, fetal growth restriction (FGR; Du et al., 2017), and endometriosis (Marí-Alexandre et al., 2016).

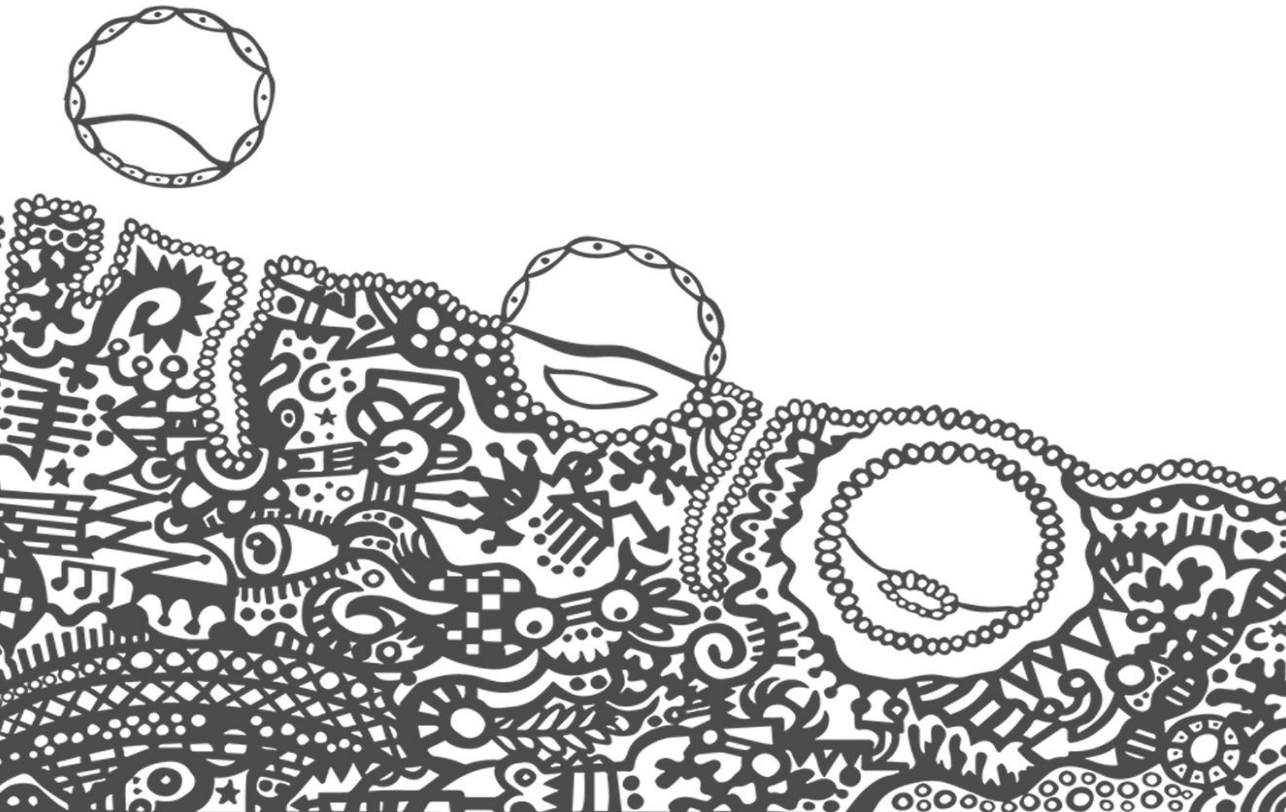
Recent studies have suggested that the EMT that occurs during implantation is partially regulated by the abundance of miR-30d (Cai et al., 2016). Specifically, reduced miR-30d expression promotes EMT and invasiveness and this impairs endometrial receptivity. Moreover, it has been suggested that miR-30d plays a functional role in TGF- β 1-induced EMT by targeting Snail 1. Therefore, it is feasible that miR-30d dysregulation could affect EMT in the KO murine model which could compromise the development of the fetal and maternal vasculature which facilitates nutrient, gas, and waste exchange. This may explain why weaned miR-30d KO mice have significantly lower weights, widths, and lengths than the WT genotype (**Figure 5.20 F, G, and H**).

Of note, pregnancy disorders arising from EMT alterations initiate at the level of defective decidualization, an event required to provide nutrients to the implanted embryo until a functional placenta is formed (Rosario and Stewart, 2016). Interestingly, LIF is an important regulator of this process, as shown by the fact that the uteri of LIF^{-/-} mice do not decidualize, even after using different well-established stimuli that induce this process (Chen et al., 2000). In line with an initial relationship between LIF and EMT, it has been suggested that, via its interaction with the apoptotic factor MCL1, STAT3 probably initiates EMTs by unknown paracrine mechanism(s) (Renjini et al., 2014). Likewise, recent studies have demonstrated that targeted inhibition of LIF signaling mid-gestation leads to abnormal trophoblast invasion and maternal decidual spiral artery (SA) remodeling in vivo in mice (Winship et al., 2015). In fact, it could be possible that fetal and

maternal vessel size may be significantly reduced in this study, thus compromising fetal-maternal exchange.

The phenotype observed in the miR-30d knockouts could result from a succession of events triggered by LIF. However, miRNAs promiscuously regulate many mRNAs (Mehta and Baltimore, 2016) and so miR-30d-deficient phenotypes could also be derived from the pleiotropic targets of miR-30d. Therefore, because current experiments only examine a limited range of this miRNA's potential range of action, further investigation and more data will be required to elucidate the full range of miR-30d regulation. However, given the effects that miR-30d had on the acquisition of a receptive endometrium and on subsequent embryo development, our initial hypothesis that this miRNA plays a role in the maternal-fetal interface has clearly been confirmed. In contrast, regarding the mechanism by which miR-30d is incorporated into exosomes, more experiments are still required to determine how the link between hnRNPC1 protein and miR-30d is established prior to this miRNA's release to the intrauterine environment.

CONCLUSIONS



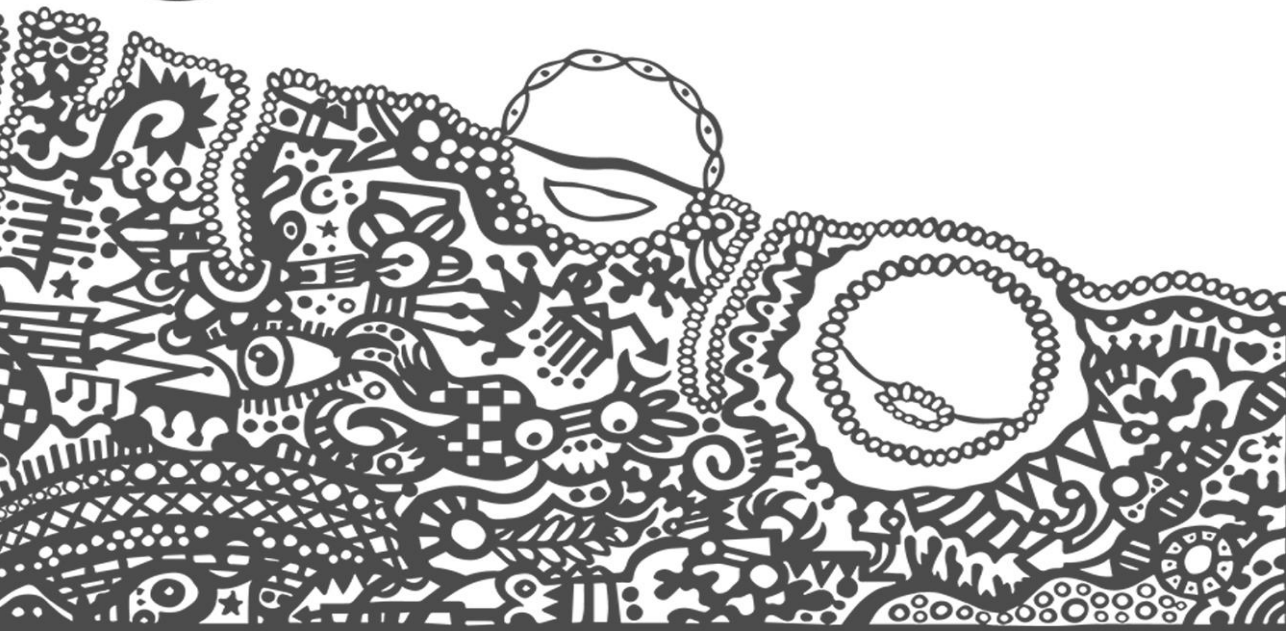
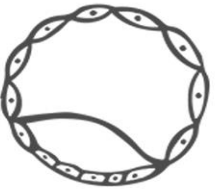
07 | CONCLUSIONS

- Mass spectrometry assays identified hnRNPC1 as a protein which might be responsible for transferring miR-30d into the inner cavity of hEEC-derived exosomes. Likewise, subsequent analysis verified both the presence of hnRNPC1 in exosomes and the link between miR-30 and hnRNPC1 inside them.
- Silencing hnRNPC1 in Ishikawa cells reduced the levels of miR-30d in the cells and their derived exosomes, suggesting that hnRNPC1 could be involved in miR-30d biogenesis. In turn, the transient silencing of hnRNPC1 resulted in a significant decrease in the adhesion rates of WT and miR-30d KO embryos, and this decrease was more significant in the KO genotype.
- Analysis of the receptivity markers in the miR-30d KO model shows that the absence of miR-30d affects LIF expression throughout the window of implantation, both in pseudopregnancy conditions as well as in different maternal-fetal communication contexts. In the latter case, transferring KO embryos pretreated with a miR-30d analog restored the basal levels of LIF fluorescence in both WT and KO uteri.
- Examination of the implantation phenotype in different maternal-fetal communication contexts revealed that blocking the transfer of miR-30d from the mother to the embryo or vice versa, significantly reduced the implantation rates achieved.
- The implantation rates in the different transfer conditions correlate with those observed for the LIF fluorescence values. Therefore, these results suggest that *Lif* constitutes a potential indirect miR-30d target.
- To some extent, the absence of miR-30d in pregnant females affects intrauterine growth, as reflected in the generation of smaller implantation

sites and higher rates of resorption in these females, as well as a significant decrease in the embryonic crown-rump-length and fetal weight/placental weight ratio parameters. Thus, the offspring from KO-genotype mice are smaller than those from the WT genotype.

- These analyses suggest that miR-30d plays an important role in regulating implantation and subsequent embryonic development through *Lif*. However, additional experiments are required to elucidate the function of miR-30d in the process of decidualization and subsequent vascularization.

REFERENCES



A

- Abdelfattah, A. M., Park, C. and Choi, M. Y. (2014)** 'Update on non-canonical microRNAs', *Biomol Concepts*, 5(4), pp. 275-87.
- Achache, H. and Revel, A. (2006)** 'Endometrial receptivity markers, the journey to successful embryo implantation', *Hum Reprod Update*, 12(6), pp. 731-46.
- Adams, N. R. and DeMayo, F. J. (2015)** 'The Role of Steroid Hormone Receptors in the Establishment of Pregnancy in Rodents', *Adv Anat Embryol Cell Biol*, 216, pp. 27-49.
- Agarwal, V., Bell, G. W., Nam, J. W. and Bartel, D. P. (2015)** 'Predicting effective microRNA target sites in mammalian mRNAs', *Elife*, 4.
- Aghajanova, L. (2010)** 'Update on the role of leukemia inhibitory factor in assisted reproduction', *Curr Opin Obstet Gynecol*, 22(3), pp. 213-9.
- Alappat, S., Zhang, Z. Y. and Chen, Y. P. (2003)** 'Msx homeobox gene family and craniofacial development', *Cell Res*, 13(6), pp. 429-42.
- Altmäe, S., Martinez-Conejero, J. A., Esteban, F. J., Ruiz-Alonso, M., Stavreus-Evers, A., Horcajadas, J. A. and Salumets, A. (2013)** 'MicroRNAs miR-30b, miR-30d, and miR-494 regulate human endometrial receptivity', *Reprod Sci*, 20(3), pp. 308-17.
- Ambros, V. (2001)** 'microRNAs: tiny regulators with great potential', *Cell*, 107(7), pp. 823-6.
- Aplin, J. D. (2006)** 'Embryo implantation: the molecular mechanism remains elusive', *Reprod Biomed Online*, 13(6), pp. 833-9.
- Arroyo, J. D., Chevillet, J. R., Kroh, E. M., Ruf, I. K., Pritchard, C. C., Gibson, D. F., Mitchell, P. S., Bennett, C. F., Pogosova-Agadjanyan, E. L., Stirewalt, D. L., Tait, J. F. and Tewari, M. (2011)** 'Argonaute2 complexes carry a population

of circulating microRNAs independent of vesicles in human plasma', *Proc Natl Acad Sci U S A*, 108(12), pp. 5003-8.

Atwood, C. S. and Vadakkadath Meethal, S. (2016) 'The spatiotemporal hormonal orchestration of human folliculogenesis, early embryogenesis and blastocyst implantation', *Mol Cell Endocrinol*, 430, pp. 33-48.

B

Barker, D. J. (2004) 'The developmental origins of adult disease', *J Am Coll Nutr*, 23(6 Suppl), pp. 588S-595S.

Basak, S., Dhar, R. and Das, C. (2002) 'Steroids modulate the expression of alpha4 integrin in mouse blastocysts and uterus during implantation', *Biol Reprod*, 66(6), pp. 1784-9.

Bass, K. E., Morrish, D., Roth, I., Bhardwaj, D., Taylor, R., Zhou, Y. and Fisher, S. J. (1994) 'Human cytotrophoblast invasion is up-regulated by epidermal growth factor: evidence that paracrine factors modify this process', *Dev Biol*, 164(2), pp. 550-61.

Bazer, F. W., Wu, G., Spencer, T. E., Johnson, G. A., Burghardt, R. C. and Bayless, K. (2010) 'Novel pathways for implantation and establishment and maintenance of pregnancy in mammals', *Mol Hum Reprod*, 16(3), pp. 135-52.

Ben-Shlomo, I. (2005) 'Sharing of unrelated receptors and ligands by cognate partners: possible implications for ovarian and endometrial physiology', *Reprod Biomed Online*, 11(2), pp. 259-69.

Bidarimath, M., Khalaj, K., Kridli, R. T., Kan, F. W., Koti, M. and Tayade, C. (2017) 'Extracellular vesicle mediated intercellular communication at the porcine maternal-fetal interface: A new paradigm for conceptus-endometrial cross-talk', *Sci Rep*, 7, pp. 40476.

Bidarimath, M., Khalaj, K., Wessels, J. M. and Tayade, C. (2014) 'MicroRNAs, immune cells and pregnancy', *Cell Mol Immunol*, 11(6), pp. 538-47.

- Bigsby, R. and Bethin, K. (2008)** 'Paracrine mediators of endometrial growth and differentiation', in Aplin, J., Fazleabas, A., Glasser, S. & Giudice, G. (eds.) *The endometrium*. Boca Ratón, FL: CRC Press, pp. 319-330
- Binder, N. K., Evans, J., Gardner, D. K., Salamonsen, L. A. and Hannan, N. J. (2014)** 'Endometrial signals improve embryo outcome: functional role of vascular endothelial growth factor isoforms on embryo development and implantation in mice', *Hum Reprod*, 29(10), pp. 2278-86.
- Bloor, D. J., Metcalfe, A. D., Rutherford, A., Brison, D. R. and Kimber, S. J. (2002)** 'Expression of cell adhesion molecules during human preimplantation embryo development', *Mol Hum Reprod*, 8(3), pp. 237-45.
- Bolte, S. and Cordelières, F. P. (2006)** 'A guided tour into subcellular colocalization analysis in light microscopy', *J Microsc*, 224(Pt 3), pp. 213-32.
- Borchert, G. M., Lanier, W. and Davidson, B. L. (2006)** 'RNA polymerase III transcribes human microRNAs', *Nat Struct Mol Biol*, 13(12), pp. 1097-101.
- Bowen, J. A. and Hunt, J. S. (2000)** 'The role of integrins in reproduction', *Proc Soc Exp Biol Med*, 223(4), pp. 331-43.
- Bratu, D. P., Catrina, I. E. and Marras, S. A. (2011)** 'Tiny molecular beacons for in vivo mRNA detection', *Methods Mol Biol*, 714, pp. 141-57.
- Brinsden, P. R., Alam, V., de Moustier, B. and Engrand, P. (2009)** 'Recombinant human leukemia inhibitory factor does not improve implantation and pregnancy outcomes after assisted reproductive techniques in women with recurrent unexplained implantation failure', *Fertil Steril*, 91(4 Suppl), pp. 1445-7.
- Bromfield, J. J., Schjenken, J. E., Chin, P. Y., Care, A. S., Jasper, M. J. and Robertson, S. A. (2014)** 'Maternal tract factors contribute to paternal seminal fluid impact on metabolic phenotype in offspring', *Proc Natl Acad Sci U S A*, 111(6), pp. 2200-5.
- Bui, T. D., Zhang, L., Rees, M. C., Bicknell, R. and Harris, A. L. (1997)** 'Expression and hormone regulation of Wnt2, 3, 4, 5a, 7a, 7b and 10b in normal

human endometrium and endometrial carcinoma', *Br J Cancer*, 75(8), pp. 1131-6.

Burd, C. G., Swanson, M. S., Görlach, M. and Dreyfuss, G. (1989) 'Primary structures of the heterogeneous nuclear ribonucleoprotein A2, B1, and C2 proteins: a diversity of RNA binding proteins is generated by small peptide inserts', *Proc Natl Acad Sci U S A*, 86(24), pp. 9788-92.

Burns, G., Brooks, K., Wildung, M., Navakanitworakul, R., Christenson, L. K. and Spencer, T. E. (2014) 'Extracellular vesicles in luminal fluid of the ovine uterus', *PLoS One*, 9(3), pp. e90913.

Burns, G. W., Brooks, K. E. and Spencer, T. E. (2016) 'Extracellular Vesicles Originate from the Conceptus and Uterus During Early Pregnancy in Sheep', *Biol Reprod*, 94(3), pp. 56.

C

Caballero-Campo, P., Domínguez, F., Coloma, J., Meseguer, M., Remohí, J., Pellicer, A. and Simón, C. (2002) 'Hormonal and embryonic regulation of chemokines IL-8, MCP-1 and RANTES in the human endometrium during the window of implantation', *Mol Hum Reprod*, 8(4), pp. 375-84.

Cai, J. L., Liu, L. L., Hu, Y., Jiang, X. M., Qiu, H. L., Sha, A. G., Wang, C. G., Zuo, Z. H. and Ren, J. Z. (2016) 'Polychlorinated biphenyls impair endometrial receptivity in vitro via regulating mir-30d expression and epithelial mesenchymal transition', *Toxicology*, 365, pp. 25-34.

Calkins, K. and Devaskar, S. U. (2011) 'Fetal origins of adult disease', *Curr Probl Pediatr Adolesc Health Care*, 41(6), pp. 158-76.

Capalbo, A., Ubaldi, F. M., Cimadomo, D., Noli, L., Khalaf, Y., Farcomeni, A., Ilic, D. and Rienzi, L. (2016) 'MicroRNAs in spent blastocyst culture medium are derived from trophoblast cells and can be explored for human embryo reproductive competence assessment', *Fertil Steril*, 105(1), pp. 225-35.e1-3.

- Carvalho-Gaspar, M., Billing, J. S., Spriewald, B. M. and Wood, K. J. (2005)** 'Chemokine gene expression during allograft rejection: comparison of two quantitative PCR techniques', *J Immunol Methods*, 301(1-2), pp. 41-52.
- Cha, J., Sun, X. and Dey, S. K. (2012)** 'Mechanisms of implantation: strategies for successful pregnancy', *Nat Med*, 18(12), pp. 1754-67.
- Cha, J., Vilella, F., Dey, S. K. and Simón, C. (2013)** 'Molecular interplay in successful implantation', *Science/AAAS*, (no. Ten critical topics in reproductive medicine), pp. 44-48.
- Chen, J. R., Cheng, J. G., Shatzer, T., Sewell, L., Hernandez, L. and Stewart, C. L. (2000)** 'Leukemia inhibitory factor can substitute for nidatory estrogen and is essential to inducing a receptive uterus for implantation but is not essential for subsequent embryogenesis', *Endocrinology*, 141(12), pp. 4365-72.
- Chen, X., Ba, Y., Ma, L., Cai, X., Yin, Y., Wang, K., Guo, J., Zhang, Y., Chen, J., Guo, X., Li, Q., Li, X., Wang, W., Wang, J., Jiang, X., Xiang, Y., Xu, C., Zheng, P., Zhang, J., Li, R., Zhang, H., Shang, X., Gong, T., Ning, G., Zen, K. and Zhang, C. Y. (2008)** 'Characterization of microRNAs in serum: a novel class of biomarkers for diagnosis of cancer and other diseases', *Cell Res*, 18(10), pp. 997-1006.
- Chimote, N. (2010)** 'Cytokines and growth factors in implantation', *Journal of Reproductive Biotechnology and Fertility*, 132(2), pp. 219-243.
- Chobotova, K., Spyropoulou, I., Carver, J., Manek, S., Heath, J. K., Gullick, W. J., Barlow, D. H., Sargent, I. L. and Mardon, H. J. (2002)** 'Heparin-binding epidermal growth factor and its receptor ErbB4 mediate implantation of the human blastocyst', *Mech Dev*, 119(2), pp. 137-44.
- Choi, S. Y., Yun, J., Lee, O. J., Han, H. S., Yeo, M. K., Lee, M. A. and Suh, K. S. (2013)** 'MicroRNA expression profiles in placenta with severe preeclampsia using a PNA-based microarray', *Placenta*, 34(9), pp. 799-804.

- Chu, B., Zhong, L., Dou, S., Wang, J., Li, J., Wang, M., Shi, Q., Mei, Y. and Wu, M. (2015)** 'miRNA-181 regulates embryo implantation in mice through targeting leukemia inhibitory factor', *J Mol Cell Biol*, 7(1), pp. 12-22.
- Clark, K., Pankov, R., Travis, M. A., Askari, J. A., Mould, A. P., Craig, S. E., Newham, P., Yamada, K. M. and Humphries, M. J. (2005)** 'A specific alpha5beta1-integrin conformation promotes directional integrin translocation and fibronectin matrix formation', *J Cell Sci*, 118(Pt 2), pp. 291-300.
- Cork, B. A., Li, T. C., Warren, M. A. and Laird, S. M. (2001)** 'Interleukin-11 (IL-11) in human endometrium: expression throughout the menstrual cycle and the effects of cytokines on endometrial IL-11 production in vitro', *J Reprod Immunol*, 50(1), pp. 3-17.
- Cork, B. A., Tuckerman, E. M., Li, T. C. and Laird, S. M. (2002)** 'Expression of interleukin (IL)-11 receptor by the human endometrium in vivo and effects of IL-11, IL-6 and LIF on the production of MMP and cytokines by human endometrial cells in vitro', *Mol Hum Reprod*, 8(9), pp. 841-8.
- Cuman, C., Van Sinderen, M., Gantier, M. P., Rainczuk, K., Sorby, K., Rombauts, L., Osianlis, T. and Dimitriadis, E. (2015)** 'Human Blastocyst Secreted microRNA Regulate Endometrial Epithelial Cell Adhesion', *EBioMedicine*, 2(10), pp. 1528-35.

D

- Daikoku, T., Cha, J., Sun, X., Tranguch, S., Xie, H., Fujita, T., Hirota, Y., Lydon, J., DeMayo, F., Maxson, R. and Dey, S. K. (2011)** 'Conditional deletion of Msx homeobox genes in the uterus inhibits blastocyst implantation by altering uterine receptivity', *Dev Cell*, 21(6), pp. 1014-25.
- Dakour, J., Li, H., Chen, H. and Morrish, D. W. (1999)** 'EGF promotes development of a differentiated trophoblast phenotype having c-myc and junB proto-oncogene activation', *Placenta*, 20(1), pp. 119-26.

- DaSilva-Arnold, S., James, J. L., Al-Khan, A., Zamudio, S. and Illsley, N. P. (2015)** 'Differentiation of first trimester cytotrophoblast to extravillous trophoblast involves an epithelial-mesenchymal transition', *Placenta*, 36(12), pp. 1412-8.
- Davidson, L. M. and Coward, K. (2016)** 'Molecular mechanisms of membrane interaction at implantation', *Birth Defects Res C Embryo Today*, 108(1), pp. 19-32.
- Dey, S. K., Lim, H., Das, S. K., Reese, J., Paria, B. C., Daikoku, T. and Wang, H. (2004)** 'Molecular cues to implantation', *Endocr Rev*, 25(3), pp. 341-73.
- Dimitriadis, E., Salamonsen, L. A. and Robb, L. (2000)** 'Expression of interleukin-11 during the human menstrual cycle: coincidence with stromal cell decidualization and relationship to leukaemia inhibitory factor and prolactin', *Mol Hum Reprod*, 6(10), pp. 907-14.
- Dimitriadis, E., White, C. A., Jones, R. L. and Salamonsen, L. A. (2005)** 'Cytokines, chemokines and growth factors in endometrium related to implantation', *Hum Reprod Update*, 11(6), pp. 613-30.
- Dominguez, F., Gadea, B., Mercader, A., Esteban, F. J., Pellicer, A. and Simón, C. (2010)** 'Embryologic outcome and secretome profile of implanted blastocysts obtained after coculture in human endometrial epithelial cells versus the sequential system', *Fertil Steril*, 93(3), pp. 774-782.e1.
- Dominguez, F., Galan, A., Martin, J. J., Remohi, J., Pellicer, A. and Simón, C. (2003)** 'Hormonal and embryonic regulation of chemokine receptors CXCR1, CXCR4, CCR5 and CCR2B in the human endometrium and the human blastocyst', *Mol Hum Reprod*, 9(4), pp. 189-98.
- Dong, X., Sui, C., Huang, K., Wang, L., Hu, D., Xiong, T., Wang, R. and Zhang, H. (2016)** 'MicroRNA-223-3p suppresses leukemia inhibitory factor expression and pinopodes formation during embryo implantation in mice', *Am J Transl Res*, 8(2), pp. 1155-63.

- Douglas, A. J. (2011)** 'Mother-offspring dialogue in early pregnancy: impact of adverse environment on pregnancy maintenance and neurobiology', *Prog Neuropsychopharmacol Biol Psychiatry*, 35(5), pp. 1167-77.
- Dreyfuss, G., Matunis, M. J., Piñol-Roma, S. and Burd, C. G. (1993)** 'hnRNP proteins and the biogenesis of mRNA', *Annu Rev Biochem*, 62, pp. 289-321.
- Du, L., Kuang, L., He, F., Tang, W., Sun, W. and Chen, D. (2017)** 'Mesenchymal-to-epithelial transition in the placental tissues of patients with preeclampsia', *Hypertens Res*, 40(1), pp. 67-72.
- Du, M. R., Wang, S. C. and Li, D. J. (2014)** 'The integrative roles of chemokines at the maternal-fetal interface in early pregnancy', *Cell Mol Immunol*, 11(5), pp. 438-48.
- Dunlap, K. A., Filant, J., Hayashi, K., Rucker, E. B., Song, G., Deng, J. M., Behringer, R. R., DeMayo, F. J., Lydon, J., Jeong, J. W. and Spencer, T. E. (2011)** 'Postnatal deletion of Wnt7a inhibits uterine gland morphogenesis and compromises adult fertility in mice', *Biol Reprod*, 85(2), pp. 386-96.

E

- E Davies, J., Pollheimer, J., Yong, H. E., Kokkinos, M. I., Kalionis, B., Knöfler, M. and Murthi, P. (2016)** 'Epithelial-mesenchymal transition during extravillous trophoblast differentiation', *Cell Adh Migr*, 10(3), pp. 310-21.
- Elovitz, M. A., Anton, L., Bastek, J. and Brown, A. G. (2015)** 'Can microRNA profiling in maternal blood identify women at risk for preterm birth?', *Am J Obstet Gynecol*, 212(6), pp. 782.e1-5.
- Elovitz, M. A., Brown, A. G., Anton, L., Gilstrop, M., Heiser, L. and Bastek, J. (2014)** 'Distinct cervical microRNA profiles are present in women destined to have a preterm birth', *Am J Obstet Gynecol*, 210(3), pp. 221.e1-11.
- Eun Kwon, H. and Taylor, H. S. (2004)** 'The role of HOX genes in human implantation', *Ann N Y Acad Sci*, 1034, pp. 1-18.

F

-
- Fischer, C. P., Kayisili, U. and Taylor, H. S. (2011)** 'HOXA10 expression is decreased in endometrium of women with adenomyosis', *Fertil Steril*, 95(3), pp. 1133-6.
- Fischer, S., Mathias, S., Schaz, S., Emmerling, V. V., Buck, T., Kleemann, M., Hackl, M., Grillari, J., Aschrafi, A., Handrick, R. and Otte, K. (2015)** 'Enhanced protein production by microRNA-30 family in CHO cells is mediated by the modulation of the ubiquitin pathway', *J Biotechnol*, 212, pp. 32-43.
- Foulk, R. A., Zdravkovic, T., Genbacev, O. and Prakobphol, A. (2007)** 'Expression of L-selectin ligand MECA-79 as a predictive marker of human uterine receptivity', *J Assist Reprod Genet*, 24(7), pp. 316-21.
- Franasiak, J. M., Holoch, K. J., Yuan, L., Schammel, D. P., Young, S. L. and Lessey, B. A. (2014)** 'Prospective assessment of midsecretory endometrial leukemia inhibitor factor expression versus $\alpha\beta 3$ testing in women with unexplained infertility', *Fertil Steril*, 101(6), pp. 1724-31.
- Friedman, R. C., Farh, K. K., Burge, C. B. and Bartel, D. P. (2009)** 'Most mammalian mRNAs are conserved targets of microRNAs', *Genome Res*, 19(1), pp. 92-105.
- Fujimoto, J., Hori, M., Ichigo, S. and Tamaya, T. (1997)** 'Ovarian steroids regulate the expression of basic fibroblast growth factor and its mRNA in fibroblasts derived from uterine endometrium', *Ann Clin Biochem*, 34 (Pt 1), pp. 91-6.
- Fässler, R. and Meyer, M. (1995)** 'Consequences of lack of beta 1 integrin gene expression in mice', *Genes Dev*, 9(15), pp. 1896-908.

G

- Gadina, M., Hilton, D., Johnston, J. A., Morinobu, A., Lighvani, A., Zhou, Y. J., Visconti, R. and O'Shea, J. J. (2001)** 'Signaling by type I and II cytokine receptors: ten years after', *Curr Opin Immunol*, 13(3), pp. 363-73.
- Gendron, R. L., Paradis, H., Hsieh-Li, H. M., Lee, D. W., Potter, S. S. and Markoff, E. (1997)** 'Abnormal uterine stromal and glandular function associated with maternal reproductive defects in Hoxa-11 null mice', *Biol Reprod*, 56(5), pp. 1097-105.
- Giudice, L. C. and Saleh, W. (1995)** 'Growth factors in reproduction', *Trends Endocrinol Metab*, 6(2), pp. 60-9.
- Gu, G., Gao, Q., Yuan, X., Huang, L. and Ge, L. (2012)** 'Immunolocalization of adipocytes and prostaglandin E2 and its four receptor proteins EP1, EP2, EP3, and EP4 in the caprine cervix during spontaneous term labor', *Biol Reprod*, 86(5), pp. 159, 1-10.
- Guduric-Fuchs, J., O'Connor, A., Camp, B., O'Neill, C. L., Medina, R. J. and Simpson, D. A. (2012)** 'Selective extracellular vesicle-mediated export of an overlapping set of microRNAs from multiple cell types', *BMC Genomics*, 13, pp. 357.
- Gustin, K. E. and Sarnow, P. (2001)** 'Effects of poliovirus infection on nucleocytoplasmic trafficking and nuclear pore complex composition', *EMBO J*, 20(1-2), pp. 240-9.
- Gustin, K. E. and Sarnow, P. (2002)** 'Inhibition of nuclear import and alteration of nuclear pore complex composition by rhinovirus', *J Virol*, 76(17), pp. 8787-96.

H

-
- Ha, M. and Kim, V. N. (2014)** 'Regulation of microRNA biogenesis', *Nat Rev Mol Cell Biol*, 15(8), pp. 509-24.
- Hambartsoumian, E. (1998)** 'Endometrial leukemia inhibitory factor (LIF) as a possible cause of unexplained infertility and multiple failures of implantation', *Am J Reprod Immunol*, 39(2), pp. 137-43.
- Han, S. P., Tang, Y. H. and Smith, R. (2010)** 'Functional diversity of the hnRNPs: past, present and perspectives', *Biochem J*, 430(3), pp. 379-92.
- Hanke, M., Hoefig, K., Merz, H., Feller, A. C., Kausch, I., Jocham, D., Warnecke, J. M. and Sczakiel, G. (2010)** 'A robust methodology to study urine microRNA as tumor marker: microRNA-126 and microRNA-182 are related to urinary bladder cancer', *Urol Oncol*, 28(6), pp. 655-61.
- Hannan, N. J., Paiva, P., Meehan, K. L., Rombauts, L. J., Gardner, D. K. and Salamonsen, L. A. (2011)** 'Analysis of fertility-related soluble mediators in human uterine fluid identifies VEGF as a key regulator of embryo implantation', *Endocrinology*, 152(12), pp. 4948-56.
- Hara, S., Kamei, D., Sasaki, Y., Tanemoto, A., Nakatani, Y. and Murakami, M. (2010)** 'Prostaglandin E synthases: Understanding their pathophysiological roles through mouse genetic models', *Biochimie*, 92(6), pp. 651-9.
- Hardy, K. and Spanos, S. (2002)** 'Growth factor expression and function in the human and mouse preimplantation embryo', *J Endocrinol*, 172(2), pp. 221-36.
- He, L. and Hannon, G. J. (2004)** 'MicroRNAs: small RNAs with a big role in gene regulation', *Nat Rev Genet*, 5(7), pp. 522-31.
- Hedlund, M., Stenqvist, A. C., Nagaeva, O., Kjellberg, L., Wulff, M., Baranov, V. and Mincheva-Nilsson, L. (2009)** 'Human placenta expresses and secretes NKG2D ligands via exosomes that down-modulate the cognate receptor

- expression: evidence for immunosuppressive function', *J Immunol*, 183(1), pp. 340-51.
- Hewitt, S. C. and Korach, K. S. (2003)** 'Oestrogen receptor knockout mice: roles for oestrogen receptors alpha and beta in reproductive tissues', *Reproduction*, 125(2), pp. 143-9.
- Hewitt, S. C., Li, L., Grimm, S. A., Chen, Y., Liu, L., Li, Y., Bushel, P. R., Fargo, D. and Korach, K. S. (2012)** 'Research resource: whole-genome estrogen receptor α binding in mouse uterine tissue revealed by ChIP-seq', *Mol Endocrinol*, 26(5), pp. 887-98.
- Holcík, M., Gordon, B. W. and Korneluk, R. G. (2003)** 'The internal ribosome entry site-mediated translation of antiapoptotic protein XIAP is modulated by the heterogeneous nuclear ribonucleoproteins C1 and C2', *Mol Cell Biol*, 23(1), pp. 280-8.
- Hoozemans, D. A., Schats, R., Lambalk, C. B., Homburg, R. and Hompes, P. G. (2004)** 'Human embryo implantation: current knowledge and clinical implications in assisted reproductive technology', *Reprod Biomed Online*, 9(6), pp. 692-715.
- Hromadnikova, I., Kotlabova, K., Ivankova, K. and Krofta, L. (2017)** 'First trimester screening of circulating C19MC microRNAs and the evaluation of their potential to predict the onset of preeclampsia and IUGR', *PLoS One*, 12(2), pp. e0171756.
- Hu, L., Han, J., Zheng, F., Ma, H., Chen, J., Jiang, Y. and Jiang, H. (2014)** 'Early second-trimester serum microRNAs as potential biomarker for nondiabetic macrosomia', *Biomed Res Int*, 2014, pp. 394125.
- Hunter, M. P., Ismail, N., Zhang, X., Aguda, B. D., Lee, E. J., Yu, L., Xiao, T., Schafer, J., Lee, M. L., Schmittgen, T. D., Nana-Sinkam, S. P., Jarjoura, D. and Marsh, C. B. (2008)** 'Detection of microRNA expression in human peripheral blood microvesicles', *PLoS One*, 3(11), pp. e3694.

I

- Ihle, J. N. (1995)** 'Cytokine receptor signalling', *Nature*, 377(6550), pp. 591-4.
- Ihle, J. N. (2001)** 'The Stat family in cytokine signaling', *Curr Opin Cell Biol*, 13(2), pp. 211-7.
- Irvine, R. F. (1982)** 'How is the level of free arachidonic acid controlled in mammalian cells?', *Biochem J*, 204(1), pp. 3-16.

J

- Jones, R. L., Stoikos, C., Findlay, J. K. and Salamonsen, L. A. (2006)** 'TGF-beta superfamily expression and actions in the endometrium and placenta', *Reproduction*, 132(2), pp. 217-32.

K

- Kalluri, R. and Weinberg, R. A. (2009)** 'The basics of epithelial-mesenchymal transition', *J Clin Invest*, 119(6), pp. 1420-8.
- Kaye, P. L. (1997)** 'Preimplantation growth factor physiology', *Rev Reprod*, 2(2), pp. 121-7.
- Kim, J. H., Paek, K. Y., Choi, K., Kim, T. D., Hahm, B., Kim, K. T. and Jang, S. K. (2003)** 'Heterogeneous nuclear ribonucleoprotein C modulates translation of c-myc mRNA in a cell cycle phase-dependent manner', *Mol Cell Biol*, 23(2), pp. 708-20.
- Kingsley, D. M. (1994)** 'The TGF-beta superfamily: new members, new receptors, and new genetic tests of function in different organisms', *Genes Dev*, 8(2), pp. 133-46.
- Komatsu, M., Carraway, C. A., Fregien, N. L. and Carraway, K. L. (1997)** 'Reversible disruption of cell-matrix and cell-cell interactions by overexpression of sialomucin complex', *J Biol Chem*, 272(52), pp. 33245-54.

- Koppers-Lalic, D., Hackenberg, M., Bijnsdorp, I. V., van Eijndhoven, M. A. J., Sadek, P., Sie, D., Zini, N., Middeldorp, J. M., Ylstra, B., de Menezes, R. X., Würdinger, T., Meijer, G. A. and Pegtel, D. M. (2014)** 'Nontemplated nucleotide additions distinguish the small RNA composition in cells from exosomes', *Cell Rep*, 8(6), pp. 1649-1658.
- Kosaka, N., Iguchi, H., Yoshioka, Y., Takeshita, F., Matsuki, Y. and Ochiya, T. (2010)** 'Secretory mechanisms and intercellular transfer of microRNAs in living cells', *J Biol Chem*, 285(23), pp. 17442-52.
- Krege, J. H., Hodgin, J. B., Couse, J. F., Enmark, E., Warner, M., Mahler, J. F., Sar, M., Korach, K. S., Gustafsson, J. A. and Smithies, O. (1998)** 'Generation and reproductive phenotypes of mice lacking estrogen receptor beta', *Proc Natl Acad Sci U S A*, 95(26), pp. 15677-82.
- Kropp, J. and Khatib, H. (2015)** 'Characterization of microRNA in bovine in vitro culture media associated with embryo quality and development', *J Dairy Sci*, 98(9), pp. 6552-63.
- Kropp, J., Salih, S. M. and Khatib, H. (2014)** 'Expression of microRNAs in bovine and human preimplantation embryo culture media', *Front Genet*, 5, pp. 91.
- Krumlauf, R. (1994)** 'Hox genes in vertebrate development', *Cell*, 78(2), pp. 191-201.
- Kuokkanen, S., Chen, B., Ojalvo, L., Benard, L., Santoro, N. and Pollard, J. W. (2010)** 'Genomic profiling of microRNAs and messenger RNAs reveals hormonal regulation in microRNA expression in human endometrium', *Biol Reprod*, 82(4), pp. 791-801.

L

- Larrea, E., Sole, C., Manterola, L., Goicoechea, I., Armesto, M., Arestin, M., Caffarel, M. M., Araujo, A. M., Araiz, M., Fernandez-Mercado, M. and Lawrie, C. H. (2016)** 'New Concepts in Cancer Biomarkers: Circulating miRNAs in Liquid Biopsies', *Int J Mol Sci*, 17(5).

- Lee, H. H., Chien, C. L., Liao, H. K., Chen, Y. J. and Chang, Z. F. (2004a)** 'Nuclear efflux of heterogeneous nuclear ribonucleoprotein C1/C2 in apoptotic cells: a novel nuclear export dependent on Rho-associated kinase activation', *J Cell Sci*, 117(Pt 23), pp. 5579-89.
- Lee, K., Jeong, J., Kwak, I., Yu, C. T., Lanske, B., Soegiarto, D. W., Toftgard, R., Tsai, M. J., Tsai, S., Lydon, J. P. and DeMayo, F. J. (2006)** 'Indian hedgehog is a major mediator of progesterone signaling in the mouse uterus', *Nat Genet*, 38(10), pp. 1204-9.
- Lee, Y., Kim, M., Han, J., Yeom, K. H., Lee, S., Baek, S. H. and Kim, V. N. (2004b)** 'MicroRNA genes are transcribed by RNA polymerase II', *EMBO J*, 23(20), pp. 4051-60.
- Lessey, B. A., Castelbaum, A. J., Sawin, S. W., Buck, C. A., Schinnar, R., Bilker, W. and Strom, B. L. (1994)** 'Aberrant integrin expression in the endometrium of women with endometriosis', *J Clin Endocrinol Metab*, 79(2), pp. 643-9.
- Lessey, B. A., Damjanovich, L., Coutifaris, C., Castelbaum, A., Albelda, S. M. and Buck, C. A. (1992)** 'Integrin adhesion molecules in the human endometrium. Correlation with the normal and abnormal menstrual cycle', *J Clin Invest*, 90(1), pp. 188-95.
- Li, H., Ge, Q., Guo, L. and Lu, Z. (2013)** 'Maternal plasma miRNAs expression in preeclamptic pregnancies', *Biomed Res Int*, 2013, pp. 970265.
- Li, R. H. and Zhuang, L. Z. (1997)** 'The effects of growth factors on human normal placental cytotrophoblast cell proliferation', *Hum Reprod*, 12(4), pp. 830-4.
- Liang, J., Wang, S. and Wang, Z. (2017)** 'Role of microRNAs in embryo implantation', *Reprod Biol Endocrinol*, 15(1), pp. 90.
- Lim, H., Das, S. K. and Dey, S. K. (1998)** 'erbB genes in the mouse uterus: cell-specific signaling by epidermal growth factor (EGF) family of growth factors during implantation', *Dev Biol*, 204(1), pp. 97-110.
- Lim, H., Gupta, R. A., Ma, W. G., Paria, B. C., Moller, D. E., Morrow, J. D., DuBois, R. N., Trzaskos, J. M. and Dey, S. K. (1999a)** 'Cyclo-oxygenase-2-derived

- prostacyclin mediates embryo implantation in the mouse via PPARdelta', *Genes Dev*, 13(12), pp. 1561-74.
- Lim, H., Ma, L., Ma, W. G., Maas, R. L. and Dey, S. K. (1999b)** 'Hoxa-10 regulates uterine stromal cell responsiveness to progesterone during implantation and decidualization in the mouse', *Mol Endocrinol*, 13(6), pp. 1005-17.
- Lim, H., Paria, B. C., Das, S. K., Dinchuk, J. E., Langenbach, R., Trzaskos, J. M. and Dey, S. K. (1997)** 'Multiple female reproductive failures in cyclooxygenase 2-deficient mice', *Cell*, 91(2), pp. 197-208.
- Linjawi, S., Li, T. C., Tuckerman, E. M., Blakemore, A. I. and Laird, S. M. (2004)** 'Expression of interleukin-11 receptor alpha and interleukin-11 protein in the endometrium of normal fertile women and women with recurrent miscarriage', *J Reprod Immunol*, 64(1-2), pp. 145-55.
- Liu, W., Niu, Z., Li, Q., Pang, R. T., Chiu, P. C. and Yeung, W. S. (2016)** 'MicroRNA and Embryo Implantation', *Am J Reprod Immunol*, 75(3), pp. 263-71.
- Luo, S. S., Ishibashi, O., Ishikawa, G., Ishikawa, T., Katayama, A., Mishima, T., Takizawa, T., Shigihara, T., Goto, T., Izumi, A., Ohkuchi, A., Matsubara, S. and Takeshita, T. (2009)** 'Human villous trophoblasts express and secrete placenta-specific microRNAs into maternal circulation via exosomes', *Biol Reprod*, 81(4), pp. 717-29.
- Lydon, J. P., DeMayo, F. J., Funk, C. R., Mani, S. K., Hughes, A. R., Montgomery, C. A., Shyamala, G., Conneely, O. M. and O'Malley, B. W. (1995)** 'Mice lacking progesterone receptor exhibit pleiotropic reproductive abnormalities', *Genes Dev*, 9(18), pp. 2266-78.

M

- Maccani, M. A. and Marsit, C. J. (2009)** 'Epigenetics in the placenta', *Am J Reprod Immunol*, 62(2), pp. 78-89.

- Makrigiannakis, A., Minas, V., Kalantaridou, S. N., Nikas, G. and Chrousos, G. P. (2006)** 'Hormonal and cytokine regulation of early implantation', *Trends Endocrinol Metab*, 17(5), pp. 178-85.
- Maruo, T., Matsuo, H., Otani, T. and Mochizuki, M. (1995)** 'Role of epidermal growth factor (EGF) and its receptor in the development of the human placenta', *Reprod Fertil Dev*, 7(6), pp. 1465-70.
- Marí-Alexandre, J., Sánchez-Izquierdo, D., Gilabert-Estellés, J., Barceló-Molina, M., Braza-Boïls, A. and Sandoval, J. (2016)** 'miRNAs Regulation and Its Role as Biomarkers in Endometriosis', *Int J Mol Sci*, 17(1).
- Matsuzaki, S., Canis, M., Darcha, C., Pouly, J. L. and Mage, G. (2009)** 'HOXA-10 expression in the mid-secretory endometrium of infertile patients with either endometriosis, uterine fibromas or unexplained infertility', *Hum Reprod*, 24(12), pp. 3180-7.
- McAfee, J. G., Soltaninassab, S. R., Lindsay, M. E. and LeSturgeon, W. M. (1996)** 'Proteins C1 and C2 of heterogeneous nuclear ribonucleoprotein complexes bind RNA in a highly cooperative fashion: support for their contiguous deposition on pre-mRNA during transcription', *Biochemistry*, 35(4), pp. 1212-22.
- Mehta, A. and Baltimore, D. (2016)** 'MicroRNAs as regulatory elements in immune system logic', *Nat Rev Immunol*, 16(5), pp. 279-94.
- Meseguer, M., Aplin, J. D., Caballero-Campo, P., O'Connor, J. E., Martín, J. C., Remohí, J., Pellicer, A. and Simón, C. (2001)** 'Human endometrial mucin MUC1 is up-regulated by progesterone and down-regulated in vitro by the human blastocyst', *Biol Reprod*, 64(2), pp. 590-601.
- Michell, D. L. and Vickers, K. C. (2016)** 'Lipoprotein carriers of microRNAs', *Biochim Biophys Acta*, 1861(12 Pt B), pp. 2069-2074.
- Michlewski, G., Guil, S., Semple, C. A. and Cáceres, J. F. (2008)** 'Posttranscriptional regulation of miRNAs harboring conserved terminal loops', *Mol Cell*, 32(3), pp. 383-93.

- Mikolajczyk, M., Wirstlein, P. and Skrzypczak, J. (2007)** 'The impact of leukemia inhibitory factor in uterine flushing on the reproductive potential of infertile women--a prospective study', *Am J Reprod Immunol*, 58(1), pp. 65-74.
- Minas, V., Loutradis, D. and Makrigiannakis, A. (2005)** 'Factors controlling blastocyst implantation', *Reprod Biomed Online*, 10(2), pp. 205-16.
- Mitchell, P. S., Parkin, R. K., Kroh, E. M., Fritz, B. R., Wyman, S. K., Pogosova-Agadjanyan, E. L., Peterson, A., Noteboom, J., O'Briant, K. C., Allen, A., Lin, D. W., Urban, N., Drescher, C. W., Knudsen, B. S., Stirewalt, D. L., Gentleman, R., Vessella, R. L., Nelson, P. S., Martin, D. B. and Tewari, M. (2008)** 'Circulating microRNAs as stable blood-based markers for cancer detection', *Proc Natl Acad Sci U S A*, 105(30), pp. 10513-8.
- Morales Prieto, D. M. and Markert, U. R. (2011)** 'MicroRNAs in pregnancy', *J Reprod Immunol*, 88(2), pp. 106-11.
- Munaut, C., Tebache, L., Blacher, S., Noël, A., Nisolle, M. and Chantraine, F. (2016)** 'Dysregulated circulating miRNAs in preeclampsia', *Biomed Rep*, 5(6), pp. 686-692.
- Murphy, C. R. (2004)** 'Uterine receptivity and the plasma membrane transformation', *Cell Res*, 14(4), pp. 259-67.

N

- Nakielny, S. and Dreyfuss, G. (1996)** 'The hnRNP C proteins contain a nuclear retention sequence that can override nuclear export signals', *J Cell Biol*, 134(6), pp. 1365-73.
- Nallasamy, S., Li, Q., Bagchi, M. K. and Bagchi, I. C. (2012)** 'Msx homeobox genes critically regulate embryo implantation by controlling paracrine signaling between uterine stroma and epithelium', *PLoS Genet*, 8(2), pp. e1002500.

- Ng, Y. H., Rome, S., Jalabert, A., Forterre, A., Singh, H., Hincks, C. L. and Salamonsen, L. A. (2013)** 'Endometrial exosomes/microvesicles in the uterine microenvironment: a new paradigm for embryo-endometrial cross talk at implantation', *PLoS One*, 8(3), pp. e58502.
- Nikas, G. and Psychoyos, A. (1997)** 'Uterine pinopodes in peri-implantation human endometrium. Clinical relevance', *Ann N Y Acad Sci*, 816, pp. 129-42.
- Nishida, M. (2002)** 'The Ishikawa cells from birth to the present', *Hum Cell*, 15(3), pp. 104-17.

O

- O'Neill, C. (2008)** 'The potential roles for embryotrophic ligands in preimplantation embryo development', *Hum Reprod Update*, 14(3), pp. 275-88.
- Olayioye, M. A., Neve, R. M., Lane, H. A. and Hynes, N. E. (2000)** 'The ErbB signaling network: receptor heterodimerization in development and cancer', *EMBO J*, 19(13), pp. 3159-67.
- Ozbilgin, K., Karaca, F., Turan, A., Köse, C., Vatanserver, S. and Ozcakir, T. (2015)** 'The higher heparin-binding epidermal growth factor (HB-EGF) in missed abortion', *Taiwan J Obstet Gynecol*, 54(1), pp. 13-8.

P

- P. Hess, A., R. Nayak, N. and Giudice, L. (2006)** *Oviduct and Endometrium Cyclic Changes in the Primate Oviduct and Endometrium*.
- Paria, B. C., Elenius, K., Klagsbrun, M. and Dey, S. K. (1999)** 'Heparin-binding EGF-like growth factor interacts with mouse blastocysts independently of ErbB1: a possible role for heparan sulfate proteoglycans and ErbB4 in blastocyst implantation', *Development*, 126(9), pp. 1997-2005.

- Park, N. J., Zhou, H., Elashoff, D., Henson, B. S., Kastratovic, D. A., Abemayor, E. and Wong, D. T. (2009)** 'Salivary microRNA: discovery, characterization, and clinical utility for oral cancer detection', *Clin Cancer Res*, 15(17), pp. 5473-7.
- Park, Y. M., Hwang, S. J., Masuda, K., Choi, K. M., Jeong, M. R., Nam, D. H., Gorospe, M. and Kim, H. H. (2012)** 'Heterogeneous nuclear ribonucleoprotein C1/C2 controls the metastatic potential of glioblastoma by regulating PDCD4', *Mol Cell Biol*, 32(20), pp. 4237-44.
- Pavelock, K., Braas, K., Ouafik, L., Osol, G. and May, V. (2001)** 'Differential expression and regulation of the vascular endothelial growth factor receptors neuropilin-1 and neuropilin-2 in rat uterus', *Endocrinology*, 142(2), pp. 613-22.
- Peck, B. C., Sincavage, J., Feinstein, S., Mah, A. T., Simmons, J. G., Lund, P. K. and Sethupathy, P. (2016)** 'miR-30 Family Controls Proliferation and Differentiation of Intestinal Epithelial Cell Models by Directing a Broad Gene Expression Program That Includes SOX9 and the Ubiquitin Ligase Pathway', *J Biol Chem*, 291(31), pp. 15975-84.
- Pellicer, A., Ardiles, G., Neuspiller, F., Remohí, J., Simón, C. and Bonilla-Musoles, F. (1998)** 'Evaluation of the ovarian reserve in young low responders with normal basal levels of follicle-stimulating hormone using three-dimensional ultrasonography', *Fertil Steril*, 70(4), pp. 671-5.
- Pettit Kneller, E. L., Connor, J. H. and Lyles, D. S. (2009)** 'hnRNPs Relocalize to the cytoplasm following infection with vesicular stomatitis virus', *J Virol*, 83(2), pp. 770-80.
- Piek, E., Heldin, C. H. and Ten Dijke, P. (1999)** 'Specificity, diversity, and regulation in TGF-beta superfamily signaling', *FASEB J*, 13(15), pp. 2105-24.
- Pieters, B. C., Arntz, O. J., Bennink, M. B., Broeren, M. G., van Caam, A. P., Koenders, M. I., van Lent, P. L., van den Berg, W. B., de Vries, M., van der Kraan, P. M. and van de Loo, F. A. (2015)** 'Commercial cow milk contains

physically stable extracellular vesicles expressing immunoregulatory TGF- β ', *PLoS One*, 10(3), pp. e0121123.

Q

Qian, K., Hu, L., Chen, H., Li, H., Liu, N., Li, Y., Ai, J., Zhu, G., Tang, Z. and Zhang, H. (2009) 'Hsa-miR-222 is involved in differentiation of endometrial stromal cells in vitro', *Endocrinology*, 150(10), pp. 4734-43.

R

Rajagopalan, L. E., Westmark, C. J., Jarzembowski, J. A. and Malter, J. S. (1998) 'hnRNP C increases amyloid precursor protein (APP) production by stabilizing APP mRNA', *Nucleic Acids Res*, 26(14), pp. 3418-23.

Ramathal, C. Y., Bagchi, I. C., Taylor, R. N. and Bagchi, M. K. (2010) 'Endometrial decidualization: of mice and men', *Semin Reprod Med*, 28(1), pp. 17-26.

Raposo, G. and Stoorvogel, W. (2013) 'Extracellular vesicles: exosomes, microvesicles, and friends', *J Cell Biol*, 200(4), pp. 373-83.

Rathjen, P. D., Toth, S., Willis, A., Heath, J. K. and Smith, A. G. (1990) 'Differentiation inhibiting activity is produced in matrix-associated and diffusible forms that are generated by alternate promoter usage', *Cell*, 62(6), pp. 1105-14.

Record, M., Carayon, K., Poirot, M. and Silvente-Poirot, S. (2014) 'Exosomes as new vesicular lipid transporters involved in cell-cell communication and various pathophysiologicals', *Biochim Biophys Acta*, 1841(1), pp. 108-20.

Redman, C. W., Tannetta, D. S., Dragovic, R. A., Gardiner, C., Southcombe, J. H., Collett, G. P. and Sargent, I. L. (2012) 'Review: Does size matter? Placental debris and the pathophysiology of pre-eclampsia', *Placenta*, 33 Suppl, pp. S48-54.

- Renjini, A. P., Titus, S., Narayan, P., Murali, M., Jha, R. K. and Laloraya, M. (2014)** 'STAT3 and MCL-1 associate to cause a mesenchymal epithelial transition', *J Cell Sci*, 127(Pt 8), pp. 1738-50.
- Revel, A., Achache, H., Stevens, J., Smith, Y. and Reich, R. (2011)** 'MicroRNAs are associated with human embryo implantation defects', *Hum Reprod*, 26(10), pp. 2830-40.
- Richter, K. S. (2008)** 'The importance of growth factors for preimplantation embryo development and in-vitro culture', *Curr Opin Obstet Gynecol*, 20(3), pp. 292-304.
- Robertson, S., Aplin, J. and Fazleabas, A. (2008)** 'Cytokine and chemokine regulation of endometrial immunobiology', in Aplin, J., Fazleabas, A., Glasser, S. & Giudice, L. (eds.) *The endometrium*. Second ed. Boca Ratón: CRC Press, pp. 547-569
- Robertson, S. A. and Moldenhauer, L. M. (2014)** 'Immunological determinants of implantation success', *Int J Dev Biol*, 58(2-4), pp. 205-17.
- Robertson, S. A., O'Connell, A. and Ramsey, A. (2000)** *The effect of interleukin-6 deficiency on implantation, fetal development and parturition in mice*.
- Robertson, S. A., Seamark, R. F., Guilbert, L. J. and Wegmann, T. G. (1994)** 'The role of cytokines in gestation', *Crit Rev Immunol*, 14(3-4), pp. 239-92.
- Rosario, G. X., Hondo, E., Jeong, J. W., Mutalif, R., Ye, X., Yee, L. X. and Stewart, C. L. (2014)** 'The LIF-mediated molecular signature regulating murine embryo implantation', *Biol Reprod*, 91(3), pp. 66.
- Rosario, G. X. and Stewart, C. L. (2016)** 'The Multifaceted Actions of Leukaemia Inhibitory Factor in Mediating Uterine Receptivity and Embryo Implantation', *Am J Reprod Immunol*, 75(3), pp. 246-55.
- Rosenbluth, E. M., Shelton, D. N., Wells, L. M., Sparks, A. E. and Van Voorhis, B. J. (2014)** 'Human embryos secrete microRNAs into culture media--a potential biomarker for implantation', *Fertil Steril*, 101(5), pp. 1493-500.

Ruan, Y. C., Guo, J. H., Liu, X., Zhang, R., Tsang, L. L., Dong, J. D., Chen, H., Yu, M. K., Jiang, X., Zhang, X. H., Fok, K. L., Chung, Y. W., Huang, H., Zhou, W. L. and Chan, H. C. (2012) 'Activation of the epithelial Na⁺ channel triggers prostaglandin E₂ release and production required for embryo implantation', *Nat Med*, 18(7), pp. 1112-7.

Rubel, C. A., Lanz, R. B., Kommagani, R., Franco, H. L., Lydon, J. P. and DeMayo, F. J. (2012) 'Research resource: Genome-wide profiling of progesterone receptor binding in the mouse uterus', *Mol Endocrinol*, 26(8), pp. 1428-42.

S

Saadeldin, I. M., Kim, S. J., Choi, Y. B. and Lee, B. C. (2014) 'Improvement of cloned embryos development by co-culturing with parthenotes: a possible role of exosomes/microvesicles for embryos paracrine communication', *Cell Reprogram*, 16(3), pp. 223-34.

Saadeldin, I. M., Oh, H. J. and Lee, B. C. (2015) 'Embryonic-maternal cross-talk via exosomes: potential implications', *Stem Cells Cloning*, 8, pp. 103-7.

Sadowski, M., Suryadinata, R., Tan, A. R., Roesley, S. N. and Sarcevic, B. (2012) 'Protein monoubiquitination and polyubiquitination generate structural diversity to control distinct biological processes', *IUBMB Life*, 64(2), pp. 136-42.

Saeki, Y., Wataya-Kaneda, M., Tanaka, K. and Kaneda, Y. (1998) 'Sustained transgene expression in vitro and in vivo using an Epstein-Barr virus replicon vector system combined with HVJ liposomes', *Gene Ther*, 5(8), pp. 1031-7.

Salamonsen, L. A., Evans, J., Nguyen, H. P. and Edgell, T. A. (2016) 'The Microenvironment of Human Implantation: Determinant of Reproductive Success', *Am J Reprod Immunol*, 75(3), pp. 218-25.

Salleh, N. (2014) 'Diverse roles of prostaglandins in blastocyst implantation', *ScientificWorldJournal*, 2014, pp. 968141.

- Salomon, C., Kobayashi, M., Ashman, K., Sobrevia, L., Mitchell, M. D. and Rice, G. E. (2013a)** 'Hypoxia-induced changes in the bioactivity of cytotrophoblast-derived exosomes', *PLoS One*, 8(11), pp. e79636.
- Salomon, C., Ryan, J., Sobrevia, L., Kobayashi, M., Ashman, K., Mitchell, M. and Rice, G. E. (2013b)** 'Exosomal signaling during hypoxia mediates microvascular endothelial cell migration and vasculogenesis', *PLoS One*, 8(7), pp. e68451.
- Salomon, C., Yee, S., Scholz-Romero, K., Kobayashi, M., Vaswani, K., Kvaskoff, D., Illanes, S. E., Mitchell, M. D. and Rice, G. E. (2014)** 'Extravillous trophoblast cells-derived exosomes promote vascular smooth muscle cell migration', *Front Pharmacol*, 5, pp. 175.
- Sanders, A. P., Burris, H. H., Just, A. C., Motta, V., Svensson, K., Mercado-Garcia, A., Pantic, I., Schwartz, J., Tellez-Rojo, M. M., Wright, R. O. and Baccarelli, A. A. (2015)** 'microRNA expression in the cervix during pregnancy is associated with length of gestation', *Epigenetics*, 10(3), pp. 221-8.
- Santonocito, M., Vento, M., Guglielmino, M. R., Battaglia, R., Wahlgren, J., Ragusa, M., Barbagallo, D., Borzì, P., Rizzari, S., Maugeri, M., Scollo, P., Tatone, C., Valadi, H., Purrello, M. and Di Pietro, C. (2014)** 'Molecular characterization of exosomes and their microRNA cargo in human follicular fluid: bioinformatic analysis reveals that exosomal microRNAs control pathways involved in follicular maturation', *Fertil Steril*, 102(6), pp. 1751-61.e1.
- Sha, A. G., Liu, J. L., Jiang, X. M., Ren, J. Z., Ma, C. H., Lei, W., Su, R. W. and Yang, Z. M. (2011)** 'Genome-wide identification of micro-ribonucleic acids associated with human endometrial receptivity in natural and stimulated cycles by deep sequencing', *Fertil Steril*, 96(1), pp. 150-155.e5.
- Shetty, S. (2005)** 'Regulation of urokinase receptor mRNA stability by hnRNP C in lung epithelial cells', *Mol Cell Biochem*, 272(1-2), pp. 107-18.

- Simon, C., Greening, D. W., Bolumar, D., Balaguer, N., Salamonsen, L. A. and Vilella, F. (2018)** 'Extracellular Vesicles in Human Reproduction in Health and Disease', *Endocr Rev.*
- Simpson, R. J., Kalra, H. and Mathivanan, S. (2012)** 'ExoCarta as a resource for exosomal research', *J Extracell Vesicles*, 1.
- Simón, C., Gimeno, M. J., Mercader, A., O'Connor, J. E., Remohí, J., Polan, M. L. and Pellicer, A. (1997)** 'Embryonic regulation of integrins beta 3, alpha 4, and alpha 1 in human endometrial epithelial cells in vitro', *J Clin Endocrinol Metab*, 82(8), pp. 2607-16.
- Singh, H. and Aplin, J. D. (2009)** 'Adhesion molecules in endometrial epithelium: tissue integrity and embryo implantation', *J Anat*, 215(1), pp. 3-13.
- Sohel, M. M., Hoelker, M., Noferesti, S. S., Salilew-Wondim, D., Tholen, E., Looft, C., Rings, F., Uddin, M. J., Spencer, T. E., Schellander, K. and Tesfaye, D. (2013)** 'Exosomal and Non-Exosomal Transport of Extra-Cellular microRNAs in Follicular Fluid: Implications for Bovine Oocyte Developmental Competence', *PLoS One*, 8(11), pp. e78505.
- Song, H., Lim, H., Das, S. K., Paria, B. C. and Dey, S. K. (2000)** 'Dysregulation of EGF family of growth factors and COX-2 in the uterus during the preattachment and attachment reactions of the blastocyst with the luminal epithelium correlates with implantation failure in LIF-deficient mice', *Mol Endocrinol*, 14(8), pp. 1147-61.
- Song, H., Lim, H., Paria, B. C., Matsumoto, H., Swift, L. L., Morrow, J., Bonventre, J. V. and Dey, S. K. (2002)** 'Cytosolic phospholipase A2alpha is crucial [correction of A2alpha deficiency is crucial] for 'on-time' embryo implantation that directs subsequent development', *Development*, 129(12), pp. 2879-89.
- Song, G. Y., Song, W. W., Han, Y., Wang, D. and Na, Q. (2013)** 'Characterization of the role of microRNA-517a expression in low birth weight infants', *J Dev Orig Health Dis*, 4(6), pp. 522-6.

- Sporn, M. B., Roberts, A. B., Wakefield, L. M. and Assoian, R. K. (1986)** 'Transforming growth factor-beta: biological function and chemical structure', *Science*, 233(4763), pp. 532-4.
- Squadrito, M. L., Baer, C., Burdet, F., Maderna, C., Gilfillan, G. D., Lyle, R., Ibberson, M. and De Palma, M. (2014)** 'Endogenous RNAs modulate microRNA sorting to exosomes and transfer to acceptor cells', *Cell Rep*, 8(5), pp. 1432-46.
- Staun-Ram, E., Goldman, S., Gabarin, D. and Shalev, E. (2004)** 'Expression and importance of matrix metalloproteinase 2 and 9 (MMP-2 and -9) in human trophoblast invasion', *Reprod Biol Endocrinol*, 2, pp. 59.
- Stenqvist, A. C., Nagaeva, O., Baranov, V. and Mincheva-Nilsson, L. (2013)** 'Exosomes secreted by human placenta carry functional Fas ligand and TRAIL molecules and convey apoptosis in activated immune cells, suggesting exosome-mediated immune privilege of the fetus', *J Immunol*, 191(11), pp. 5515-23.
- Stewart, C. L. (1994)** 'Leukaemia inhibitory factor and the regulation of preimplantation development of the mammalian embryo', *Mol Reprod Dev*, 39(2), pp. 233-8.
- Sun, X., Park, C. B., Deng, W., Potter, S. S. and Dey, S. K. (2016)** 'Uterine inactivation of muscle segment homeobox (Msx) genes alters epithelial cell junction proteins during embryo implantation', *FASEB J*, 30(4), pp. 1425-35.
- Surveyor, G. A., Gendler, S. J., Pemberton, L., Das, S. K., Chakraborty, I., Julian, J., Pimental, R. A., Wegner, C. C., Dey, S. K. and Carson, D. D. (1995)** 'Expression and steroid hormonal control of Muc-1 in the mouse uterus', *Endocrinology*, 136(8), pp. 3639-47.
- Sutherland, A. E., Calarco, P. G. and Damsky, C. H. (1993)** 'Developmental regulation of integrin expression at the time of implantation in the mouse embryo', *Development*, 119(4), pp. 1175-86.

T

- Tabibzadeh, S. and Babaknia, A. (1995)** 'The signals and molecular pathways involved in implantation, a symbiotic interaction between blastocyst and endometrium involving adhesion and tissue invasion', *Hum Reprod*, 10(6), pp. 1579-602.
- Takamoto, N., Kurihara, I., Lee, K., Demayo, F. J., Tsai, M. J. and Tsai, S. Y. (2005)** 'Haploinsufficiency of chicken ovalbumin upstream promoter transcription factor II in female reproduction', *Mol Endocrinol*, 19(9), pp. 2299-308.
- Takamoto, N., Zhao, B., Tsai, S. Y. and DeMayo, F. J. (2002)** 'Identification of Indian hedgehog as a progesterone-responsive gene in the murine uterus', *Mol Endocrinol*, 16(10), pp. 2338-48.
- Tan, J., Raja, S., Davis, M. K., Tawfik, O., Dey, S. K. and Das, S. K. (2002)** 'Evidence for coordinated interaction of cyclin D3 with p21 and cdk6 in directing the development of uterine stromal cell decidualization and polyploidy during implantation', *Mech Dev*, 111(1-2), pp. 99-113.
- Taylor, H. S. (2000)** 'The role of HOX genes in human implantation', *Hum Reprod Update*, 6(1), pp. 75-9.
- Teh, W. T., McBain, J. and Rogers, P. (2016)** 'What is the contribution of embryo-endometrial asynchrony to implantation failure?', *J Assist Reprod Genet*, 33(11), pp. 1419-1430.
- Teklenburg, G., Salker, M., Molokhia, M., Lavery, S., Trew, G., Aojanepong, T., Mardon, H. J., Lokugamage, A. U., Rai, R., Landles, C., Roelen, B. A., Quenby, S., Kuijk, E. W., Kavelaars, A., Heijnen, C. J., Regan, L., Brosens, J. J. and Macklon, N. S. (2010)** 'Natural selection of human embryos: decidualizing endometrial stromal cells serve as sensors of embryo quality upon implantation', *PLoS One*, 5(4), pp. e10258.

- Thie, M., Harrach-Ruprecht, B., Sauer, H., Fuchs, P., Albers, A. and Denker, H. W. (1995)** 'Cell adhesion to the apical pole of epithelium: a function of cell polarity', *Eur J Cell Biol*, 66(2), pp. 180-91.
- Thouas, G. A., Dominguez, F., Green, M. P., Vilella, F., Simon, C. and Gardner, D. K. (2015)** 'Soluble ligands and their receptors in human embryo development and implantation', *Endocr Rev*, 36(1), pp. 92-130.
- Torry, D. S., Leavenworth, J., Chang, M., Maheshwari, V., Groesch, K., Ball, E. R. and Torry, R. J. (2007)** 'Angiogenesis in implantation', *J Assist Reprod Genet*, 24(7), pp. 303-15.
- Trabucchi, M., Briata, P., Garcia-Mayoral, M., Haase, A. D., Filipowicz, W., Ramos, A., Gherzi, R. and Rosenfeld, M. G. (2009)** 'The RNA-binding protein KSRP promotes the biogenesis of a subset of microRNAs', *Nature*, 459(7249), pp. 1010-4.
- Tsai, S. J., Wu, M. H., Chen, H. M., Chuang, P. C. and Wing, L. Y. (2002)** 'Fibroblast growth factor-9 is an endometrial stromal growth factor', *Endocrinology*, 143(7), pp. 2715-21.
- Tulac, S., Nayak, N. R., Kao, L. C., Van Waes, M., Huang, J., Lobo, S., Germeyer, A., Lessey, B. A., Taylor, R. N., Suchanek, E. and Giudice, L. C. (2003)** 'Identification, characterization, and regulation of the canonical Wnt signaling pathway in human endometrium', *J Clin Endocrinol Metab*, 88(8), pp. 3860-6.
- Turchinovich, A., Samatov, T. R., Tonevitsky, A. G. and Burwinkel, B. (2013)** 'Circulating miRNAs: cell-cell communication function?', *Front Genet*, 4, pp. 119.
- Turchinovich, A., Weiz, L., Langheinz, A. and Burwinkel, B. (2011)** 'Characterization of extracellular circulating microRNA', *Nucleic Acids Res*, 39(16), pp. 7223-33.

-
- Valadi, H., Ekström, K., Bossios, A., Sjöstrand, M., Lee, J. J. and Lötval, J. O. (2007)** 'Exosome-mediated transfer of mRNAs and microRNAs is a novel mechanism of genetic exchange between cells', *Nat Cell Biol*, 9(6), pp. 654-9.
- Van Kouwenhove, M., Kedde, M. and Agami, R. (2011)** 'MicroRNA regulation by RNA-binding proteins and its implications for cancer', *Nat Rev Cancer*, 11(9), pp. 644-56.
- Vandermolen, D. T. and Gu, Y. (1996)** 'Human endometrial interleukin-6 (IL-6): in vivo messenger ribonucleic acid expression, in vitro protein production, and stimulation thereof by IL-1 beta', *Fertil Steril*, 66(5), pp. 741-7.
- Vickers, K. C., Palmisano, B. T., Shoucri, B. M., Shamburek, R. D. and Remaley, A. T. (2011)** 'MicroRNAs are transported in plasma and delivered to recipient cells by high-density lipoproteins', *Nat Cell Biol*, 13(4), pp. 423-33.
- Vilella, F., Moreno-Moya, J. M., Balaguer, N., Grasso, A., Herrero, M., Martínez, S., Marcilla, A. and Simón, C. (2015)** 'Hsa-miR-30d, secreted by the human endometrium, is taken up by the preimplantation embryo and might modify its transcriptome', *Development*, 142(18), pp. 3210-21.
- Vilella, F., Ramirez, L., Berlanga, O., Martínez, S., Alamá, P., Meseguer, M., Pellicer, A. and Simón, C. (2013)** 'PGE2 and PGF2 α concentrations in human endometrial fluid as biomarkers for embryonic implantation', *J Clin Endocrinol Metab*, 98(10), pp. 4123-32.
- Villarroya-Beltri, C., Gutiérrez-Vázquez, C., Sánchez-Cabo, F., Pérez-Hernández, D., Vázquez, J., Martín-Cofreces, N., Martínez-Herrera, D. J., Pascual-Montano, A., Mittelbrunn, M. and Sánchez-Madrid, F. (2013)** 'Sumoylated hnRNPA2B1 controls the sorting of miRNAs into exosomes through binding to specific motifs', *Nat Commun*, 4, pp. 2980.

- Von Rango, U., Alfer, J., Kertschanska, S., Kemp, B., Müller-Newen, G., Heinrich, P. C., Beier, H. M. and Classen-Linke, I. (2004)** 'Interleukin-11 expression: its significance in eutopic and ectopic human implantation', *Mol Hum Reprod*, 10(11), pp. 783-92.
- Von Wolff, M., Thaler, C. J., Strowitzki, T., Broome, J., Stolz, W. and Tabibzadeh, S. (2000)** 'Regulated expression of cytokines in human endometrium throughout the menstrual cycle: dysregulation in habitual abortion', *Mol Hum Reprod*, 6(7), pp. 627-34.

W

- Waclawik, A. (2011)** 'Novel insights into the mechanisms of pregnancy establishment: regulation of prostaglandin synthesis and signaling in the pig', *Reproduction*, 142(3), pp. 389-99.
- Wang, H., Xie, H., Sun, X., Tranguch, S., Zhang, H., Jia, X., Wang, D., Das, S. K., Desvergne, B., Wahli, W., DuBois, R. N. and Dey, S. K. (2007)** 'Stage-specific integration of maternal and embryonic peroxisome proliferator-activated receptor delta signaling is critical to pregnancy success', *J Biol Chem*, 282(52), pp. 37770-82.
- Wang, J. and Maldonado, M. A. (2006)** 'The ubiquitin-proteasome system and its role in inflammatory and autoimmune diseases', *Cell Mol Immunol*, 3(4), pp. 255-61.
- Wang, K., Zhang, S., Weber, J., Baxter, D. and Galas, D. J. (2010)** 'Export of microRNAs and microRNA-protective protein by mammalian cells', *Nucleic Acids Res*, 38(20), pp. 7248-59.
- Wang, W., Van De Water, T. and Lufkin, T. (1998)** 'Inner ear and maternal reproductive defects in mice lacking the Hmx3 homeobox gene', *Development*, 125(4), pp. 621-34.

- Wetendorf, M. and DeMayo, F. J. (2014)** 'Progesterone receptor signaling in the initiation of pregnancy and preservation of a healthy uterus', *Int J Dev Biol*, 58(2-4), pp. 95-106.
- Wilkins-Haug, L. (2009)** 'Epigenetics and assisted reproduction', *Curr Opin Obstet Gynecol*, 21(3), pp. 201-6.
- Winship, A., Correia, J., Zhang, J. G., Nicola, N. A. and Dimitriadis, E. (2015)** 'Leukemia Inhibitory Factor (LIF) Inhibition during Mid-Gestation Impairs Trophoblast Invasion and Spiral Artery Remodelling during Pregnancy in Mice', *PLoS One*, 10(10), pp. e0129110.
- Winter, J., Jung, S., Keller, S., Gregory, R. I. and Diederichs, S. (2009)** 'Many roads to maturity: microRNA biogenesis pathways and their regulation', *Nat Cell Biol*, 11(3), pp. 228-34.

Y

- Ye, X., Hama, K., Contos, J. J., Anliker, B., Inoue, A., Skinner, M. K., Suzuki, H., Amano, T., Kennedy, G., Arai, H., Aoki, J. and Chun, J. (2005)** 'LPA3-mediated lysophosphatidic acid signalling in embryo implantation and spacing', *Nature*, 435(7038), pp. 104-8.

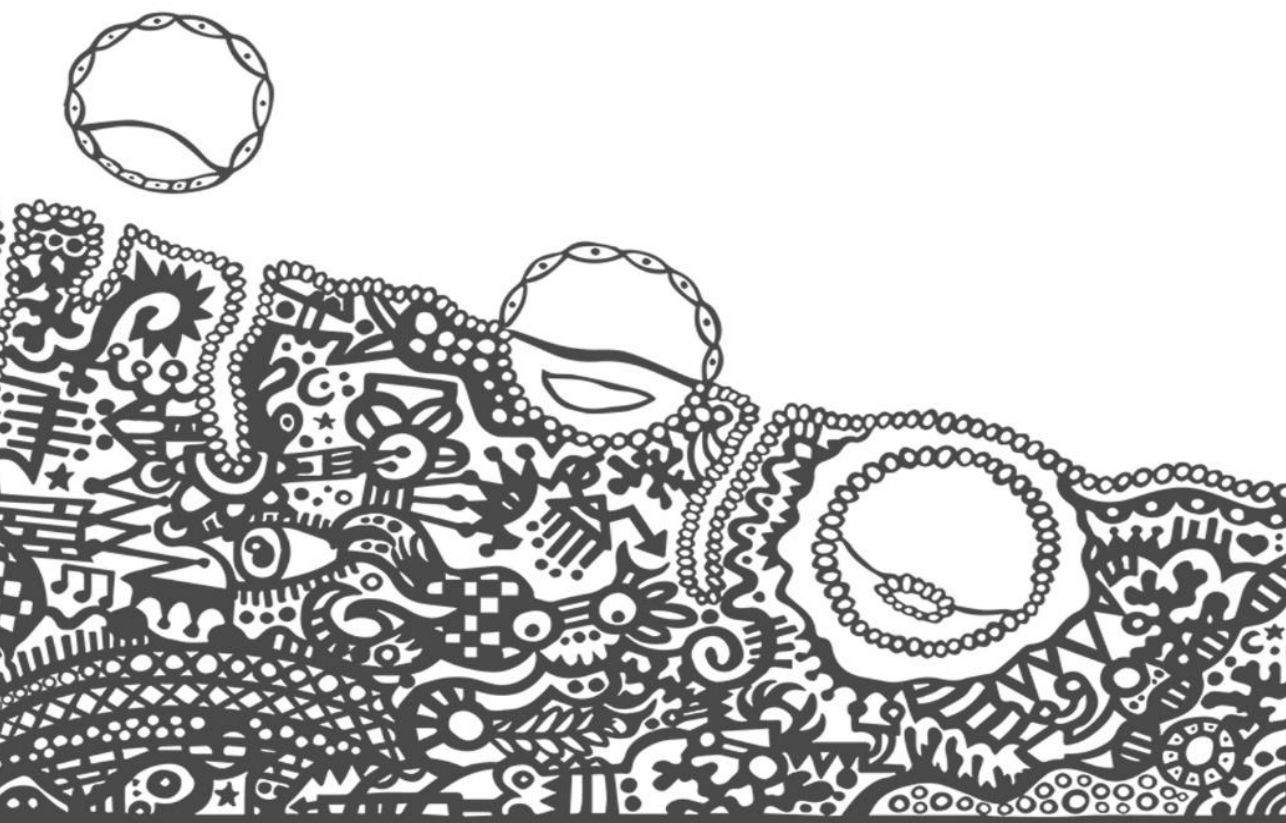
Z

- Zernecke, A., Bidzhekov, K., Noels, H., Shagdarsuren, E., Gan, L., Denecke, B., Hristov, M., Köppel, T., Jahantigh, M. N., Lutgens, E., Wang, S., Olson, E. N., Schober, A. and Weber, C. (2009)** 'Delivery of microRNA-126 by apoptotic bodies induces CXCL12-dependent vascular protection', *Sci Signal*, 2(100), pp. ra81.
- Zhang, Q., Zhang, H., Jiang, Y., Xue, B., Diao, Z., Ding, L., . . . Hu, Y. (2015).** MicroRNA-181a is involved in the regulation of human endometrial

stromal cell decidualization by inhibiting Krüppel-like factor 12. *Reprod Biol Endocrinol*, 13, 23. doi:10.1186/s12958-015-0019-y

Zhao, Z., Zhao, Q., Warrick, J., Lockwood, C. M., Woodworth, A., Moley, K. H., & Gronowski, A. M. (2012). Circulating microRNA miR-323-3p as a biomarker of ectopic pregnancy. *Clin Chem*, 58(5), 896-905. doi:10.1373/clinchem.2011.179283.

APPENDIX



09 | **APPENDIX**

9.1 Supplementary files

Supplementary file 1 | Data showing the FDR calculation for the proteins identified after performing the pull-down with a biotinylated miR-30d in the hEEC sample 1. Sheet1: Protein level summary; Sheet2: Distinct peptide level summary; Sheet3: Spectral level summary; Sheet4: Protein level data; Sheet5: Distinct peptide level data; Sheet6: Spectral level data; Sheet7: Single results table; Sheet8: Protein Summary; Sheet9: Peptide Summary.

Supplementary file 2 | Data showing the false discovery rate (FDR) calculation for the proteins identified after performing the pull-down with a biotinylated polyA in the human endometrial epithelial cell (hEEC) sample 1. Sheet1: Protein level summary; Sheet2: Distinct peptide level summary; Sheet3: Spectral level summary; Sheet4: Protein level data; Sheet5: Distinct peptide level data; Sheet6: Spectral level data; Sheet7: Single results table; Sheet8: Protein Summary; Sheet9: Peptide Summary.

Supplementary file 3 | Data showing the false discovery rate (FDR) calculation for the proteins identified after performing the pull-down with a biotinylated miR-30d in the human endometrial epithelial cell (hEEC) sample 2. Sheet1: Protein level summary; Sheet2: Distinct peptide level summary; Sheet3: Spectral level summary; Sheet4: Protein level data; Sheet5: Distinct peptide level data; Sheet6: Spectral level data; Sheet7: Single results table; Sheet8: Protein Summary; Sheet9: Peptide Summary.

Supplementary file 4 | Data showing the false discovery rate (FDR) calculation for the proteins identified after performing the pull-down with a biotinylated polyA in the human endometrial epithelial cell (hEEC) sample 2. Sheet1: Protein level

summary; Sheet2: Distinct peptide level summary; Sheet3: Spectral level summary; Sheet4: Protein level data; Sheet5: Distinct peptide level data; Sheet6: Spectral level data; Sheet7: Single results table; Sheet8: Protein Summary; Sheet9: Peptide Summary.

Supplementary file 5 | Data showing the false discovery rate (FDR) calculation for the proteins identified after performing the pull-down with a biotinylated miR-30d in a pool of exosomes obtained from 4 human endometrial epithelial cell (hEEC) samples. Sheet1: Protein level summary; Sheet2: Distinct peptide level summary; Sheet3: Spectral level summary; Sheet4: Protein level data; Sheet5: Distinct peptide level data; Sheet6: Spectral level data; Sheet7: Single results table; Sheet8: Protein Summary; Sheet9: Peptide Summary.

Supplementary file 6 | Data showing the false discovery rate (FDR) calculation for the proteins identified after performing the pull-down with a biotinylated polyA in a pool of exosomes obtained from 4 human endometrial epithelial cell (hEEC) samples. Sheet1: Protein level summary; Sheet2: Distinct peptide level summary; Sheet3: Spectral level summary; Sheet4: Protein level data; Sheet5: Distinct peptide level data; Sheet6: Spectral level data; Sheet7: Single results table; Sheet8: Protein Summary; Sheet9: Peptide Summary.

Supplementary file 7 | Information related to the protein profile obtained in all the analyzed samples. Sheet1: Protein summary interpretation; Sheet2: Protein summary; Sheet3: Pre-selected proteins.

9.2 Supplementary movies

Supplementary video 1 | Live animation showing a wild type (WT) hatching mouse blastocyst beginning the adhesion process on hEECs previously treated with molecular beacon (MB) probes intended to recognize the miRNA miR-30d in living cells. Dyes: in blue Hoechst 33342 (nucleus), in green WGA-Alexa 488 (cell membrane), in red Cy3 (miR-30d).

Supplementary video 2 | Live animation showing a wild type (WT) mouse blastocyst, during the invasion stage, on human endometrial epithelial cells (hEECs) previously treated with molecular beacon (MB) probes intended to recognize the miRNA miR-30d in living cells. Dyes: in blue Hoechst 33342 (nucleus), in green WGA-Alexa 488 (cell membrane), in red Cy3 (miR-30d).

Supplementary video 3 | Live animation showing a knockout (KO) hatching mouse blastocyst beginning the adhesion process on human endometrial epithelial cells (hEECs) previously treated with molecular beacon (MB) probes intended to recognize the miRNA miR-30d in living cells. Dyes: in blue Hoechst 33342 (nucleus), in green WGA-Alexa 488 (cell membrane), in red Cy3 (miR-30d).

Supplementary video 4 | Live animation showing a knockout (KO) mouse blastocyst, during the invasion stage, on human endometrial epithelial cells (hEECs) previously treated with molecular beacon (MB) probes intended to recognize the miRNA miR-30d in living cells. Dyes: in blue Hoechst 33342 (nucleus), in green WGA-Alexa 488 (cell membrane), in red Cy3 (miR-30d).

9.3 Publications

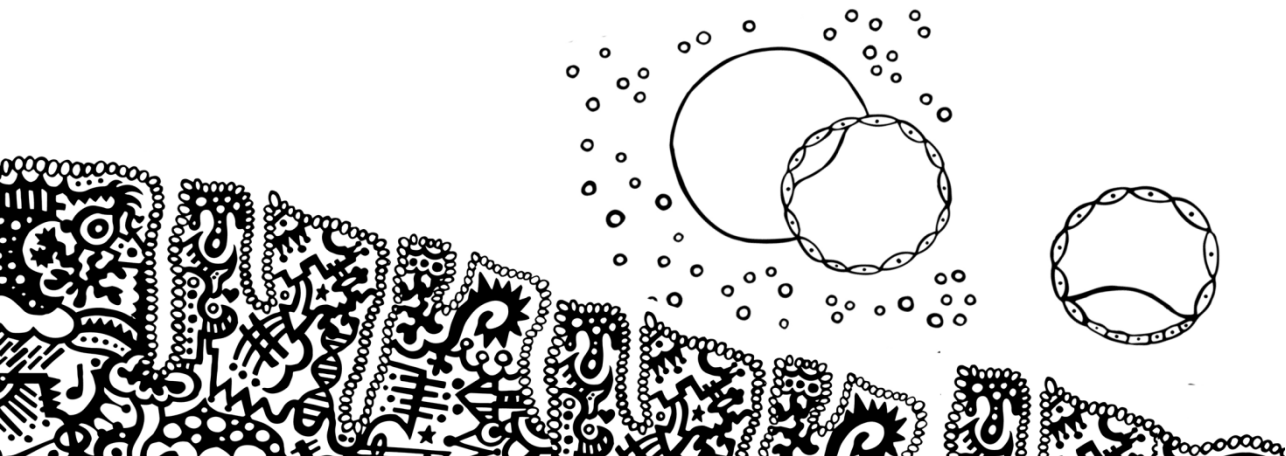
Vilella, F., Moreno-Moya, J. M., Balaguer, N., Grasso, A., Herrero, M., Martínez, S., Marcilla, A. and Simón, C. (2015) 'Hsa-miR-30d, secreted by the human endometrium, is taken up by the pre-implantation embryo and might modify its transcriptome', *Development*, 142(18), pp. 3210-21.

Balaguer, N., Moreno, I., Herrero, M., González, M., Simón, C. and Vilella, F. (2018) 'Heterogeneous nuclear ribonucleoprotein C1 may control miR-30d levels in endometrial exosomes affecting early embryo implantation', *Mol Hum Reprod*, pp. 1-15.

Balaguer, N., Moreno I., Herrero, M., González-Monfort, M., Vilella, F. and Simón, C. (2018) 'Reproductive and fetal outcome of miR-30d deficiency at the maternal-embryonic interface', *Ajog*. **(Under Review)**

Balaguer, N., Domínguez, F., Simón, C. and Vilella, F. (2017) 'Embryo/fetal maternal cross-talk', in Simón, C. & Giudice, L.C. (eds.) *The endometrial factor. A reproductive precision medicine approach*: CRC Press, pp. 241-255.

Hsa-miR-30d secreted by the human endometrium is taken up by the pre-implantation embryo and might modify its transcriptome



RESEARCH ARTICLE

Hsa-miR-30d, secreted by the human endometrium, is taken up by the pre-implantation embryo and might modify its transcriptome

Felipe Vilella^{1,*}, Juan M. Moreno-Moya^{1,*}, Nuria Balaguer^{1,*}, Alessia Grasso¹, Maria Herrero¹, Sebastian Martínez¹, Antonio Marcilla² and Carlos Simón^{1,3}

ABSTRACT

During embryo implantation, the blastocyst interacts with and regulates the endometrium, and endometrial fluid secreted by the endometrial epithelium nurtures the embryo. Here, we propose that maternal microRNAs (miRNAs) might act as transcriptomic modifier of the pre-implantation embryo. Microarray profiling revealed that six of 27 specific, maternal miRNAs were differentially expressed in the human endometrial epithelium during the window of implantation – a brief phase of endometrial receptivity to the blastocyst – and were released into the endometrial fluid. Further investigation revealed that hsa-miR-30d, the expression levels of which were most significantly upregulated, was secreted as an exosome-associated molecule. Exosome-associated and free hsa-miR-30d was internalized by mouse embryos via the trophectoderm, resulting in an indirect overexpression of genes encoding for certain molecules involved in the murine embryonic adhesion phenomenon – *Itgb3*, *Itga7* and *Cdh5*. Indeed, this finding was supported by evidence *in vitro*: treating murine embryos with miR-30d resulted in a notable increase in embryo adhesion. Our results suggest a model in which maternal endometrial miRNAs act as transcriptomic modifiers of the pre-implantation embryo.

KEY WORDS: Has-miR-30d, Pre-implantation embryo, Endometrial fluid, Embryo adhesion

INTRODUCTION

In 2010, 45 million couples were affected by infertility (Mascarenhas et al., 2012), and this number is expected to rise as child-bearing is increasingly postponed. More than 5 million children have been born through assisted reproduction (Mansour et al., 2014), and research in this area is moving toward the improvement of success rates, and improvement of success rates through a better understanding of embryo and uterine physiology.

The human embryo undergoes complex developmental modifications throughout the pre-implantation period (Niakan et al., 2012), during which it enters the uterine cavity at the blastocyst stage and embeds in the endometrial fluid (EF) (Cross et al., 1994). During the implantation process, the blastocyst regulates the expression and secretion of integrins $\beta 3$, $\alpha 4$ and $\alpha 1$ (Simón et al., 1997), the interleukin-1 (IL-1) system (De los Santos

et al., 1996), chemokines IL-8, MCP-1 and RANTES (Caballero-Campo et al., 2002), leptin (Cervero et al., 2004; González et al., 2000) and hCG (Licht et al., 2001; Paiva et al., 2011) by the endometrial epithelium during the window of implantation (WOI), the period when the endometrium is receptive to a blastocyst. The EF, a viscous fluid secreted by the endometrial glands into the uterine cavity, nurtures the embryo and constitutes the microenvironment in which the first bidirectional dialogue between the maternal endometrium and the embryo occurs during the WOI (Cha et al., 2012, 2013; Thouas et al., 2014; Tranguch et al., 2005).

The developmental origins of adult disease are now recognized to reflect intrauterine conditions during embryonic and fetal life (Turchinovich et al., 2011). Accumulated evidence suggests that the EF serves as the ‘uterine milk’ (Burton et al., 2007; Khalil et al., 2009) that nurtures the embryo not only during implantation but beyond (Godfrey and Barker, 2001; Kennedy et al., 2007). The EF contains a variety of molecules, including glycodefin (van der Gaast et al., 2009), cytokines (Boomsma et al., 2009; Simón et al., 1996), lipids (Vilella et al., 2013) and proteins (Dominguez et al., 2009; Hannan et al., 2010), but their impacts on embryo physiology and the putative developmental origins of adult diseases are unknown (Barker, 1990).

Of increasing importance to all aspects of human physiology, including development, are microRNAs (miRNAs), the small, 19–22 nucleotide sequences of non-coding RNA that function as regulators of endogenous gene expression (Ambros and Chen, 2007; Bartel, 2004). miRNAs are secreted by cells and incorporated into microvesicles or associated with proteins that protect them from RNase degradation, endowing them with a long half-life (Turchinovich et al., 2011; Yoshizawa and Wong, 2013). These molecules have been implicated in the regulation of the WOI (Altmäe et al., 2010; Kuokkanen et al., 2010; Ng et al., 2013; Sha et al., 2011), decidualization (Estella et al., 2012a,b) and embryo development in humans (Mincheva-Nilsson and Baranov, 2010), and, more recently, embryo implantation in mice (Chen et al., 2015; Kang et al., 2015; Liu et al., 2013; Revel et al., 2011). In the present study, we aimed to elucidate the role of and mechanisms by which maternal miRNAs secreted into the EF act as transcriptomic regulators of the reprogramming of pre-implantation embryos by the maternal intrauterine environment.

RESULTS**Human EF miRNA profile**

First, a microarray analysis of RNA transcripts present in EF was conducted to determine the global expression profile; this revealed a large proportion of miRNAs (supplementary material Fig. S1A), as well as a differential expression pattern among the different phases of the menstrual cycle. Thus, to establish a specific analysis, EF samples were classified into the following groups based on the

¹Fundación Instituto Valenciano de Infertilidad (FIVI), Department of Obstetrics and Gynecology, Universitat de València, Instituto Universitario IVI/INCLIVA, 46980 Valencia, Spain. ²Departamento de Biología Celular y Parasitología, Facultad de Farmacia, Universitat de València, 46100 Burjassot (Valencia), Spain. ³Department of Obstetrics and Gynecology, School of Medicine, Stanford University, Palo Alto, CA 94304, USA.

*These authors contributed equally to this work

†Author for correspondence (felipe.vilella@ivi.es)

Received 12 March 2015; Accepted 30 July 2015

3210

timing of sample collection: early proliferative (EP; days 6-8; $n=4$), late proliferative (LP; days 9-14; $n=4$), early secretory (ES; days 15-18; $n=4$), WOI (days 19-23; $n=4$) or late secretory (LS; days 24-28; $n=4$).

Microarray technology was used to compare the expression of miRNAs in EF during other phases of the menstrual cycle with that exhibited during the WOI. Significance analysis of microarrays (SAM) with a false discovery rate (FDR) correction $<5\%$ allowed us to identify differential miRNA expression across the menstrual cycle. Compared with the WOI, nine differentially expressed miRNAs were identified in the EP phase, eight in the LP phase, six in the ES phase and four in the LS phase (Fig. 1A). Bioinformatics analysis to predict the function(s) of these differentially expressed miRNAs primarily targeted cell cycle and endocrine processes (supplementary material Fig. S1B). As shown on the heat map in Fig. 1A, miRNAs tended to be downregulated in the proliferative

phase and upregulated in the secretory phase compared with the WOI. Supervised principal components analysis (PCA) revealed that the EF obtained from the WOI was different from EF secreted at different points of the cycle based on miRNA composition (Fig. 1B). Interestingly, hsa-miR-30d was the most differentially secreted maternal miRNA in the EF during the WOI compared with the rest of the menstrual cycle (Fig. 1C). The hsa-miR-30d concentration in the EF during the WOI, corresponding to the time when an embryo would be present in a conception cycle, was 194.68 ± 29.90 nM (Fig. 1D).

Hsa-miR-30d is secreted by the endometrial glands and transported as an exosome-associated molecule

Next, the cellular origin and mechanism of secretion of endometrial miRNAs into the EF were investigated. As miRNAs are usually secreted in exosomes and carried by Argonau proteins (Valadi

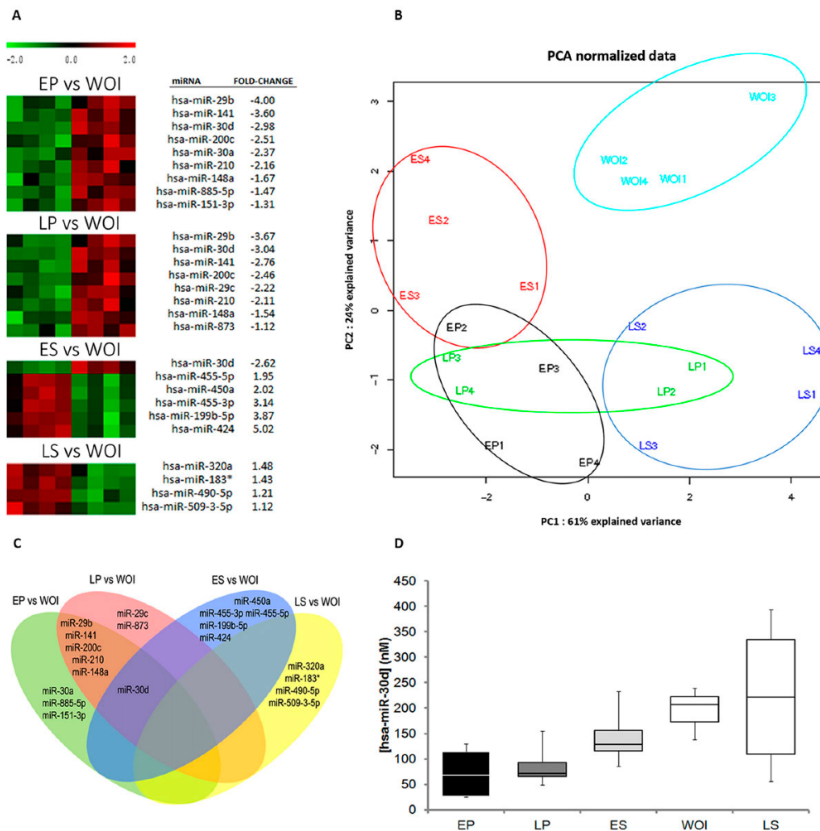


Fig. 1. Study of the specific miRNA profile during the window of implantation (WOI). (A) Heat map of the differential expression of secreted maternal miRNAs during the WOI relative to other phases of the menstrual cycle. (B) Supervised principal components analysis (PCA) to distinguish differentially expressed miRNAs in endometrial fluid (EF) obtained throughout the menstrual cycle relative to the WOI. (C) Venn diagram demonstrating the overlap in expression of miRNAs at different phases of the menstrual cycle, with special attention on hsa-miR-30d in the WOI. (D) Hsa-miR-30d concentration in the EF throughout the menstrual cycle. Boxes represent the first quartile, median and third quartile, and error bars represent maximum and minimum values.

et al., 2007), an initial search for these extracellular vesicles in the human endometrium was performed. To identify exosomes, CD63, a well-known exosome marker (Colombo et al., 2014), was detected by immunohistochemistry. CD63 staining was observed to be localized

in apical and glycocalyx regions of the glandular epithelium during the WOI. By contrast, relatively less intense staining was observed in the ES endometrium, corresponding to the pre-receptive phase (Fig. 2A). Using transmission electron microscopy (TEM),

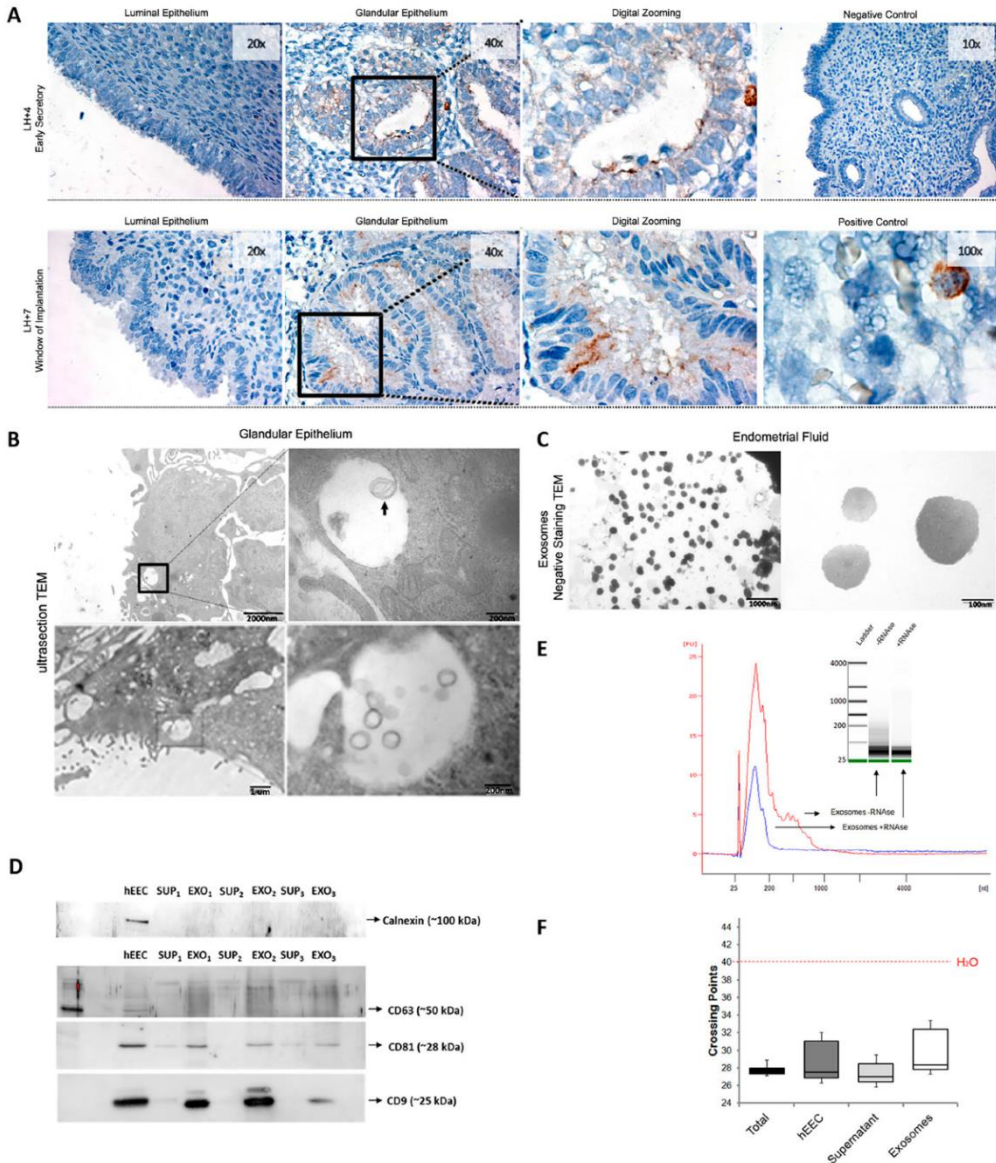


Fig. 2. See next page for legend.

Fig. 2. Identification of the secretion of exosomes loaded with RNA from hEECs into the EF. (A) Immunohistochemical staining of CD63 in the human glandular and luminal epithelium during the early secretory phase (4 days after luteinizing hormone peak; LH+4), the WOI (LH+7) and in the negative (no primary antibody) and positive (immune cell) controls. (B) Transmission electron microscopy (TEM) images of glandular hEECs showing an endosome proximal to the plasma membrane with a small exosome (arrow). Another glandular hEEC shows the same type of endosome compartment in which it is possible to distinguish several exosomes. (C) Electron micrographs of negative staining with uranyl acetate for exosomes purified from EF. (D) Western blot identifying calnexin (negative control) and possible exosome markers CD63, CD9 and CD81 in protein extracts from hEECs, three fractions of exosomes derived from three different human biopsies, and their respective supernatants obtained after ultracentrifugation. (E) Results from a small RNA lab chip assay showing the RNA content of primary hEEC-derived exosomes with or without treatment with RNase A. (F) Crossing points (*y*-axis) for hsa-miR-30d in cells, supernatant, exosomes purified from primary hEEC cultures and total supernatant without depletion of exosomes. The box represents the first quartile, median and third quartile, and the error bars represent maximum and minimum values.

glandular epithelial cells in the secretory phase were verified to have high endosome content, with sizes ranging from 50 to 250 nm (Fig. 2B). These endosomes contained vesicles the size of which was consistent with the exosomes that appear to be secreted into the endometrial cavity. Negative-staining electron microscopy, after ultracentrifugation of human EF, corroborated the presence of these exosomes (Fig. 2C). Western blot analysis showed that the exosome fraction from primary human endometrial epithelial cell (hEEC) culture was positive for the three exosomal tetraspanins CD63, CD81 and CD9 (Colombo et al., 2014; Mathivanan et al., 2011; Ng et al., 2013) and negative for calnexin (Tian et al., 2013) (Fig. 2D).

After verifying that human endometrial epithelium produces and secretes exosomes, in support of Ng et al. (2013), an *in vitro* model of primary hEECs was used to obtain large quantities of exosomes (3.5±1.26 µg of total protein from hEEC-conditioned media). A small RNA LabChip was used to detect the presence of miRNAs within vesicles. RNase treatment did not result in an absence of miRNAs, demonstrating that exosomes protected miRNAs from degradation (Fig. 2E). Among potential miRNAs, hsa-miR-30d was identified in exosomes obtained from hEEC-conditioned media, primary hEECs and exosome-depleted conditioned media (Fig. 2F).

Next, the endogenous production of miR-30d by hEECs and its secretion in exosomes were identified by using a specific custom probe (SmartFlare, Millipore). Each probe consists of a gold nanoparticle conjugated to many copies of the same double-stranded oligonucleotide encoding the target sequence (in this case, hsa-miR-30d). One strand of the oligonucleotide bears a fluorophore (Cy3) that is quenched by its proximity to the gold core. When the nanoparticle contacts its target, the target RNA displaces the fluorophore. The reporter strand, now unquenched, fluoresces and can be detected using any fluorescence detection platform, like a confocal microscope (Fig. 3A; supplementary material Movie 1). A scrambled sequence that does not recognize any target in cells was used as a background control. To delimit the main location of the gold nanoparticles, and, consequently, the one for the hsa-miR-30d, a TEM assay was performed. As the micrographs show, most of these nanoparticles were included inside vesicles (Fig. 3B).

This finding demonstrates that maternal endometrial miRNAs are transported inside exosomes. Taken together, these observations suggest that maternal miRNAs, specifically hsa-miR-30d, are actively produced and secreted from the glandular epithelium into the lumen of the endometrial cavity.

Embryos take up free and/or exosome-associated hsa-miR-30d from the EF

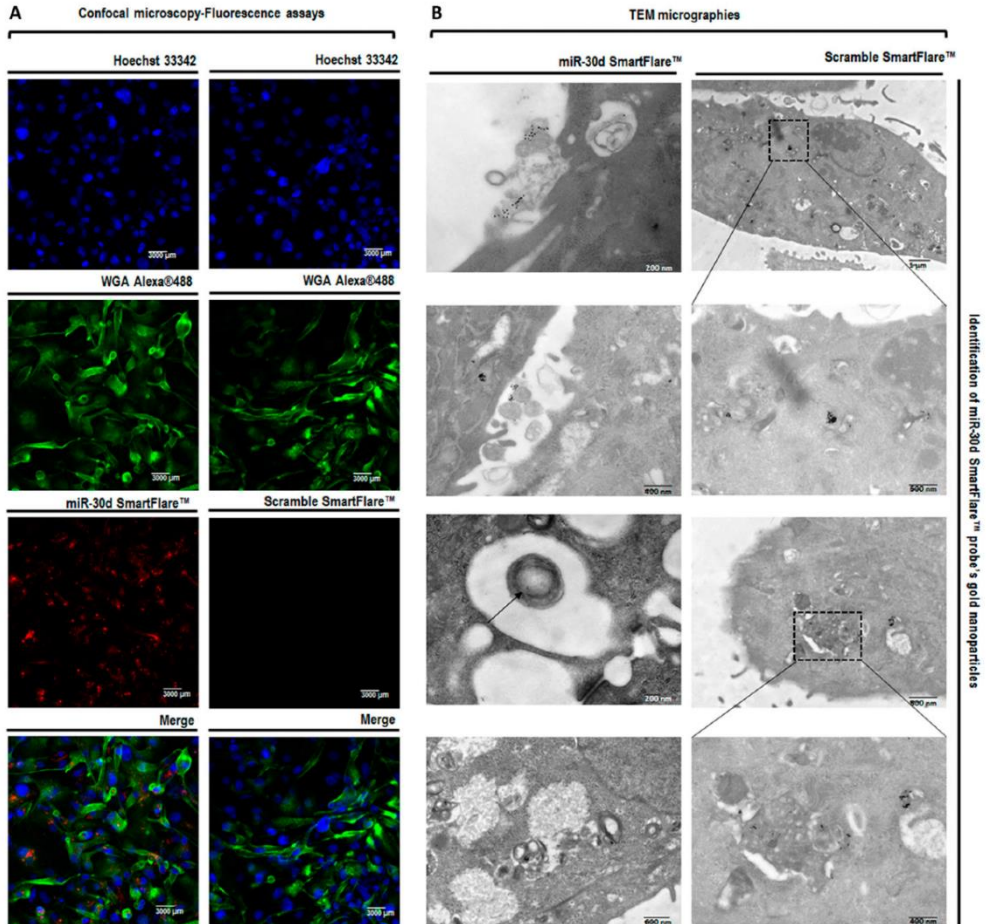
To investigate the hypothesis that the embryo is able to take up free and/or exosome-associated miRNAs from the EF, uptake of free hsa-miR-30d was tested in an *in vitro* mouse model. Day-1.5 embryos (*n*=30) were cultured for 72 h with 400 nM Alexa 488-labeled scramble miRNA. Uptake by trophectoderm cells was confirmed by immunofluorescence in either the hatched area or the trophectoderm after zona pellucida removal without affecting embryo quality (Fig. 4A; supplementary material Movie 2). The embryos (*n*=60) were incubated with 50 nM, 100 nM or 400 nM free synthetic miR-30d (to mimic) using scramble miRNA as a negative control, and miR-30d uptake was validated by real-time quantitative PCR (Fig. 4C).

To test the embryo acquisition of exosome-secreted miRNAs, the vesicles isolated from primary hEECs were stained with the exosome membrane marker Vybrant DiO and added to the culture media containing day-4.5 mouse blastocysts (*n*=15) for 24 h. As seen for free miR-30d, the trophectoderm in the hatched area or after zona pellucida removal exhibited the ability to take up exosomes (Fig. 4B; supplementary material Movie 3). This finding was validated using scanning electron microscopy (SEM) to visualize the trophectoderm surface of exosome-co-cultured embryos (Fig. 4D). Small, rounded vesicles surrounded by microvilli were attached to the apical trophectoderm membrane, close to pores or cell membrane invaginations in treated embryos.

In addition, an *in vitro* assay was performed in which miR-30d-labeled hEECs were co-cultured with unstained mouse embryos. The miR-30d signal was observed to transfer from the hEECs to the trophectoderm of embryos when they were attached to the hEEC monolayer. However, when the attachment was not present, no fluorescence was observed in the embryo. The red signal of miR-30d was evident in embryo cells in the rolling stage, an event confirmed in the adhesion and invasion phases (Fig. 5; supplementary material Fig. S2). These results demonstrate that secreted maternal miRNAs, specifically miR-30d, either free or in exosome-associated form, can be incorporated into the embryo via the trophectoderm.

Hsa-miR-30d secreted by hEECs induces transcriptional and functional embryo modifications

Finally, to demonstrate the functional relevance of this novel maternal tissue-embryo communication mechanism, we investigated the effects of endometrial miRNA uptake on the embryonic transcriptome and phenotype. A gene expression microarray of day-1.5 mouse embryos (*n*=360, performing triplicates), cultured in the presence of either 400 nM hsa-miR-30d or scramble miRNA for 72 h, revealed an overexpression of ten genes in embryos cultured with miR-30d mimic (Fig. 6A; supplementary material Fig. S3 and Tables S2-7 include all comparisons between the different groups, i.e. non-treated, scramble, mimic miR-30d and inhibitor of miR-30d). These genes were investigated using the web-based tool DAVID (<http://david.abcc.ncifcr.gov/home.jsp>) to identify the most likely affected biological processes. The regulated genes were related to cell adhesion, integrin-mediated signaling pathways and developmental maturation (Fig. 6B). The phenotypic effect of this transcriptomic regulation was demonstrated using an *in vitro* model of embryo adhesion (Garrido-Gómez et al., 2012; Martín et al., 2000). Four conditions were compared in six different experiments (15 embryos per condition, *n*=6): control without miRNA, scramble miRNA, mimic miR-30d and miR-30d inhibitor. After 32 h of co-culture, the presence of mimic miR-30d resulted in an increased rate of embryonic adhesion to the



Identification of miR-30d SmartFlare™ probe's gold nanoparticles

Fig. 3. *In vitro* identification of miR-30d production by hEECs. (A) Confocal microscopy images showing *in vitro* identification of miR-30d production by the human luminal epithelium. The first column shows the information obtained with a SmartFlare probe that specifically recognizes the presence of miR-30d in cells (labeled in red). Each probe consists of a gold nanoparticle conjugated to many copies of the same double-stranded oligonucleotide encoding the target sequence. One strand of the oligonucleotide bears a fluorophore (Cy3) that is quenched by its proximity to the gold core. When the nanoparticle contacts its target, the target RNA displaces the fluorophore. The reporter strand, now unquenched, fluoresces and can be detected using any fluorescence detection platform. The second column shows the images acquired with the control provided by the company (Millipore; Scramble SmartFlare probe). In this case, the capture strand is a scrambled sequence that does not recognize any target in cells and can therefore be used as a background control. In both cases, cell membranes appear to be labeled with WGA-Alexa 488 (green). (B) Transmission electron micrographs showing the location of the gold nanoparticles from the SmartFlare probes. The first column refers to the miR-30d SmartFlare probe, whereas the second column marks the location of the scramble probe within cells. The gold nanoparticles appear preferably located within multivesicular bodies and exosomes, thus suggesting that part of the miR-30d produced in cells can be found inside these membrane-bound organelles.

endometrial epithelium compared with that of scramble miRNA; this adhesive phenotype was significantly reduced when a specific miR-30d inhibitor blocking endogenous miR-30d was used (53.44±6.4% versus 18.55±3.72%, $P=0.004$; Fig. 6C). To analyze this effect in a homologous human model, a co-culture of a choriocarcinoma human cell line (JEG3, extravillous trophoblast used for its invasive

phenotype) on top of hEECs was conducted for 24 h under three conditions: control without miRNA, in the presence of mimic miR-30d or in the presence of miR-30d inhibitor, in media previously conditioned for 72 h ($n=15$ spheroids per condition in each experiment). Analysis indicated there were no significant differences ($P>0.05$) in adhesion among the three conditions tested.

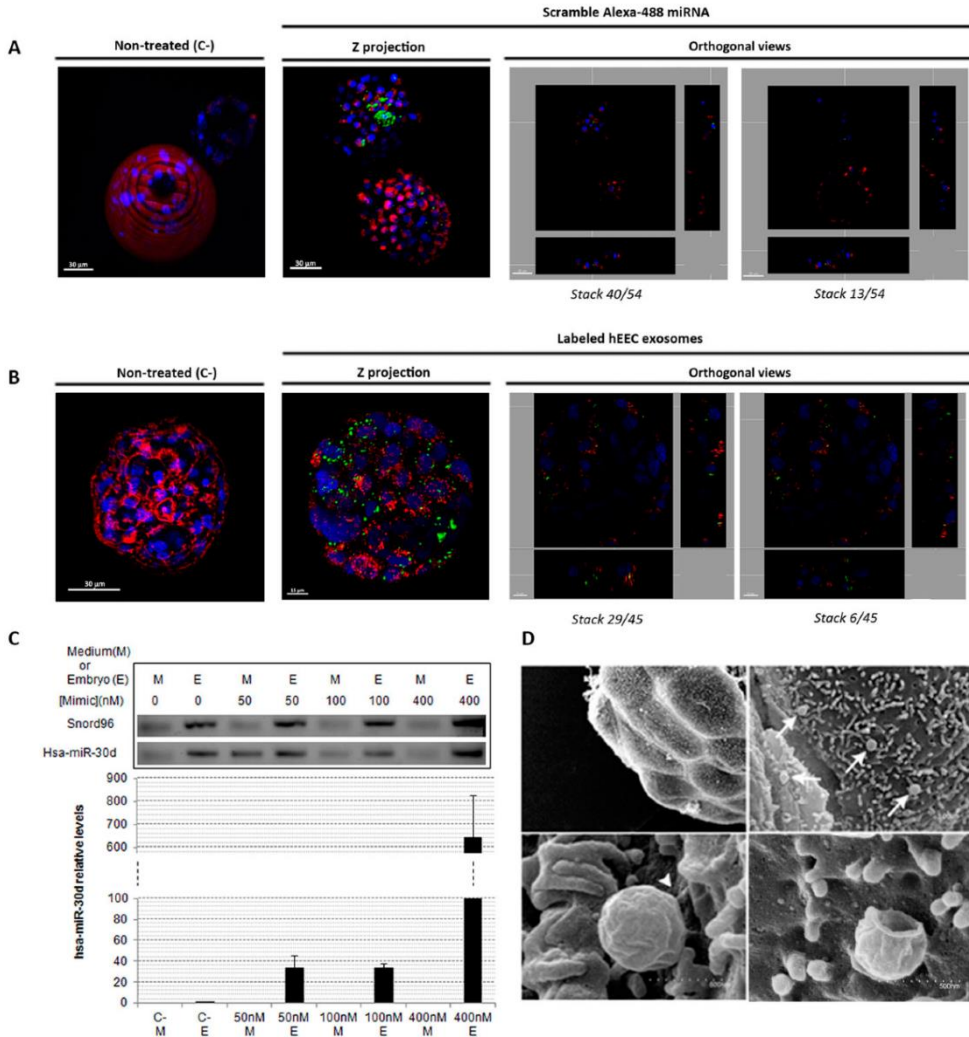


Fig. 4. Study of the ability of mouse embryos to take up free and exosome-associated miRNAs from the EF. (A) Confocal fluorescence microscopy of a live, hatching mouse blastocyst treated with 400 nM Alexa 488-scramble (green) miRNA for 72 h. Orthogonal sections performed with Imapris software confirm the internalization of free miRNAs inside embryos, discounting the possibility that these miRNAs could be adhered to the trophectoderm membrane (labeled in red). (B) Confocal microscopy images of a hatched blastocyst cultured with hEEC exosomes labeled with Vybrant DiO (green) for 24 h. Orthogonal sections performed with Imapris software confirm the internalization of exosomes inside embryos, discounting the possibility that these vesicles could be adhered to the trophectoderm membrane (labeled in red). (C) qPCR of embryos (E) treated with 0, 50, 100 or 400 nM mimic miR-30d (M). Gel bands, indicating the absence of Snord96 (housekeeping) or hsa-miR-30d in the final wash medium, are shown. (D) SEM images of a hatched mouse blastocyst with typical rounded vesicles (similar to exosomes) adhering to the trophectoderm. Arrows indicate vesicles adhering to the trophectoderm surface, arrowhead indicates a contact zone.

DISCUSSION

The 'Barker hypothesis' suggests that "the womb may be more important than the home", emphasizing the concept that the maternal endometrium has a reprogramming effect on the embryo,

fetus and adult (Barker, 1990, 1997). To date, no strong evidence has implicated molecules secreted in the EF in the origin of adult diseases. However, accumulated evidence suggests that intrauterine exposure of fetuses in patients with diabetes or obesity confers an

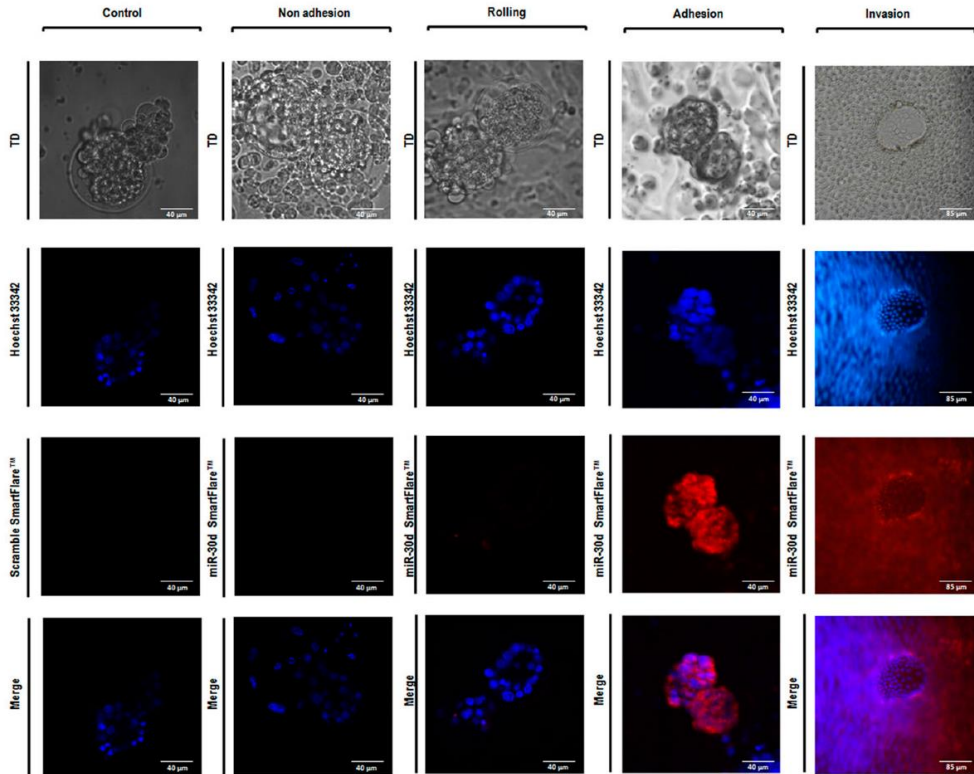


Fig. 5. *In vitro* identification of hsa-miR-30d uptake from HEECs by mouse embryos. Confocal microscopy images show the projection in the z-plane of mouse embryos that are specifically acquiring hsa-miR-30d (red) from SmartFlare-labeled-human epithelium. Micrographs are obtained in different moments of the co-culture, so the distinct stages of the implantation procedure could be identified. The intensity of the red signal progressively increases as implantation occurs. This phenomenon suggests that a direct cell-to-cell contact would probably be necessary for the transfer of hsa-miR-30d. This would explain why, in the adhesion stage, in which the contact is complete, the Cy3 label is distributed throughout the embryo, whereas just those cells of the trophoctoderm directly polarized towards the epithelium are marked in the rolling stage.

increased risk of these diseases in the adult life of offspring (Clausen et al., 2008). Similarly, follow-up studies of the Pima Native American community in Arizona, a population with an extremely high prevalence of type-2 diabetes (T2D) and obesity, demonstrate that the offspring of mothers affected by T2D during pregnancy were at substantially higher risks of developing both T2D (45% versus 1.4%) and obesity (58% versus 17%) than children born to the same mother in a non-diabetic status (Dabelea et al., 2000).

Our study, which is consistent with other evidence (Ng et al., 2013), demonstrates the presence of miRNAs differentially secreted in human EF throughout the menstrual cycle. In this study, hsa-miR-30d was the most differentially expressed miRNA during the WOI; miR-30d was previously described in endometrial physiology (Moreno-Moya et al., 2014). Therefore, we used this molecule as the paradigm for our hypothesis regarding maternal transcriptomic reprogramming of the pre-implantation embryo. Hsa-miR-30d belongs to the miR-30 family comprising six molecules (hsa-

miR-30a-f) that possess a sequence highly conserved between species. In general, the miR-30 family is ubiquitously expressed in humans and has been associated with several functions in different cell types. For example, this family participates in the epithelial-to-mesenchymal transition (Özcan, 2014), confers an epithelial phenotype to human pancreatic cells (Joglekar et al., 2014), regulates apoptosis through TP53 targeting and the mitochondrial fusion machinery (Li et al., 2010), and participates in ectoderm differentiation during embryonic development by targeting the embryonic ectoderm development (EED) protein (Song et al., 2011).

MiRNAs are often transported through exosomes, which are emerging as important mediators of intercellular communication. The secretion of exosomes from the apical surface of endometrial glands was confirmed here by electron microscopy, which is consistent with the existence of endosomes in epithelial cells and small vesicles in EF observed by immunohistochemistry. Further, primary HEECs were found to actively secrete large quantities of

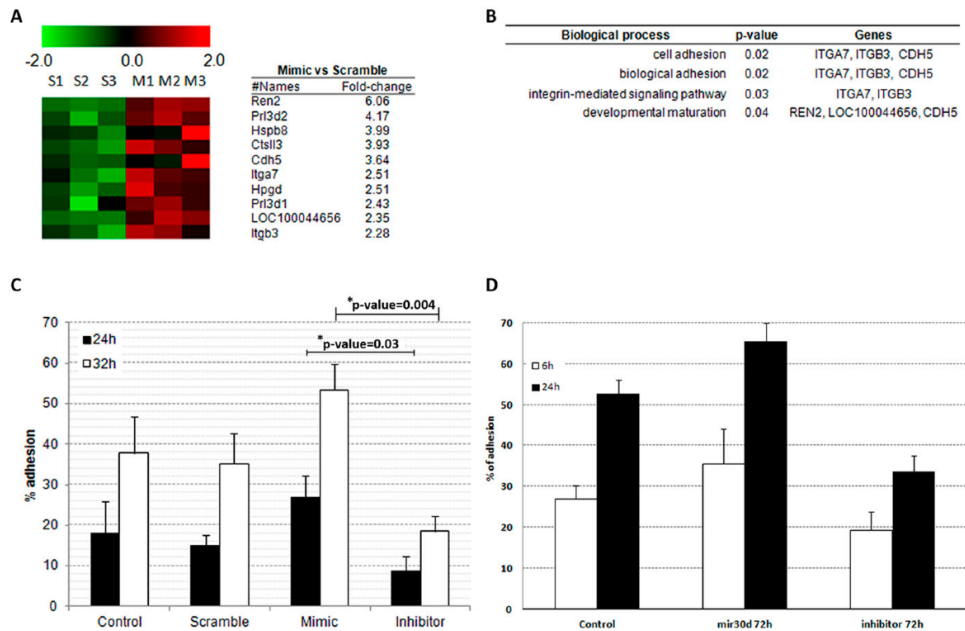


Fig. 6. Transcriptional and functional modifications in mouse embryos induced by hsa-miR-30d. (A) Supervised and standardized heat map of differentially expressed genes obtained from gene expression microarrays in embryos treated with scramble miRNA (S) or mimic miR-30d (M). (B) Significantly affected biological processes based on predictions made by the web-based tool DAVID. (C) Mouse blastocyst adhesion assay showing a functional effect related to miR-30d uptake. (D) JEG3 adhesion assay showing a functional effect related to miR-30d uptake. (C,D) Data are expressed as means \pm e.m.

exosomes into the conditioned media, and labeling experiments with miR30-d revealed that this miRNA is internalized in vesicles and secreted in exosomes. In addition, miR-30d was detected in the remaining supernatant from EF and conditioned media samples after harvesting of exosomes by ultracentrifugation, suggesting that other soluble forms are also present in the EF. Several tracking experiments showed that exosomes loaded with miR-30d were secreted from hEECs and could be internalized by trophoblastic cells of murine embryos adhered to hEECs. These findings demonstrate that the maternal factors can be transmitted through EF to the embryo.

Several mechanisms, such as endocytosis or fusion of the exosomes with the plasma membrane (Colombo et al., 2014), have been proposed to explain how exosome content is released into target cells. Here, the addition of free miRNAs into culture media at different concentrations resulted in the incorporation of these molecules into the hatched trophoblastic cells. In electron microscopy images, we observed that murine embryos presented microvilli and what appeared to be small pores interspaced along the trophoblastic surface. This finding could explain how blastocysts mediate a fast exchange of nutrients and molecules.

To understand the functional role of maternal miR-30d incorporation into the embryo, transcriptomic studies were performed to compare the effects of mimic miR-30d miRNAs and scramble miRNA in murine embryos. Expression arrays demonstrated that embryos treated with miR-30d exhibited increased expression of ten genes, including those encoding

adhesion molecules such as ITGB3, ITGA7 and CDH5. The induction of this adhesive phenotype was validated *in vitro* by adhesion assays showing a significant increase in the adhesion of murine embryos treated with miR-30d mimic versus miR-30d inhibitor. To clarify whether these findings could be extrapolated to humans, an *in silico* analysis of the putative targets of miR-30d in mice and humans was performed using the TargetScan database (<http://www.targetscan.org>). Specifically, 1594 targets were identified in humans and 1396 in mice, with 1108 common targets between both species (supplementary material Table S8). As most of the target genes coincided, we expected that the physiological functions in which they were involved could be similar. The gene ontology (GO) terms associated with these genes were analyzed using the Ensembl database (<http://www.ensembl.org/>), identifying a total of 2422 common terms between humans and mice (supplementary material Tables S9, S10). Notably, among the common terms, 19 were involved in embryonic development, highlighting the relevance of this paradigm.

In summary, we have identified a novel cell-to-cell communication mechanism that involves the delivery of endometrial miRNAs from the maternal endometrium to the pre-implantation embryo. Exosome-associated and free hsa-miR-30d was taken up by the embryo from the EF. Trophoblast cells are able to take up maternal miRNAs; these miRNAs are proposed to be incorporated into the RISC complex to exert gene regulation under physiological conditions, thereby resulting in the observed modifications to the transcriptome and embryo adhesion (Fig. 7).

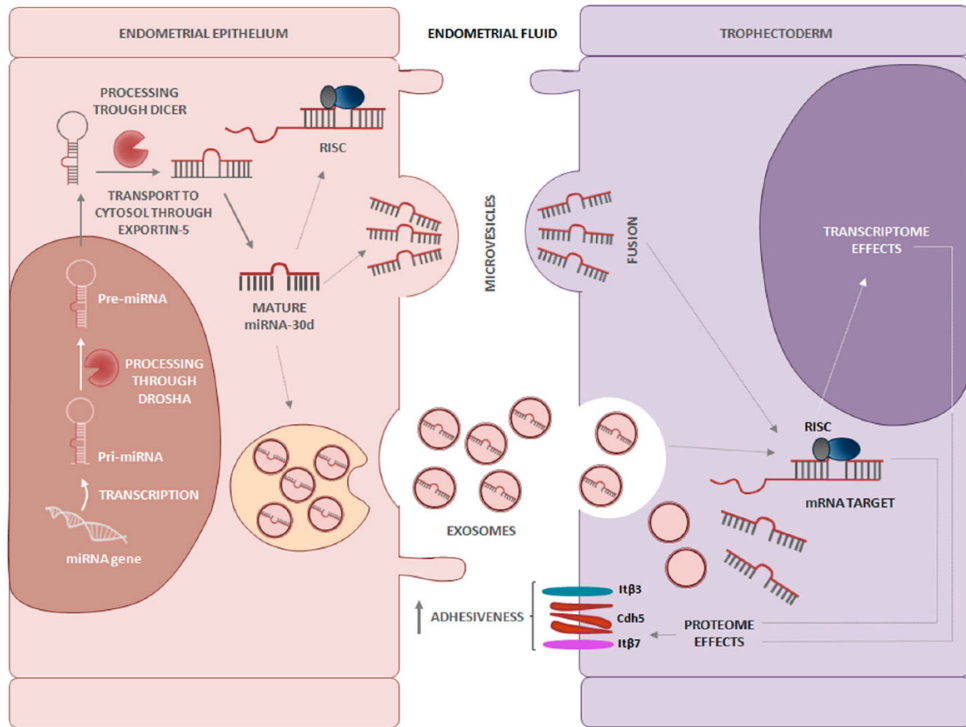


Fig. 7. Schematic of a novel maternal-fetal cross-talk mechanism promoted by hsa-miR-30d. Hsa-miR-30d is delivered to the EF from the maternal endometrium, modifying the embryo transcriptome and its adhesive phenotype.

MATERIALS AND METHODS

EF samples

This study was approved by the institutional review board of the Instituto Valenciano de Infertilidad (IVI) (project number 1204-C-102-FV-F), Valencia, Spain. Written informed consent was obtained from all donors involved in this prospective study. Healthy participants with regular menstrual cycles of 25-33 days and without underlying endometrial pathologies were selected for collection of EF samples ($n=20$). None of the women received hormonal treatment in the 3 months preceding biopsy and EF collection. Women were divided into five groups ($n=4$ per group), according to the stage of the cycle when the samples were obtained (EP, LP, ES, LS and WOI), based on the date of the last menstruation (supplementary material Table S1). Briefly, a speculum was inserted into the subject while in the lithotomy position. Next, the cervix was cleansed and a flexible catheter (Wallace; Smiths Medical) gently introduced to aspirate 20-50 μ l of endometrial secretion. EF samples were preserved at -80°C until they were used for RNA extraction.

RNA extraction from EF

RNA extraction was performed using the miRNeasy Kit (Qiagen) and quantified using a NanoDrop spectrophotometer (Thermo Fisher Scientific). To characterize the fraction of miRNAs present, a Small RNA kit and a Small RNA assay were used on samples with the Agilent 2100 Bioanalyzer (Agilent Technologies). MiRNA microarray analysis was performed in triplicate. miRNAs were quantified using the Small RNA LabChip

Bioanalyzer 2100 (Agilent Technologies) (see supplementary material Table S1A and Fig. S1).

miRNA microarray analysis

The grouped EF cohorts were analyzed using human miRNA v3.0 8×15 K microarrays (Agilent Technologies), which evaluate the expression of 866 human miRNAs. Total RNA was processed from each sample according to the manufacturer's instructions and then scanned. Data obtained for each probe were normalized and \log_2 -transformed using R software and Bioconductor database libraries. The web-based Babelomics tool (Medina et al., 2010) was used for merging the resulting data matrix in accordance with the mean number of replicates for each probe. Next, the data matrix was analyzed, and differentially expressed miRNAs were listed together with their fold change. PCA of the differentially expressed miRNAs was performed using Babelomics. IPA software (Ingenuity Systems) was used for predicting the affected biological functions and any previously reported interactions between the miRNAs and target genes. Raw data are available in the Gene Expression Omnibus (GEO) database under the accession number GSE44558.

miRNA PCR validation

To confirm the results of the miRNA microarrays, hsa-miR-30d was selected due to its significantly higher expression during the WOI. Absolute qPCR was performed using the miScript reverse transcription and miScript SYBR Green PCR kits (Qiagen). hsa-miR-30d concentration was estimated using a standard curve ranging from 20 fM to 2 mM.

Immunohistochemistry

Formalin-fixed and paraffin-embedded human endometrial biopsies were sectioned and mounted on glass slides coated with IHC (DAKO) as described previously (Dominguez et al., 2010). The primary antibody was mouse monoclonal anti-CD63 (Abcam), which was incubated overnight. Secondary antibodies were included in the LSAB Peroxidase Kit (DAKO) and were valid against mouse-origin primary antibodies.

Isolation of exosomes from EF

EF samples were diluted in PBS (Life Technologies), vortexed vigorously and filtered using a 0.22- μ m syringe filter (Pall). The filtrates were centrifuged at 300 *g* for 10 min to remove whole cells. The supernatant was subjected to a second centrifugation at 2000 *g* for 10 min to remove dead cells, then centrifuged again at 10,000 *g* for 30 min to remove cell debris. The supernatants were re-filtered with a 0.22- μ m syringe filter (Pall) and ultracentrifuged at 120,000 *g* for 70 min. Pellets containing exosomes were used for electron microscopy, embryo uptake assays, RNA extraction and qPCR.

hEEC cultures and exosome isolation

Endometrial biopsy samples obtained from healthy donors were processed to separate the epithelial and stromal cell fractions by collagenase digestion as described previously (Simón et al., 1997), and the purified hEECs were plated into 24-well plates (Falcon; Becton Dickinson). When cultures reached confluence, they were washed with DMEM (Sigma-Aldrich) to remove FBS-contaminated exosomes and cultured in DMEM (Sigma-Aldrich). After 48 h, the conditioned medium was collected and exosomes were isolated as described in the section above.

Western blotting

Antibodies against human CD63, CD9, CD81 (System Biosciences) and calnexin (Enzo Life Sciences) were used for western blotting. Isolated exosomes secreted from primary hEEC cultures were lysed in RIPA buffer at 4°C for 20 min. Samples were quantified using a BCA protein assay kit (Pierce) and separated by SDS-PAGE before electro-transfer to PVDF membranes (Bio-Rad). Membranes were incubated overnight with specific primary antibodies diluted 1:1000 in 5% BSA. Next, membranes were washed three times with PBS-T 1% and incubated with secondary anti-mouse and anti-rabbit antibodies (System Biosciences) at a concentration of 1:20,000. Finally, target proteins were detected by using the SuperSignal West Femto Chemiluminescent kit (Thermo Fisher Scientific).

RNAse treatment of exosomes

To test whether miRNAs contained in exosomes were protected from degradation, total RNA extraction was performed on isolated exosomes using the miRNeasy Kit (Qiagen). Extracted RNA was treated with 10 ng/ μ l of RNase A (Sigma-Aldrich) at room temperature for 30 min. RNA was quantified using a NanoDrop spectrophotometer (Thermo Fisher Scientific) and the miRNA fraction evaluated using a Small RNA kit and a Small RNA assay on an Agilent 2100 Bioanalyzer (supplementary material Table S1 and Fig. S1).

In vitro identification of miR-30d production by hEECs

Confluent hEECs were incubated for 20 h with 8 μ l of a work solution comprised of a SmartFlare probe (miR-30d probe or scramble control) (Millipore) and PBS in a proportion of 1:20. After labeling was completed, cells were incubated with 5 μ g/ml Hoechst 33342 (Sigma-Aldrich) and WGA Alexa 488 (Life Technologies, Molecular Probes). Next, hEECs were washed three times with medium and visualized with a 60 \times water immersion confocal microscope (FV1000, Olympus). When the confocal assay was finished, cells were used in a TEM study to identify the location of the gold nanoparticles from the SmartFlare probes.

Recovery of pre-implantation mouse embryos

The B6C3F₁ mouse strain was purchased from Charles River Laboratories. Female mice, ages 6-8 weeks, were primed to ovulate by administering 10 IU of pregnant mare serum gonadotropin (Sigma-Aldrich). Then, 48 h later, 10 IU of human chorionic gonadotropin (Sigma-Aldrich) were

administered. Females were housed overnight with male studs and examined the following morning for the presence of a vaginal plug (classified as day 1 of pregnancy). On day 1.5 of pregnancy, the mice were euthanized by cervical dislocation and embryos were flushed from the oviduct with PBS (Life Technologies) using a 30-gauge blunt needle (code procedure 2015/VSC/PEA/00048). Embryos were then washed four times in fresh CCM-30 (Qiagen) medium and used for transcriptomic assays, electron microscopy, confocal microscopy and adhesion assays. Studies were carried out using protocols (Garrido-Gomez et al., 2012; 2014/VSC/PEA/00119 tipo2 and 2015/VSC/PEA/00048) approved by the Ministry of Presidency, Agriculture, Fisheries, Food and Water, Valencia (Spain) and the Animal Care and Use Committee of the Valencia University.

Free miRNA uptake by embryo

Before studying the internalization of free miRNAs by confocal microscopy, an *in vitro* time course to select the most suitable concentration of hsa-miR-30d was performed. For this, day-1.5 mouse embryos were cultured for 72 h with 50, 100 and 400 nM mimic hsa-miR-30d and Alexa 488 scramble miRNA. To validate the success of the internalization process, a qPCR was performed in both control and hsa-miR-30d-treated embryos. miRNA extraction was performed with Arcturus PicoPure RNA Isolation Kit (Life Technologies). Once the working concentration (400 nM) was selected, confocal microscopy assays were performed.

Exosome staining and embryo co-culture

Previously isolated exosomes were incubated with 5 μ M fluorescent Vybrant DiO (Life Technologies) at 37°C for 30 min. After labeling, exosomes were collected and ultracentrifuged to wash off the excess dye, added to hatching embryos and incubated for 12-24 h.

Confocal fluorescence microscopy

For visual inspection of the uptake of free miRNA and exosomes by mouse embryos, the aforementioned samples were incubated at 37°C for 30 min with 5 μ g/ml of Hoechst 33342 (Sigma-Aldrich) and 10 μ g/ml of WGA-Texas Red (Life Technologies, Molecular Probes) for nuclear and membrane staining, respectively. Next, excess dye was removed by transferring the embryos to new wells covered with fresh medium. Finally, embryos were placed in an 8-well μ -Slide chamber (Ibidi) filled with PBS and visualized with a 60 \times water immersion confocal microscope (FV1000, Olympus). Data analysis renderings and live animations were carried out using Imaris software (Oxford Instruments).

Electron microscopy

To assess the presence of exosomes in primary hEECs, cells and isolated exosomes were fixed in Karnovsky's solution (Doughty et al., 1997). After incubation with isolated exosomes, pre-implantation mouse embryos were fixed for 2-24 h. Briefly, freshly isolated primary hEECs were post-fixed in osmium tetroxide, washed and stained with uranyl acetate. Samples were dehydrated, embedded in epoxy resin, ultrasectioned, transferred to carbon-coated grids, and observed using a JEM-1010 transmission electron microscope (Jeol Korea) at 100 kV. Pre-implantation mouse embryos were processed for TEM in the same way but were embedded in agarose before post-fixation. Exosomes were re-suspended in 50 μ l of Karnovsky's solution, incubated for 1 h on a Formvar carbon-coated grid and contrasted with uranyl acetate. For SEM, post-fixed embryos were subjected to critical point dehydration and observed in an S-4100 scanning electron microscope (Hitachi) at 10 kV.

In vitro identification of miR-30d uptake by mouse embryos

Day-1.5 mouse embryos were incubated with hEEC previously labeled with the SmartFlare probe (miR-30d probe or scramble control) (Millipore). Before the co-culture took place, medium was removed from the cells to ensure that the signal transferred to the embryos came from the hEEC. After 30 h of co-culture, 5 μ g/ml of Hoechst 33342 (Sigma-Aldrich) was added, and analysis was performed with a 60 \times water immersion confocal microscope (FV1000, Olympus).

Transcriptomic microarray analyses

A total of 360 mouse embryos from day 1.5 (30 per condition, four conditions, including the untreated, all conditions in triplicate) were treated with either 400 nM of scramble miRNA or mimic or inhibitor of miR-30d for 72 h; we performed three biological replicates, and the total number of mouse embryos used was 1080. Next, embryos were analyzed using Agilent GE 4×44 K Mouse v3 microarrays. Total RNA from each sample was processed according to the manufacturer's instructions. After scanning, microarray data were preprocessed and normalized using the R/Bioconductor package *limma*. Quantile normalization was applied to standardize probe intensities across samples. Differential gene expression was assessed using the *RankProd* library of Bioconductor (<http://bioconductor.org>). The *RankProd* methodology uses a non-parametric statistic to estimate differential expression for each gene and a permutation scheme to estimate *P*-values and control for the FDR. Log fold changes created by *RankProd* were used to rank miRNAs according to the mean expression differences between groups. Microarray results were validated by qPCR as previously described (Estella et al., 2012b) using two of the most significantly upregulated genes, *Cdh5* and *Igf3* (supplementary material Fig. S3 and Table S1B).

Embryo adhesion assay

Epithelial endometrial cells from six donors were cultured until confluence, and 15 embryos per condition (total of four conditions) were added in three independent experiments (i.e. 360 embryos). Mouse blastocysts expanded with normal morphology were cultured in the presence of 400 nM mimic miR-30d, Alexa 488-scramble miRNA or miR-30d inhibitor (Qiagen) for 72 h. The attachment of mouse blastocysts to the epithelial cell monolayer was measured after 24 and 32 h by mechanical assay. Briefly, plates were moved on a rotation shaker for 10 s, and floating blastocysts were deemed to be unattached.

JEG3 adhesion assay

JEG3 cells, a human choriocarcinoma cell line used as a model to simulate primary trophoblast cells, were grown in a monolayer with Eagle's Minimal Essential Medium (EMEM; PPA) supplemented with 10% FBS, 0.1% fungizone and 0.1% gentamicin until 80% confluence. JEG3 cells were cultured in the presence of 400 nM miR-30 mimic, Alexa 488-scramble miRNA or miR-30d inhibitor (Qiagen) for 72 h and then plated in an ultra-low-attachment plate for spheroid formation with the same culture medium. Spheroids were observed after 24 h. hEECs from three donors were cultured until confluence and 15 spheroids added per condition. Adhesion was analyzed after 6 and 24 h by mechanical assays. After a brief rotation on the shaker, floating spheroids were considered to be unattached.

Statistical analysis

For miRNA microarrays of EF, the pre-processed (log-transformed, normalized and merged based on the number of probe replicates) data matrix was introduced into an SAM module in the MeV statistical analysis software. Samples were grouped into EP, LP, ES, WOI and LS phases and each group analyzed relative to the WOI group using an FDR correction of <5%. The fold changes in miRNA among the various samples and groups were calculated. For embryo gene expression microarrays, the pre-processed data matrix was introduced into a *Rank Product* module in MeV. Samples were assigned to their respective categories based on the intended comparison. Median differences among conditions in embryo adhesion experiments were evaluated using the Kruskal–Wallis test, after confirming that data did not follow a normal distribution. A one-way ANOVA was applied for the analysis of JEG3 adhesion assays. In both cases, Statgraphics Centurion software package (v.16.1.11) was used. *P*-values <0.05 were considered significant.

In silico analysis of transcriptomic effects

To explore how the transcriptomic effects caused by hsa-miR-30d in mouse could relate to human, the TargetScan database was used to find potential targets of miR-30d in both species. Once these were established, the Ensembl website (<http://www.ensembl.org/>) was used to determine which

GO terms were associated with the output of targets obtained. With all the information available, a screening of the coincidences existing between the two species was conducted.

Acknowledgements

We thank Prof. Eulogio Valentin for helping with the exosome separation protocol. We also thank David Montaner from Genometra Company for his excellent work on the microarrays analysis and helping us with the statistical methodology. We thank Blanca Simon and Inmaculada Moreno, PhD, for help in reading and correcting the manuscript. We thank Sheila M. Cherry, PhD, ELS, President and Senior Editor from Fresh Eyes Editing, LLC for her excellent work editing this manuscript. Finally, we are grateful to the Electronic Microscopy Service (SCSIE) at the University of Valencia for their help.

Competing interests

The authors declare no competing or financial interests.

Author contributions

F.V.: conception and design, collection and assembly of data, data analysis and interpretation, manuscript writing, final approval of manuscript and fundraising; J.M.M.-M.: conception and design, collection and assembly of data, data analysis and interpretation, and final approval of manuscript; N.B.: collection and assembly of data, data analysis and interpretation, manuscript writing and final approval of manuscript; A.G.: collection and assembly of data and final approval of manuscript; M.H.: collection and assembly of data and final approval of manuscript; S.M.: collection and assembly of data and final approval of manuscript; A.M.: data analysis and interpretation and final approval of manuscript; C.S.: conception and design, data analysis and interpretation, manuscript writing, final approval of manuscript and fundraising.

Funding

This work was supported by the IVI Foundation and Miguel Servet Program Type I of Instituto de Salud Carlos III (CP13/00038); FIS project [P14/00545] and Fondos Feder to F.V.; and the 'Atracció de Talent' Program from VLC-CAMPUS [UV-INV-PREDOC14-178329 to N.B.].

Supplementary material

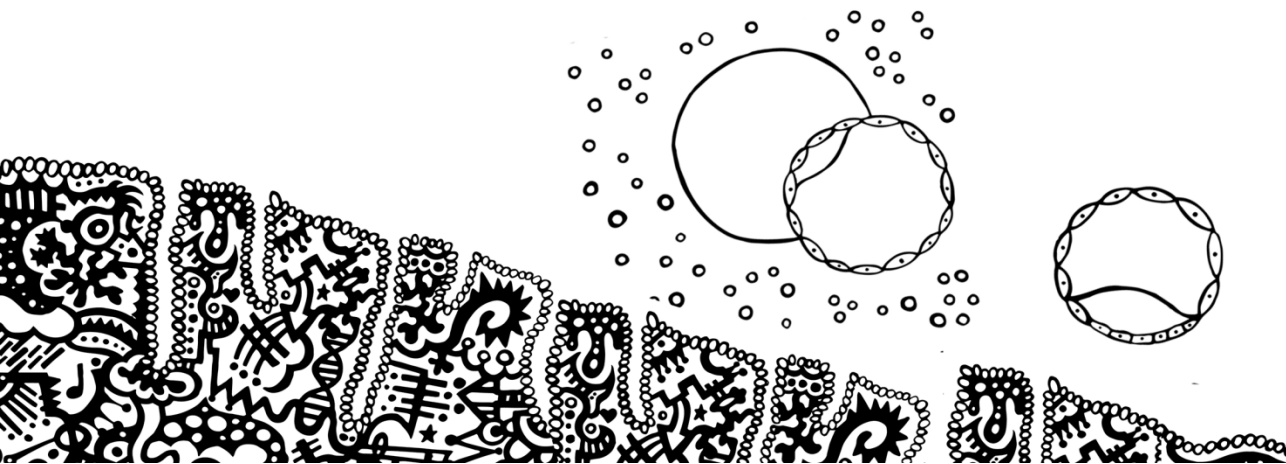
Supplementary material available online at <http://dev.biologists.org/lookup/suppl/doi:10.1242/dev.124289/-DC1>

References

- Aitmae, S., Martínez-Conejero, J. A., Salumets, A., Simón, C., Horcajadas, J. A. and Stavreus-Evers, A. (2010). Endometrial gene expression analysis at the time of embryo implantation in women with unexplained infertility. *Mol. Hum. Reprod.* **16**, 178–187.
- Ambros, V. and Chen, X. (2007). The regulation of genes and genomes by small RNAs. *Development* **134**, 1635–1641.
- Barker, D. J. (1990). The fetal and infant origins of adult disease. *BMJ* **301**, 1111.
- Barker, D. J. P. (1997). The long-term outcome of retarded fetal growth. *Clin. Obstet. Gynecol.* **40**, 853–863.
- Bartel, D. P. (2004). MicroRNAs: genomics, biogenesis, mechanism, and function. *Cell* **116**, 281–297.
- Boomsma, C. M., Kavelaars, A., Eijkemans, M. J. C., Amarouchi, K., Teklenburg, G., Gutknecht, D., Fauser, B. J. C. M., Heijnen, C. J. and Macklon, N. S. (2009). Cytokine profiling in endometrial secretions: a non-invasive window on endometrial receptivity. *Reprod. Biomed. Online* **18**, 85–94.
- Burton, G. J., Jauniaux, E. and Charnock-Jones, D. S. (2007). Human early placental development: potential roles of the endometrial glands. *Placenta* **28**, S64–S69.
- Caballero-Campo, P., Dominguez, F., Coloma, J., Meseguer, M., Remohí, J., Pellicer, A. and Simón, C. (2002). Hormonal and embryonic regulation of chemokines IL-8, MCP-1 and RANTES in the human endometrium during the window of implantation. *Mol. Hum. Reprod.* **8**, 375–384.
- Cervero, A., Horcajadas, J. A., Martín, J., Pellicer, A. and Simón, C. (2004). The leptin system during human endometrial receptivity and preimplantation development. *J. Clin. Endocrinol. Metab.* **89**, 2442–2451.
- Cha, J., Sun, X. and Dey, S. K. (2012). Mechanisms of implantation: strategies for successful pregnancy. *Nat. Med.* **18**, 1754–1767.
- Cha, J., Vilella, F., Dey, S. K. and Simón, C. (2013). Molecular interplay in successful implantation. *Science Ten critical Topics in Reproductive Medicine*, 44–48.
- Chen, K., Chen, X., He, J., Ding, Y., Geng, Y., Liu, S., Liu, X. and Wang, Y. (2015). Mouse endometrium temporal and spatial expression mma and microrna associated with embryo implantation. *Reprod. Sci.*
- Clausen, T. D., Mathiesen, E. R., Hansen, T., Pedersen, O., Jensen, D. M., Lauenborg, J. Damme, P. (2008). High Prevalence of Type 2 Diabetes and

- Pre-Diabetes in Adult Offspring of Women With Gestational Diabetes Mellitus or Type 1 Diabetes.
- Colombo, M., Raposo, G. and Théry, C. (2014). Biogenesis, secretion, and intercellular interactions of exosomes and other extracellular vesicles. *Annu. Rev. Cell Dev. Biol.* **30**, 255-289.
- Cross, J. C., Werb, Z. and Fisher, S. J. (1994). Implantation and the placenta: key pieces of the development puzzle. *Science* **266**, 1508-1518.
- Dabelea, D., Hanson, R. L., Lindsay, R. S., Pettitt, D. J., Imperatore, G., Gabir, M. M., Roumain, J., Bennett, P. H. and Knowler, W. C. (2000). Intrauterine exposure to diabetes conveys risks for type 2 diabetes and obesity: a study of discordant sibships. *Diabetes* **49**, 2208-2211.
- De los Santos, M. J., Mercader, A., Francés, A., Portolés, E., Remohí, J., Pellicer, A. and Simón, C. (1996). Role of endometrial factors in regulating secretion of components of the immunoreactive human embryonic interleukin-1 system during embryonic development. *Biol. Reprod.* **54**, 563-574.
- Dominguez, F., Garrido-Gómez, T., López, J. A., Camafeita, E., Quiñero, A., Pellicer, A. and Simón, C. (2009). Proteomic analysis of the human receptive versus non-receptive endometrium using differential in-gel electrophoresis and MALDI-MS unveils stathmin 1 and annexin A2 as differentially regulated. *Hum. Reprod.* **24**, 2607-2617.
- Dominguez, F., Simón, C., Quiñero, A., Ramirez, M. A., González-Muñoz, E., Burghardt, H., Cervero, A., Martínez, S., Pellicer, A., Palacin, M. et al. (2010). Human endometrial CD98 is essential for blastocyst adhesion. *PLoS ONE* **5**, e13380.
- Doughty, M. J., Bergmanson, J. P. and Blocker, Y. (1997). Shrinkage and distortion of the rabbit corneal endothelial cell mosaic caused by a high osmolality glutaraldehyde-formaldehyde fixative compared to glutaraldehyde. *Tissue Cell* **29**, 533-547.
- Estella, C., Herrero, I., Atkinson, S. P., Quiñero, A., Martínez, S., Pellicer, A. and Simón, C. (2012a). Inhibition of histone deacetylase activity in human endometrial stromal cells promotes extracellular matrix remodeling and limits embryo invasion. *PLoS ONE* **7**, e30508.
- Estella, C., Herrero, I., Moreno-Moya, J. M., Quiñero, A., Martínez, S., Pellicer, A. and Simón, C. (2012b). miRNA signature and Dicer requirement during human endometrial stromal decidualization in vitro. *PLoS ONE* **7**, e41080.
- Garrido-Gómez, T., Dominguez, F., Quiñero, A., Estella, C., Vilella, F., Pellicer, A. and Simón, C. (2012). Annexin A2 is critical for embryo adhesiveness to the human endometrium by RhoA activation through F-actin regulation. *FASEB J.* **26**, 3715-3727.
- Godfrey, K. M. and Barker, D. J. P. (2001). Fetal programming and adult health. *Public Health Nutr.* **4**, 611-624.
- González, R. R., Caballero-Campo, P., Jasper, M., Mercader, A., Devoto, L., Pellicer, A. and Simón, C. (2000). Leptin and leptin receptor are expressed in the human endometrium and endometrial epithelial secretion is regulated by the human blastocyst. *J. Clin. Endocrinol. Metab.* **85**, 4883-4888.
- Hannan, N. J., Stephens, A. N., Rainczuk, A., Hincks, C., Rombauts, L. J. F. and Salomonsen, L. A. (2010). 2D-DIGE analysis of the human endometrial secretome reveals differences between receptive and nonreceptive states in fertile and infertile women. *J. Proteome Res.* **9**, 6256-6264.
- Joglekar, M. V., Patil, D., Joglekar, V. M., Rao, G. V., Reddy, N. D., Mitnala, S., Shouche, Y. and Hardikar, A. (2014). The miR-30 family microRNAs confer epithelial phenotype to human pancreatic cells. *Islets* **1**, 137-147.
- Kang, Y.-J., Lees, M., Matthews, L. C., Kimber, S. J., Forbes, K. and Aplin, J. D. (2015). MiR-145 suppresses embryo-epithelial junctional communication at implantation by modulating maternal IGF1R. *J. Cell Sci.* **128**, 804-814.
- Kennedy, A. R., Pliossios, P., Otu, H., Xue, B., Asakura, K., Furukawa, N., Marino, F. E., Liu, F.-F., Kahn, B. B., Libermann, T. A., et al. (2007). A high-fat, ketogenic diet induces a unique metabolic state in mice. *Am. J. Physiol. Endocrinol. Metab.* **292**, E1724-E1739.
- Khalil, A., Jauniaux, E., Cooper, D. and Harrington, K. (2009). Pulse Wave Analysis in Normal Pregnancy: A Prospective Longitudinal Study. *PLoS ONE* **4**, e6134.
- Kuokkanen, S., Chen, B., Ojalvo, L., Benard, L., Santoro, N. and Pollard, J. W. (2010). Genomic profiling of microRNAs and messenger RNAs reveals hormonal regulation in microRNA expression in human endometrium. *Biol. Reprod.* **82**, 791-801.
- Li, J., Donath, S., Li, Y., Qin, D., Prabhakar, B. S. and Li, P. (2010). miR-30 regulates mitochondrial fission through targeting p53 and the dynamin-related protein-1 pathway. *PLoS Genet.* **6**, e1000795.
- Licht, P., Russu, V. and Wildt, L. (2001). On the role of human chorionic gonadotropin (hCG) in the embryo-endometrial microenvironment: implications for differentiation and implantation. *Semin. Reprod. Med.* **19**, 37-48.
- Liu, X., Gao, R., Chen, X., Zhang, H., Zheng, A., Yang, D., Ding, Y., Wang, Y. and He, J. (2013). Possible roles of mmu-miR-141 in the endometrium of mice in early pregnancy following embryo implantation. *PLoS ONE* **8**, e67382.
- Mansour, R., Ishihara, O., Adamson, G. D., Dyer, S., de Mouzon, J., Nygren, K.-G., Sullivan, E. and Zegers-Hochschild, F. (2014). International committee for monitoring assisted reproductive technologies world report: assisted reproductive technology 2006. *Hum. Reprod.* **29**, 1536-1551.
- Martín, J. C., Jasper, M. J., Valbuena, D., Meseguer, M., Remohí, J., Pellicer, A. and Simón, C. (2000). Increased adhesiveness in cultured endometrial-derived cells is related to the absence of moesin expression. *Biol. Reprod.* **63**, 1370-1376.
- Mascarenhas, M. N., Flaxman, S. R., Boerma, T., Vanderpoel, S. and Stevens, G. A. (2012). National, regional, and global trends in infertility prevalence since 1990: a systematic analysis of 277 health surveys. *PLoS Med.* **9**, e1001356.
- Mathivanan, S., Fahner, C. J., Reid, G. E. and Simpson, R. J. (2011). ExoCarta 2012: database of exosomal proteins, RNA and lipids. *Nucleic Acids Res.* **40**, D1241-D1244.
- Medina, I., Carbonell, J., Pulido, L., Madeira, S. C., Goetz, S., Conesa, A., Tárrega, J., Pascual-Montano, A., Nogales-Cadenas, R., Santoyo, J. et al. (2010). Babelomics: an integrative platform for the analysis of transcriptomics, proteomics and genomic data with advanced functional profiling. *Nucleic Acids Res.* **38**, W210-W213.
- Mincheva-Nilsson, L. and Baranov, V. (2010). The role of placental exosomes in reproduction. *Am. J. Reprod. Immunol.* **63**, 520-533.
- Moreno-Moya, J. M., Vilella, F., Martínez, S., Pellicer, A. and Simón, C. (2014). The transcriptomic and proteomic effects of ectopic overexpression of miR-30d in human endometrial epithelial cells. *Mol. Hum. Reprod.* **20**, 550-566.
- Ng, Y. H., Rome, S., Jalabert, A., Forterre, A., Singh, H., Hincks, C. L. and Salomonsen, L. A. (2013). Endometrial exosomes/microvesicles in the uterine microenvironment: a new paradigm for embryo-endometrial cross talk at implantation. *PLoS ONE* **8**, e58502.
- Niakan, K. K., Han, J., Pedersen, R. A., Simón, C. and Pera, R. A. R. (2012). Human pre-implantation embryo development. *Development* **139**, 829-841.
- Özcan, S. (2014). MiR-30 family and EMT in human fetal pancreatic islets. *Islets* **1**, 283-285.
- Paiva, P., Hannan, N. J., Hincks, C., Meehan, K. L., Pruysers, E., Dimitriadis, E. and Salomonsen, L. A. (2011). Human chorionic gonadotropin regulates GF2 and other cytokines produced by human endometrial epithelial cells, providing a mechanism for enhancing endometrial receptivity. *Hum. Reprod.* **26**, 1153-1162.
- Revel, A., Achache, H., Stevens, J., Smith, Y. and Reich, R. (2011). MicroRNAs are associated with human embryo implantation defects. *Hum. Reprod.* **26**, 2830-2840.
- Sha, A.-G., Liu, J.-L., Jiang, X.-M., Ren, J.-Z., Ma, C.-H., Lei, W., Su, R.-W. and Yang, Z.-M. (2011). Genome-wide identification of micro-ribonucleic acids associated with human endometrial receptivity in natural and stimulated cycles by deep sequencing. *Fertil. Steril.* **96**, 150-155.e5.
- Simón, C., Mercader, A., Francés, A., Gimeno, M. J., Polan, M. L., Remohí, J. and Pellicer, A. (1996). Hormonal regulation of serum and endometrial IL-1 alpha, IL-1 beta and IL-1ra: IL-1 endometrial microenvironment of the human embryo at the apposition phase under physiological and supraphysiological steroid level conditions. *J. Reprod. Immunol.* **31**, 165-184.
- Simón, C., Gimeno, M. J., Mercader, A., O'Connor, J. E., Remohí, J., Polan, M. L. and Pellicer, A. (1997). Embryonic regulation of integrins beta 3, alpha 4, and alpha 1 in human endometrial epithelial cells in vitro. *J. Clin. Endocrinol. Metab.* **82**, 2607-2616.
- Song, P.-P., Hu, Y., Liu, C.-M., Yan, M.-J., Song, G., Cui, Y., Xia, H.-F. and Ma, X. (2011). Embryonic ectoderm development protein is regulated by microRNAs in human neural tube defects. *Am. J. Obstet. Gynecol.* **204**, 544.e9-544.e17.
- Thouas, G. A., Dominguez, F., Green, M. P., Vilella, F., Simón, C. and Gardner, D. K. (2014). Soluble ligands and their receptors in human embryo development and implantation. *Endocr. Rev.* **36**, e20141046.
- Tian, T., Zhu, Y.-L., Hu, F.-H., Wang, Y.-Y., Huang, N.-P. and Xiao, Z.-D. (2013). Dynamics of exosome internalization and trafficking. *J. Cell. Physiol.* **228**, 1487-1495.
- Tranguch, S., Daikoku, T., Guo, Y., Wang, H. and Dey, S. K. (2005). Molecular complexity in establishing uterine receptivity and implantation. *Cell. Mol. Life Sci.* **62**, 1964-1973.
- Turchinovich, A., Weiz, L., Langheinz, A. and Burwinkel, B. (2011). Characterization of extracellular circulating microRNA. *Nucleic Acids Res.* **39**, 7223-7233.
- Valadi, H., Ekström, K., Bossios, A., Sjöstrand, M., Lee, J. J. and Lötvall, J. O. (2007). Exosome-mediated transfer of mRNAs and microRNAs is a novel mechanism of genetic exchange between cells. *Nat. Cell Biol.* **9**, 654-659.
- van der Gaast, M. H., Macklon, N. S., Beier-Hellwig, K., Krusche, C. A., Fauser, B. C. J. M., Beier, H. M. and Classen-Linke, I. (2009). The feasibility of a less invasive method to assess endometrial maturation-comparison of simultaneously obtained uterine secretion and tissue biopsy. *BJOG* **116**, 304-312.
- Vilella, F., Ramirez, L., Berlanga, O., Martínez, S., Alamá, P., Meseguer, M., Pellicer, A. and Simón, C. (2013). PGE2 and PGE2α Concentrations in Human Endometrial Fluid as Biomarkers for Embryonic Implantation. *J. Clin. Endocrinol. Metab.* **98**, 4123-4132.
- Yoshizawa, J. M. and Wong, D. T. W. (2013). Salivary MicroRNAs and oral cancer detection. *Methods Mol. Biol.* **936**, 313-324.


Heterogeneous ribonucleoprotein C1 may control miR-30d levels in endometrial exosomes affecting early embryo implantation



Heterogeneous nuclear ribonucleoprotein C1 may control miR-30d levels in endometrial exosomes affecting early embryo implantation

N. Balaguer¹, I. Moreno^{2,3}, M. Herrero², M. González²,
C. Simón^{1,2,3,4,*},†, and F. Vilella^{1b} 3,4,*

¹Department of Pediatrics, Obstetrics and Gynecology, School of Medicine, University of Valencia, 46010 Valencia, Spain ²Department of Basic Research, Igenomix, S.L. Parque Tecnológico de Paterna, 46980 Valencia, Spain ³Department of Obstetrics and Gynecology, School of Medicine, Stanford University, CA 94305, USA ⁴Department of Reproductive Medicine, Igenomix Foundation, Instituto de Investigación Sanitaria Hospital Clínico (INCLIVA), 46010 Valencia, Spain

*Correspondence address: Igenomix, S.L. Ronda Narciso Monturiol, 11B. Edificios Europark. Parque Tecnológico, 46980, Paterna (Valencia), Spain. Tel: 963905310; Fax: 963902522; E-mail: carlos.simon@igenomix.com (C.S.); felipe.vilella@igenomix.com (F.V.)  orcid.org/0000-0002-0039-9846

Submitted on February 1, 2018; resubmitted on May 16, 2018; editorial decision on May 25, 2018; accepted on May 28, 2018

STUDY QUESTION: Is there a specific mechanism to load the microRNA (miRNA), hsa-miR-30d, into exosomes to facilitate maternal communication with preimplantation embryos?

SUMMARY ANSWER: The heterogeneous nuclear ribonucleoprotein C1 (hnRNPC1) is involved in the internalization of endometrial miR-30d into exosomes to prepare for its subsequent incorporation into trophoctoderm cells.

WHAT IS KNOWN ALREADY: Our group previously described a novel cell-to-cell communication mechanism involving the delivery of endometrial miRNAs from the maternal endometrium to the trophoctoderm cells of preimplantation embryos. Specifically, human endometrial miR-30d is taken up by murine blastocysts causing the overexpression of certain genes involved in embryonic adhesion (Itb3, Itga7 and Cdh5) increasing embryo adhesion rates.

STUDY DESIGN, SIZE, DURATION: Transfer of maternal miR-30d to preimplantation embryos was confirmed by co-culture of wild-type (WT) and miR-30d knockout (KO) murine embryos with primary cultures of human endometrial epithelial cells (hEECs) in which miR-30d was labeled with specific Molecular Beacon (MB) or SmartFlare probes. Potential molecules responsible for the miR-30d loading into exosomes were purified by pull-down analysis with a biotinylated form of miR-30d on protein lysates with human endometrial exosomes, identified using mass spectrometry and assessed by flow cytometry, western blotting and co-localization studies. The role of hnRNPC1 in the miR-30d loading and transportation was interrogated by quantification of this miRNA in exosomes isolated from endometrial cells in which hnRNPC1 was transiently silenced using small interference RNA. Finally, the transfer of miR-30d to WT and KO embryos was assessed upon co-culture with sihnRNPC1 transfected cells.

PARTICIPANTS/MATERIALS, SETTING, METHODS: Murine embryos from miR-30d WT and KO mice, (strain MirC26tm1Mtm/Mmjax), were obtained by oviduct flushing of superovulated females. Endometrial Exosomes were purified by ultracentrifugation of supernatants from primary cultures of hEECs or Ishikawa cells. MB and Smartflare miR-30d probes were detected by confocal and/or transmission electron microscopy (TEM). hEECs and exosomes derived from them were subjected to pull-down with a biotinylated form of miR-30d. Captured proteins were identified by mass spectrometry (MS/MS). Western blotting was performed to detect hnRNPC1 and CYR61 in whole lysates, subcellular fractions and secreted vesicles from hEECs. Co-localization studies of the selected proteins with the exosomal marker CD63 were performed. FACS analysis was carried out to determine the presence of hnRNPC1 inside exosomes. Silencing of hnRNPC1 was conducted in the Ishikawa Cell Line with the Smart Pool Accell HNRNPC siRNA at a final concentration of 50 nM. RT-qPCRs

[†]Contributed equally to this work.

were done to determine the messenger levels of miR-30d in cells and exosomes. Co-cultures of WT and KO embryos were established with Ishikawa cells double-transfected with sihnRNPCI and MB probes.

MAIN RESULTS AND THE ROLE OF CHANCE: MS/MS analysis allowed us to identify hnRNPCI as a possible protein to influence miR-30d loading into exosomes. Co-localization studies of hnRNPCI with CD63 and FACS analyses suggested the presence of hnRNPCI inside exosomes. Silencing of hnRNPCI in Ishikawa cells resulted in a sharp decrease of the levels of miR-30d in both epithelial-like cells ($P = 0.0001$) and exosomes ($P = 0.0152$), suggesting its potential role in miR-30d biogenesis and transfer. Co-culture assays of miR-30d KO embryos with sihnRNPCI hEECs revealed a decrease in embryo-miR-30d acquisition during the adhesion and invasion stages. In turn, transient silencing of hnRNPCI results in a significant decrease of blastocyst adhesion compared to mock transfection conditions using Block-it, in both WT [Mean \pm SD; $67 \pm 10.0\%$ vs. $38 \pm 8.5\%$ ($P = 0.0006$)] and miR-30d KO embryos [Mean \pm SD; $50 \pm 11.5\%$ vs. $26 \pm 8.8\%$ ($P = 0.0029$) ($n = 2$); 14 embryos transferred per condition tested].

LARGE-SCALE DATA: MS/MS data are available via ProteomeXchange with identifier PXD008773.

LIMITATIONS, REASONS FOR CAUTION: The Ishikawa Cell Line was used as a model of hEECs in silencing experiments due to the low survival rates of primary hEECs after transfection.

WIDER IMPLICATIONS OF THE FINDINGS: The data show that hnRNPCI may be involved in the internalization of miR-30d inside exosomes. The decreased rates of embryo adhesion in endometrial epithelial-like cells transiently silenced with sihnRNPCI evidence that hnRNPCI could be an important player in the maternal-embryo communication established in the early stages of implantation.

STUDY FUNDING AND COMPETING INTEREST(S): This work was supported by the Miguel Servet Program Type I of Instituto de Salud Carlos III [CPI3/00038]; FIS project [PI14/00545] to F.V.; the 'Atracció de Talent' Program from VLC-CAMPUS [UV-INV-PREDOC14-178329 to NB]; a Torres-Quevedo grant (PTQ-13-06133) by the Spanish Ministry of Economy and Competitiveness to IM and MINECO/FEDER Grant [SAF2015-67154-R] to C.S. The authors declare there is no conflict of interest.

Key words: hnRNPCI / implantation / crosstalk / miRNAs / extracellular vesicles

Introduction

Currently, microRNAs (miRNAs) constitute a promising model for cell-to-cell communication (Valadi et al., 2007) since they are transferred between cells to execute essential roles in many processes. Their structure and size, in addition to various transport mechanisms, allow them to remain stable within various biological fluids (Turchinovich et al., 2013; Larrea et al., 2016), surviving in extremely adverse conditions, including low pH, boiling and freezing (Pieters et al., 2015). The presence of miRNAs in reproductive fluids, such as follicular, uterine and seminal fluid, indicate potential roles in the reproductive system. These extracellular miRNAs can be transported by lipoproteins [both high-density lipoprotein (HDL) and low-density lipoprotein (LDL)] (Vickers et al., 2011; Michell and Vickers, 2016 or other proteins, including Argonaute2 (AGO2) (Arroyo et al., 2011; Turchinovich et al., 2011) and nucleophosmin1 (NPM1) (Wang et al., 2010). Another transport system is mediated by extracellular vesicles (EVs), such as apoptotic bodies (Zernecke et al., 2009), microvesicles (MVs) (Hunter et al., 2008) and/or exosome-like vesicles (Harding et al., 2013). EVs protect miRNAs from degradation and contribute to their stability within biological fluids (Pieters et al., 2015). Furthermore, EVs can transport a wide range of components packaged in a selective way. For instance, Squadrito et al. (2014), used macrophages and endothelial cells to demonstrate that the sorting of miRNAs into EVs for heterotrophic cell communication is altered by both, the presence of target transcripts and presence of the miRNAs themselves (Squadrito et al., 2014). In addition, the repertoire of miRNAs found in the exosomes significantly differs for that in the parent cells (Koppers-Lalic et al., 2014).

To date, mechanisms controlling the specific loading of miRNAs into exosomes remain unclear. Indeed, several mechanisms may

govern exosome sorting of specific subsets of miRNAs (Santangelo et al., 2016). miRNA sorting appears to be influenced by different pathways and molecules in different cell types and tissues (Villarroya-Beltri et al., 2013; Janas et al., 2015; Zhang et al., 2015), and miRNAs contain well-defined motifs (i.e. EXOmotifs), that direct the miRNA allocation into exosomes before delivery into recipient cells (Villarroya-Beltri et al., 2013). A recent study showed that this RNA sequence can be recognized by the sumoylated form of the heterogeneous ribonucleoprotein A2B1 (hnRNPA2B1; Villarroya-Beltri et al., 2013). Moreover, a terminal 30 nucleotide addition in miRNAs affects their selective sorting in B cells (Koppers-Lalic et al., 2014). Another hypothesis suggests that RNAs are selectively sorted depending on the differential affinity of RNA motifs towards the raft-like region of the cytoplasmic surface of multivesicular body (MVB) limiting membranes (Janas et al., 2015).

Current data indicate that cells can communicate with each other through the transfer of miRNA-loaded exosomes (Zhang et al., 2010; Mittelbrunn et al., 2011; Hergenreider et al., 2012; Montecalvo et al., 2012; Roccaro et al., 2013). For example, monocyte-derived exosomes deliver miR-150 to endothelial cells and enhance endothelial cell migration by reducing c-myc expression (Zhang et al., 2010). The miRNA content of exosomes plays a critical role in such cell-to-cell communication and determines the fate of recipient cells. Thus, exosomes derived from the bone marrow mesenchymal stromal cells of myeloma patients promote tumor growth depending on the content of miR-15a in exosomes (Roccaro et al., 2013).

Our group has described a novel cell-to-cell communication mechanism involving the delivery of endometrial miRNAs from the maternal endometrium to the trophoblast cells of preimplantation embryos (Vilella et al., 2015). Specifically, in B6C3 derived mouse embryos, we found EV-associated and free miR-30d to cause overexpression of

genes involved in embryonic adhesion processes, including *Irb3*, *Irga7* and *Cdh5* (Vilella et al., 2015). Furthermore, supplementing murine embryos with miR-30d significantly improved embryo adhesion, suggesting that external miRNAs may have a functional role as transcriptional modifiers of preimplantation embryos. Based on profiling of miRNAs in endometrial fluid, maternally-derived miRNAs are present within EVs in the uterine microenvironment. The internalization of maternally-derived exosomes has been visualized, but the mechanism by which miR-30d becomes incorporated into exosomes remains unknown. The present study aimed to elucidate the underlying mechanism of hsa-miR-30d transfer from human endometrial epithelial cells (hEECs) to the interior of exosomes and eventually to early-stage blastocysts, using a miR-30d knockout (KO) murine model.

Materials and Methods

Recovery of preimplantation mouse embryos

Mice lacking miR-30d and their wild-type (WT) counterparts, were obtained from Jackson laboratories for the strain MirC26tm1Mtm/Mmjx using as background C57BL/6, Fvb and 192P2. Adult mice were caged in a controlled environment with a cycle of 14L:10D. All animal procedures were approved by the Ethics Commission in Experimental Research of the University of Valencia authorized by the Department of Agriculture, Livestock and Fisheries of the Spanish Government (Code: 2015/VSC/PEA/00048). Female mice, aged 6–8 weeks, were primed to ovulate by administering 10 IU of pregnant mare serum gonadotropin (Sigma-Aldrich, Madrid, Spain). Forty-eight hours later, 10 IU of hCG (Sigma-Aldrich) were administered. Females were housed overnight with male studs and examined the following morning for the presence of a vaginal plug (classified as Day 1 of pregnancy). On day E1.5 of pregnancy, the mice were euthanized by cervical dislocation and embryos flushed from the oviduct with PBS (Life Technologies, Waltham, MA, USA) using a 30-gauge blunt needle. Embryos were then washed four times in fresh CCM-30 medium (Vitrolife, Englewood, CO, USA). After washing was completed, embryos were incubated at 37°C, 5% CO₂ in air in CCM-30 medium for 72 h until they arrived at a hatching stage.

Detection of miR-30d using confocal microscopy

WT or KO embryos at day E4.5 were co-cultured in μ -Slide 8-Well ibiTreat plates (Ibidi GmbH, Planegg/Martinsried, Germany) on hEECs previously transfected with Molecular Beacon (MB) probes (200 ng/ μ l) specifically customized to recognize miR-30d *in vivo*. The design of the miR-30d MB was performed by Dharmacon (Lafayette, CO, USA). MBs are internally quenched hairpin-shaped oligonucleotide probes that fluoresce upon hybridization with their target sequence. Target-bound probes fluoresce as much as 100 times more intensely than background levels of unbound probes, enabling highly sensitive detection. Due to their stem, the recognition of targets by an MB is so specific that if the target differs even by a single nucleotide, the probe will not bind (Bratu et al., 2011). Sequences of the MB targeting miR-30d and the one used as a negative control are: (miR-30d)- 5'-CAC UGC AGU CGG CGA UGU UUA CCA GUG-3 and (negative control)-5'-CUC AGA AAA AAA AAA AAA AAC UGA C. The transfection was performed using HiPerfect (Qiagen, Hilden, Germany) transfection reagent following manufacturer's instructions. After 6 h of treatment, the medium was replaced. Twenty-four hours after transfection, fluorescence could be observed. For visual inspection of the uptake of miR-30d by mouse embryos, the cell embryo co-culture was incubated at 37°C, under 5% CO₂ in air for 30 min with 5 μ g/ml of

Hoechst 33342 (Sigma-Aldrich, Madrid, Spain) and 10 μ g/ml of WGA-Alexa 488 (Life Technologies, Molecular Probes, Eugene, OR, USA), for nuclear and membrane staining, respectively. Once the labeling was completed, samples were visualized at 60 \times with a water immersion confocal microscope (FV1000, Olympus). 3D modeling and live animations were carried out using Imaris software. Quantification of intensity fluorescence was performed with ImageJ software. Experiments were performed in triplicate, so that in each replicate, the signal distribution of 3–4 embryos, per condition tested, was analyzed. In the results, a representative experiment is shown.

Thermal denaturation profiles of the MB

Thermal denaturation profiles were used to determine the specificity of the molecular beacon probe used in this study. The changes in fluorescence of a 10- μ l solution containing 0.2 μ M of the beacon probe with [miR-30d mimic: 5'-UGUAAACAUCGCCGACUGGAAG; Ref: MSY0000245; Qiagen, Hilden, Germany] or without 1 μ M of a complementary single-stranded oligonucleotide were measured. Solutions were analyzed in Quantum Studio 5 Real-time PCR system. Specifically, samples were initially heated to 95°C and held at this temperature for 10 min; then, they were gradually cooled to 25°C at a rate of 1.6°C/s. As a negative control, the miRNA, miR-190 was used (miR-190 mimic: 5'-UGAUAUGUUUGAUUAUUUAGGU; Ref: MS00008911).

Detection of miR-30d using transmission electron microscopy

WT and KO embryos at day E4.5 were co-cultured in μ -Slide 8-Well ibiTreat plates (Ibidi GmbH, Planegg/Martinsried, Germany) with hEEC cells that were previously transfected with Smartflare probes (Millipore, Burlington, MA, USA). Confluent hEECs were incubated for 20 h with 8 μ l of a work solution comprised of a Smartflare probe (miR-30d probe or Scramble control) at a 1:20 dilution in PBS. Smartflare probes comprise a gold nanoparticle conjugated with many copies of the same double-stranded oligonucleotide encoding the target sequence. After 24 h of co-culture, samples were processed to identify the location of the gold nanoparticles within epithelial and trophoblast cells. For this, the co-culture was fixed with Karnovsky's solution for 1 h; and then a post-fixation process in osmium tetroxide was performed. Next, several washes were done prior to staining with uranyl acetate. Samples were dehydrated, embedded in epoxy resin, ultrasonicated, transferred to carbon-coated grids, and observed using a JEM-1010 transmission electron microscope (Jeol Korea Ltd) at 100 000 kV.

hEEC primary cultures and exosome isolation

Endometrial biopsies were obtained at day LH+0 from healthy 18–35-year-old donors. Patients diagnosed with endometriosis and/or endometritis were excluded. All patients signed informed consent prior to the sample collection; procedures were approved by the local Ethical Committee at IV Valencia, Spain (code:1308-FVI-127-FV). Endometrial samples were processed to separate the epithelial and stromal fractions by collagenase digestion and gravity sedimentation as previously described (Simón et al., 1997). When cultures reached confluence, they were washed with DMEM (Sigma-Aldrich, Madrid, Spain) to remove FBS-contaminated exosomes and then cultured in serum-depleted hEEC medium. After 24 h, the conditioned medium was collected, and cells were incubated again with hEEC medium without serum for 24 h. All collected conditioned media was subjected to a series of differential centrifugations: (1) media were centrifuged at 300g for 10 min to pellet residual cells; (2) next, supernatants were centrifuged at 2000g for 10 min; (3) the supernatants from step 2 were centrifuged at 10 000g for

30 min; (4) the supernatants from step 3 were passed through 0.22- μ m diameter filters (Acrodisc[®] syringe filters, Pall Corporation, Newquay Cornwall, UK) and centrifuged at 120 000g for 70 min using a P50AT4 Hitachi rotor. Step 4 supernatants were kept as extracellular vesicles (EV)-negative controls for further analysis. Step 4 pellets were resuspended in 1 ml PBS and centrifuged again under the same conditions (120 000g, 70 min). The pellet obtained contained the exosome enriched fraction.

miRNA pull-down

Two biological samples of hEECs and a pool of Exosomes obtained from four hEECs cultures were subjected to pull-down with a biotinylated miR-30d. Briefly, samples were isolated, resuspended in 400 μ l of buffer 1 (TBS pH 7.5, 0.5% NP-40 (v/v), 2.5 mM MgCl₂, 40 U/ml RNase inhibitor (Invitrogen, Carlsbad, CA, USA) and protease inhibitors (Complete, [Roche, Basel, Switzerland]) and precleared by incubation with streptavidin–sepharose beads (GE Healthcare, Little Chalfont, UK) for 1.5 h at 4°C. Biotinylated miR-30d [Biotin-CCCUUUA-UGUAAACAUCGCCGACUGGAAG] or poly-A [Biotin-CCCUUUA-AAAAAAAAAAAAAAAAAAAAAAAAA] (20 nmol; Thermo Fisher Scientific, Waltham, MA, USA) were resuspended in TBS with RNase inhibitor (40 U/ml; Invitrogen, Carlsbad, CA, USA) and incubated with 40 μ l streptavidin–sepharose beads (4 h at 4°C). Beads were washed twice with TBS and incubated with lysates (overnight at 4°C). Beads were washed six times in buffer 2 (TBS, 0.05% NP-40, RNase inhibitor and protease inhibitors). Protein loading buffer (Fermentas, Waltham, MA, USA) was added and beads were heated at 90°C for 10 min before proteomics analysis.

Protein identification by mass spectroscopy

In-gel digestion of proteins

Samples were digested with sequencing grade trypsin (500 ng; Promega, Madison, WI, USA) as described elsewhere (Shevchenko et al., 1996). Briefly, each slide was cut and small pieces of ~1 mm² in size were transferred into 1.5 ml Eppendorf tubes. After washing in 50 mM ammonium bicarbonate (ABC) in water pH 8 (Sigma-Aldrich, Madrid, Spain) the gel was dehydrated in acetonitrile (ACN; Fisher Scientific, Waltham, MA, USA), reduced with dithiothreitol (DTT; 10 mM in 50 mM ABC; 20 min at 60°C) and alkylated with iodoacetamide (IAM; 50 mM in 50 mM ABC; 30 min RT in the dark). For protein digestion, 500 ng of trypsin in 200 μ l of 50 mM ABC was added to each dried gel piece and digestion was done at 37°C overnight. The trypsin digestion was stopped by adding 10% trifluoroacetic acid (TFA) to 1% final concentration, and the supernatant, containing the extracted digests, was carefully removed, leaving behind the sliced gels in the Eppendorf tube. Then, for additional peptide extraction, 200 μ l of pure ACN, were added to each tube and incubated for 15 min at 37°C in a shaker. The new supernatant containing the new peptide mixture was carefully withdrawn. Both supernatants were mixed in a tube and dried in a speed vacuum (ISS 110 SpeedVac System, Thermo Savant, ThermoScientific, Langensfeld, Germany) for 20 min and re-suspended in 15 μ l of 2% ACN and 0.1% TFA prior to LC and MS analysis.

Nano-liquid chromatography tandem-mass spectrometry analysis

The peptides recovered from in-gel digestion processing were analyzed by liquid chromatography (LC) using a NanoLC Ultra I-D plus Eksigent[®] (Eksigent Technologies, Dublin, CA, USA) which was directly connected to an SCIEX TripleTOF 5600 mass spectrometer (SCIEX, Framingham, MA, USA) in direct injection mode.

Briefly, 5 μ l from each digested sample was trapped on a NanoLC pre-column (3 μ m particles size C18-CL, 350 μ m diameter x 0.5 mm long; Eksigent) and desalted with 0.1% TFA at 3 μ l/min during 5 min. Then, the digested peptides present in the samples were separated using an analytical

LC column (3 μ m particles size C18-CL, 75 μ m diameter x 12 cm long, Nipkyo Technos Co[®], Tokyo, Japan) equilibrated in 5% ACN 0.1% formic acid (FA; Fisher Scientific, Waltham, MA, USA). The peptides were eluted from the column with a linear gradient from 5–40% of solvent B at a constant flow rate of 300 nL/min over 120 min. Solvent A being 0.1% FA in water and solvent B being 0.1% FA in ACN.

Eluted peptides were ionized applying 2.8 kV to the spray emitter on an ESI Nanospray III (SCIEX). Analysis was carried out in a data-dependent mode. Survey MS1 scans were acquired from 350 to 1250 m/z for 250 ms. The quadrupole resolution was set to 'UNIT' for MS2 experiments, which were acquired 100–1500 m/z for 50 ms in 'high sensitivity' mode. Following dynamic selection criteria were used: charge: 2+ to 5+; minimum intensity; 70 counts per second (cps). Up to 50 ions were selected for fragmentation after each survey scan. Dynamic exclusion time was set to 15 s. Collision energy was automatically set by the instrument according to its Rolling collision energy equations.

The mass spectrometry proteomics data have been deposited to the ProteomeXchange Consortium via the PRIDE (Vizcaino et al., 2016) partner repository, with the dataset identifier PXD008773 and 10.6019/PXD008773.

Protein identification

The MS/MS information was sent to PARAGON algorithm via the software ProteinPilot v 4.5 (ABSciex). ProteinPilot default parameters were used to generate peak list directly from 5600 TripleTOF. The Paragon algorithm of ProteinPilot was used to search ExPASy protein database with the following parameters: trypsin specificity, cys-alkylation, no taxonomy restriction and the search effort set to through. To avoid using the same spectral evidence for more than one protein, the identified proteins were grouped based on MS/MS spectra by the ProteinPilot Progroup algorithm. A protein group in a Pro Group Report is a set of proteins that share some spectral evidence. Then, unobserved regions of protein sequence play no role in explaining the data. The False Discovery Rate (FDR) analysis was performed with the PSPEP algorithm implemented in ProteinPilot (see Supplementary files 1–6).

Endometrial epithelial cell lysates

hEECs used for exosome collection served as positive controls for western blot analysis. To obtain cellular lysates, cells were washed with PBS and frozen at –80°C for at least 1 h. Then, they were incubated with 1.5 ml of RIPA buffer (150 mM NaCl, 1% IGEPAL CA 630, 0.5% Na-DOC, 0.1% SDS, 0.5 M EDTA, 50 mM Tris-HCl, pH 8) with protease inhibitors [1% PMSF 0.1 M (Sigma-Aldrich, Madrid, Spain), 10% Roche mini complete (Roche, Basel, Switzerland)] for 10–15 min. Once lysis was complete, the supernatant was centrifuged for 13 000g for 15 min. The pellet obtained was discarded and the resulting supernatant frozen until use. Quantification of proteins was performed by BCA protein assay kit (Pierce, Rockford, IL, USA).

Western blot

Antibodies against human CD63, CD9, CD81, HSP70 (System Biosciences, Palo Alto, CA, USA), actin (ab8227, Abcam, Cambridge, UK), CYR61 (ab24448, Abcam, Cambridge, UK), hnRNPC1 (ab10294, Abcam, Cambridge, UK) and calnexin (Enzo Life Sciences, Farmingdale, NY, USA) were used for western blotting. Isolated exosomes secreted from primary hEECs cultures were lysed in RIPA buffer at 4°C for 20 min. Samples were quantified using a BCA protein assay kit (Pierce, Rockford, IL, USA) and analyzed by SDS-PAGE, followed by electroblotting onto PVDF membranes (Bio-Rad Laboratories, Hercules, CA, USA). Membranes were incubated overnight with specific primary (1:1000) antibodies diluted in 3% skimmed milk, following the specifications of the manufacturers. After three washes with 1% PBST, membranes were incubated with a 1:20 000 dilution of secondary antibodies (Santa Cruz Biotechnology, Dallas, TX,

USA). Finally, target proteins were detected by using the SuperSignal West Femto Chemiluminescent kit (Thermo Fisher Scientific, Waltham, MA, USA). Western blots of the whole lysates and exosomes were performed in triplicate, a representative image is shown.

Subcellular fractionation

hEEC subcellular compartments were fractionated with the Subcellular Proteome Extraction kit (Calbiochem, Burlington, MA, USA). Cytosol, membranous organelles, and nuclear fractions were blotted for hnRNPC1 (ab10294, Abcam, Cambridge, UK), the cytosolic marker HSP70 (System biosciences, Palo Alto, CA, USA), the tetraspanin markers CD81, CD63 and CD9 (System biosciences, Palo Alto, CA, USA), the membrane organelle marker Calnexin (Enzo Life Sciences, Farmingdale, NY, USA), the nuclear marker Histone 4 (ab10158, Abcam, Cambridge, UK) and the cytoskeletal marker Actin (ab8227, Abcam, Cambridge, UK). Western blots of the subcellular fractions were performed twice. A representative image is shown.

Immunofluorescence

hEECs were grown on μ -Slide 8-Well ibiTreat plates (Ibidi GmbH, Planegg/Martinsried, Germany) until 50–70% confluent. Then, cells were fixed with 4% of paraformaldehyde for 15–20 min at RT. Two washes were performed with 1x TBST (20 mM Tris-HCl pH 7.4, 0.15 mM NaCl, 0.05% Tween 20). Permeabilization of the cells was carried out with 0.1% Triton X-100/PBS (Ca^{2+} , Mg^{2+}) for 10 min at RT. Blocking was done with 4% normal goat serum for 30 min at RT. Incubation with a 1:50 dilution of primary antibodies against hnRNPC1 (ab10294, Abcam, Cambridge, UK) and CYR61 (ab24448, Abcam, Cambridge, UK) was performed o/n following the manufacturers' instructions. Cells were washed three times before a 60-min incubation with secondary antibodies. Alexa 488 and Alexa 555 labeled antibodies (5 $\mu\text{g}/\text{ml}$) (Life technologies, Molecular Probes, Eugene, OR, USA) were used to identify the proteins of interest and the exosome marker CD63. The labeled cells were washed three times and protein co-localization visualized with a 60x water immersion confocal microscope (FV1000, Olympus). Images were processed and assembled using Imaris software. Co-localization studies were performed in triplicate, representative images are presented. For within-cell immunofluorescence analysis of hnRNPC1, plates (Nunc 146485 24-well plates, Waltham, MA, USA) intended for In-Cell analysis (In-Cell Analyzer 2000) were used. In-Cell analysis was performed in triplicate.

Flow cytometry analysis of exosome-coupled beads

Exosomes were obtained using ultracentrifugation, resuspended in PBS and coupled to 4 mm aldehyde-sulfate beads (Invitrogen, Carlsbad, CA, USA) overnight at RT with rotation. Beads were washed and blocked for 60 min at RT in 4% bovine serum albumin in PBS. For intracellular staining, bead-bound exosomes were permeabilized and fixed for 5 min at RT with 0.2% Triton X-100, 2% formaldehyde in PBS. Beads were incubated with anti-hnRNPC1 (Abcam, Cambridge, UK) or anti-CD9 (System biosciences, Palo Alto, CA, USA) for 1 h at 4°C, washed and incubated with Alexa 488-goat-anti-mouse IgG (Invitrogen, Carlsbad, CA, USA) for 30 min. Bead signals were acquired on a FACSCalibur (BD Biosciences, USA) and data were analyzed with FlowJo software (Tree Star). Negative controls were obtained with exosome-coupled beads incubated with the secondary antibody. FACS was performed twice, a representative experiment is presented.

Validation of the miRNA pull-down assay

Sample preparation

The Ishikawa endometrial carcinoma cell line purchased from Sigma-Aldrich (Ref: 99040201) was used to validate the results obtained from the miRNA pull-down assay. Cells were grown in T-175 flask until reaching confluence, using the following culture media: MEM (Sigma-Aldrich, Madrid, Spain), 2 mM glutamine, 1% non-essential amino acids (NEAA), 5% FBS, 0.2% gentamycin and 0.2% fungizone. Next, they were washed with DMEM (Sigma-Aldrich, Madrid, Spain) to remove FBS-contaminated exosomes and then cultured in serum-depleted medium. After 24 h, the conditioned medium was collected in order to isolate the exosomes as described. A pool of the media from five flask T-175 was used to obtain the exosomes. Once the isolation was finished, exosomes were lysed in the following buffer (25 mM Tris pH 8, 150 mM NaCl, 2 mM MgCl_2 , 0.5% NP-40, 5 mM DTT, protease inhibitors and 40 U/ml RNase inhibitor (Invitrogen)). Regarding the cell lysate, this was collected in the same way as the hEEC extract was obtained.

Immunoprecipitation

Protein G Dynabeads (50 μl per condition) (Invitrogen, Carlsbad, CA, USA) were washed twice in buffer 3 (PBS, 0.01% Tween) and resuspended in 200 μl of buffer 3 containing 10 μg mouse anti-hnRNPA2B1 (Santa Cruz Biotechnology, Dallas, TX, USA) or mouse anti-IgG control (Santa Cruz Biotechnology, Dallas, TX, USA) and incubated overnight at 4°C. Isolated exosomes and cell lysates were incubated (1 h, 4°C) with non-conjugated Dynabeads (50 μl per condition). The precleared lysates were incubated with 50 μl of Ab-conjugated Dynabeads (1.5 h, 4°C), which were then washed twice with buffer 4 (25 mM Tris pH 8, 150 mM NaCl, 2 mM MgCl_2 , 0.5% NP-40, 5 mM DTT), protease inhibitors and 40 U/ml RNase inhibitor (Invitrogen, Carlsbad, CA, USA) and three times with buffer 5 (25 mM Tris pH 8, 900 mM NaCl, 2 mM MgCl_2 , 1% NP-40, 5 mM DTT, protease inhibitors and 40 U/ml RNase inhibitor). Next, they were transferred to clean tubes and washed with buffer 6 (25 mM Tris pH 8, 150 mM NaCl, 2 mM MgCl_2 , 0.05% NP-40, 5 mM DTT; protease inhibitors and 40 U/ml RNase inhibitor). For qPCR analysis, 700 μl of Qiazol lysis reagent (Qiagen) was added and samples were vortexed. Finally, miRNA extraction was performed according to the manufacturer's instructions of the kit miRneasy (Qiagen, Hilden, Germany).

miRNA extraction and qPCR

RT and qPCR for miR-30d and miR-450 (used in this experiment to test unspecific binding) were performed with miScript reverse transcription and miScript SYBR Green PCR kits (Qiagen, Hilden, Germany), respectively. In order to quantify the miRNA levels recovered from the immunoprecipitation (ip), standard curves were done for each miRNA. To do that, mimics for the miR-30d (Ref: MSY0000245, Qiagen, Hilden, Germany) and the miR-450 (Ref: MSY0001545, Qiagen, Hilden, Germany) were retro-transcribed and the following concentrations to construct the curve were used: 0, 5, 15, 20, 25, 50 and 75 pM. The primers used to conduct the qPCR are detailed next: Primer miR-450a-5p: 5'-UUUUGCGAUGU GUUCCUAAUUAU; Primer miR-30d: 5'-UGUAACAUCCTCCGACUGG AAG.

Silencing of hnRNPC1 in the Ishikawa cell line

Ishikawa cells were grown in 24-well plates until reaching 70% of confluence. Silencing was performed using Smart Pool Accell HNRNPC siRNA (Dharmacon, Lafayette, CO, USA). This pool consists of several siRNA sequences intended to target different regions of the RNA. Invitrogen™ BLOCK-iT™ Alexa Fluor™ Red Fluorescent Control (Invitrogen,

Carlsbad, CA, USA) was used to test the efficiency of the transfection. The Accell non-targeting control siRNA (Dharmacon, Lafayette, CO, USA) was used as a negative control. A time course experiment (24 h, 48 h, 72 h, 90 h and 96 h) was designed to determine the time yielding a maximum reduction in protein. Transfections were performed using Lipofectamine™ (Thermo Fisher Scientific, Waltham, MA, USA), following the manufacturer's instructions. The final concentration of siRNAs in the cell culture was 50 nM. At all analyzed time points, cells were recovered for both RNA and protein extraction. Spent media was also collected to isolate exosomes for detecting packaged miR-30d. For protein and RNA extraction, cells were trypsinized for 5 min, centrifuged at 300g for 5 min and washed twice with PBS before extraction. RNA extraction was done using the RNeasy Kit (Qiagen, Hilden, Germany) and quantified using a NanoDrop spectrophotometer (Thermo Fisher Scientific Inc., MA, USA). Protein isolation was carried out by using RIPA buffer as previously described. Western blotting for hnRNPC1 (ab10294, Abcam, Cambridge, UK) was performed as previously described. Actin (ab8227, Abcam, Cambridge, UK) was used as a housekeeping control. Experiments were performed in triplicate.

RT-qPCR

RT-qPCR was performed to determine the messenger levels of hnRNPC1 in cells and miR-30d in both, cells and exosomes. RT and qPCR for miR-30d were performed with miScript reverse transcription and miScript SYBR Green PCR kits (Qiagen, Hilden, Germany), respectively. For the determination of the relative quantity of hnRNPC1, the PrimeScript™ RT reagent Kit -Perfect Real Time- (Clontech Laboratories, Mountain View, CA, USA) and LightCycler FastStart DNA Master SYBR (Roche, Basel, Switzerland) were used. Fold changes were estimated using the $-2^{\Delta\Delta Ct}$ formula. Actin and Snord 96 were used as housekeeping controls for relative quantification of hnRNPC1 and miR-30d, respectively. Primer sequences were: hnRNPC1: FW: 5'-AGACGAAGACTGAGCGTTG-3'; RV: 5'-AGCCGAAAACAAGAAGGGGA-3'; Actin: FW: 5'-GATCATTG CTCCTCTGAGC-3'; RV: 5'-AGTCCGCCTAGAAGCACTTG-3'; miR-30d: 5'-UGUAAACAUCCTCCGACUGGAAG-3' (Ref: MS0009387, Qiagen), SNORD 96: Hs_SNORD96A.11 miScript Primer Assay (Ref: 218300, Qiagen, Hilden, Germany). Experiments were performed in triplicate.

Co-culture of murine embryos with siRNA hnRNPC1-transfected cells

Ishikawa endometrial carcinoma cells were seeded at a density of 80 000 cell/cm² in μ -Slide 8-Well ibiTreat plates (Ibidi GmbH, Planegg/Martinsried, Germany). At 70% confluency, cells were transfected simultaneously with Smart Pool Accell HNRNPC siRNA (Dharmacon, Lafayette, CO, USA) and the MB probe for detecting miR-30d. After 90 h of transfection, cells were washed with PBS and refreshed with new media. WT and KO blastocysts were transferred onto and allowed to contact the cells for 24 h at 37°C under 5% CO₂ in air. Then, the co-culture was incubated at 37°C for 30 min with 5 μ g/ml Hoechst 33342 (Sigma-Aldrich, Madrid, Spain) and 10 μ g/ml of WGA-Alexa 488 (Life Technologies, Molecular Probes, Eugene, OR, USA), for nuclear and the membrane staining, respectively. Once labeling was complete, co-cultures were visualized at 60 \times with a water immersion confocal microscope (FV1000, Olympus). 3D modeling was carried out using Imaris software. Quantification of intensity fluorescence was performed with ImageJ software. Experiments were performed in duplicate, so that in each replicate, the signal distribution of 3–4 embryos, per condition tested, was analyzed. In the results, a representative experiment is shown.

Embryo adhesion assay

Ishikawa cells transfected with Block-It or sihnRNPC1 and untransfected controls were cultured until confluence in μ -Slide 8-Well ibiTreat plates (Ibidi GmbH, Planegg/Martinsried, Germany). Then, WT or miR-30d KO embryos were added (14 embryos per condition, six conditions) in two independent experiments ($n = 168$, total embryos). The attachment of mouse blastocysts to the epithelial cell monolayer was measured after 24 h by mechanical assay. Briefly, plates were moved on a rotation shaker for 10 s, and floating blastocysts were deemed to be unattached.

Statistical analysis

The Statgraphics Centurion software package (v.16.1.11) was used to study the significance of the results. One-way ANOVA was applied with a P -value < 0.05 indicating significance.

Results

Transfer of hsa-miR-30d from human endometrial epithelial cells to trophectoderm cells of invading and hatching miR-30d KO embryos

Here, we co-cultured WT or miR-30d KO blastocysts on hEECs previously transfected with MB probes customized to specifically recognize hsa-miR-30d within living cells (Fig. 1A). Prior to doing the assays, MB probes were initially characterized to evaluate their specificity for the miR-30d. (Supplementary Fig. 1). As it can be seen by the thermal denaturation profiles, fluorescence of the MB is higher with the miR-30d compared to the cases where no target or a mismatch target oligonucleotide are used.

Figure 1B displays micrographs of hatching and invading embryos obtained from WT and KO mice. The Cy3 fluorophore appears concentrated in the trophectoderm cells of hatching embryos that remain in direct contact with hEECs. However, in the blastocoel cavity of blastocysts still protected by the zona pellucida, the signal was barely detected. In contrast, in invading embryos, the signal was widely distributed throughout the blastocoel, confirming that an intimate cell-to-cell contact was necessary for the miRNA transfer. Orthogonal sections of different z-stacks verified that the signal was located inside cells and not attached to surface membranes (Fig. 1B). The 3D reconstruction of the embryos shown in the Supplementary videos 1–4 corroborates this fact. Moreover, it is noteworthy that the intensity of the signal identified is significantly decreased in KO embryos regardless of the grade of invasion accomplished (Fig. 1C).

To further understand the transfer of miR-30d from the maternal endometrium to the trophectoderm cells of embryos, WT or KO embryos were co-cultured with hEECs previously transfected with SmartFlare probes, designed specifically for miR-30d recognition. The main characteristic of these probes is the presence of a gold nanoparticle conjugated with many copies of the same double-stranded oligonucleotide encoding the target sequence. In Fig. 2A, a topographic reconstruction of a KO embryo during the adhesion process is presented showing trophectodermal cells establishing contact with hEECs. The areas with the miR-30d coupled to gold nanoparticles are highlighted in the frames, showing the presence of this probe in miR-30d KO blastocyst, transferred from hEECs. The particles were widely

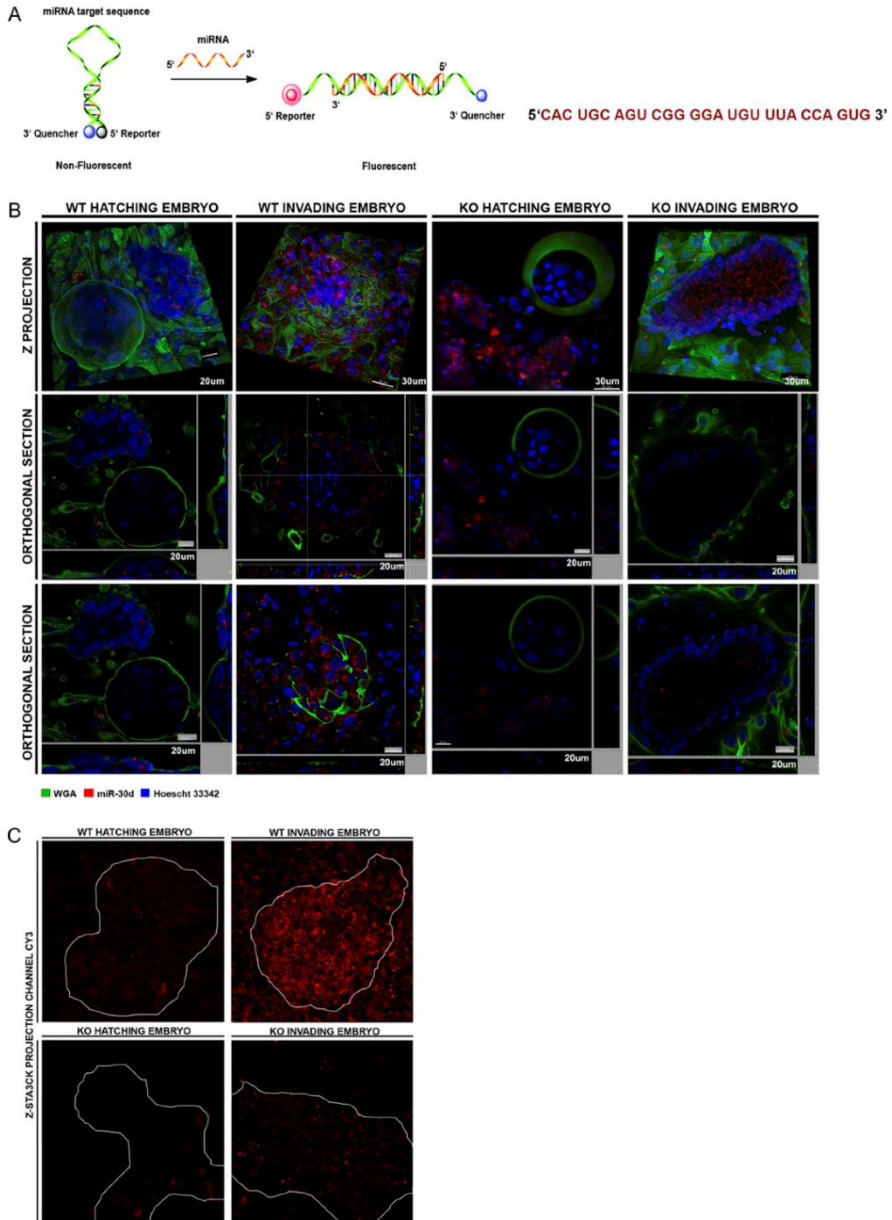


Figure 1 Studying miR-30d transfer from human endometrial epithelial cells (hEECs) to trophectoderm cells in a miR-30d knockout (KO) and wild-type (WT) murine embryos **(A)** Image of the molecular beacon (MB) structure. On the right, the MB sequence used to detect miR-30d in living cells is shown. **(B)** Confocal images of a co-culture of WT and miR-30d KO embryos with hEECs previously transfected with an MB probe. Cy3: miR-30d, WGA-Alexa 488: membrane labeling, Hoechst 33382: nuclear staining. **(C)** Relative intensity fluorescence calculated for each of the conditions tested.

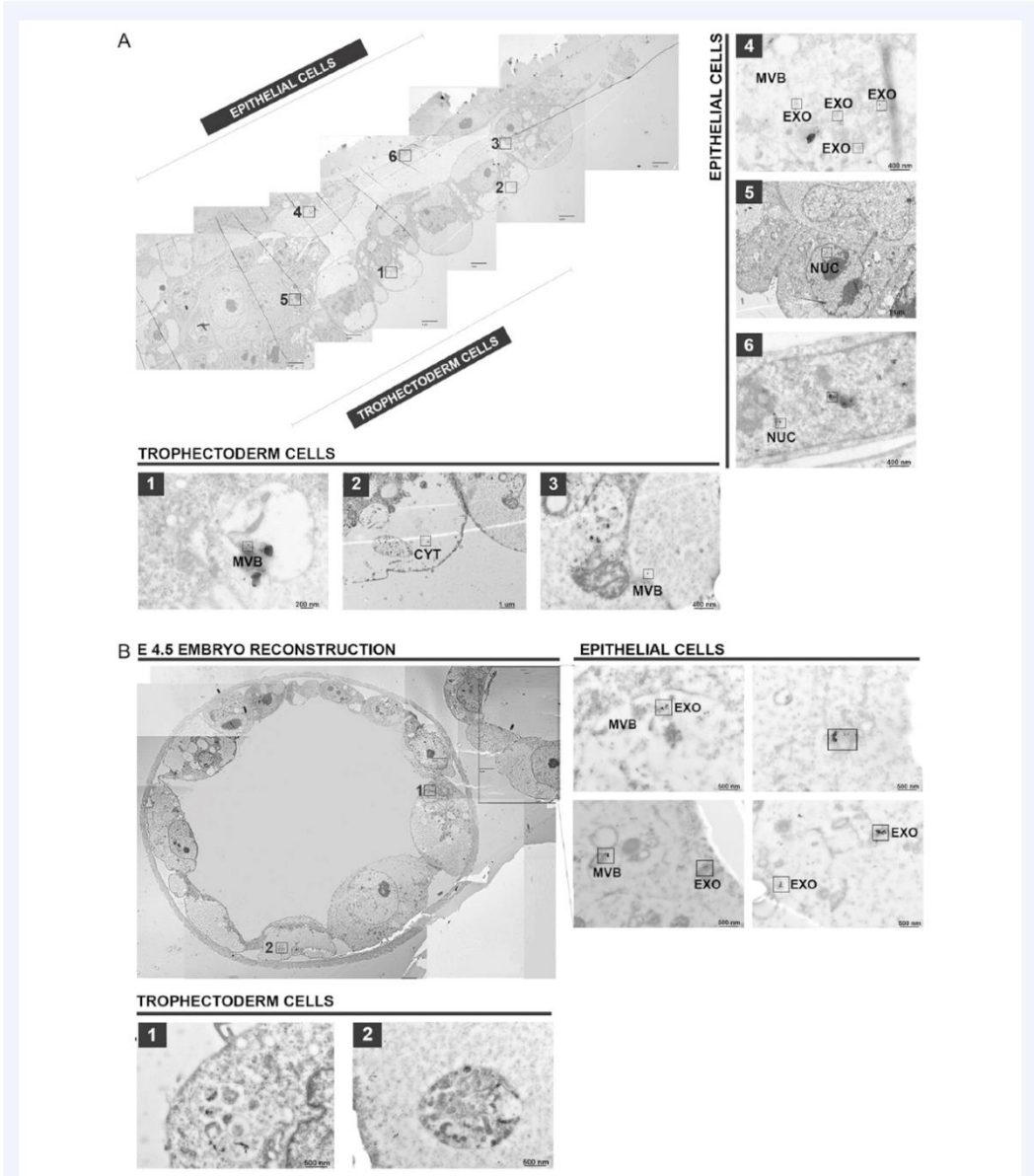


Figure 2 Studying miR-30d transfer from human endometrial epithelial cells (hEECs) to trophoblast cells in a miR-30d knockout (KO) murine embryos (**A**) Topographic reconstruction obtained by transmission electron microscopy (TEM) of a co-culture of a miR-30d KO embryo with hEECs previously transfected with miR-30d SmartFlare probes. The areas where the gold nanoparticles were found are highlighted in frames. Next to the frames, the subcellular location is indicated: EXO: Exosomes; NUC: Nucleus; MVB: Multivesicular body; CYT: Cytoplasm. (**B**) Topographic reconstruction obtained by TEM of a co-culture of a wild-type (WT) embryo with hEECs previously transfected with miR-30d SmartFlare probes. In hEECs, the areas where the gold nanoparticles were found are highlighted. Next to the frames, the subcellular location is indicated: EXO: Exosomes; NUC: Nucleus; MVB: Multivesicular body; CYT: Cytoplasm.

distributed in the cytoplasm as well as in the perinuclear regions of the blastocyst cells embedded into MVBs. Figure 2B shows a reconstruction of a WT embryo on hEECs. Unlike the KO embryo, the zona pellucida of the WT embryo was intact, explaining why gold nanoparticles could only be detected in the transfected epithelial cells.

Screening for the transporter protein of hsa-miR-30d in exosomes

Having phenotypically characterized the transfer of miR-30d in our murine model, we then wanted to elucidate the molecular mechanism responsible for sorting the miRNA into endometrial exosomes before its incorporation into trophoblast cells. First, we screened for those proteins present in the endometrium and endometrial exosomes that could exert this role within cells. To achieve this, extracts from hEECs ($n = 2$) and exosomes isolated by ultracentrifugation (pool of supernatants obtained from four T75 hEEC cultures) were incubated with streptavidin beads coated with several copies of a biotinylated miR-30d. As a negative control, poly-A coated beads were used. Once the pull-down was finished, proteins were identified by mass spectrometry. We performed an initial sieving by discarding the proteins that appeared linked to the poly-A beads as well as the ones belonging to the keratins (KRT) gene family. Next, we selected only the set of proteins identified specifically in exosomes and whose ProtScore was ≥ 2 or the level of confidence $\geq 99\%$ (Supplementary file 7).

Functional analysis revealed that the proteins detected were mainly associated with transcriptional, post-transcriptional modifications, and embryonic morphogenesis (Supplementary Table I). To proceed with the study, it was considered interesting to select those proteins whose biological function was related in some way with the intercellular mRNA transport. In accordance with this criterion, the heterogeneous ribonucleoprotein C1 (hnRNPCI) was preselected based on a previous report showing its role in the transport of mRNA from the nucleus to the cytosol (Pettit Kneller *et al.*, 2009). In addition, Cysteine-rich angiogenic inducer 61 (CYR61), a predominantly detected protein in every condition tested was also used for further studies as an unspecific miR-30d binding protein (see Supplementary file 7).

The presence of both proteins in endometrial exosomal fraction was confirmed by western blot analysis ($n = 3$) (Fig. 3A). Supernatant obtained in the ultracentrifugation process was used as the negative control. In addition, a western blot of subcellular fractions was performed and detected the enrichment of hnRNPCI in the protein fraction associated with membranous organelles (Fig. 3B). CYR61 was detected in the membranous fraction, but its location was predominantly cytoplasmic (Fig. 3B). We used confocal microscopy to examine co-localization of these proteins with an exosomal marker (CD63) (Fig. 4A) confirming the western blot results. Since, the analyzed subcellular structures are close to the resolution limit of the microscope, we decided to identify the regions of interest (ROI) manually and subsequently measure their fluorescence intensity curves (Bolte and Cordelières, 2006). To achieve this, we drew vectors through these structures and plotted the fluorescence intensity for the green and red channels against the length of the vector (Fig. 4A). In the left panel, the results for CYR61 are shown. In this particular example, the exosome marker CD63 appears in green whereas CYR61 is in red. Noticeably, there is no coincidence of the fluorescence intensity distributions for

the indicated randomly selected ROI. These results suggest that CYR61 and exosomes do not co-localize, supporting the previous observation that this is not an exosomal protein, so it is unlikely that CYR61 could be involved in miR-30d loading into exosomes.

The right panel of Fig. 4A displays the results for hnRNPCI and CD63 co-localization, this time with hnRNPCI in green and the exosomal marker CD63 in red. It is important to note that hnRNPCI was predominantly nuclear, but there is also considerable cytoplasmic staining. Unlike the CYR61 distribution, the hnRNPCI fluorescence intensity distribution overlapped with CD63 for certain regions of the traced vectors in the cytoplasmic compartment. This phenomenon suggests a partial co-localization between hnRNPCI and the exosomes. To eliminate the possibility that this protein might adhere to the membranes of exosomes, a fluorescence-activated cell sorting (FACS) analysis was performed (Fig. 4B), suggesting that hnRNPCI fluorescence was higher in permeabilized compared to non-permeabilized exosomes (Fig. 4B). This suggests hnRNPCI could be located inside exosomal structures.

Since hnRNPCI has been described to be predominantly nuclear (Dreyfuss *et al.*, 1993), we investigated whether this protein could be found in the cytoplasm of cells in a conventional hEEC culture. To achieve this, we compared the protein's fluorescence distribution signal between the nucleus and the cytoplasm with an In-Cell Analyzer (Fig. 4C). The percentage of signal found in the cytoplasm was higher than the percentage from the nucleus. Feasibly, this sharp difference could be attributed to the surface area analyzed; however, these results seem to confirm the presence of this protein in the cytoplasm of hEECs. This also accords with the study by Kim *et al.* (2003) that found this protein has the ability to migrate to the cytoplasm depending on the phase of the cell cycle (Kim *et al.*, 2003).

Finally, specific binding of hnRNPCI to miR-30d was verified with Ip of hnRNPCI from exosome lysates followed by qPCR of miRNAs (Supplementary Fig. 2). MiR-30d, but not miR-450, was amplified from hnRNPCI immunoprecipitates, demonstrating specific binding of hnRNPCI and miR-30d in exosomes *in vitro*. Therefore, from the results obtained and given that hnRNPCI has already been identified as a possible miRNA transporter (Villarroya-Beltri *et al.*, 2013), it is feasible the existence of an interaction between the protein hnRNPCI and the miRNA miR-30d prior to its loading into the inner cavity of the exosomes.

Silencing of hnRNPCI in Ishikawa cells affects the hsa-miR-30d levels within endometrial exosomes

To investigate the possible function of hnRNPCI in the packaging of miR-30d into exosomes, we assessed the effect of silencing hnRNPCI in Ishikawa cells. Due to the low survival rate of primary hEECs to transfection, the Ishikawa cell line was selected for silencing of hnRNPCI. This endometrial cancer cell line has provided a good model to study normal endometrium due to its capacity to maintain normal hormonal responsiveness to ovarian steroids (Nishida, 2002).

Initially, we performed a time course experiment to identify the moment of maximum silencing efficiency (Fig. 5A). The greatest degree of messenger silencing was achieved 72 h post-transfection (Fig. 5A). This is in accordance with the results obtained by western blotting,

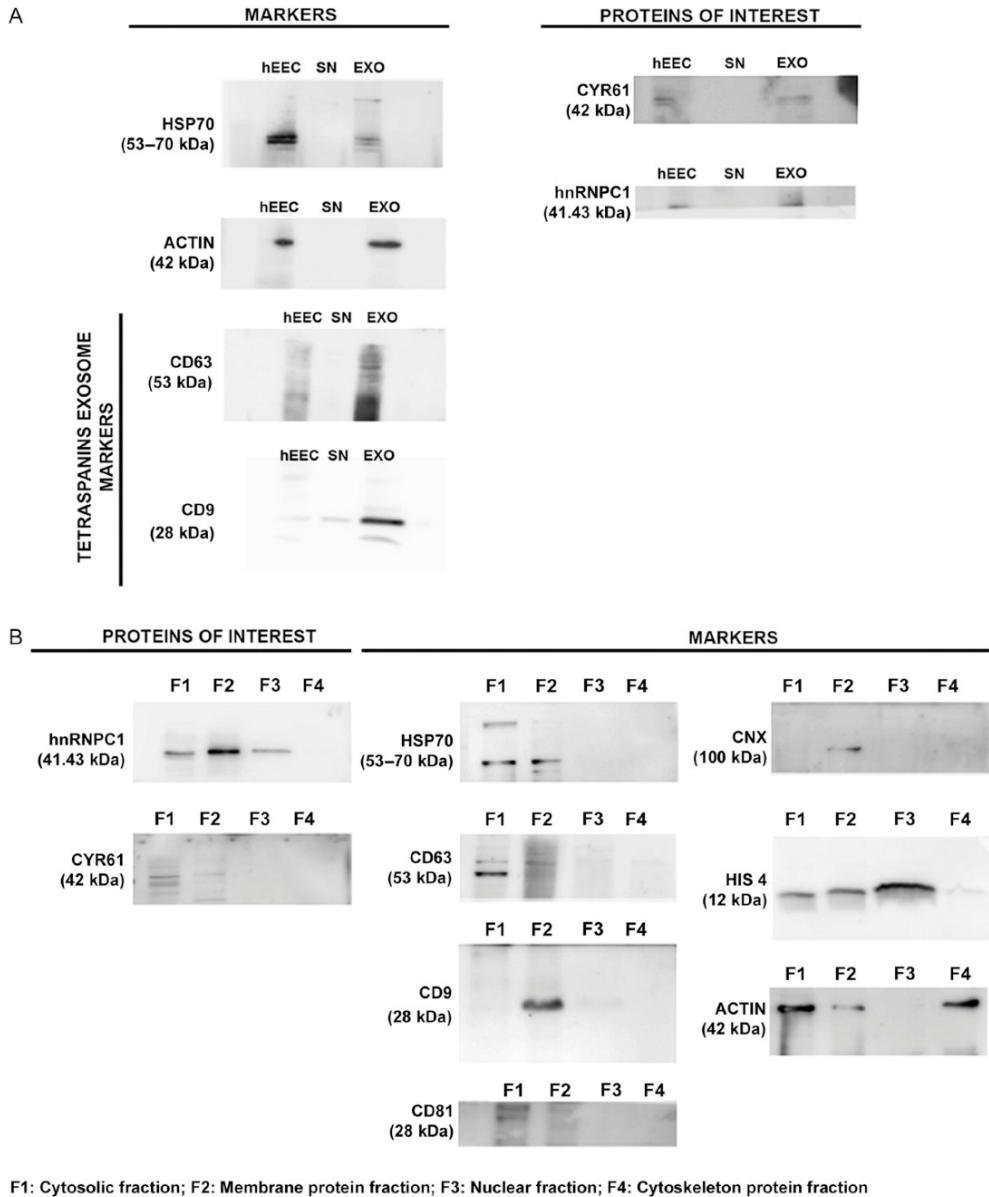


Figure 3 Screening for proteins directing the loading of miR-30d within exosomes. **(A)** Western blot analysis of CYR61 and hnRNPC1 in human endometrial epithelial cell (hEEC) lysate and exosomes. CD63, CD9, HSP70 and actin were used as exosomal markers. **(B)** Western blot of the sub-cellular fractionation performed to test for enrichment of the main candidate protein in the membrane organelle fraction. HSP70 and CD63 were used as cytosol and membrane markers; CD9, CD81 and Calnexin (CNX) were markers for the membrane organelle fraction, His4 was used as a reference for the nuclear fraction, and actin as a marker for the cytoskeletal fraction.

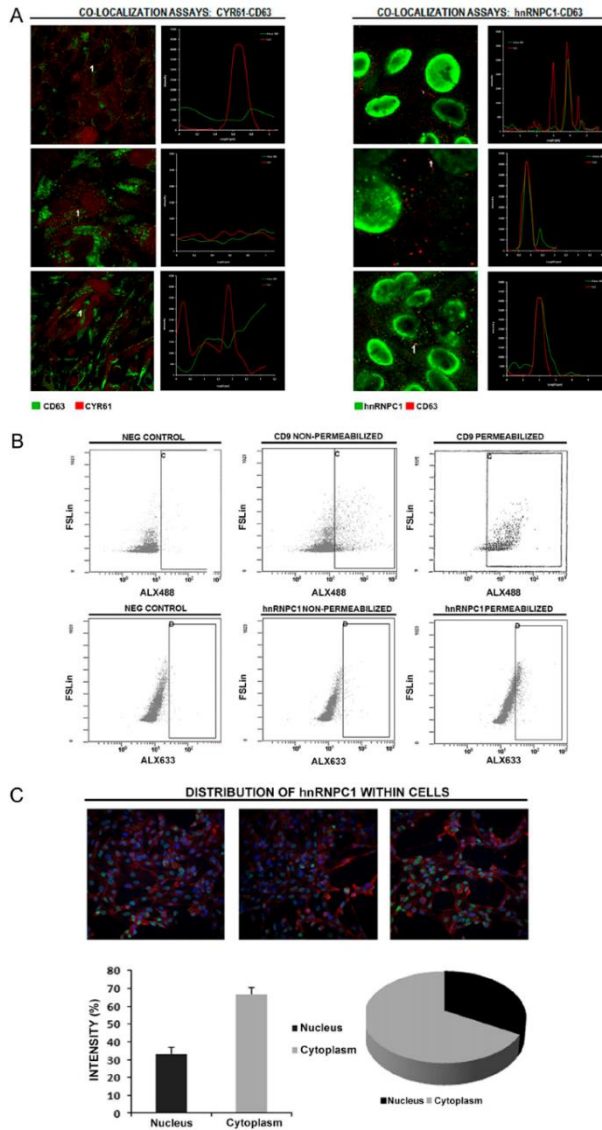


Figure 4 Identification of hnRNPC1 inside exosomes. **(A)** Co-localization assays to determine if the proteins of interest were in the inner cavity of exosomes. In the left panel, staining for CYR61 (red) and the exosome marker CD63 (green) can be observed. The lack of coincidence between the fluorescence intensity distributions for the defined ROI indicates that CYR61 was not present inside exosomes. In the right panel, the co-localization assay for hnRNPC1 (green) and the exosome marker CD63 (red) is shown. The overlap between the fluorescence intensity distributions suggests hnRNPC1 is a possible candidate for loading miR-30d into exosomes. **(B)** FACS analysis of hnRNPC1 and CD9 in exosome-coupled beads. Exosomes were coupled to aldehyde-sulfate beads, permeabilized or left intact, and incubated with antibodies to hnRNPC1 (lower panels) or CD9 (upper panels) and secondary antibody. Exosome-coupled beads incubated just with secondary antibodies were used as negative controls (left panels). **(C)** In-Cell analysis to determine the distribution of hnRNPC1 within cells. On the top, three representative fluorescence images obtained by In-Cell analysis are shown: Nucleus in blue (Hoechst 33382), hnRNPC1-Alexa 488 in green and WGA-Texas red in red. On the bottom, the proportion of hnRNPC1 in either the cytoplasm or the nucleus is presented.

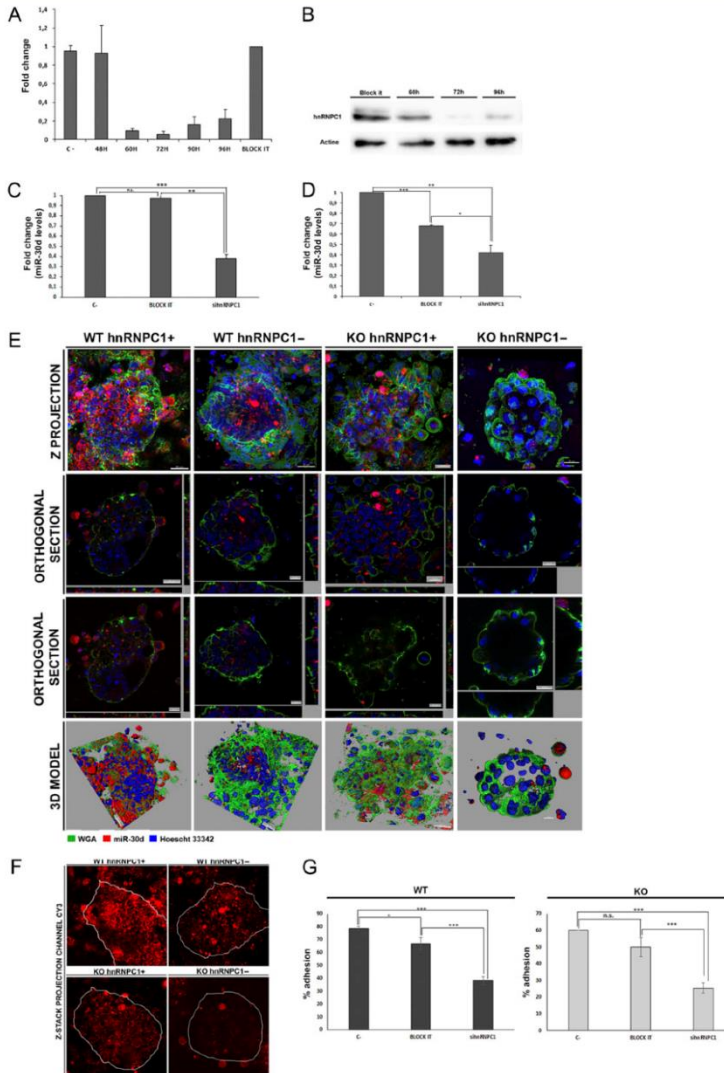


Figure 5 Silencing of hnRNPC1 in Ishikawa cells affects the hsa-miR-30d levels within endometrial exosomes. **(A)** RT-qPCR to detect mRNA levels of hnRNPC1 in Ishikawa cells previously transfected with shRNPC1 at different time points: 48, 60, 72, 90 and 96 h post-transfection. As a blank of transfection, a negative control siRNA was transfected for 96 h (Block-It). The results suggest that, at 72 h, the levels of hnRNPC1 have reached their minimum. **(B)** Western blot analyses performed to detect the best time frame to obtain maximum silencing efficiency. Actin was used as a housekeeping control. Results indicate that after 72 h, the levels of hnRNPC1 decrease dramatically. **(C)** miR-30d levels significantly decrease in Ishikawa cells at 90 h after silencing of hnRNPC1 ($P = 0.0001$). **(D)** miR-30d levels significantly decrease in exosomes isolated from Ishikawa cells' spent media at 90 h after silencing of hnRNPC1 ($P = 0.0152$). **(E)** Confocal images of the co-culture established between WT and miR-30d KO embryos with Ishikawa cells previously transfected simultaneously with shRNPC1 and the miR-30d MB probe. In red Cy3: miR-30d, in green WGA-Alexa 488: membrane labeling, in blue Hoechst 33382: nuclear staining. **(F)** Relative intensity fluorescence showed for each of the conditions tested, a representative experiment. **(G)** Adhesion assays of wild-type (WT) (Left graph) and knockout (KO) embryos (right graph) with Ishikawa cells previously transfected with either a

where the lowest yield of protein was obtained 72–96 h post-transfection (Fig. 5B).

After 90 h of hnRNPC1 knock-down, there was a reduced level of miR-30d in the cellular cytoplasm ($P = 0.0001$) ($n = 3$) (Fig. 5C) as well as in the inner exosomal cavity ($P = 0.0152$) ($n = 3$) (Fig. 5D). WT or miR-30d KO embryos were co-cultured with Ishikawa cells doubly-transfected with the hnRNPC1 siRNA and the MB probe intended for the detection of miR-30d in living cells ($n = 2$) (Fig. 5E). Images obtained by confocal microscopy showed that, following hnRNPC1 silencing, there is a reduction of miR-30d transfer between epithelial-like cells and trophectoderm cells (Fig. 5E). In fact, subsequent image analysis indicates a considerable decrease of the transferred signal, and hence of the miR-30d, in those co-cultures where hnRNPC1 was silenced (Fig. 5F).

Finally, to determine if a reduction in hnRNPC1 and miR-30d levels may impair blastocyst adhesion to hEEC, *in vitro* embryo adhesion assays were performed (Fig. 5G). Specifically, WT or miR-30d KO embryos were added to a monolayer of Ishikawa cells, previously transfected with either sihnRNPC1 or the negative control (Block-It). Adhesion assays show that in non-transfected cells (C-), the adhesion rates on KO embryos are significantly lower than WT (WT: $78.75 \pm 2.50\%$ (\pm SD) versus KO: $60 \pm 0.00\%$ (\pm SD); $P = 0.0000$) ($n = 2$; 14 embryos transferred per condition, six conditions tested. Total embryos used: 168). Likewise, transient silencing of hnRNPC1 results in a significant decrease of blastocyst adhesion compared to mock transfection conditions using Block-it, in both WT [$66.67 \pm 10.01\%$ versus $38.33 \pm 8.45\%$ ($P = 0.0006$)] and miR-30d KO embryos [$50.00 \pm 11.50\%$ versus $25.50 \pm 8.76\%$ ($P = 0.0029$)]. These results confirm that the highest decrease in the adhesion levels of KO embryos is due to the combined effect of the intrinsic reduction of the endogenous levels of miR-30d and the diminution linked with the drop in hnRNPC1 levels.

Discussion

This study focused on elucidating the possible molecular machinery responsible for the transfer of miR-30d into exosomes during the first stages of maternal-fetal communication. First, we examined the phenotypic characteristics of mouse embryos with a constitutive knock-down of miR-30d. *In vitro* adhesion assays with hEECs, previously transfected with MB and SmartFlare probes validated our previous results showing that an intimate cell-to-cell contact is necessary for the transfer of miRNAs between cells. This is in accordance with the work of Mittelbrunn *et al.* (2011), who determined that exosomes could be transferred between immune cells at a distance, but the formation of an immunological synapse is necessary to enhance the exosomal transition (Mittelbrunn *et al.*, 2011).

miRNA pull-down assay was used to determine which protein could be responsible for the internalization of miR-30d in epithelial-derived

exosomes. Results derived from MS/MS revealed the presence of proteins involved in several biological processes including transcriptional changes, post-transcriptional modifications or embryonic morphogenesis. Among the proteins detected, hnRNPC1 seems the most plausible to exert a transport role since both co-localization and FACS analyses demonstrated the presence of this protein in the inner cavity of exosomes.

hnRNPC1 has multiple functions within the eukaryotic cell. It is involved in splicing (Dreyfuss *et al.*, 1993), stabilization, transport and biogenesis of mRNA (Rajagopalan *et al.*, 1998; Shetty, 2005) and in internal ribosome entry site (IRES)-dependent translation of proteins implicated in cell division and apoptosis (Holcik *et al.*, 2003; Kim *et al.*, 2003). It performs these functions as stable heterotetramers (Dreyfuss *et al.*, 1993; McAfee *et al.*, 1996) comprised of three molecules of the more abundant hnRNPC1 and one molecule of a slightly larger splice variant, hnRNPC2, which contains a 13-aa insertion (Burd *et al.*, 1989). Both hnRNPC1 isoforms contain a basic leucine zipper-like RNA-binding motif, but the functional difference between the two variants remains unclear (McAfee *et al.*, 1996). Normally, hnRNPC1/C2 resides mainly in the nucleus (Lee *et al.*, 2004), but certain cellular conditions (e.g. apoptosis, mitosis and viral infection) induce hnRNPC1/C2 to translocate from the nucleus to the cytoplasm (Nakiely and Dreyfuss, 1996; Gustin and Sarnow, 2001, 2002; Kim *et al.*, 2003; Lee *et al.*, 2004; Pettit Kneller *et al.*, 2009). In fact, the results obtained from the In-Cell analyses allowed us to determine that in hEECs the greater proportion of hnRNPC1 in our conditions is cytoplasmic.

The evidence that hnRNPC1 is a plausible transporter of miR-30d into exosomes comes from our silencing assays where a clear decrease in the levels of miR-30d was found in both Ishikawa cells and epithelial-derived exosomes. This sharp reduction of miR-30d inside cells could be associated with a deficiency in the miRNA biogenesis machinery. The ribonucleoprotein family plays pivotal roles in miRNA function by regulating their biogenesis, localization, and degradation (van Kouwenhove *et al.*, 2011). The KH-type splicing regulatory protein (KSRP) promotes the biogenesis of a subset of miRNAs containing a GGG triplet motif in their terminal loop by enhancing Drosha-mediated microprocessing. More specifically, phosphorylation of KSRP increases the accessibility of pre-miRNAs thus promoting miRNA biogenesis (Trabucchi *et al.*, 2009). Similarly, hnRNPA1 binds to a conserved loop region of miRNAs facilitating Drosha-mediated cleavage (Michlewski *et al.*, 2008). Although more exhaustive research is needed to determine the exact way in which hnRNPC1 interacts with miR-30d, it seems that its biological role in RNA splicing and mRNA stability could be compromising both miR-30d biogenesis and its subsequent transfer. A similar conclusion was obtained by Park *et al.* (2012) who described that the silencing of hnRNPC1 was closely related with reduced levels of miR-21 in glioblastoma cells (Park *et al.*, 2012).

negative control (Block-It) and sihnRNPC1. Showed adhesion rates are significantly lower in case of using KO embryos (WT: $78.75 \pm 2.50\%$ versus KO: $60 \pm 0.00\%$; $P < 0.0001$) in baseline conditions. In both cases, there exists a significant decrease in the adhesion percentages after conducting the transient silencing of hnRNPC1. This decrease is relevant in the comparison established with baseline conditions [WT: $78.75 \pm 2.50\%$ versus $38.33 \pm 8.45\%$ ($P < 0.0001$); KO: $60 \pm 0.0\%$ versus $25.50 \pm 8.76\%$ ($P < 0.0001$)], as in the case of carrying out a transfection with the negative control Block-it [WT: $66.67 \pm 10.01\%$ versus $38.33 \pm 8.45\%$ ($P = 0.0006$); KO: $50 \pm 11.5\%$ versus $25.5 \pm 8.76\%$ ($P = 0.0029$)]. Results are presented in the format mean \pm SD ($n = 2$; 14 embryos transfer per condition, six conditions tested; Total embryos transferred $n = 168$).

Finally, proof-of-concept evidence for the possible role of hnRNPCI in miR-30d transfer comes from the co-culture of WT or miR-30d KO embryos with sihnRNPCI cells. Knocking down hnRNPCI compromises the detection of the miR-30d-CY3 signal throughout the embryo structure in two of the main stages of implantation: adhesion and invasion. Regardless the embryo was WT or KO, the levels of miR-30d were significantly reduced. In turn, adhesion assays showed that the transient silencing of hnRNPCI resulted in a significant decrease of the adhesion rates in both genotypes, being this reduction more pronounced in miR-30d KO embryos. This negative effect at the beginning of embryo implantation could be associated to an additive effect derived from a simultaneous absence of the miRNA miR-30d and the protein hnRNPCI.

It is important to note that although the experiments were done in cells derived from human adenocarcinomas (Ishikawa cells), they are likely to be relevant for human embryo implantation since Ishikawa cells have been the most useful models for examining the early events and interactions that occur between the endometrium and the trophoblast (Hannan et al., 2009). In fact, Zhang et al. (2012) developed a similar model of embryo implantation using mouse blastocysts and Ishikawa cells in which the blastocyst ultimately attached and grew. Scanning electron micrographs and immunocytochemical results of the implantation marker Leukemia Inhibitory Factor (LIF), confirmed the viability, biochemical integrity and responsiveness to implantation events of the Ishikawa cell line. Therefore, given these results, we consider that hnRNPCI could exert a relevant role in the maternal-fetal communication by participating both, in the biogenesis of miR-30d and its subsequent transport to trophoblast cells.

Supplementary data

Supplementary data are available at *Molecular Human Reproduction* online.

Acknowledgements

We thank Sheila M. Cherry, PhD, ELS, President and Senior Editor from Fresh Eyes Editing, LLC, for her work editing this manuscript. Also, to the SCSIE Proteomics laboratory, a member of ISCIII Carlos III Networked Proteomics Platform.

Authors' role

N.B., C.S. and F.V. designed the study; N.B., M.H., M.G. and F.V. performed the research; N.B., I.M., C.S. and F.V. analyzed data; N.B., C.S. and F.V. wrote the paper; all the authors performed the final approval of the manuscript; C.S. and F.V. contributed to the fundraising for the research.

Funding

This work was supported by the Miguel Servet Program Type I of Instituto de Salud Carlos III [CPI3/00038]; FIS project [PI14/00545] to F.V.; the 'Atracció de Talent' Program from VLC-CAMPUS [UV-INV-PREDOC14-178329 to N.B.]; a Torres-Quevedo grant (PTQ-13-06133) by the Spanish Ministry of Economy and Competitiveness to I.M.; and MINECO/FEDER Grant [SAF2015-67154-R] to C.S.

Conflict of interest

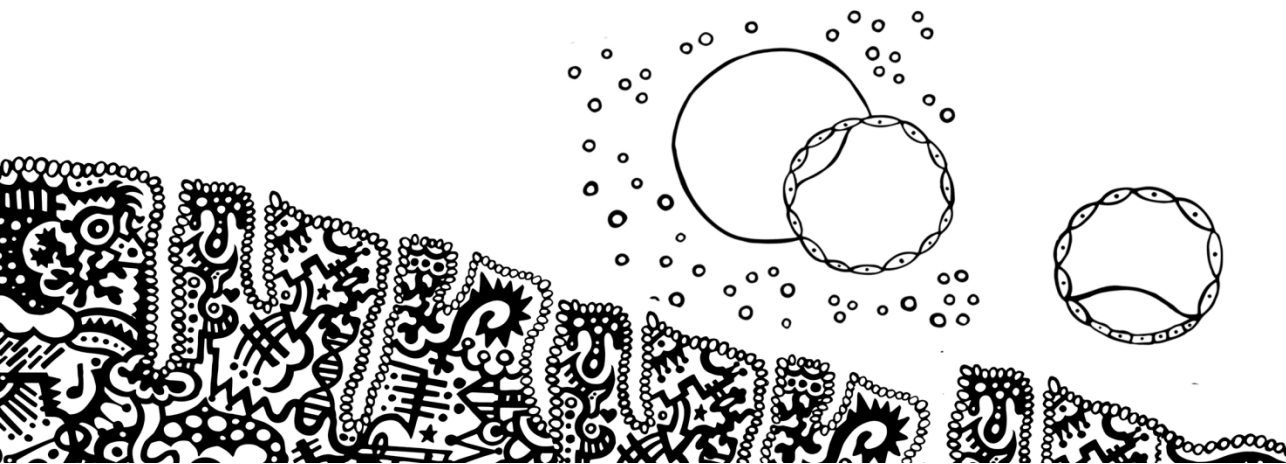
The authors have no conflict of interest.

References

- Arroyo JD, Chevillet JR, Kroh EM, Ruf IK, Pritchard CC, Gibson DF, Mitchell PS, Bennett CF, Pogosova-Agadjanyan EL, Stirewalt DL et al. Argonaute2 complexes carry a population of circulating microRNAs independent of vesicles in human plasma. *Proc Natl Acad Sci USA* 2011; **108**:5003–5008.
- Bolte S, Cordelières FP. A guided tour into subcellular colocalization analysis in light microscopy. *J Microsc* 2006; **224**:213–232.
- Bratu DP, Catrina IE, Marras SAE. Tiny molecular beacons for in vivo mRNA detection. *Methods Mol Biol* 2011; **714**:141–157.
- Burd CG, Swanson MS, Görlich M, Dreyfuss G. Primary structures of the heterogeneous nuclear ribonucleoprotein A2, B1, and C2 proteins: a diversity of RNA binding proteins is generated by small peptide inserts. *Proc Natl Acad Sci USA* 1989; **86**:9788–9792.
- Dreyfuss G, Matunis MJ, Piñol-Roma S, Burd CG. hnRNP proteins and the biogenesis of mRNA. *Annu Rev Biochem* 1993; **62**:289–321.
- Gustin KE, Sarnow P. Effects of poliovirus infection on nucleocytoplasmic trafficking and nuclear pore complex composition. *EMBO J* 2001; **20**:240–249.
- Gustin KE, Sarnow P. Inhibition of nuclear import and alteration of nuclear pore complex composition by rhinovirus. *J Virol* 2002; **76**:8787–8796.
- Hannan NJ, Paiva P, Dimitriadis E, Salomonson LA. Models for study of human embryo implantation: choice of cell lines. *Biol Reprod* 2009; **82**:235–245.
- Harding CV, Heuser JE, Stahl PD. Extracellular vesicles: exosomes, microvesicles, and friends. *J Cell Biol* 2013; **200**:373–383.
- Hergenreider E, Heydt S, Tréguer K, Boettger T, Horrevoets AJG, Zeiher AM, Scheffer MP, Frangakis AS, Yin X, Mayr M et al. Atheroprotective communication between endothelial cells and smooth muscle cells through miRNAs. *Nat Cell Biol* 2012; **14**:249–256.
- Holcik M, Gordon BW, Korneluk RG. The internal ribosome entry site-mediated translation of antiapoptotic protein XIAP is modulated by the heterogeneous nuclear ribonucleoproteins C1 and C2. *Mol Cell Biol* 2003; **23**:280–288.
- Hunter MP, Ismail N, Zhang X, Aguda BD, Lee EJ, Yu L, Xiao T, Schafer J, Lee M-LT, Schmittgen TD et al. Detection of microRNA expression in human peripheral blood microvesicles. In Lo YMD, editor. *PLoS One* 2008; **3**:e3694.
- Janas T, Janas MM, Sapoń K, Janas T. Mechanisms of RNA loading into exosomes. *FEBS Lett* 2015; **589**:1391–1398.
- Kim JH, Paek KY, Choi K, Kim T-D, Hahm B, Kim K-T, Jang SK. Heterogeneous nuclear ribonucleoprotein C modulates translation of c-myc mRNA in a cell cycle phase-dependent manner. *Mol Cell Biol* 2003; **23**:708–720.
- Koppers-Lalic D, Hackenberg M, Bijnsdorp IV, van Eijndhoven MAJ, Sadek P, Sie D, Zini N, Middeldorp JM, Ylstra B, de Menezes RX et al. Nontemplated nucleotide additions distinguish the small RNA composition in cells from exosomes. *Cell Rep* 2014; **8**:1649–1658.
- Larrea E, Sole C, Manterola L, Goicoechea I, Armesto M, Arestin M, Caffarel MM, Araujo AM, Araiz M, Fernandez-Mercado M et al. New concepts in cancer biomarkers: circulating miRNAs in liquid biopsies. *Int J Mol Sci* 2016; **17**:627.
- Lee H-H, Chien C-L, Liao H-K, Chen Y-J, Chang Z-F. Nuclear efflux of heterogeneous nuclear ribonucleoprotein C1/C2 in apoptotic cells: a novel nuclear export dependent on Rho-associated kinase activation. *J Cell Sci* 2004; **117**:5579–5589.
- McAfee JG, Soltaninassab SR, Lindsay ME, LeSturgeon WM. Proteins C1 and C2 of heterogeneous nuclear ribonucleoprotein complexes bind RNA

- in a highly cooperative fashion: support for their contiguous deposition on pre-mRNA during transcription. *Biochemistry* 1996;**35**:1212–1222.
- Michell DL, Vickers KC. Lipoprotein carriers of microRNAs. *Biochim Biophys Acta* 2016;**1861**:2069–2074.
- Michlewski G, Guil S, Semple CA, Cáceres JF. Posttranscriptional regulation of miRNAs harboring conserved terminal loops. *Mol Cell* 2008;**32**:383–393.
- Mittelbrunn M, Gutiérrez-Vázquez C, Villarroya-Beltri C, González S, Sánchez-Cabo F, González MÁ, Bernad A, Sánchez-Madrid F. Unidirectional transfer of microRNA-loaded exosomes from T cells to antigen-presenting cells. *Nat Commun* 2011;**2**:282. Nature Publishing Group.
- Montecalvo A, Larregina AT, Shufesky WJ, Stolz DB, Sullivan MLG, Karlsson JM, Baty CJ, Gibson GA, Erdos G, Wang Z *et al*. Mechanism of transfer of functional microRNAs between mouse dendritic cells via exosomes. *Blood* 2012;**119**:756–766.
- Nakiely S, Dreyfuss G. The hnRNP C proteins contain a nuclear retention sequence that can override nuclear export signals. *J Cell Biol* 1996;**134**:1365–1373.
- Nishida M. The Ishikawa cells from birth to the present. *Hum Cell* 2002;**15**:104–117.
- Park YM, Hwang SJ, Masuda K, Choi K-M, Jeong M-R, Nam D-H, Gorospe M, Kim HH. Heterogeneous nuclear ribonucleoprotein C1/C2 controls the metastatic potential of glioblastoma by regulating PDCD4. *Mol Cell Biol* 2012;**32**:4237–4244.
- Pettit Kneller EL, Connor JH, Lyles DS. hnRNPs relocate to the cytoplasm following infection with vesicular stomatitis virus. *J Virol* 2009;**83**:770–780.
- Pieters BCH, Arntz OJ, Bennink MB, Broeren MGA, van Caam APM, Koenders MI, van Lent PLEM, van den Berg WB, de Vries M, van der Kraan PM *et al*. Commercial cow milk contains physically stable extracellular vesicles expressing immunoregulatory TGF- β . *PLoS One* 2015;**10**:e0121123.
- Rajagopalan LE, Westmark CJ, Jarzembowski JA, Malter JS. hnRNP C increases amyloid precursor protein (APP) production by stabilizing APP mRNA. *Nucleic Acids Res* 1998;**26**:3418–3423.
- Roccaro AM, Sacco A, Maiso P, Azab AK, Tai Y-T, Reagan M, Azab F, Flores LM, Campigotto F, Weller E *et al*. BM mesenchymal stromal cell-derived exosomes facilitate multiple myeloma progression. *J Clin Invest* 2013;**123**:1542–1555.
- Santangelo L, Giurato G, Cicchini C, Montaldo C, Mancone C, Tarallo R, Battistelli C, Alonzi T, Weisz A, Tripodi M. The RNA-binding protein SYNCRIP is a component of the hepatocyte exosomal machinery controlling MicroRNA sorting. *Cell Rep* 2016;**17**:799–808.
- Shetty S. Regulation of urokinase receptor mRNA stability by hnRNP C in lung epithelial cells. *Mol Cell Biochem* 2005;**272**:107–118.
- Shevchenko A, Jensen ON, Podtelejnikov AV, Sagliocco F, Wilm M, Vorm O, Mortensen P, Shevchenko A, Boucherie H, Mann M. Linking genome and proteome by mass spectrometry: large-scale identification of yeast proteins from two dimensional gels. *Proc Natl Acad Sci USA* 1996;**93**:14440–14445.
- Simón C, Gimeno MJ, Mercader A, O'Connor JE, Remohí J, Polan ML, Pellicer A. Embryonic regulation of integrins beta 3, alpha 4, and alpha 1 in human endometrial epithelial cells *in vitro*. *J Clin Endocrinol Metab* 1997;**82**:2607–2616.
- Squadrito ML, Baer C, Burdet F, Maderna C, Gilfillan GD, Lyle R, Ibberson M, De Palma M. Endogenous RNAs modulate microRNA sorting to exosomes and transfer to acceptor cells. *Cell Rep* 2014;**8**:1432–1446.
- Trabucchi M, Briata P, Garcia-Mayoral M, Haase AD, Filipowicz W, Ramos A, Gherzi R, Rosenfeld MG. The RNA-binding protein KSRP promotes the biogenesis of a subset of microRNAs. *Nature* 2009;**459**:1010–1014.
- Turchinovich A, Samatov TR, Tonevitsky AG, Burwinkel B. Circulating miRNAs: cell-cell communication function? *Front Genet* 2013;**4**:119.
- Turchinovich A, Weiz L, Langheinz A, Burwinkel B. Characterization of extracellular circulating microRNA. *Nucleic Acids Res* 2011;**39**:7223–7233.
- Valadi H, Ekström K, Bossios A, Sjöstrand M, Lee JJ, Lötvall JO. Exosome-mediated transfer of mRNAs and microRNAs is a novel mechanism of genetic exchange between cells. *Nat Cell Biol* 2007;**9**:654–659.
- van Kouwenhove M, Kedde M, Agami R. MicroRNA regulation by RNA-binding proteins and its implications for cancer. *Nat Rev Cancer* 2011;**11**:644–656.
- Vickers KC, Palmisano BT, Shoucri BM, Shamburek RD, Remaley AT. MicroRNAs are transported in plasma and delivered to recipient cells by high-density lipoproteins. *Nat Cell Biol* 2011;**13**:423–433. Nature Publishing Group.
- Vilella F, Moreno-Moya JM, Balaguer N, Grasso A, Herrero M, Martínez S, Marcella A, Simón C. Hsa-miR-30d, secreted by the human endometrium, is taken up by the pre-implantation embryo and might modify its transcriptome. *Development* 2015;**142**:3210–3221.
- Villarroya-Beltri C, Gutiérrez-Vázquez C, Sánchez-Cabo F, Pérez-Hernández D, Vázquez J, Martín-Cofreces N, Martínez-Herrera DJ, Pascual-Montano A, Mittelbrunn M, Sánchez-Madrid F. Sumoylated hnRNPA2B1 controls the sorting of miRNAs into exosomes through binding to specific motifs. *Nat Commun* 2013;**4**:1–10. Nature Publishing Group.
- Vizcaino JA, Csordas A, Del-Toro N, Dianas JA, Griss J, Lavidas I, Mayer G, Perez-Riverol Y, Reisinger F, Tertent T *et al*. 2016 update of the PRIDE database and its related tools. *Nucleic Acids Res* 2016;**44**:11033–11033.
- Wang K, Zhang S, Weber J, Baxter D, Galas DJ. Export of microRNAs and microRNA-protective protein by mammalian cells. *Nucleic Acids Res* 2010;**38**:7248–7259.
- Zernecke A, Bidzhekov K, Noels H, Shagdarsuren E, Gan L, Denecke B, Hristov M, Köppl T, Jahantigh MN, Lutgens E *et al*. Delivery of microRNA-126 by apoptotic bodies induces CXCL12-dependent vascular protection. *Sci Signal* 2009;**2**:ra81.
- Zhang J, Li S, Li L, Li M, Guo C, Yao J, Mi S. Exosome and exosomal microRNA: trafficking, sorting, and function. *Genomics Proteomics Bioinformatics* 2015;**13**:17–24.
- Zhang Y, Liu D, Chen X, Li J, Li L, Bian Z, Sun F, Lu J, Yin Y, Cai X *et al*. Secreted monocyte miR-150 enhances targeted endothelial cell migration. *Molecular Cell* 2010;**39**:133–144. Elsevier Ltd.
- Zhang D, Lv P, Zhang R, Luo Q, Ding G, Ying L, Li J, Xu G, Qu F, Sheng J *et al*. A new model for embryo implantation: co-culture of blastocysts and Ishikawa cells. *Gynecol Endocrinol* 2012;**28**:288–292.

**Reproductive and fetal outcome of miR-30d deficiency at
the maternal embryonic interface**



Elsevier Editorial System(tm) for American
Journal of Obstetrics and Gynecology
Manuscript Draft

Manuscript Number: W18-1006

Title: Reproductive and fetal outcome of murine miR-30d deficiency at the maternal-embryonic interface

Article Type: Original Research

Section/Category: Reproductive Endocrinology/Infertility

Corresponding Author: Dr. Felipe Vilella, Ph.D.

Corresponding Author's Institution: Igenomix Foundation / INCLIVA

First Author: Nuria Balaguer

Order of Authors: Nuria Balaguer; Inmaculada Moreno; Maria Herrero; Marta Gonzalez-Monfort; Felipe Vilella, Ph.D.; Carlos Simon

Manuscript Region of Origin: SPAIN

Abstract: BACKGROUND: Reciprocal communication between the maternal endometrium and the preimplantation embryo is required for normal pregnancy. Our previous work demonstrated that maternal microRNAs (miRNAs), specifically miR-30d, secreted into the endometrial fluid act as transcriptomic regulator of the pre-implantation embryos by the maternal intrauterine environment.

OBJECTIVE: In this study, we investigated the reproductive and fetal effects of murine miR-30d deficiency at the maternal-embryonic interface according to its maternal or embryonic default.

STUDY DESIGN: miR-30d knockout mice were produced by Jackson laboratories from the microRNA cluster 26 (miR-30b/miR-30d) (MirC26tm1Mtm/Mmjax) on a mixed C57BL/6, Fvb, and 192P2 background. Uterine tissues were isolated from non-pregnant [day 0 (E0)], pseudopregnant [day 4 (E4), and day 5 (E5)] and pregnant [d4; and d5] wildtype and miR-30d knockout mice that were synchronized in estrus. RT-qPCR, immunofluorescence, and western blot analysis were performed for key receptivity markers Cox2, Lif, Msx1, Msx2: Esr, Pgr, and Act. Six different transfer conditions were used to analyze the influence of the maternal and/or embryonic deficiency of miR-30d: 1) wildtype embryos transferred into wildtype recipients (WTE-WTR), (2) knockout embryos into wildtype recipients (KOE-WTR), (3) miR-30d pre-treated knockout embryos into wildtype recipients (PTKOE-WTR), (4) wildtype embryos into knockout recipients (WTE-KOR), (5) knockout embryos into knockout recipients (KOE-KOR) and (6) miR-30d pre-treated knockout embryos into knockout recipients (PTKOE-KOR). We assessed the course of gestation, characterizing implantation site size, resorption sites, crown-rump length (cm) and fetal weight: placental weight (FW: PW) ratio at days 5, 6, 8 and 12 of pregnancy. Finally, parturition was monitored from days 17 through 21, and pups were allowed to grow until weaning (21 days post-birth) at which their weights (mg), widths (cm) and the lengths (cm) were recorded (wildtype, n = 40; knockout, n=37). Statgraphics Centurion software package (v.16.1.11) was used to compare results using one-way ANOVA, with a p-value < 0.05 indicating statistical significance.

RESULTS: Maternal miR-30d deficiency induced a significant downregulation of endometrial receptivity markers including LIF. Different maternal-embryonic crosstalk scenarios were tested by controlling the source of miR-30d deficiency by transferring wildtype, miR-30d knockout, or miR-30d knockout embryos pre-treated with miR-30d into WT or KO recipients. When transferred into wildtype recipients, miR-30d knockout embryos had poorer implantation rates (IR) than wildtype embryos ($48.86 \pm 14.33\%$ vs $75.00 \pm 10.47\%$, respectively, $p = 0.0061$). The lowest implantation rates were observed when comparing knockout embryos were transferred into knockout dams ($26.04 \pm 7.15\%$ and $49.71 \pm 8.59\%$, respectively, $p = 0.0059$). A positive correlation ($r = 0.9978$) was observed for maternal LIF expression and the implantation rate, suggesting that dysregulation of LIF is associated with miR-30d knockdown. Further, the course of gestation was compromised in miR-30d knockout mothers, which had smaller implantation sites, higher rates of resorption, and fetuses with smaller crown-rump length and FW:PW ratios.

CONCLUSION: Our results demonstrate that a maternal and/or embryonic miR-30d deficiency impairs embryonic implantation and fetal development in mice. This finding adds a novel miRNA dimension to the understanding of intrauterine growth restriction.

1 **Reproductive and fetal outcome of murine miR-30d deficiency at**
 2 **the maternal-embryonic interface**

3 N. Balaguer, I. Moreno, M. Herrero, M. González-Monfort, F. Vilella^{*§}, C.
 4 Simón[§]

5 * Contributed equally to this work

6 Nuria BALAGUER, Ms. Valencia, Spain. Department of Pediatrics, Obstetrics,
 7 and Gynecology, Universidad de Valencia.

8 Inmaculada MORENO, Ph.D. Valencia, Spain. R&D Department, Igenomix
 9 Foundation.

10 María HERRERO. Ms. Valencia, Spain. R&D Department, Igenomix
 11 Foundation.

12 Marta GONZÁLEZ. Ms. Valencia, Spain. R&D Department, Igenomix
 13 Foundation.

14 Felipe VILELLA, Ph.D. Valencia, Spain. R&D Department, Igenomix
 15 Foundation. Department of Obstetrics and and Gynecology, School of Medicine,
 16 Stanford University, CA, USA. Instituto de Investigación Sanitaria Hospital
 17 Clínico (INCLIVA), Valencia, Spain.

18 Carlos SIMÓN. M.D., Ph.D. Valencia, Spain. Igenomix S.L. Department of
 19 Pediatrics, Obstetrics and Gynecology, Universidad de Valencia. INCLIVA,
 20 Valencia, Spain. Department of Obstetrics and Gynecology, School of Medicine,
 21 Stanford University, Stanford, CA, USA.

22 **Conflict of interest and financial disclosure:** I.M., M.H., M.G. and C.S. are
 23 employed by Igenomix S.L. NB and FV report no conflict of interest.

24 This work was supported by the Miguel Servet Program Type I of Instituto de
 25 Salud Carlos III [CP13/00038]; FIS project [PI14/00545] to F.V.; the 'Atracció de
 26 Talent' Program from VLC-CAMPUS [UV-INV-PREDOC14-178329 to N.B.]; and
 27 MINECO/FEDER Grant [SAF2015-67154-R] to C.S.

28 Preliminary results were presented at the 64th Annual Scientific Meeting of the
 29 Society for Reproduction Investigation, Orlando, FL, March 15-18, 2015, and at

30 the 2018 Gordon Research Conference on Mammalian Reproduction, Barga,
31 Italy, July 29-August 3, 2018.

32 **Corresponding author:** Carlos Simón, M.D., Ph.D. and Felipe Vilella, Ph.D.
33 Igenomix, S.L. Parque tecnológico. Ronda Narciso Monturiol, 11B. Edificios
34 Europark. Cp46980, Paterna (Valencia), Spain. Phone: +34 963905310. Fax:
35 +34 963902522. Email: carlos.simon@igenomix.com;
36 felipe.vilella@igenomix.com.

37 **Word count:** Abstract: 504; Main text: 4672.

38 **Condensation:** A maternal and/or embryonic miR-30d deficiency impairs
39 embryonic implantation and fetal development.

40 **Short title:** miR-30d deficiency impairs embryo implantation and fetal
41 development.

42 **AJOG at a Glance**

43 **A. Why was this study conducted?** This study follows our previously
44 published observations demonstrating that maternal microRNAs
45 (miRNAs), specifically miR-30d, secreted into the endometrial fluid (EF)
46 act as transcriptomic regulators of the pre-implantation embryo. Our
47 results suggested a model in which maternal endometrial miRNAs act as
48 transcriptomic modifiers of the preimplantation embryo (Vilella et al.,
49 Development 2015) and therefore the development of the fetus.

50 **B. What are the key findings?** Maternal miR-30d deficiency induces a
51 significant downregulation of LIF. Different maternal-embryonic miR-30d
52 deficiency scenarios demonstrate that a maternal and/or embryonic miR-
53 30d deficiency impairs embryonic implantation and fetal development.

54 **C. What does this study add to what is already known?** The effect of
55 endometrial and/or embryonic miR-30d deficiency on pregnancy is a
56 novel finding. Furthermore, in a mouse model miR-30d deficiency affects
57 fetal development by causing intrauterine growth restriction (IUGR), with
58 consequent implications for health during adulthood.

59

1
2
3
4
5
6
7
8
9
10
11
12
13
14
15
16
17
18
19
20
21
22
23
24
25
26
27
28
29
30
31
32
33
34
35
36
37
38
39
40
41
42
43
44
45
46
47
48
49
50
51
52
53
54
55
56
57
58
59
60
61
62
63
64
65

60 ABSTRACT

61 BACKGROUND: Reciprocal communication between the maternal
62 endometrium and the preimplantation embryo is required for normal pregnancy.
63 Our previous work demonstrated that maternal microRNAs (miRNAs),
64 specifically miR-30d, secreted into the endometrial fluid act as transcriptomic
65 regulator of the pre-implantation embryos by the maternal intrauterine
66 environment.

67 OBJECTIVE: In this study, we investigated the reproductive and fetal effects of
68 murine miR-30d deficiency at the maternal-embryonic interface according to its
69 maternal or embryonic default.

70 STUDY DESIGN: miR-30d knockout mice were produced by Jackson
71 laboratories from the microRNA cluster 26 (miR-30b/miR-30d)
72 (MirC26tm1Mtm/Mmjax) on a mixed C57BL/6, Fvb, and 192P2 background.
73 Uterine tissues were isolated from non-pregnant [day 0 (E0)], pseudopregnant
74 [day 4 (E4), and day 5 (E5)] and pregnant [d4; and d5] wildtype and miR-30d
75 knockout mice that were synchronized in estrus. RT-qPCR,
76 immunofluorescence, and western blot analysis were performed for key
77 receptivity markers *Cox2*, *Lif*, *Msx1*, *Msx2*: *Esr*, *Pgr*, and *Act*. Six different
78 transfer conditions were used to analyze the influence of the maternal and/or
79 embryonic deficiency of miR-30d: 1) wildtype embryos transferred into wildtype
80 recipients (WTE-WTR), (2) knockout embryos into wildtype recipients (KOE-
81 WTR), (3) miR-30d pre-treated knockout embryos into wildtype recipients
82 (PTKOE-WTR), (4) wildtype embryos into knockout recipients (WTE-KOR), (5)
83 knockout embryos into knockout recipients (KOE-KOR) and (6) miR-30d pre-
84 treated knockout embryos into knockout recipients (PTKOE-KOR). We
85 assessed the course of gestation, characterizing implantation site size,
86 resorption sites, crown-rump length (cm) and fetal weight: placental weight (FW:
87 PW) ratio at days 5, 6, 8 and 12 of pregnancy. Finally, parturition was monitored
88 from days 17 through 21, and pups were allowed to grow until weaning (21 days
89 post-birth) at which their weights (mg), widths (cm) and the lengths (cm) were
90 recorded (wildtype, n = 40; knockout, n=37). Statgraphics Centurion software
91 package (v.16.1.11) was used to compare results using one-way ANOVA, with a
92 p-value < 0.05 indicating statistical significance.

1
2
3
4
5
6
7
8
9
10
11
12
13
14
15
16
17
18
19
20
21
22
23
24
25
26
27
28
29
30
31
32
33
34
35
36
37
38
39
40
41
42
43
44
45
46
47
48
49
50
51
52
53
54
55
56
57
58
59
60
61
62
63
64
65

93 **RESULTS:** Maternal miR-30d deficiency induced a significant downregulation of
94 endometrial receptivity markers including LIF. Different maternal-embryonic
95 crosstalk scenarios were tested by controlling the source of miR-30d deficiency
96 by transferring wildtype, miR-30d knockout, or miR-30d knockout embryos pre-
97 treated with miR-30d into WT or KO recipients. When transferred into wildtype
98 recipients, miR-30d knockout embryos had poorer implantation rates (IR) than
99 wildtype embryos ($48.86 \pm 14.33\%$ vs $75.00 \pm 10.47\%$, respectively, $p =$
100 0.0061). The lowest implantation rates were observed when comparing
101 knockout embryos were transferred into knockout dams ($26.04 \pm 7.15\%$ and
102 $49.71 \pm 8.59\%$, respectively, $p = 0.0059$). A positive correlation ($r = 0.9978$) was
103 observed for maternal LIF expression and the implantation rate, suggesting that
104 dysregulation of LIF is associated with miR-30d knockdown. Further, the course
105 of gestation was compromised in miR-30d knockout mothers, which had smaller
106 implantation sites, higher rates of resorption, and fetuses with smaller crown-
107 rump length and FW:PW ratios.

108 **CONCLUSION:** Our results demonstrate that a maternal and/or embryonic miR-
109 30d deficiency impairs embryonic implantation and fetal development in mice.
110 This finding adds a novel miRNA dimension to the understanding of intrauterine
111 growth restriction.

112 **Key words:** implantation, intrauterine growth retardation, LIF, maternal-
113 embryonic crosstalk, miR-30d

114

115 **INTRODUCTION**1
2
3
4
5
6
7
8
9
10
11
12
13
14
15
16
17
18
19
20
21
22
23
24
25
26
27
28
29
30
31
32
33
34
35
36
37
38
39
40
41
42
43
44
45
46
47
48
49
50
51
52
53
54
55
56
57
58
59
60
61
62
63
64
65

116 Defects in the intrauterine environment can negatively impact the health
117 of the fetus well into adulthood ¹. A key intrauterine factor is the bi-directional
118 communication between the endometrium and the preimplantation embryo and,
119 later, the fetus, to support both implantation and fetal development. Establishing
120 adequate maternal-embryonic crosstalk is complex² and requires the
121 coordination of both soluble embryo-derived factors and maternal secreted
122 molecules³. Factors involved in this dialogue include chemokines, cytokines,
123 adhesion molecules, and growth factors ⁴⁻⁷.

124 MicroRNAs (miRNAs), which have emerged as novel regulators of cell-
125 cell communication, are essential for regulating gene expression in fetal and
126 maternal tissues during conception and through the course of pregnancy ⁸.
127 miRNAs contained within exosomes/microvesicles have been detected in
128 human endometrial fluid, suggesting their potential role in embryo-maternal
129 interactions during the early stages of implantation ^{9,10}. Moreover, a broad range
130 of miRNAs has been linked with pregnancy-related disorders, such as
131 implantation failure, preeclampsia, preterm labor, and intrauterine growth
132 retardation¹¹.

133 Several miRNAs are implicated in endometrial receptivity: hsa-miR-30b
134 and -30d, which have been found to be upregulated, and hsa-miR-494, which is
135 downregulated, during the window of implantation (WOI) in humans ¹². The
136 predicted target genes of these miRNAs have been related to cyclic remodeling
137 of the endometrium, including endometrial maturation to the receptive stage ¹².
138 Our previous results demonstrated that endometrial miR-30d dysregulation
139 during the window of implantation leads to abnormal implantation rates by
140 impairing the expression of adhesion molecules (ITGB3, ITA7, and CDH5) in
141 trophoctoderm cells of murine blastocysts ⁹.

142 Due to the pleiotropic effects caused by miRNAs, it is difficult to define
143 the specific role of a particular miRNA. To date, most miRNA experiments have
144 been conducted on a cellular level in vitro. Others have generated in vivo
145 models by injecting miRNA mimics and/or inhibitors, producing phenotypic
146 changes by means of transcriptional modifications on their specific predicted

147 target genes. However, there are no in vivo models demonstrating the impact of
148 an specific miRNA deficiency in the initiation of conception as well as during
149 pregnancy, in a bi-directional communication context. Here, we use a miR-30d
150 knockout mouse model to test the reproductive and fetal impact of the miR-30d
151 deficiency at the maternal-embryonic interface and its relevance depending on
152 whether the miR-30d deficiency originates from the maternal endometrium and/
153 or the embryo.

154 **MATERIALS AND METHODS**

155 **Animal models and facilities**

156 miR-30d knockout (KO) mice were produced by Jackson laboratories
157 from the microRNA cluster 26 (miR-30b/miR-30d) (MirC26tm1Mtm/Mmjax) on a
158 mixed C57BL/6, Fvb, and 192P2 background. Mature mice were caged in a
159 controlled environment with a cycle of 14L:10D. All animal procedures were
160 revised by the Ethics Commission on Experimental Research at the University
161 of Valencia and approved by the Spanish Government Ministry of Agriculture,
162 Livestock, and Fisheries of the Spain Government
163 (Code:2017/VSC/PEA/00005). To confirm the reproducibility of the results, at
164 least three mice per group were used for each stage or treatment in this study.

165 **Uterine sample collections**

166 Uterine tissues were isolated from non-pregnant [day 0 (E0)],
167 pseudopregnant [day 4 (E4), and day 5 (E5)] and pregnant [d4; and d5] WT and
168 miR-30d KO that were synchronized in estrus. Synchronization was achieved
169 by introducing bedding material from cages housing males to cages housing
170 females¹³. Three days later, some females were euthanized by cervical
171 dislocation to harvest E0 samples, while the others were housed overnight with
172 non-vasectomized mice (to generate pregnant females) or vasectomized mice
173 (to generate pseudopregnant mice) at a ratio of two females per male. Females
174 presenting vaginal plugs (classified as day 1 of pregnancy or pseudopregnancy)
175 were separated and euthanized at day 4 or 5, as appropriate, to obtain uteri for
176 RT-qPCR (n = 6 uteri per condition tested and genotype analyzed; total uteri
177 per time point: WT, n = 18; KO, n = 18), immunofluorescence (n = 3 uteri per
178 condition tested and genotype analyzed; total uteri per timepoint: WT, n = 9; KO,

179 n = 9), and western blot (n = 6 uteri per condition tested and genotype
 180 analyzed; total uteri per time point: WT; n = 18; KO, n = 18). Uteri for RNA
 181 extraction were placed in 1.5 mL Eppendorf tubes filled with an RNA
 182 stabilization reagent, *RNA/later* (Qiagen, Hilden, Germany) until processed. Uteri
 183 for protein extraction were frozen directly at -80°C. Finally, uteri for IF assays
 184 were flash frozen, and stored in cryovials at -80°C until processed.

185 **Study of key receptivity markers by RT-qPCR**

186 RT-qPCR was used to assess mRNA expression levels of key receptivity
 187 markers in non-pregnant and pseudopregnant females at days 4 and 5 of
 188 pseudopregnancy (n = 6 uteri per condition tested and genotype analyzed; total
 189 uteri per timepoint: WT, n = 18; KO, n = 18). RNA was extracted from uterine
 190 tissue using the RNeasy Kit (Qiagen, Hilden, Germany) and quantified using
 191 NanoDrop spectrophotometer (ThermoFisher Scientific Inc., MA, USA). RT was
 192 performed using the PrimeScript™ RT reagent Kit (Perfect Real Time)
 193 (Clontech Laboratories, Mountain View, CA, USA), and qPCR was conducted
 194 using the “Kapa Sybr fast master mix universal 2x qPCR master mix” (Sigma
 195 Aldrich, St Louis, Mi, USA) in a QuantumStudio 5 Real-Time PCR system.
 196 Conditions for the qPCR were as follows: enzyme activation at 95°C for 10 min
 197 and 40 two-step cycles 10s at 95°C and 30s at 60°C. Fold changes were
 198 estimated using the $-2^{\Delta\Delta Ct}$ formula. Actin was used as a housekeeping control to
 199 determine the relative quantification of the analyzed genes. Primer sequences
 200 were as follows. *Cox2*: (FW: 5'-AACCGAGTCGTTCTGCCAAT-3'; RV: 5'-
 201 CTAGGGAGGGGACTGCTCAT-3'); *Lif*: (FW: TGTCGCCTAGATTACCC-3';
 202 RV: 5'-CACAAATCCCTGCATCTCATC-3'); *Msx1*: (FW: 5'-
 203 TCTCGGCCATTTCTCAGTTTCG-3'; RV: 5'-CCGATCTAGTTTCTCGGGGC-3');
 204 *Msx2*: (FW: 5'-TCGTCAAGCCCTTCGAGACC-3'; RV: 5'-
 205 TGGTGGGGCTCATATGTCTGGG-3'), *Esr*: (FW: 5'-
 206 TGCCAAGGAGACTCGCTACT-3'; RV: 5'-CTCCGGTCTTGCAATGGT-3');
 207 *Pgr*: (FW: 5'-CACAAAGCCTGACACTTCCA-3'; RV: 5'-
 208 AAACACCATCAGGCTCATCC-3') *Act*: (FW: 5'-GATCATTGCTCCTCCTGAGC-
 209 3'; RV: 5'-AGTCCGCCTAGAAGCACTTG-3').

210

5
6
7
8
9
10
11
12
13
14
15
16
17
18
19
20
21
22
23
24
25
26
27
28
29
30
31
32
33
34
35
36
37
38
39
40
41
42
43
44
45
46
47
48
49
50
51
52
53
54
55
56
57
58
59
60
61
62
63
64
65

213 **Immunofluorescence assessment of receptivity markers**

214 Uterine tissues were isolated from non-pregnant [day 0 (E0)],
215 pseudopregnant [day 4 (E4), and day 5 (E5)] and pregnant [day 4 (E4) and day
216 5 (E5)] WT and miR-30d KO females (n = 3 uteri per condition tested and
217 genotype analyzed; total uteri per timepoint: WT, n =9; KO, n = 9), flash frozen,
218 and stored in cryovials at -80°C. Next, tissues were completely embedded in an
219 OCT compound before cryostat sectioning. Cryosections were cut at 7 mm onto
220 poly-L-lysine-coated slides, rehydrated with PBS, and fixed with 4%
221 paraformaldehyde (PFA) for 10 min. Permeation was performed with PBS-1%
222 Triton X-100 for 10 min. Sections were blocked with 5% bovine serum albumin
223 (BSA)/0.05% triton/4% FBS in PBS. Sections were then incubated with the
224 following primary antibodies: COX2 (1 µg/mL) (Ref: ab15191) (Abcam,
225 Cambridge, United Kingdom), LIF (20 µg/mL) (Ref: ab11362) (Abcam,
226 Cambridge, United Kingdom), MSX-1 (1:200) (Ref: ab174207) (Abcam,
227 Cambridge, United Kingdom), MSX-2 (1:200) (Ref: HPA005652) (Sigma-
228 Aldrich, St. Louis, Mi, USA), ESR (1:200) (Ref: ab32063) (Abcam, Cambridge,
229 United Kingdom), and PGR (1:200) (Ref:8757) (Cell Signaling Technology,
230 Danvers, Ma, USA) O/N at 4°C in a humidified chamber. In addition to these
231 primary antibodies, one against Zona Occludens (ZO-1) (Abcam, Cambridge,
232 United Kingdom) was used. ZO-1 is a tight junction protein often expressed in
233 the primary decidual zone (PDZ) after implantation. It was used in this study to
234 detect the region surrounding the implantation sites. Sections were washed
235 three times with PBS-0.05%TritonX-100/0.1% BSA and incubated with a goat
236 anti-rabbit IgG (H+L) Superclonal™ secondary antibody, Alexa Fluor 555®
237 (Thermo Fisher Scientific, Waltham, MA, USA). Nuclei were stained with DAPI
238 (Thermo Fisher Scientific, Waltham, MA, USA). Aquatex® (Merck-Millipore,
239 Billerica, MA, USA) was used as the mounting medium. Tissues from control
240 (WT) and experimental uteri (KO) were processed on the same slide. Images
241 were acquired with a 60× water immersion confocal microscope (FV1000,
242 Olympus). Image processing was conducted by using Imaris software (Bitplane,

1
2
3
4
5
6
7
8
9
10
11
12
13
14
15
16
17
18
19
20
21
22
23
24
25
26
27
28
29
30
31
32
33
34
35
36
37
38
39
40
41
42
43
44
45
46
47
48
49
50
51
52
53
54
55
56
57
58
59
60
61
62
63
64
65

243 Zurich, Switzerland). Measurements of the fluorescence intensity values
244 (integrated density/area) were conducted with ImageJ software (National
245 Institute of Health (NIH), Bethesda, MD).

246

247 **Protein extraction and western blot analysis**

248 Uteri were flash frozen, cut into pieces, and homogenized in 1 mL of lysis
249 buffer (150 mM NaCl, 1% IGEPAL CA 630, 0.5% Na-DOC, 0.1% SDS, 0.5 M
250 EDTA, 50 mM Tris-HCl, pH 8) with protease inhibitors [1% PMSF 0.1 M (Sigma-
251 Aldrich, Madrid, Spain), 10% Roche mini complete (Roche, Basel, Switzerland)]
252 in a TissueLyser LT device (Qiagen, Hilden, Germany). Samples were
253 homogenized at 30 s intervals until completely dissociated (n = 6 uteri per
254 condition tested and genotype analyzed; total uteri per time point: WT, n = 18;
255 KO, n = 18). The tissue slurry was transferred into clean 1.5 mL Eppendorf
256 tubes and allowed to incubate at 4°C for 1 h. Samples were then centrifuged at
257 15,000 rpm for 30 min. The supernatant was recovered, and protein
258 concentrations quantified by a Bradford assay following the manufacturer's
259 instructions. 25 µg of each protein sample were heated in Laemli SDS sample
260 buffer (6x) (Alfa Aesar, Haverhill, MA, USA) and separated by SDS-PAGE
261 followed by electroblotting onto PVDF membranes (Bio-Rad Laboratories,
262 Hercules, CA, USA). Membranes were incubated overnight with specific primary
263 (1:1000) antibodies diluted in 3% nonfat milk, following the manufacturer's
264 specifications. Antibodies against mouse COX2 (1:1,000) (Ref: ab1519)
265 (Abcam, Cambridge, United Kingdom), LIF (1:500) (Ref: ab11362) (Abcam,
266 Cambridge, United Kingdom), MSX-1 (1:200) (Ref: ab174207) (Abcam,
267 Cambridge, United Kingdom), MSX-2 (1:500) (Ref: HPA005652) (Sigma-
268 Aldrich, St. Louis, Mi, USA), ESR (1:1,000) (Ref: ab32063) (Abcam, Cambridge,
269 United Kingdom), PGR (1:500) (Ref: 8757) (Cell Signaling Technology,
270 Danvers, Ma, USA) (Abcam, Cambridge, United Kingdom), and calnexin (Enzo
271 Life Sciences, Farmingdale, NY, USA) were used for western blotting. After
272 three washes with 1% PBST, membranes were incubated with a 1:20,000
273 dilution of secondary antibodies (Santa Cruz Biotechnology, Dallas, TX, USA).

274 Finally, target proteins were detected by using the SuperSignal West Femto
275 Chemiluminescent kit (Thermo Fisher Scientific, Waltham, MA, USA).

276

277 **Embryo transfer assays**

278 Female mice, ages 6-8 weeks, were primed to ovulate by administering
279 10 IU of pregnant mare serum gonadotropin (Sigma-Aldrich, St Louis, Mi, USA)
280 and, 48 h later, 10 IU of human chorionic gonadotropin (Sigma-Aldrich, St Louis,
281 Mi, USA). Females were housed overnight with males and examined the
282 following morning for the presence of a vaginal plug (classified as day 1 of
283 pregnancy). On day 1.5 of pregnancy, the mice were euthanized by cervical
284 dislocation and embryos flushed from the oviduct with PBS (Life Technologies
285 S.A.) using a 30-gauge blunt needle. Embryos were then washed three times
286 with fresh G2™ Plus medium (Vitrolife, Göteborg, Sweden) and incubated in
287 G2™ medium for 72h at 37°C, 5% CO₂. For rescue experiments, 123 miR-30d
288 KO embryos were pre-treated with 400 nM of an analog of miR-30d for 72h
289 (miScript miRNA Mimic [Qiagen, Cat No. MSY0000245]
290 5'UGUAAACAUCCCCGACUGGAAG). Beyond this timepoint, embryos at the
291 blastocyst stage were washed three times with PBS and used to perform the
292 embryo transfer into both WT and KO pseudopregnant females synchronized in
293 estrus, as described above. Females presenting a vaginal plug (day 1 of
294 pregnancy) either the same day or 48 h after mating were separated to undergo
295 embryo transfers on day 4. Six different transfer conditions were used to
296 analyze the influence of both maternal and embryonic factors influencing the
297 implantation process: 1) WT embryos transferred into WT recipients (WTE-
298 WTR), (2) KO embryos into WT recipients (KOE-WTR), (3) miR-30d pre-treated
299 KO embryos into WT recipients (PTKOE-WTR), (4) WT embryos into KO
300 recipients (WTE-KOR), (5) KO embryos into KO recipients (KOE-KOR) and (6)
301 miR-30d pretreated KO embryos into KO recipients (PTKOE-KOR). These
302 transfers were done using a Non-Surgical Embryo Transfer (NSET™) device for
303 mice (ParaTechs, Lexington, KY, USA). For each condition tested; an average
304 of 10-15 embryos was transferred. Three biological replicates were performed
305 for harvest on day 5 (embryos transferred per condition: ~36; total embryos
306 transferred in the six conditions tested: ~216). Six biological replicates were

307 performed for harvest on day 6.5-7 of pregnancy [embryos transferred per
 308 condition: WTE-WTR (54); KOE-WTR (87); PTKOE-WTR (67); WTE-KOR (73);
 309 KOE-KOR (58); PTKOE-KOR (84); total embryos transferred in the six
 310 conditions tested: ~423). Implantation sites were visualized using the colorant
 311 Chicago Sky blue (Sigma-Aldrich, St. Louis, Mi, USA) injected via tail vein.
 312 Finally, females were euthanized by cervical dislocation and the implantation
 313 sites counted to calculate implantation rates. Uteri obtained from
 314 pseudopregnant females euthanized at day 5 of pregnancy were flash-frozen,
 315 and stored in cryovials at -80°C. Cryosections and immunofluorescence
 316 analyses were performed following the protocol described above (n = 3 uteri per
 317 condition tested and genotype analyzed; total uteri: WT, n = 6; KO, n = 6).

318 **Characterization of the implantation phenotype and pregnancy outcomes** 319 **associated with miR-30d deficiency**

320 The course of gestation was evaluated in pregnant females on days 5, 6,
 321 8, and 12. Specifically, on days 5 and 6, implantation sites were visualized by
 322 intravenous injection of a Chicago Sky blue (Sigma-Aldrich, St. Louis, Mi, USA)
 323 solution, and the number of implantation sites — demarcated by distinct blue
 324 bands — was recorded (number of uteri evaluated: WT, n = 4; KO, n = 5).
 325 Resorption sites were identified at day 12 (number of uteri evaluated: WT, n =
 326 10; KO, n = 5). In all cases, the size of the implantation sites was evaluated.
 327 The latter was determined considering the characteristic area of an ellipsoid -
 328 see equation below-(Eqn.1).

$$329 \quad A = \pi \cdot \frac{D_1}{2} \cdot \frac{D_2}{2} \quad (\text{Eqn.1})$$

330 Where A is the area (cm²), D₁, the minor radius (cm) and D₂ the major radius
 331 (cm). Measures were done by image analysis with Adobe Photoshop software
 332 [WT: E5 (n = 16); E6 (n = 37); E8 (n = 28); E12 (n = 16); KO E5 (n = 23); E6 (n
 333 = 15); E8 (n = 20); E12 (n = 17)]. Intrauterine growth restriction (IUGR) was
 334 evaluated by analyzing the fetuses and the placentas at day 12 and 16 of
 335 pregnancy [WT: E12 (n = 14); E16 (n = 17); KO: E12 (n = 12); E16 (n = 5);]. In
 336 fetuses, two parameters were assessed, crown-rump length (CRL) (cm) and
 337 weight (mg). Placental weight was also evaluated and used to estimate the

1
2
3
4
5
6
7
8
9
10
11
12
13
14
15
16
17
18
19
20
21
22
23
24
25
26
27
28
29
30
31
32
33
34
35
36
37
38
39
40
41
42
43
44
45
46
47
48
49
50
51
52
53
54
55
56
57
58
59
60
61
62
63
64
65

338 fetal-weight: placental-weight (FW: PW) ratio. Finally, parturition events were
339 monitored from days 17 through 21 by observing mice thrice daily: morning,
340 noon, and evening. Pups were allowed to grow until weaning (21 days post-
341 birth) and were then euthanized by cervical dislocation to record their weights
342 (mg), widths (cm), and lengths (cm) (WT, n = 40; KO, n=37).

343

344 **Statistical analysis**

345 Statgraphics Centurion software package (v.16.1.11) was used to
346 compare results by one-way ANOVA. Statistical significance was accepted at a
347 p-value < 0.05.

348

349 **RESULTS**

350

351 **Impact of miR-30d deficiency on endometrial receptivity**

352 To examine the effects of miR-30 deficiency on endometrial receptivity,
353 we analyzed the expression of cyclooxygenase-2 (*Cox2*), leukemia inhibitory
354 factor (*Lif*), Msh homeobox 1 (*Msx1*), Msh homeobox 2 (*Msx2*), estrogen
355 receptor (*Esr*), and progesterone receptor (*Pgr*) in the mouse endometrium at
356 days 0, 4, and 5 of pseudopregnancy. Thus, in the non-pregnant endometrium
357 condition (E0), *Lif* mRNA levels were significantly reduced ($p = 0.0355$) and
358 *Msx1* mRNA levels were increased in KO compared to WT tissues ($p = 0.0014$;
359 Fig. 1A). Of note, all the receptivity markers were significantly reduced at the
360 beginning of implantation (E4) in KO uteri, but once implantation was
361 established (E5) differences remained significant only for *Msx2* (Fig 1A).

362 To determine if the mRNA expression changes were also reproduced at
363 the protein level, immunofluorescence (IF) and western blot (WB) analyses
364 were performed. The changes in the protein levels of COX2, LIF, and ESR were
365 like those detected for their respective mRNAs over the time course (E0, E4,
366 and E5; Fig. 1B) and the expression of these markers was higher in WT than in
367 KO uteri. WB analysis (Fig. 1C) revealed significant genotype-dependent
368 differences between COX2, LIF, and MSX1 at E0, for LIF at E4, and for LIF and

369 MSX1 at E5, while MSX2 was barely detectable in either genotype during
370 implantation (Fig. 1B, 1C). Finally, PGR levels were similar in WT and KO uteri
371 at all the analyzed time points (Fig. 1B, 1C).

372

373 **Reproductive impact of maternal and/or embryonic miR-30d deficiency**

374 Next, we investigated the reproductive phenotype according to the
375 maternal or embryonic origin of the miR-30d deficiency. WT, miR-30d KO, and
376 miR-30d KO embryos pretreated with 400 nM of synthetic miR-30d (Vilella et
377 al., 2015) were transferred into either WT or KO pseudopregnant mice in which
378 estrus had been synchronized. The different conditions evaluated were: (1) WT
379 embryos transferred into WT recipients (WTE-WTR); (2) KO embryos into WT
380 recipients (KOE-WTR); (3) miR-30d-pretreated KO embryos into WT recipients
381 (PTKOE-WTR); (4) WT embryos into KO recipients (WTE-KOR); (5), KO
382 embryos into KO recipients (KOE-KOR); and (6) miR-30d-pretreated KO
383 embryos into KO recipients (PTKOE-KOR).

384 Fig. 2 reflects the implantation sites (IS) (Fig. 2A) and implantation rates
385 (IR) (Fig. 2B) in uteri surgically removed at day 6.5–7 of pregnancy after these
386 transfers were performed. Note that average and standard deviations are
387 calculated from 6 biological replicates, with a total of 12–15 embryos per
388 condition transferred in each replicate (total of 423 embryos transferred in six
389 tested conditions).

390 KO embryos transferred into WT recipients had a lower IR than WT
391 embryos transferred into WT recipients ($48.86 \pm 14.33\%$ vs $75.00 \pm 10.47\%$,
392 respectively; $p = 0.0061$). Similarly, when transferred into KO recipients, KO
393 embryos had lower IR than WT embryos ($26.04 \pm 7.15\%$ vs $49.71 \pm 8.59\%$;
394 $p = 0.0059$). Interestingly, KO embryos pretreated with miR-30d and transferred
395 into KO uteri had a higher implantation rate than untreated KO embryos
396 ($54.39 \pm 10.13\%$ vs. $26.04 \pm 7.15\%$, respectively; $p = 0.0025$), but this rescue
397 was not observed in WT uteri ($56.26 \pm 2.44\%$ vs. $48.86 \pm 14.33\%$; $p = 0.3288$;
398 Fig. 2B), suggesting that the maternal and embryonic expression of miR-30d
399 are equally important for achieving pregnancy.

1
2
3
4
5
6
7
8
9
10
11
12
13
14
15
16
17
18
19
20
21
22
23
24
25
26
27
28
29
30
31
32
33
34
35
36
37
38
39
40
41
42
43
44
45
46
47
48
49
50
51
52
53
54
55
56
57
58
59
60
61
62
63
64
65

400 To determine if the implantation rates observed in the different conditions
401 were associated with deregulation of receptivity markers during gestation, we
402 evaluated marker expression on days 4 (E4) and 5 (E5) of pregnancy under
403 physiological conditions (i.e., with no embryo transfer) as compared to
404 expression in the different transfer conditions indicated (Fig. 3A, 3B and Suppl.
405 Fig. 1). Under physiological conditions, the mean receptivity marker
406 fluorescence intensity value (FIV) on day 4 was lower in KO than WT samples;
407 however, this generalized trend was not significant when the complete panel of
408 micrographs from all the biological replicates was considered (Fig. 3A and
409 Suppl. Fig. 1). In contrast, on day 5 of pregnancy (E5) the FIV of LIF was
410 significantly lower in the KO relative to the WT uteri (64.73 ± 3.86 and
411 49.15 ± 9.05 , respectively; $p = 0.0336$; Suppl. Fig. 1), although there were no
412 statistically significant differences in expression for any other markers.

413 Yet, it is interesting to consider the implication of FIV patterns for
414 endometrial-embryo communication in the different embryo transfer conditions
415 (Figs. 3B and 3C). Although in some cases changes in the FIVs failed to reach
416 significance, the expression levels of LIF were significantly different in all the
417 conditions tested (Fig. 3C). Thus, KO embryos transferred into either WT or KO
418 mothers elicited considerably less LIF expression than WT embryos under the
419 same conditions (WT uteri [42.82 ± 11.85 and 64.74 ± 8.63 , respectively;
420 $p = 0.0381$] and KO uteri [66.25 ± 9.05 and 88.54 ± 7.18 , respectively;
421 $p = 0.0061$]). Interestingly, treatment of KO embryos with a miR-30d analog
422 before transfer normalized, or even increased, the mean FIV for LIF, regardless
423 of whether the recipient uterus was WT or KO (WT uteri [miR-30d treated:
424 81.83 ± 3.49 ; untreated: 42.82 ± 11.85 ; $p = 0.0467$ and KO uteri [miR-30d
425 treated: 94.50 ± 9.31 ; untreated: 66.25 ± 9.05 ; $p = 0.0046$]). Finally, COX2
426 exhibited perhaps the most intriguing changes. miR-30d pretreatment of KO
427 embryos significantly increased the COX2 FIVs in WT hosts (miR-30d treated:
428 34.52 ± 6.40 ; vs untreated 60.54 ± 1.24 , $p = 0.0299$), thus recovering or
429 exceeding the basal conditions (Fig. 3C).

430 Notably, the IR pattern of the different transfer conditions coincided with
431 the LIF mean FIV pattern (Fig. 4A), and there was a positive correlation
432 ($r = 0.9978$) between the LIF mean FIV and the IR for KO recipients (Fig. 4B).

433 Fetal development impairment linked to a miR-30d deficiency

1
2
3
4
5
6
7
8
9
10
11
12
13
14
15
16
17
18
19
20
21
22
23
24
25
26
27
28
29
30
31
32
33
34
35
36
37
38
39
40
41
42
43
44
45
46
47
48
49
50
51
52
53
54
55
56
57
58
59
60
61
62
63
64
65

434 Considering the observed changes in maternal-embryo communication,
435 we hypothesized that mir-30d deficiency in the mother or embryo would also
436 affect placentation and fetal development. IS size and the number of resorptions
437 were first assessed on days 5, 6, 8, and 12 of pregnancy in both WT and KO
438 genotypes under physiological conditions. The IS sizes were significantly
439 smaller ($p < 0.001$) in KO mothers at all time points analyzed (Fig. 5A).
440 Likewise, the number of resorptions identified by day 12 of pregnancy was
441 slightly higher in KO females compared to the WTs (25% and 10%,
442 respectively; Fig. 5B).

443 To determine if these defects impact fetoplacental growth, we analyzed
444 fetuses and placentas on day 12 (E12) and 16 (E16) of pregnancy (Fig. 5C and
445 D). Placentas and fetuses obtained from KO females were significantly smaller
446 ($p < 0.001$) in terms of CRL ($p < 0.001$) and fetal/placental weight ratio (FW:PW
447 at E12 [$p = 0.012$] and FW:PW_at E16 [$p = 0.001$]), compared to WT females
448 (Fig. 5C-F). The FW:PW is a proxy for placental efficiency¹⁴, defined as the
449 grams of fetus produced per gram of placenta. These results suggest that miR-
450 30 deficiency might affect the nutrient supply, resulting in smaller offspring. This
451 hypothesis is supported by the observation that the weight (Fig. 5G and H),
452 length (Fig. 5G and I), and width (Fig. 5G and J) of weaned offspring derived
453 from KO dams were also significantly less than the controls ($p \leq 0.05$).

454

455 COMMENT

456 This study analyzed the reproductive and fetal effect of bi-directional
457 miR-30d deficiency in vivo at the maternal-embryonic interface and its
458 subsequent effect on gestation.

459 In mice, the uterus is non-responsive to blastocysts during the pre-
460 receptive phase (days 1–3) but becomes receptive on day 4 of pregnancy or
461 pseudopregnancy^{15,16}. When we evaluated the expression of essential
462 receptivity markers (*Cox2*, *Lif*, *Msx1*, *Msx2*, *Esr*, and *Pgr*), we found a
463 significant difference in marker mRNA levels in the early stages of receptivity in

1
2
3
4
5
6
7
8
9
10
11
12
13
14
15
16
17
18
19
20
21
22
23
24
25
26
27
28
29
30
31
32
33
34
35
36
37
38
39
40
41
42
43
44
45
46
47
48
49
50
51
52
53
54
55
56
57
58
59
60
61
62
63
64
65

464 KO uteri. Surprisingly, this difference was not observed in the late stages. On
465 the other hand, LIF protein levels were reduced in KO uteri throughout the WOI.
466 It is generally assumed that miRNAs negatively regulate mRNA expression.
467 However, this is not the first time that a member of the miR-30d family has been
468 implicated in physiological contexts where the absence of one of its members
469 causes protein downregulation¹⁷. These observations suggest that miR-30d
470 could be involved in managing protein balance, depending on internal or
471 external stimuli. As a result, fundamental cellular processes including cell cycle
472 regulation, gene expression, apoptosis, and signal transduction^{18,19} could be
473 compromised.

474 Hence, given the possible impairment of protein expression in the miR-
475 30d KO model, variation in receptivity marker expression was evaluated in a
476 maternal-fetal crosstalk context regulated by bi-directional miR-30d transfer.
477 With that purpose, different embryo-transfer combinations were performed in
478 both WT and KO females to cover all the possible maternal-embryo crosstalk
479 scenarios. Interestingly, re-analysis of receptivity marker expression showed
480 evidence of an intriguing modified fluorescence pattern for LIF. This
481 dysregulation was accompanied by a lower IR at days 6.5–7 of pregnancy,
482 suggesting that a miR-30d-transfer deficiency between the mother and the
483 embryo impaired implantation. Of note, impaired implantation was substantially
484 recovered in the KO genotype after transferring KO embryos pre-treated with a
485 miR-30d analog.

486 Interestingly, the variation in IR among the mice in the different transfer
487 conditions coincided with that observed for the mean FIVs for LIF. Furthermore,
488 there was a positive correlation between the mean FIV for LIF and the IR
489 registered, suggesting LIF as a potential indirect miR-30d target. LIF is an
490 essential regulator of embryo implantation in mice and is a crucial receptivity
491 marker in several mammalian species, including humans. Deregulation of LIF
492 expression has been linked to several cases of female infertility associated with
493 defective implantation²⁰⁻²². Other researchers have suggested that LIF is
494 regulated by miRNAs. The LIF mRNA expression pattern has been found to be
495 virtually the inverse of miR-181a and miR-181b expression during pregnancy²³.
496 In addition, administering miR-181a or miR-181b mimics to mice led to

1
2
3
4
5
6
7
8
9
10
11
12
13
14
15
16
17
18
19
20
21
22
23
24
25
26
27
28
29
30
31
32
33
34
35
36
37
38
39
40
41
42
43
44
45
46
47
48
49
50
51
52
53
54
55
56
57
58
59
60
61
62
63
64
65

497 decreased LIF mRNA and protein levels in their uteri on day 4 of pregnancy.
498 Likewise, miR-223-39 has been described to affect embryo implantation by
499 suppressing the expression of LIF and pinopodes in the endometrium of
500 pregnant mice ²⁴.

501 Yet, it is important to consider that most researchers studying the role of
502 miRNAs in endometrial receptivity, highlight the effect exerted by the
503 endometrium on the embryo, but not how this might influence the acquisition of
504 endometrial receptivity. To date, the closest described in the literature is that of
505 human endometrial epithelial cells (hEECs), which were able to acquire
506 fluorescently-tagged miR-661, a miRNA present in non-implanted blastocyst-
507 conditioned medium ²⁵. Extracellular miR-661 reduced trophoblast spheroid
508 adhesion to hEECs, thus establishing a functional role for extracellular miRNAs
509 in the maternal-fetal interface. Similarly, infusion of fluorescently-labeled
510 embryo-derived EVs into the uterine horns of ewes near the time of implantation
511 resulted in the detection of fluorescence in the cytoplasm of the uterine luminal
512 and glandular epithelium ²⁶. These studies established that extracellular
513 miRNAs originating from the embryo are internalized by uterine cells and
514 modulate maternal gene expression, highlighting the presence of a functional
515 signaling role between the blastocyst and maternal endometrium during the
516 WOI. In this context, here we show evidence that miRNAs transferred from
517 early developmental-stage embryos impact endometrial function, influencing
518 levels of LIF as well as IR.

519 Defective implantation leads to adverse 'ripple' effects throughout
520 pregnancy, including abnormal embryo spacing, retarded fetoplacental growth,
521 and higher rates of resorption ^{27,28}. Consistent with this, IS sizes in miR30d-KO
522 females were significantly smaller at all the analyzed time points and, based on
523 the CRL and FW:PW analysis, their fetuses exhibited retarded fetoplacental
524 growth. These results suggest that miR-30d deficiency is associated with a
525 modest effect on placental development

526 The observed miR-30d-associated phenotypes, particularly those evident
527 during implantation, might arise from altered epithelial-to-mesenchymal
528 transition (EMT). Recent studies have suggested that EMT during implantation

1
2
3
4
5
6
7
8
9
10
11
12
13
14
15
16
17
18
19
20
21
22
23
24
25
26
27
28
29
30
31
32
33
34
35
36
37
38
39
40
41
42
43
44
45
46
47
48
49
50
51
52
53
54
55
56
57
58
59
60
61
62
63
64
65

529 is partially regulated by the abundance of miR-30d²⁹. Specifically, reduced miR-
530 30d expression promotes EMT and invasiveness, and this impairs endometrial
531 receptivity. Therefore, it is feasible that miR-30d dysregulation could affect EMT
532 in the KO murine model, thereby compromising the development of the fetal
533 and maternal vasculature that facilitates nutrient, gas, and waste exchange.
534 This may explain the smaller size of weaned miR-30d KO mice compared to
535 WT genotype.

536 Pregnancy disorders arising from EMT alterations initiate at the level of
537 defective decidualization, an event required to provide nutrients to the implanted
538 embryo until a functional placenta is formed³⁰. Interestingly, LIF is an important
539 regulator of this process; the uteri of *Lif* null mice do not decidualize, even after
540 using different well-established stimuli that induce this process³¹. The
541 phenotype observed in the miR-30d knockouts could result from a succession
542 of events triggered by LIF deficiency. However, miRNAs promiscuously regulate
543 many mRNAs³², and miR-30d-deficient phenotypes could also be derived from
544 the pleiotropic targets of this miRNA. Therefore, because current experiments
545 only examine a limited range of this miRNA's potential range of action, further
546 investigation and more data will be required to elucidate the full range of miR-
547 30d regulation. However, what is clear is that depending on the source of miR-
548 30d deficiency, the deleterious impact on the implantation process considerably
549 varies, highlighting the importance of optimal bi-directional communication in
550 the first stages of conception and later fetal development. Hence, this work
551 opens the door for the investigation of the role of miR-30d in IUGR.

552 ACKNOWLEDGMENTS

553 We thank Fresh Eyes Editing, LLC., for editing this manuscript.

554 REFERENCES

- 555 1. Barker DJ. The developmental origins of adult disease. *J Am Coll Nutr.* 2004;23(6
556 Suppl):588S-595S.
557 2. Douglas AJ. Mother-offspring dialogue in early pregnancy: impact of adverse
558 environment on pregnancy maintenance and neurobiology. *Prog*
559 *Neuropsychopharmacol Biol Psychiatry.* 2011;35(5):1167-1177.
560 3. [Soluble ligands and their receptors in human embryo development and implantation.](#)
561 Thouas GA, Dominguez F, Green MP, Vilella F, Simon C, Gardner D. *Endocr Rev.* 2015;
562 36(1):92-130.

- 1 563 4. Salamonsen LA, Evans J, Nguyen HP, Edgell TA. The Microenvironment of Human
2 564 Implantation: Determinant of Reproductive Success. *Am J Reprod Immunol.*
3 565 2016;75(3):218-225.
4 566 5. Atwood CS, Vadakkadath Meethal S. The spatiotemporal hormonal orchestration of
5 567 human folliculogenesis, early embryogenesis and blastocyst implantation. *Mol Cell*
6 568 *Endocrinol.* 2016;430:33-48.
7 569 6. Bazer FW, Wu G, Spencer TE, Johnson GA, Burghardt RC, Bayless K. Novel pathways for
8 570 implantation and establishment and maintenance of pregnancy in mammals. *Mol Hum*
9 571 *Reprod.* 2010;16(3):135-152.
10 572 7. Robertson SA, Moldenhauer LM. Immunological determinants of implantation success.
11 573 *Int J Dev Biol.* 2014;58(2-4):205-217.
12 574 8. Galliano D, Pellicer A. MicroRNA and implantation. *Fertil Steril.* 2014;101(6):1531-
13 575 1544.
14 576 9. Vilella F, Moreno-Moya JM, Balaguer N, et al. Hsa-miR-30d, secreted by the human
15 577 endometrium, is taken up by the pre-implantation embryo and might modify its
16 578 transcriptome. *Development.* 2015;142(18):3210-3221.
17 579 10. Simon C, Greening DW, Bolumar D, Balaguer N, Salamonsen LA, Vilella F. Extracellular
18 580 Vesicles in Human Reproduction in Health and Disease. *Endocr Rev.* 2018, 39: 292–332.
19 581 11. Bidarimath M, Khalaj K, Wessels JM, Tayade C. MicroRNAs, immune cells and
20 582 pregnancy. *Cell Mol Immunol.* 2014;11(6):538-547.
21 583 12. Altmäe S, Martínez-Conejero JA, Esteban FJ, et al. MicroRNAs miR-30b, miR-30d, and
22 584 miR-494 regulate human endometrial receptivity. *Reprod Sci.* 2013;20(3):308-317.
23 585 13. Moreno-Moya JM, Ramírez L, Vilella F, et al. Complete method to obtain, culture, and
24 586 transfer mouse blastocysts nonsurgically to study implantation and development.
25 587 *Fertil Steril.* 2014;101(3):e13.
26 588 14. Hayward CE, Lean S, Sibley CP, et al. Placental Adaptation: What Can We Learn from
27 589 Birthweight:Placental Weight Ratio? *Front Physiol.* 2016;7:28.
28 590 15. Dey SK, Lim H, Das SK, et al. Molecular cues to implantation. *Endocr Rev.*
29 591 2004;25(3):341-373.
30 592 16. Daikoku T, Cha J, Sun X, et al. Conditional deletion of Msx homeobox genes in the
31 593 uterus inhibits blastocyst implantation by altering uterine receptivity. *Dev Cell.*
32 594 2011;21(6):1014-1025.
33 595 17. Peck BC, Sincavage J, Feinstein S, et al. miR-30 Family Controls Proliferation and
34 596 Differentiation of Intestinal Epithelial Cell Models by Directing a Broad Gene
35 597 Expression Program That Includes SOX9 and the Ubiquitin Ligase Pathway. *J Biol Chem.*
36 598 2016;291(31):15975-15984.
37 599 18. Sadowski M, Suryadinata R, Tan AR, Roesley SN, Sarcevic B. Protein
38 600 monoubiquitination and polyubiquitination generate structural diversity to control
39 601 distinct biological processes. *IUBMB Life.* 2012;64(2):136-142.
40 602 19. Wang J, Maldonado MA. The ubiquitin-proteasome system and its role in
41 603 inflammatory and autoimmune diseases. *Cell Mol Immunol.* 2006;3(4):255-261.
42 604 20. Hambartsoumian E. Endometrial leukemia inhibitory factor (LIF) as a possible cause of
43 605 unexplained infertility and multiple failures of implantation. *Am J Reprod Immunol.*
44 606 1998;39(2):137-143.
45 607 21. Mikolajczyk M, Wirstlein P, Skrzypczak J. The impact of leukemia inhibitory factor in
46 608 uterine flushing on the reproductive potential of infertile women--a prospective study.
47 609 *Am J Reprod Immunol.* 2007;58(1):65-74.
48 610 22. Frasiak JM, Holoch KJ, Yuan L, Schammel DP, Young SL, Lessey BA. Prospective
49 611 assessment of midsecretory endometrial leukemia inhibitor factor expression versus
50 612 $\alpha\beta 3$ testing in women with unexplained infertility. *Fertil Steril.* 2014;101(6):1724-
51 613 1731.
52
53
54
55
56
57
58
59
60
61
62
63
64
65

- 1 614 23. Chu B, Zhong L, Dou S, et al. miRNA-181 regulates embryo implantation in mice
2 615 through targeting leukemia inhibitory factor. *J Mol Cell Biol.* 2015;7(1):12-22.
- 3 616 24. Dong X, Sui C, Huang K, et al. MicroRNA-223-3p suppresses leukemia inhibitory factor
4 617 expression and pinopodes formation during embryo implantation in mice. *Am J Transl
5 618 Res.* 2016;8(2):1155-1163.
- 6 619 25. Cuman C, Van Sinderen M, Gantier MP, et al. Human Blastocyst Secreted microRNA
7 620 Regulate Endometrial Epithelial Cell Adhesion. *EBioMedicine.* 2015;2(10):1528-1535.
- 8 621 26. Burns GW, Brooks KE, Spencer TE. Extracellular Vesicles Originate from the Conceptus
9 622 and Uterus During Early Pregnancy in Sheep. *Biol Reprod.* 2016;94(3):56.
- 10 623 27. Song H, Lim H, Paria BC, et al. Cytosolic phospholipase A2alpha is crucial [correction of
11 624 A2alpha deficiency is crucial] for 'on-time' embryo implantation that directs
12 625 subsequent development. *Development.* 2002;129(12):2879-2889.
- 13 626 28. Ye X, Hama K, Contos JJ, et al. LPA3-mediated lysophosphatidic acid signalling in
14 627 embryo implantation and spacing. *Nature.* 2005;435(7038):104-108.
- 15 628 29. Cai JL, Liu LL, Hu Y, et al. Polychlorinated biphenyls impair endometrial receptivity in
16 629 vitro via regulating mir-30d expression and epithelial mesenchymal transition.
17 630 *Toxicology.* 2016;365:25-34.
- 18 631 30. Rosario GX, Stewart CL. The Multifaceted Actions of Leukaemia Inhibitory Factor in
19 632 Mediating Uterine Receptivity and Embryo Implantation. *Am J Reprod Immunol.*
20 633 2016;75(3):246-255.
- 21 634 31. Chen JR, Cheng JG, Shatzer T, Sewell L, Hernandez L, Stewart CL. Leukemia inhibitory
22 635 factor can substitute for nidatory estrogen and is essential to inducing a receptive
23 636 uterus for implantation but is not essential for subsequent embryogenesis.
24 637 *Endocrinology.* 2000;141(12):4365-4372.
- 25 638 32. Mehta A, Baltimore D. MicroRNAs as regulatory elements in immune system logic. *Nat
26 639 Rev Immunol.* 2016;16(5):279-294.

640

641 **FIGURE LEGENDS**

642 **Fig. 1. Analysis of receptivity markers in WT and miR-30d KO uteri at pre-**
643 **and post- implantation.** A) RT-qPCRs performed on WT and miR-30d KO uteri
644 samples during a non-pregnancy state (E0) and at day 4 (E4) and 5 (E5) of
645 pseudopregnancy (n = 6 uteri per condition tested and per genotype analyzed;
646 total uteri: WT, n = 18; KO, n = 18). Fold-change (FC) values are presented for
647 all the analyzed receptivity markers (*Cox2*, *Lif*, *Msx1*, *Msx2*, *Esr*, and *Pgr*).
648 Significant differences were observed at E0 (*Lif* [p = 0.036]; *Msx1* [p = 0.001]),
649 E4 (*Cox2* [p < 0.001]; *Lif* [p < 0.001]; *Msx1* [p < 0.001]; *Msx2* [p = 0.004]; *Esr*
650 [p < 0.001]; *Pgr* [p < 0.001]), and E5 (*Msx2* [p = 0.0355]). B) IF assays
651 performed on WT and miR-30d KO uteri in a non-pregnancy state (E0) and on
652 day 4 (E4) and day 5 (E5) of pseudopregnancy (n = 3 uteri per condition tested
653 and per genotype analyzed; total uteri: WT, n = 9; KO, n = 9). Micrographs
654 suggest that COX2, LIF, and ESR expression was higher in the WT genotype
655 than in the KO at all the stages analyzed. Staining was with Hoechst 33382

65

656 (blue): nucleus; Alexa Fluor 555 dye (red): receptivity markers COX2, LIF,
 657 MSX1, MSX2, and ESR; Alexa Fluor 488 dye (green): receptivity marker PGR.
 658 C) WB analysis performed on WT and miR-30d KO uteri at a non-pregnancy
 659 state (E0) and at day 4 (E4) and 5 (E5) of pseudopregnancy (n = 6 uteri per
 660 condition tested and genotype analyzed; total uteri: WT, n = 18; KO, n = 18).
 661 Significant differences were detected for COX2 (p < 0.001) at E0, LIF at E0
 662 (p = 0.002), E4 (p = 0.001) and E5 (p < 0.001); and ESR (p < 0.001) at E5.

663 **Fig. 2. Characterization of the implantation phenotype associated with**
 664 **miR-30d deficiency.** A) Representative images of the implantation sites
 665 (demarcated by distinct blue bands) registered for the WT and KO uteri at days
 666 6.5-7 of pregnancy. Six biological replicates were performed for day 6.5-7 of
 667 pregnancy (approximately 90 embryos transferred per condition; total of 423
 668 embryos transferred in the six conditions tested) B) Implantation rate (IR) at day
 669 6.5-7 of pregnancy. The IRs for KO embryos transferred into WT recipients was
 670 less than for the transfer of WT embryos into WT recipients (48.86% ± 14.33 vs.
 671 75.00% ± 10.47; p = 0.006); transfer of KO embryos into KO recipients led to
 672 lower IRs compared to the transfer of WT embryos into KO recipients
 673 (26.04% ± 7.15 vs. 49.71% ± 8.59; p = 0.006); pretreating KO embryos with
 674 miR-30d significantly restored these IRs in KO uteri (54.39% ± 10.13 vs.
 675 26.04 ± 7.15; p = 0.003).

676 **Fig. 3. Analysis of receptivity markers in WT or KO uteri depending on the**
 677 **miR-30d source of origin.** A) Micrographs of WT and KO uteri at day 4 (E4)
 678 and 5 (E5) of pregnancy. Representative images for every receptivity marker
 679 are presented (n = 3 uteri per condition tested and per genotype analyzed; total
 680 uteri: WT; n = 6; KO, n = 6). Staining was with Hoechst 33382 (blue): nucleus;
 681 Alexa Fluor 555 dye (red): receptivity markers COX2, LIF, MSX1, MSX2, and
 682 ESR; Alexa Fluor 488 dye (green): from rows 1–5, represents the ZO-1 location.
 683 In row 6, Alexa Fluor 488 demarcates PGR expression. B) Right panels:
 684 Micrographs of WT and KO uteri in the different transfer conditions tested. For
 685 every condition tested; an average of 10–15 embryos were introduced. Three
 686 biological replicates were performed for day 5 (E5; approximately 36 embryos
 687 transferred per condition tested). The staining was Hoechst 33382 (blue):
 688 nucleus; Alexa Fluor 555 dye (red): receptivity markers COX2, LIF, MSX1,

689 MSX2, and ESR; Alexa Fluor 488 dye (green): from rows 1–5, represents the
 690 ZO-1 location. In row 6, Alexa Fluor 488 demarcates PGR expression. C)
 691 Integrated fluorescence density/area calculated for every transfer condition
 692 tested: (1) WTE-WTR; (2) KOE-WTR; (3) PTKOE-WTR; (4) WTE-KOR; (5)
 693 KOE-KOR; (6) PTKOE-KOR. Compared to WT embryos, transfer of KO
 694 embryos significantly reduces the presence of LIF in both WT and KO uteri (WT
 695 uteri [42.82 ± 11.85 vs. 64.74 ± 8.63 ; $p = 0.038$ and KO uteri [66.25 ± 9.05 vs.
 696 88.54 ± 7.18 ; $p = 0.006$]). Transfer of miR-30d-pretreated KO embryos results in
 697 an increase of the LIF mean fluorescence intensity value (FIV) in both WT and
 698 KO recipients (WT uteri [81.83 ± 3.49 vs. 42.82 ± 11.85 ; $p = 0.047$ and KO uteri
 699 [94.50 ± 9.31 vs. 66.25 ± 9.05 ; $p = 0.005$]). Transfer of miR-30d-pretreated KO
 700 embryos increases the COX2 mean FIVs compared to transferring KO embryos
 701 to WT recipients (34.52 ± 6.40 vs. 60.54 ± 1.24 , $p = 0.03$).

702 **Fig. 4. Correlation between IR and LIF staining under the different**
 703 **maternal transfer conditions.** Graphs representing the overlapping tendency
 704 between the mean FIVs for LIF (red line) and the percentage IR (grey bars)
 705 observed for the WT (left graph) and KO (right graph) recipient. Primary axis: IR
 706 (%), secondary axis: integrated density/area. (B) Correlation between the LIF
 707 mean FIVs and the IR (%) observed in all the transfer conditions tested. A
 708 positive correlation was found for the KO recipients ($r = 0.998$).

709 **Fig. 5. Characterization of the pregnancy outcome associated with miR-**
 710 **30d deficiency.** A) Implantation site (IS) size calculated throughout gestation
 711 (days 5, 6, 8, and 12) as measured by Adobe Photoshop image analysis
 712 software (WT: E5 [n = 16]; E6 [n = 37]; E8 [n = 28]; E12 [n = 16]; KO E5
 713 [n = 23]; E6 [n = 15]; E8 [n = 20]; E12 [n = 17]). The IS sizes were significantly
 714 smaller (E5, E6, E8, E12; $p < 0.001$) in the KO genotype on all the gestation
 715 days analyzed. B) Resorption sites registered on day 12 (E12) of pregnancy
 716 [WT (n=10), KO (n=5); n is the number of mice analyzed. In the graphs,
 717 between brackets, the number of resorption sites in relation to the total number
 718 of IS analyzed is reflected. C) Intrauterine growth restriction (IUGR) was
 719 evaluated by analyzing the fetuses and the placentas on day 12 (E12) and 16
 720 (E16) of pregnancy (WT: E12 [n = 14]; E16 [n = 17]; KO: E12 [n = 12]; E16
 721 [n = 5]). Representative images of the fetuses obtained for the WT and KO

1 722 genotypes on day 12 and 16 of pregnancy. D) Representative images of the
2 723 placentas obtained for the WT and KO genotypes on day 12 (E12) and 16 (E16)
3 724 of pregnancy. E) Crown-rump length (CRL) determination for WT and KO
4 725 genotype embryos on day 12 (E12) and 16 (E16) of pregnancy. There was a
5 726 significant reduction in the RCL in the KO genotype on both days CRL_E12
6 727 [$p < 0.001$]; CRL_E16 [$p < 0.001$]). F) The FW:PW ratio estimated for the WT
7 728 and KO genotypes on day 12 (E12) and 16 (E16) of pregnancy. A significant
8 729 reduction in the FW:PW was observed in the KO genotype on both days
9 730 (FW:PW_E12 [$p = 0.012$]). G) Representative images of weaned WT and KO
10 731 mice (WT [$n = 40$]; KO [$n = 37$]). (H) Weight determination for WT and KO
11 732 weaned mice after 4 weeks of delivery; there were significant differences
12 733 between these genotypes ($p = 0.05$). I) Length determination for weaned WT
13 734 and KO mice 4 weeks after delivery; significant differences between these
14 735 genotypes were detected ($p = 0.05$). J) Width determination for WT and KO
15 736 weaned mice 4 weeks after delivery; significant differences between these
16 737 genotypes were detected ($p = 0.05$).

17 738 **Suppl. Fig. 1.** A) Right graph integrates fluorescence value (FIV) density/area
18 739 calculated for every receptivity marker at day 4 of pregnancy. In general, all the
19 740 mean FIVs decreased for all the receptivity markers, but this decrease was not
20 741 significant. Left graph integrates density/area calculated for every receptivity
21 742 marker at day 5 of pregnancy. The FIV of LIF was significantly downregulated in
22 743 KO uteri (64.73 ± 3.86 vs. 49.15 ± 9.05 ; $p = 0.034$). For the rest of the markers,
23 744 differences were not significant.

24 745

25 746

26 747

27 748

28 749

29 750

FIGURE 1

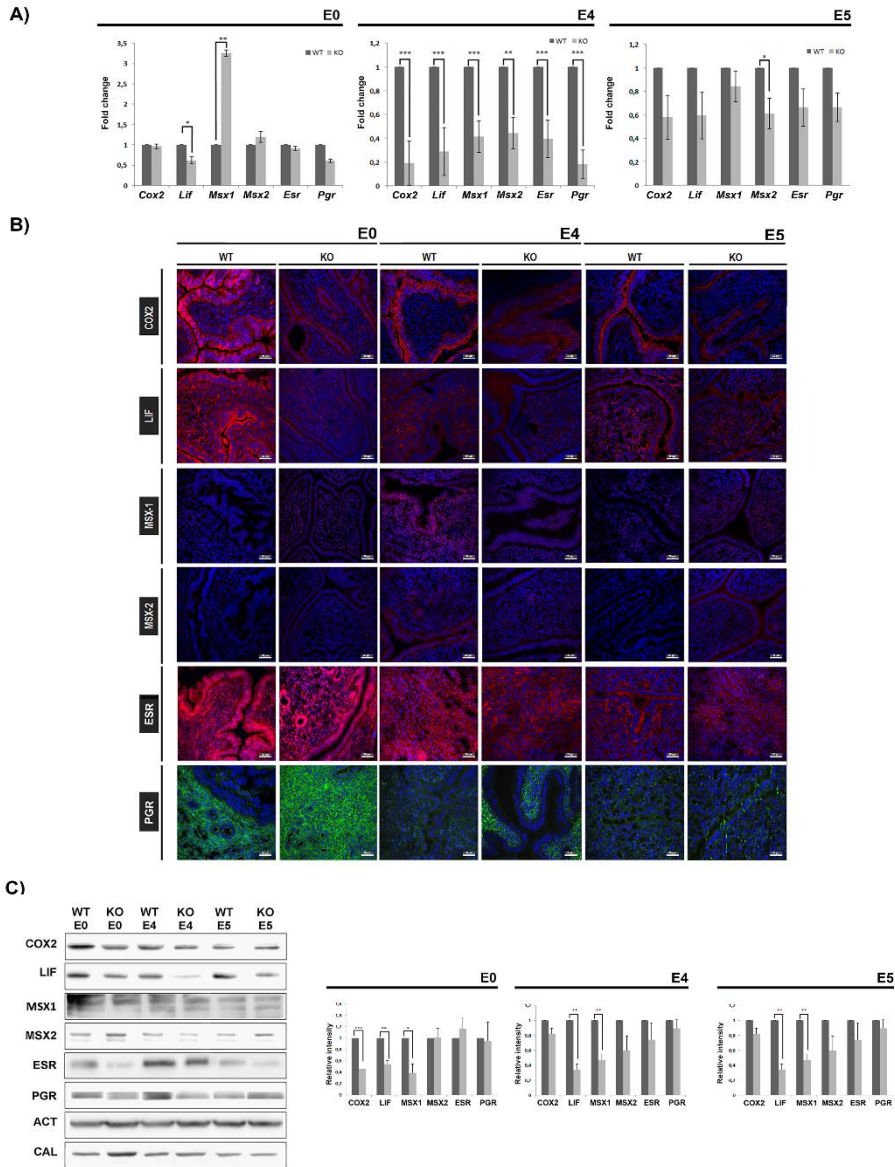


FIGURE 2

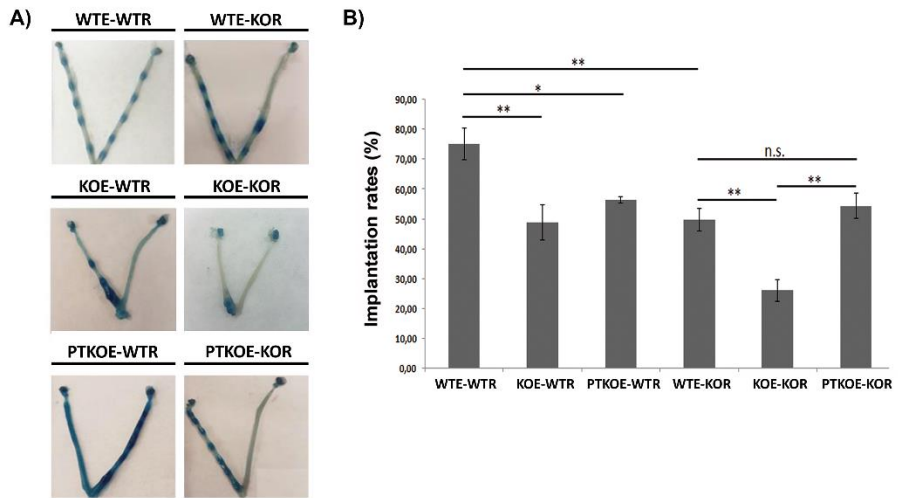


FIGURE 3

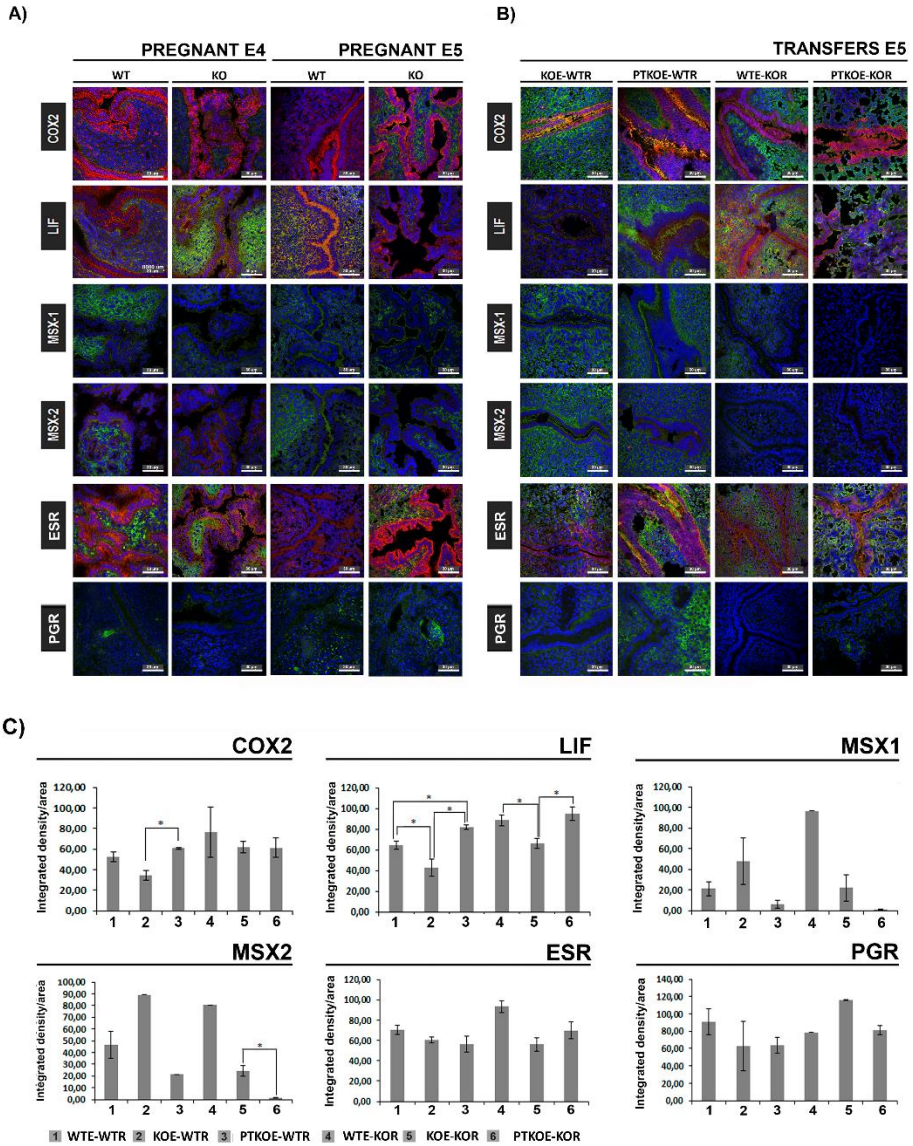
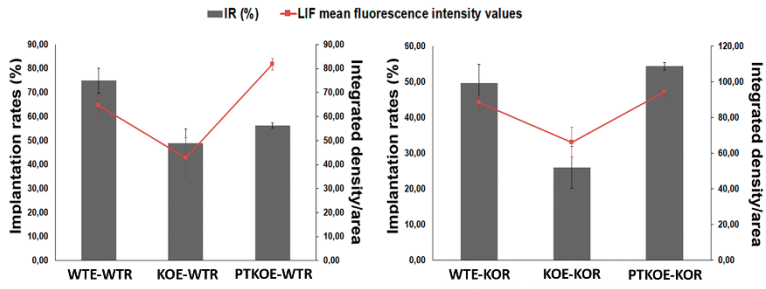


FIGURE 4

A)



B)

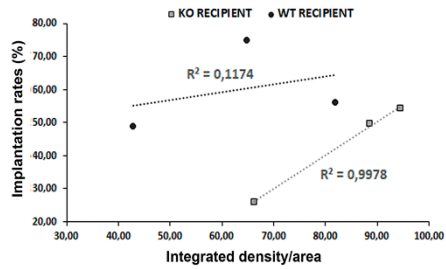
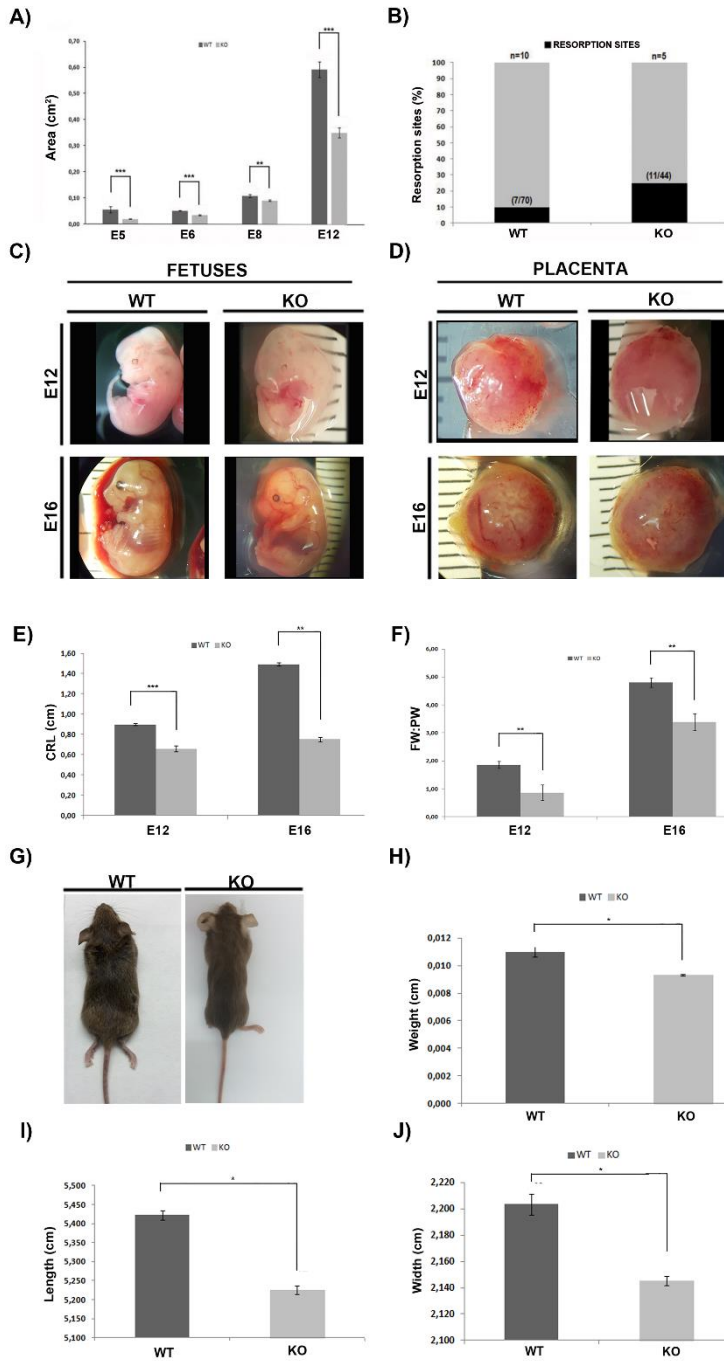
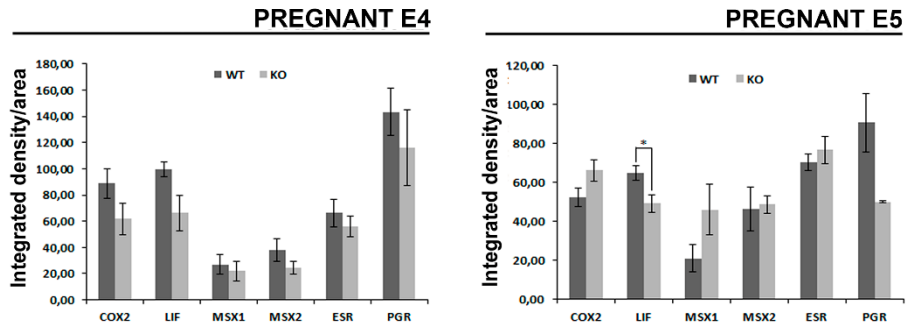


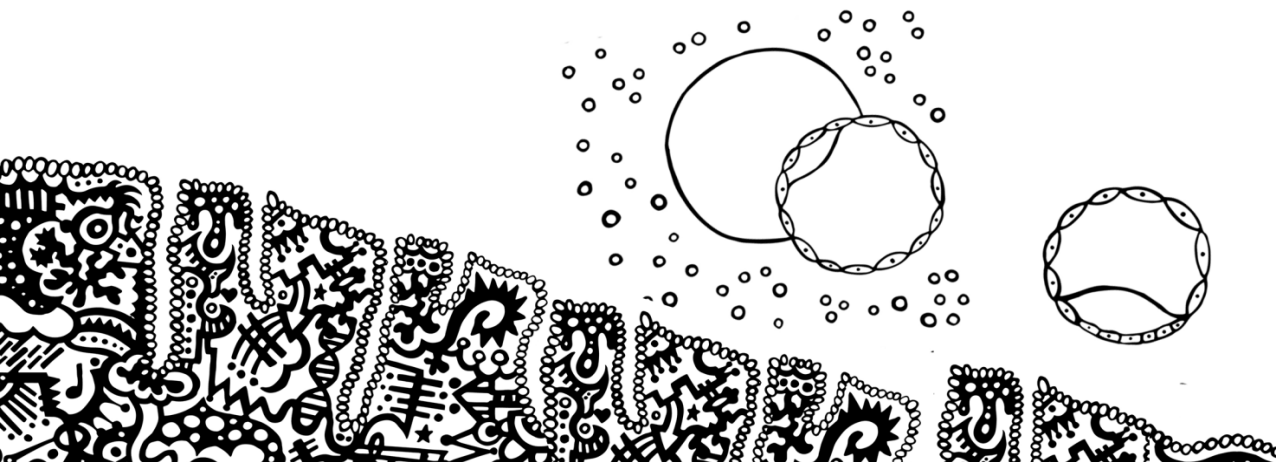
FIGURE 5



SUPPLEMENTARY FIGURE 1



Embryo/fetal maternal crosstalk



Embryo/fetal–maternal cross talk

NURIA BALAGUER, FRANCISCO DOMINGUEZ, CARLOS SIMON, and FELIPE VILELLA

INTRODUCTION

Despite the effort devoted to understanding the molecular basis of embryo implantation, the process remains a biological enigma. Following fertilization, the resulting blastocyst must signal its presence to the mother, attach to the luminal epithelium of the endometrium, and embed itself into the decidualized stroma. Failure to do so results in no pregnancy. Events producing a negative impact on this process are intrinsically linked to the development of obstetric pathologies such as intrauterine growth restriction (IUGR) and preeclampsia, or the fetal origin of adult disease (FOAD) (1).

It is widely accepted that the attainment of a successful pregnancy requires three factors: a competent euploid embryo, a receptive endometrium, and a successful dialogue between them (2–6) (Figure 19.1). In this chapter, we summarize the existing information connecting the main factors involved in embryo–endometrial or fetal–maternal cross talk, including cytokines, growth factors, prostaglandins (PGs), and microRNAs (miRNAs). Special relevance is given to the emerging role exerted by exosomes as cell communication mediators. Finally, the adverse intrauterine environment's effect on the development of adult diseases such as diabetes or obesity is discussed.

CYTOKINES AND GROWTH FACTORS IN CELL-TO-CELL COMMUNICATION

Factors released by the maternal tract, especially cytokines, are reported to exert paracrine cell-to-cell signals influencing embryo physiology and developmental potential (7–9). In turn, these factors act in synergy with autocrine growth factors and cytokines produced by the embryo itself to modulate gene expression and physiological function. As a result, the acquisition of implantation competence and postimplantation developmental ability may be profoundly affected, in both physiological and pathological conditions (10,11).

Cytokines

Cytokines are a family of several hundred small, diffusible glycoproteins that act as soluble intercellular signaling agents (12). They are the major players in the regulation of immune-related events. Binding of cytokines to specific high-affinity receptors, located in target cells, triggers activation of a broad range of tyrosine kinases belonging to the JAK/STAT family (13–15). The production of endometrial cytokines is primarily regulated by ovarian steroid hormones, but also by paracrine factors secreted by adjacent endometrial cells or emanating from microorganisms,

or the trophoblast itself. Dysregulation of cytokine production, especially those of the interleukin (IL)-6 family, is associated with implantation failure and miscarriage, even for a euploid embryo.

The IL-6 family includes leukemia inhibitory factor (LIF), IL-6, and IL-11 (16). LIF is a pro-inflammatory factor that regulates proliferation, differentiation, and cell survival (17). Expression of LIF appears to be under maternal control, and exhibits a considerable increase during the window of implantation (WOI), the period of endometrial receptivity during which a blastocyst can implant. LIF acts by binding to its receptor, LIF-R, and co-receptor, gp130; this binding triggers several signaling pathways, including JAK/STAT, MAPK, and phosphatidylinositol-3 (PI-3) kinase pathways (5). The importance of LIF to reproduction is demonstrated by the phenotype of *Lif* knockout mice: females are fertile, but their blastocysts fail to implant (18). These promising results prompted the implementation of clinical trials investigating the effect of recombinant human LIF (rhLIF) administration during the luteal phase in women with implantation failure; however, no noticeable improvements in pregnancy rates were achieved (19).

IL-6 is a multifunctional cytokine that regulates several aspects of the immune response, acute phase reaction, and hematopoiesis (20). IL-6 is minimally expressed during the proliferative phase of the menstrual cycle, but strong immunoreactivity is shown during the midsecretory phase, predominantly in the glandular and luminal epithelial cells (21). Aberrant expression of IL-6 is associated with recurrent miscarriage (22), suggesting an autocrine or paracrine role for IL-6 during implantation (23). Moreover, higher levels of IL-6 appear to be linked with lower implantation rates in patients with endometriosis through impairment of oocyte and embryo quality (24). Embryo viability is, in turn, related to the consumption of IL-6. Our group validated this finding during an investigation of the secretome profile of implanted blastocysts that were grown in sequential media versus cocultured endometrial epithelial cells (EECs) (25). We observed a differential protein pattern between culture conditions. Interestingly, IL-6 was the most abundantly secreted protein in the EEC coculture, meaning that the IL-6 present in the media could be consumed or metabolized by the blastocyst. Furthermore, IL-6 was nearly absent from the sequential media used to culture the blastocysts that later implanted successfully, compared with those blastocysts that did not implant (25), reinforcing the hypothesis that the consumed or metabolized IL-6 may be necessary for proper development and implantation of the blastocyst.

252 Embryo/fetal–maternal cross talk

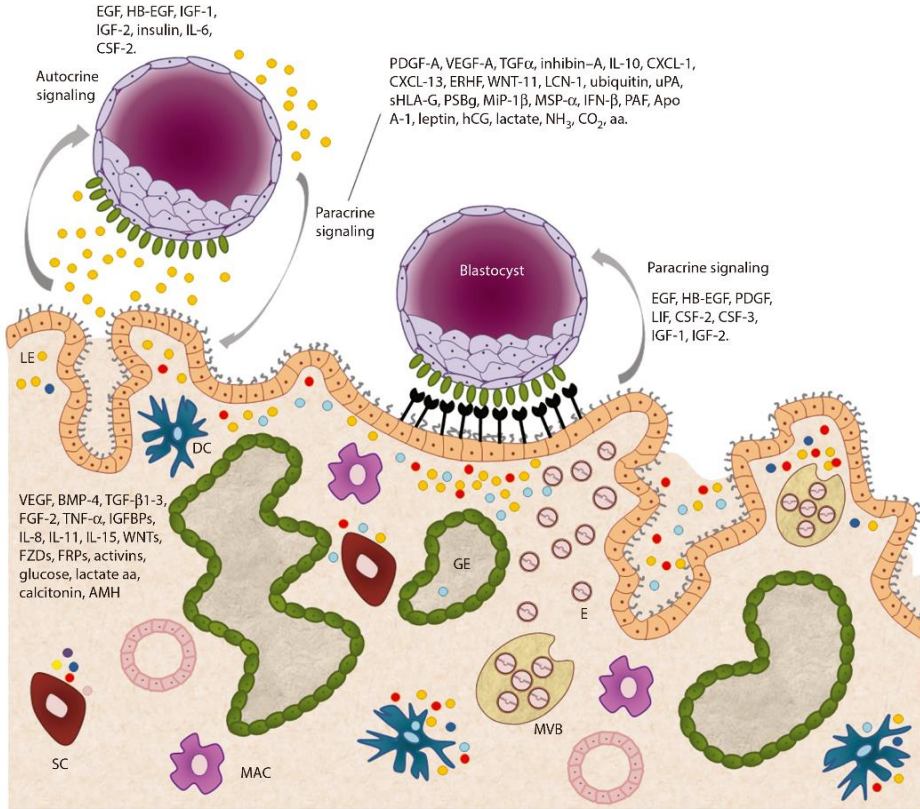


Figure 19.1 Schematic representation of the maternal–fetal cross talk. LE, luminal epithelium; GE, glandular epithelium; SC, stromal cells; DC, dendritic cells; MBV, multivesicular bodies.

IL-11 exerts important pleiotropic actions (26). Both IL-11 and its receptor IL-11R α localize to decidualized stromal cells in the midsecretory phase endometrium (27–29). Their functional relevance has been demonstrated by the existence of a phenotype in the animal model lacking IL-11, which has impaired fertility and smaller litter sizes (30). Incidentally, IL-11 deficiency has been observed in patients with recurrent miscarriage compared with fertile women (31).

During postimplantation, in the placental–decidual interface, a vast quantity of cytokines are synthesized; colony-stimulating factor (CSF) 1, transforming growth factor (TGF) β , tumor necrosis factor (TNF) α , GM-CSF, LIF, interferon (IFN) γ , IL-6, and IL-10 are the most functionally relevant in trophoblast differentiation and invasion (32). Patterns of receptor expression in specific trophoblast cell populations, combined with data from *in vitro* models, suggest that individual cytokines have

specific roles in the regulation of the invasive, adhesive, secretory, and antigenic properties of different trophoblast lineages (12). Some cytokines, such as IL-1, IL-6, IL-15, and TNF γ , enhance matrix metalloproteinase (MMP) activity, while others, like IL-10, LIF, and TGF β , inhibit MMP secretion or stimulate expression of tissue inhibitors of matrix metalloproteinases (TIMPs) (33).

Among cytokines, chemokines stand out due to the chemotactic properties that enable them to regulate leukocyte recruitment from the blood, as well as their directional movement within tissues and their exodus via the lymphatic system (34). Chemokines can be classified into different subfamilies based on their structural motifs: the CXC, CC, CX3C, and C groups, or the α , β , γ , and δ subfamilies (35). To assess the paracrine effect of the embryo on the expression of chemokine receptors on the endometrium, our group cocultured human embryos with EECs. Chemokine receptors CXCR1, CXCR4, and CCR5 were

barely detectable in an EEC monolayer. However, when a human blastocyst was present, there was an increase in the number of EECs positive for CXCR1, CXCR4, and CCR5, and these receptors were polarized in one of the cell poles of the endometrial epithelium. In another study using the same coculture model, we examined the embryonic regulation of EEC IL-8 (36). IL-8 expression (messenger RNA [mRNA]) was significantly upregulated in EEC in the presence of blastocysts compared with the control EEC (without embryos) (37). Altogether, these results show a paracrine effect of the embryo over cytokines and chemokines in the maternal endometrium.

The *in vivo* study of human implantation sites is impracticable for ethical reasons. Therefore, animal models, especially gene knockouts (38), and *in vitro* studies are of great interest in employing a human coculture model using decidualizing endometrial stromal cells (ESCs) and single hatched blastocysts to identify the soluble factors involved in implantation (39). Over a 3-day coculture period, approximately 75% of embryos arrested, whereas the remainder continued normal development. Multiplex immunoassays were used to determine the levels of 14 factors secreted by the ESCs. The presence of a normal blastocyst had no significant effect on decidual secretions; in contrast, arrested embryos triggered a response, characterized by selective inhibition of IL-1 β , IL-6, IL-10, IL-17, IL-18, eotaxin, and heparin binding epidermal growth factor (HB-EGF) secretion. The authors concluded that the response of decidual cells to a developmentally impaired embryo could represent a mechanism for controlled embryo disposal, mediated by induction of menstruation-like tissue breakdown and shedding (39).

Growth factors

Growth factors comprise a group of peptides and polypeptides that are usually divided into families based primarily on their structural characteristics (40). They interact with specific cell membrane receptors, thus initiating intracellular signaling pathways (41). The major families include epidermal growth factors (EGFs), TGF β , fibroblast growth factors (FGFs), insulin-like growth factors, and platelet-derived growth factors (PDGFs). The EGF family encompasses EGF itself, TGF α , HB-EGF, amphiregulin, β -cellulin (BTC), epiregulin (ER), and neuregulins (38). Specifically, they interact with the receptor subtypes of the ErbB family, which comprises four receptor tyrosine kinases: ErbB1 (EGF-R), ErbB2, ErbB3, and ErbB4 (42). Spatiotemporal expression patterns of EGF gene family members and ErbB in the uterus during the peri-implantation period suggest compartmentalized functions of EGF-like growth factors in implantation (43–47). HB-EGF appears to play a critical role in this process, as well as in embryo development, since its expression reaches its highest level during the late secretory phase, a period of maximum receptivity (48). Moreover, decreasing levels lead to pregnancy complications, such as preeclampsia and small for gestational age (SGA), due to aberrant trophoblast invasion, and also to IUGR due

to increased apoptosis (49). Concurrently, cells expressing the transmembrane form of HB-EGF adhere to human blastocysts displaying cell surface ErbB4 (50). In support of this molecular event, Paria et al. (51) demonstrated that ErbB4 was expressed by day 4 blastocysts at both the protein and mRNA levels. This was located primarily at the submyometrial stroma and connective tissues with basal levels of expression throughout the stroma (52). Besides HB-EGF, the luminal epithelium also expresses BTC and ER as ligands at the site of implantation that can interact with ErbB1 and ErbB4. Thus, the contribution of these various ligands to implantation may be redundant. In general, the expression of multiple ligands and multiple ErbB family receptors might be a protective mechanism to ensure a high probability of blastocyst development and implantation.

Notably, Wnt proteins may behave as growth factors in the uterus; they are reported to be involved in cell specification and epithelial–mesenchymal interactions (53–55). Wnt signaling can occur through the canonical pathway mediated by the family of receptors inducing stabilization of β -catenin, or it may work through an unrelated receptor, RYK (56). Wnt signaling also regulates vascular endothelial growth factors (VEGFs), which are effectors of angiogenesis. Splicing variants of VEGF interact differentially with the two VEGF receptors (VEGF-R1 and VEGF-R2, also known as FLT-1 and FLK-2). Moreover, one isoform of VEGF (VEGF165) binds to neuropilin proteins (NPN-1 and NPN-2), transmembrane proteins unrelated to VEGF-R. The interaction between VEGF165 and NPN-2 promotes the binding of VEGF165 to VEGF-R (57). Redundancy within pathways and cross talk between them increase the complexity of biological responses, making it very difficult to elucidate the molecular mechanisms involved in paracrine mediation of hormone action (58). Hannan et al. (59) were the first to detect high levels of VEGF165 in uterine fluid in women during the WOI, being as well significantly reduced in women with unexplained infertility. Moreover, rhVEGF administration significantly improves preimplantation mouse embryo development and embryo outgrowth *in vitro*, as well as implantation rates and aspects of fetal development *in vivo*. These findings further support the existence of a precise paracrine and autocrine dialogue between the blastocyst and endometrial epithelium during the WOI and clearly highlight the importance of the changing microenvironment as embryos develop (60).

TGF β superfamily members are associated with tissue remodeling events and reproductive processes. They include at least 42 different mammalian dimeric proteins sharing a similar structure (61,62). These are divided into two subfamilies, the TGF β /activating/nodal subfamily and the bone morphogenetic protein (BMP)/Mullerian inhibiting substance (MIS)/growth and differentiation factor (GDF) subfamily (63). Their roles in preparation for implantation have been detailed, particularly in promoting decidualization of endometrial stroma (64). However, given the grade of complexity surrounding this system,

it is not surprising that disruption of any member of the family has not resulted in alteration of implantation.

ADHESION AND ANTIADHESION MOLECULES

Adhesion molecules

Integrins are a family of transmembrane proteins formed by the interaction of two different noncovalently linked α and β subunits (65). These proteins are receptors for extracellular matrix (ECM) ligands such as collagen, laminin, and fibronectin, as well as for transducing signals from soluble ligands such as osteopontin (66). In humans, $\alpha^2\beta^1$, $\alpha^3\beta^1$, $\alpha^6\beta^1$, $\alpha^7\beta^1$, $\alpha^8\beta^1$, $\alpha^9\beta^1$, $\alpha^5\beta^1$, $\alpha^4\beta^3$, and $\alpha^6\beta^5$ are localized on the uterine luminal epithelium. The glandular epithelium exhibits the same proteins, with the exception of $\alpha^7\beta^1$ and $\alpha^8\beta^1$, as well as $\alpha^9\beta^1$ and $\alpha^4\beta^3$ (67,68). Some integrins (i.e., $\alpha^7\beta^1$ and $\alpha^8\beta^1$) are characterized for having a cycle-dependent expression in both stroma and epithelium throughout the menstrual cycle (69). During the WOI, β^3 and α^4 appear to be upregulated and downregulated, respectively, leading to the hypothesis that they could play an important role in the initial stages of blastocyst adhesion. Studies performed with β^1 -/- knockout mice demonstrated the ability of embryos to develop until the blastocyst stage, but they failed to implant, showing defects in cell lineage allocation (70). Interestingly, mice with mutations in α^4 , α^5 , or α^6 subunits or $\alpha^7\beta^1$ integrin have proper implantation. In contrast, aberrant expression of $\alpha^7\beta^1$ in humans is associated with endometriosis and in vitro fertilization (IVF) failure (71).

Selectins, the lectin-like proteins that include E-, L-, and P-selectins, are responsible for the tether and roll mechanism on endothelial surfaces (72). At the time of implantation, carbohydrate ligands (i.e., MECA-79) that bind L-selectin are present on the luminal epithelium, an event that coincides with a strong expression of L-selectin by the trophoblast after hatching. Human studies revealed that the lack of expression of MECA-79 in midluteal endometrial biopsies is indicative for low or no probability of pregnancy (73).

Antiadhesion molecules

Antiadhesion molecules (i.e., MUC-1) appear to perform a temporary role in the regulation of blastocyst implantation (65). MUC-1 is a well-described glycosylated protein (>250 kDa), which is likely to produce a steric blocking of E-cadherin-based cell-to-cell interactions (74). In humans, MUC-1 concentration increases during the WOI, and decreases in the late secretory phase. However, despite the existence of a general steroid-mediated increase of MUC-1 in the WOI, *in vitro* experiments have shown that paracrine effects from the blastocyst may cause a local clearance of MUC-1 at the place of attachment (75).

PROSTAGLANDINS

PGs are involved in vascular permeability, stromal decidualization, blastocyst growth and development, leukocyte recruitment, embryo transport, trophoblast invasion, and ECM remodeling during implantation (76).

PGs are bioactive lipid compounds of the eicosanoid family, derived from the essential fatty acid arachidonic acid (AA) (77). The participation of specific terminal PG synthases enables the formation of a set of well-known PGs: PGE₂, PGE₂, PGF_{2 α} , and PGI₂ (78); PGE₂ and PGF_{2 α} are the most relevant in acquiring a receptive endometrium (79). PGs actions are mediated by their binding to various G protein-coupled receptors (GPCRs), which include four subtypes for PGE₂ (EP1, EP2, EP3, and EP4) and one (FP) for PGF_{2 α} (80).

PG production can be inhibited in female mice lacking PLA₂ and COX enzymes, resulting in significant implantation defects (81). Specifically, *Cox-2* knockout mice show a marked infertility associated with abnormal implantation and decidualization (82). On the other hand, *Cox-1*-deficient mice do not demonstrate problems with implantation but are characterized by having anomalous parturition (83).

Our group demonstrated that PGE₂ and PGF_{2 α} concentrations in endometrial fluid (EF) aspirate 24 hours before embryo transfer can predict pregnancy outcome (79). Moreover, we showed that blocking PG receptors on the membrane of the trophoblast of mouse embryos produces a considerable reduction in embryo adhesion rates. These results suggest that the transport of PGs from mother to embryo is essential for acquiring a proper adhesion phenotype.

MicroRNAs

miRNAs are a family of 21- to 25-nucleotide small RNA molecules characterized for their ability to regulate gene expression at the posttranscriptional level through degradation, repression, or silencing (84–86). A single miRNA is able to regulate up to hundreds of mRNA targets through perfect or imperfect complementation with the 3'-untranslated regions of its target transcripts (87).

Initially, Kuokkanen et al. (88) reported the existence of differential miRNA expression patterns in EECs throughout the menstrual cycle, suggesting that some miRNAs could be hormonally regulated in the human endometrium. Later, Revel et al. (89) identified 13 differentially expressed miRNAs (i.e., miR-23b, miR-145, miR-27b, or miR-195) in the endometrium in recurrent implantation failure (RIF) patients when compared with fertile women. This study allowed them to identify a set of 23 downregulated genes with biological functions in adherens junctions, Wnt signaling, p53, the cell cycle, cell adhesion molecules, and cancer pathways, which are currently considered crucial in the implantation process. Additionally, they observed a link between the downregulation of estrogen receptor α (ER α) *in vitro* expression and the upregulation of miR-145, an event that led them to consider targeting miR-145 as a therapeutic option for these patients. Following the same line of research, Sha et al. (90), designed a clinical study where miRNAs were proposed as potential biomarkers for human endometrial receptivity. Using a deep sequencing approach, miRNA expression profiles were compared between a prereceptive

(lutinizing hormone [LH] + 2) and a receptive (LH + 7) state in both natural and stimulated cycles. In normal cycles, they found 8 upregulated miRNAs and 12 downregulated miRNAs on LH + 7 compared with LH + 2. Bioinformatic analysis revealed that those miRNAs target a set of genes differentially expressed during the WOI.

Most recently, Altmäe et al. (91) identified 4 miRNAs (miR-30b, miR-30d, miR-494, and miR-923) that are specifically regulated in receptive endometrium at the time of implantation. In particular, miR-30b and miR-30d are upregulated, whereas miR-494 and miR-923 are downregulated in receptive endometrium. These results are consistent with Sha et al. (90), who found miR-30b and miR-30d are upregulated in nonstimulated LH + 7 vs. LH + 2 in endometria of infertile women. Another study highlighted the importance of miR-30d, after demonstrating its downregulation in decidualized stromal cells vs. nondecidualized cells (92). Finally, the bioinformatic analyses revealed that several signaling pathways, such as Wnt, axon guidance, ERK/MAPK, TGF β , p53, and leukocyte extravasation, are regulated by these microRNAs, confirming their indispensable role in a successful blastocyst implantation.

Our group recently took a step forward in understanding the importance of miR-30d as a transcriptomic modifier of the preimplantation embryo (93). We not only demonstrated the upregulation of miR-30d in EF during the WOI, but also described a novel cell-to-cell communication mechanism involving the delivery of endometrial microRNAs from the maternal endometrium to the preimplantation embryo. To do so, we initially confirmed that primary human EECs (hEECs) actively secrete large quantities of exosomes into the conditioned media. Transmission electron micrographs suggested that those exosomes are loaded with miR-30d. Concurrently, several tracking experiments recognizing the miRNA *in vitro* allowed us to demonstrate that exosomes loaded with miR-30d are secreted from hEECs and can be internalized by trophoblastic cells of murine embryos adhered to hEECs.

Several mechanisms could explain how exosome content is released into target cells, such as endocytosis or fusion of the exosomes with the plasma membrane (94). Further, addition of free miRNAs into culture media at different concentrations results in the incorporation of these molecules into hatched trophoblasts. In electron micrographs, we observed that murine embryos present microvilli and what appear to be small pores interspaced along the trophoblastic surface. This finding could explain how blastocysts mediate a fast exchange of nutrients and molecules.

To understand the functional role of maternal miR-30d incorporation into the embryo, transcriptomic studies were used to compare the effects of mimic miR-30d miRNA and scramble miRNA in murine embryos. Expression arrays demonstrated that embryos treated with miR-30d have increased expression of 10 genes, including those encoding adhesion molecules such as ITGB3, ITGA7, and CDH5 (Figure 19.2). The induction of

this adhesive phenotype was validated *in vitro* by adhesion assays showing a significant increase in the adhesion of murine embryos and human trophoblastic cell lines treated with miR-30d mimic versus miR-30d inhibitor. Further studies are needed to understand the underlying molecular mechanisms that enhance this adhesion phenotype. However, this work paves the way to understanding more accurately how the intrauterine environment is important not only in the attainment of a pregnancy but also in the epigenetic reprogramming to which the embryo is exposed throughout its different developmental stages.

EXOSOMES AS A NOVEL MECHANISM OF EMBRYO–MATERNAL CROSS TALK

Exosomes are nanoscale-sized phospholipid bilayer-enclosed particles (50–120 nm diameter) actively released from cells into the extracellular space and body fluids under physiological and pathological conditions (95). To date, they have been demonstrated to contain not only proteins and bioactive lipids, but also mRNAs, cytokines, growth factors, miRNAs, and double-strand or genomic DNA (96–101). They are involved in stem cell maintenance, angiogenesis, and immune responses (102); thus, they are considered among the most powerful paracrine and long-range mediators of cellular communication.

Ng et al. (103) examined the release of exosomes from the EECs into the uterine cavity throughout the different stages of the menstrual cycle. Interestingly, they observed the existence of a specific miRNA profile within vesicles, clearly distinct from the one found in the EEC of origin. Bioinformatic analyses showed that this unique miRNA signature has potential target genes that contribute to many Kyoto Encyclopedia of Genes and Genomes (KEGG) pathways, many of which are relevant to implantation. Specifically, these included adherens junctions, ECM–receptor interactions, and VEGF, JAK–STAT, and Toll-like receptor (TLR) signaling pathways.

Most recently, Salomon et al. (104) described that exosomes released from the first trimester placental mesenchymal stem cells (pMSCs) promote endothelial cell migration and vascular tube formation *in vitro*. Similarly, cytotrophoblast-derived exosomes seem to have increased extravillous trophoblasts (EVTs) *in vitro* (105). Following the same line of research, they demonstrated that exosomes released from EVT may play a role in remodeling spiral arteries by inducing migration of vascular smooth muscle cells (VSMCs) (106). Related to this, the molecular characterization of trophoblast-derived exosomes highlights the presence of immunomodulator proteins such as fibronectin and syncytin, Wnt/ β -catenin-related molecules, galectin-3, HLA-G, bioactive lipid compounds (immunosuppressive PGE2 and PPAR γ ligand 15d-PGJ2), and miRNAs (107). This molecular profile offers evidence for exosomes as promoters of intercellular fusion and syncytiotrophoblast formation. On the other hand, syncytiotrophoblast-derived microvesicles have pro-inflammatory, antiendothelial, and procoagulant effects that appear to be involved in preeclampsia (108). Specifically, isolated

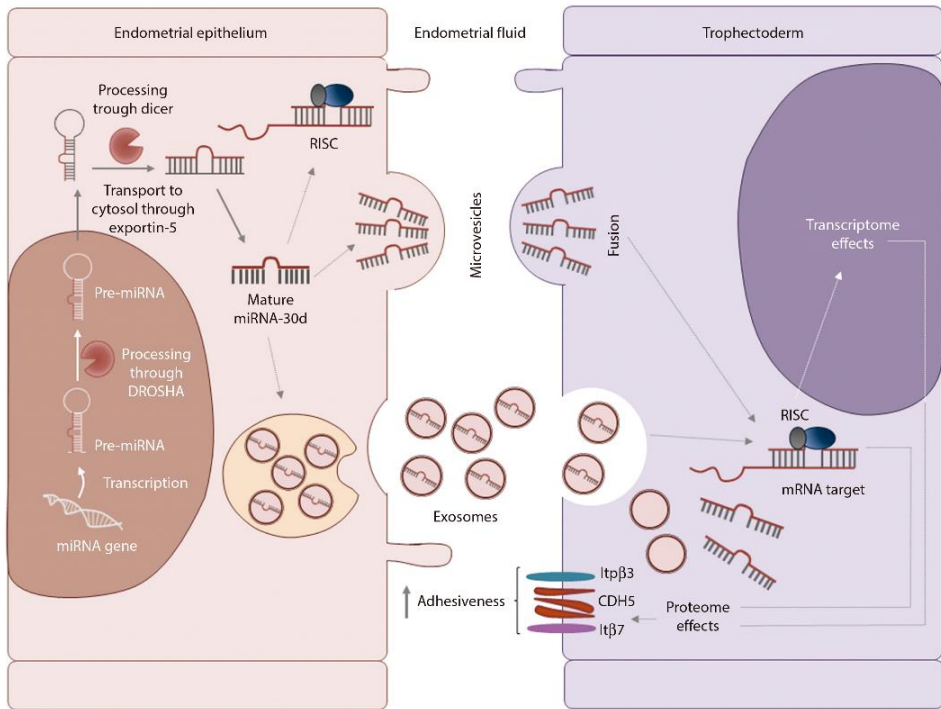


Figure 19.2 Schematic representation of a novel maternal–fetal cross talk mechanism carried out by hsa-miR-30d. The delivery of hsa-miR-30d from the maternal endometrium to the EF is able to modify the embryo transcriptome and its adhesive phenotype. (Reprinted from Vilella F et al. *Development* 2015;142(18):3210–21. With permission.)

human placental exosomes carry NKG2D ligands, ULBPs (ULBP1–5), and MIC proteins on their surface, by which they induce downregulation of the NKG2D receptor on natural killer (NK), CD8(+), and gamma delta T cells (109). Moreover, bioactive FasL- and TRAIL-carrying exosomes, which are able to trigger apoptosis, are secreted by the placenta and responsible for the immunomodulatory and protective role of the human placenta (110).

Embryo-derived exosomes may also be important markers. With routine clinical morphological grading performed on 239 embryos from 18 couples, the embryo culture supernatant (148 at day 3 and 91 at day 5) was collected and investigated by nanoparticle tracking analysis (NTA). The authors found a strong correlation between median-sized EVs and the grade of development of the embryos at days 3 and 5 ($r=0.50$, $p=0.0001$). Further, they observed that as the size of median EV increased, there was a reduction in the embryo quality attained (202 nm good, 218 nm average, 222 nm poor, and 227 nm slow development; $p=0.004$). Additionally, DNA was detected in the EVs. This finding could allow, in the near future, the implementation of a noninvasive method for

assessing embryo quality and implantation ability, offering an alternative to the current invasive prenatal diagnosis (preimplantation genetic diagnosis [PGD]) technique (111). Moreover, given these promising results, elucidating the regulation and function of exosomes in the uterine cavity will improve our understanding of the early embryo–maternal dialogue, with potential impacts on our perception of infertility and success rates of IVF.

Saadeldin et al. (112) showed that the addition of exosomes isolated from the conditioned medium of parthenogenetic embryos can increase the developmental competence of cloned embryos. Whether this positive influence is attributable to proteins, lipids, or miRNAs present in these exosomes remains to be clarified. Nonetheless, the concept of a dynamic microenvironment or niche among cultured embryos was confirmed, highlighting the advantage of a continuous transfer of mRNA cargoes via exosomes over an acute transfer of mRNA by the conditioned medium. In any case, it would be interesting to add exosome-encapsulated proteins with possible autocrine functions to the culture medium of preimplantation embryos and compare these results with the

addition of the proteins alone. This approach may contribute to the development of new synthetic media for embryo production, improving rates of embryo development and viability (113).

PREIMPLANTATION MATERNAL ORIGIN OF ADULT DISEASE IN THE EMBRYO

The FOAD hypothesis holds that events during early development have a profound impact on the risk of specific diseases in adulthood (114). Barker and his colleagues were the first to describe the concept of FOAD based on significant associations between low birth weight and the development of coronary artery disease, hypertension and stroke, type 2 diabetes (T2D), and osteoporosis (115). Long-term susceptibility to these pathologies appears conditioned to adverse intrauterine environments, like gestational diabetes mellitus (GDM), obesity, intrauterine undernutrition, and preeclampsia, the most common and severe gestational complications (116).

Lifelong programming of the ACTH/hypothalamic-pituitary-adrenal (HPA) axis has been proposed as a mechanism to explain the association between low-birth-weight infants and later development of metabolic syndrome and hypertension in adult life. Increased cortisol levels due to alterations in the regulation of the ACTH/glucocorticoid axis may constitute one mediating mechanism. In fact, significant exposure to stressful conditions has been related to SGA children who have blunted HPA axis responses to stressors if compared with appropriate for gestational age (AGA) neonates (117).

However, genetic mutations and environmental triggers are not sufficient to explain the pathogenesis and the rising incidence of cancer, obesity, and T2D. Epigenetic mechanisms (i.e., DNA methylation, histone, and noncoding RNA modification) may permanently modulate gene expression profiles in progeny during critical developmental windows wherein adverse parental nutrition has taken place (118). Einstein et al. (119) identified epigenetic modifications that link IUGR with T2D in adulthood. Specifically, they found that IUGR subjects were distinctive for having a number of consistent differences in methylation patterns near genes involved in critical processes for stem cell function, including cell cycle and cellular maintenance. Moreover, the results indicated that variation in methylation in the *HNF4A* promoter region may be responsible for diabetes onset later in life.

Additional human studies also demonstrated a connection between exposure to famine and altered DNA methylation at multiple sites within the insulin-like growth factor (IGF) 2 differentially methylated region (DMR). Similarly, perinatally unbalanced maternal diet induces epigenetic changes in offspring genomes, resulting in long-lasting modification of the transcriptional control of adipogenesis or inflammation (120).

Related to this, a wide variety of animal studies have been performed to understand the molecular mechanisms responsible for nutritional programming. Jousse et al. (121) investigated the consequences of maternal

undernutrition during gestation and lactation on DNA methylation and leptin gene expression in rodents. They showed that animals born to mothers fed a low-protein diet had lower body weight and adiposity and exhibited a higher food intake than the control group. This nutritional stress resulted in the removal of methyl groups at CpG islands located in the leptin promoter. Maternal obesity in female mice induces increased expression of *Zfp423*, a key transcriptional factor in charge of initiating adipogenic commitment, along with lower promoter methylation levels in fetal offspring (122).

Likewise, weaned rats from obese dams display greater adipocyte differentiation and increased *Zfp423*, *Ppar γ* , and *C/Ebp β* mRNA expression levels, along with specific alterations in DNA methylation of CpG sites (123). On the other hand, maternal high-fat diet during pregnancy has been described as a possible mechanism for histone modifications within leptin and adiponectin promoter regions, thus resulting in altered adipocytokine gene expression in offspring (124).

From the results obtained to date, it follows that many efforts have been made to elucidate the molecular nature of inherited epigenetic marks responsible for phenotypic transmission of chronic adult disease. However, most studies investigating this question have focused mainly on DNA methylation, thus only scratching the surface of the complete landscape of epigenomic variation. Fortunately, thanks to next-generation global DNA sequencing techniques, there are numerous advances in revealing the complete epigenomic map. Thus, it is now possible to engineer site-specific modifications in the epigenome in a targeted and reproducible manner, opening the door to the establishment of a causal relationship between transgenerational transmission of diseases and specific epigenetic marks (125).

CONCLUSIONS

1. The maternal-fetal cross talk constitutes a complex event, as in any dialogue, in which a large number of molecules and their respective receptors act in coordination to promote the process of embryo implantation. Cytokines, sex steroids, ECM proteins, growth factors, and PGs appear to be orchestrating innumerable metabolic pathways designed to promote proper embryonic differentiation, the acquisition of a receptive endometrium, and embryonic implantation (for specific information see Table 19.1).
2. Exosomes have been recently discovered as an essential component of cell communication in mammals. Deepening our knowledge about the content of exosomes will be critical in understanding the physiology and pathophysiology of the early stages of pregnancy recognition.
3. Adverse intrauterine environments, prior to implantation and during fetal development, adversely influence the health of offspring during gestation and adulthood.

Table 19.1

Molecule	Messenger	Source	Physiological role	References
Cytokines	IL-6	Glandular and luminal epithelial cells/trophoblast cells	Contributes to trophoblast growth and placental development. Aberrant expression has been associated with recurrent miscarriage. Reduced fertility, viable implantation sites decreased 48%. Higher amounts have been linked with lower implantation rates in patients with endometriosis, through impairment of oocyte and embryo quality.	21
	IL-11	Glandular and luminal epithelium, decidualized stromal cells	Exerts inflammatory activities and pleiotropic action in multiple cell types. Aberrant expression has been associated with recurrent miscarriage. Fertility defect that, unlike that in LIF-deficient mice, occurs in the postimplantation response to the implanting blastocyst.	16,26–29,31
	LIF	Endometrium/trophoblast cells	Involved in preimplantation, implantation, embryo development, and placentation. Abnormal expression of LIF in the endometrium has been associated with unexplained infertility. Inhibits MMP secretion and stimulates expression of TIMPs.	5,17,33
	IL-17 IL-18	Stromal cells	Inhibition of these cytokines has been observed in the presence of arrested embryos.	39
	TNF α	Endometrium/placenta/decidua	Expression of high levels is associated with arrest in growth and development at both morula and blastocyst stages, along with ultrastructural features of degeneration. Mediator in apoptosis processes.	126
Growth factors	EGF	Decidual and trophoblastic cells	Induces trophoblast invasion, trophoblast differentiation.	43–47
	HB-EGF	Stromal, decidual, and trophoblastic cells	Decidualization factor and trophoblastic invasion modulator. Decreasing levels lead to pregnancy complications, such as preeclampsia and SGA, due to aberrant trophoblast invasion, and also to IUGR due to increasing apoptosis.	49
	TGF β 1 TGF β 2 TGF β 3	Endometrial stromal, epithelial, and decidual cells/villous and extravillous CTB and in STB	Controls trophoblast invasion during implantation and placentation. TGF β exerts an anti-invasive effect by stimulating the secretion of TIMP, by downregulating urokinase plasminogen activator (plasmin being a known activator of MMPs), and by inhibiting CTB migration. GF-b3 is overexpressed in preeclamptic placentas, and antisense mRNA to this cytokine favors the formation of invasive CTB columns and induces invasion.	127,128
	VEGF-A	Luminal epithelium	Appears reduced in women with unexplained infertility.	59
	Wnt proteins	Epithelial and stromal cells	Implicated in decidualization and implantation. Involved in cell specification and epithelial–mesenchymal interactions. A targeted gene deletion of <i>Wnt7a</i> in mice results in the absence of uterine glands and infertility.	53–55
Adhesion molecules	Integrins β 1, β 3, β 4	Luminal epithelium	They seem to play a role in the initial stages of blastocyst adhesion. Embryos from β 1–/– mice develop themselves until the blastocyst stage but fail to implant with defects in cell lineage allocation.	70

(Continued)

Table 19.1 (Continued)

Molecule	Messenger	Source	Physiological role	References
miRNAs	miR-23b	Endometrium	Involved in Wnt signaling, p53, cell cycle, cancer pathways, and adhesion molecules.	89
	miR-145			
	miR-27b			
	miR-195			
	miR-30b	Endometrium	Involved in Wnt, axon guidance, ERK/MAPK, TGF β , p53, leukocyte extravasation pathways	91
	miR-494			
	miR-923			
	miR-30d	Endometrium	Involved in Wnt, axon guidance, ERK/MAPK, TGF β , p53, leukocyte extravasation pathways. Promotes overexpression of the adhesion molecules ITGB3, ITGA7, CDH5.	90–93
Exosomes	Placental exosomes	Endosomal compartment of syncytiotrophoblast (secretory mechanisms of production)	Promotion of maternal immunotolerance. Suppression of NK- and T-cell-induced cytotoxicity, impairment of T-cell response, activation of apoptosis in cytotoxic immune cells at the fetal–maternal surface. Transport of mRNAs and miRNAs. Promotes VSMCs and endothelial migration.	110,104,105
	STMBs	Apical plasma membrane of the syncytiotrophoblast (production via shedding)	Pro-inflammatory, pro-coagulant, and antiendothelial effects. Activation of immune response.	108
	Endometrial exosomes	Uterus	Possible role in regulation of endometrial receptivity and embryo implantation.	93,103

REFERENCES

- Sharkey AM, Macklon NS. The science of implantation emerges blinking into the light. *Reprod Biomed Online* 2013;27(5):453–60.
- Grümmer R, Winterhager E. Connexins: Indicators for hormonal and blastocyst-mediated endometrial differentiation. In: Aplin JD, Fazleabas AT, Glasser SR, Giudice LC, eds. *The Endometrium*. Second ed. Boca Raton, FL: CRC Press; 2008:319–30.
- Aghajanova L, Hamilton AE, Giudice LC. Uterine receptivity to human embryonic implantation: Histology, biomarkers, and transcriptomics. *Semin Cell Dev Biol* 2008;19:204–11.
- Simón C, Martín JC, Pellicer A. Paracrine regulators of implantation. *Baillieres Best Pract Res Clin Obstet Gynaecol* 2000;14:815–26.
- Cha J, Vilella F, Dey SK, Simón C. Molecular interplay in successful implantation. In: Sanders S, ed. *Ten Critical Topics in Reproductive Medicine*. Washington, DC: Science/AAAS; 2013:44–8.
- Norwitz ER, Schust DJ, Fisher SJ. Implantation and the survival of early pregnancy. *N Engl J Med* 2001;345(19):1400–8.
- Kaye P. Preimplantation growth factor physiology. *Rev Reprod* 1997;2(2):121–7.
- Hardy K, Spanos S. Growth factor expression and function in the human and mouse preimplantation embryo. *J Endocrinol* 2002;172(2):221–36.
- Richter KS. The importance of growth factors for preimplantation embryo development and in-vitro culture. *Curr Opin Obstet Gynecol* 2008;20(3):292–304.
- O'Neill C. The potential roles for embryotrophic ligands in preimplantation embryo development. *Hum Reprod Update* 2008;14(3):275–88.
- Bromfield JJ, Schjenken JE, Chin PY, Care AS, Jasper MJ, Robertson SA. Maternal tract factors contribute to paternal seminal fluid impact on metabolic phenotype in offspring. *Proc Natl Acad Sci USA* 2014;111(6):2200–5.
- Robertson SA, Aplin JD, Fazleabas AT. Cytokine and chemokine regulation of endometrial immunobiology. In: Aplin JD, Fazleabas AT, Glasser SR, Giudice LC, eds. *The Endometrium*. Second ed. Boca Raton, FL: CRC Press; 2008:547–69.
- Ihle JN. The Stat family in cytokine signaling. *Curr Opin Cell Biol* 2001;13(2):211–7.
- Ihle JN. Cytokine receptor signalling. *Nature* 1995;377(6550):591–4.
- Gadina M, Hilton D, Johnston JA et al. Signaling by type I and II cytokine receptors: Ten years after. *Curr Opin Immunol* 2001;13(3):363–73.
- Cork BA, Tuckerman EM, Li TC, Laird SM. Expression of interleukin (IL)-11 receptor by the human endometrium in vivo and effects of IL-11, IL-6 and LIF on the production of MMP and cytokines by human endometrial cells in vitro. *Mol Hum Reprod* 2002;8(9):841–8.

17. L Stewart C. Leukaemia inhibitory factor and the regulation of pre-implantation development of the mammalian embryo. *Mol Reprod Dev* 1994;39(2):233–8.
18. Song H, Lim H, Das SK, Paria BC, Dey SK. Dysregulation of EGF family of growth factors and COX-2 in the uterus during the preattachment and attachment reactions of the blastocyst with the luminal epithelium correlates with implantation failure in LIF-deficient mice. *Mol Endocrinol* 2000;14(8):1147–61.
19. Brinsden PR, Alam V, de Moustier B, Engrand P. Recombinant human leukemia inhibitory factor does not improve implantation and pregnancy outcomes after assisted reproductive techniques in women with recurrent unexplained implantation failure. *Fertil Steril* 2009;91(4 Suppl):1445–7.
20. Robertson SA, O'Connell A, Ramsey A. The effect of interleukin-6 deficiency on implantation, fetal development and parturition in mice. *Proc Aust Soc Reprod Biol* 2000;31:97.
21. Tabibzadeh S, Babaknia A. The signals and molecular pathways involved in implantation, a symbiotic interaction between blastocyst and endometrium involving adhesion and tissue invasion. *Hum Reprod* 1995;10(6):1579–602.
22. von Wolff M, Thaler CJ, Strowitzki T, Broome J, Stolz W, Tabibzadeh S. Regulated expression of cytokines in human endometrium throughout the menstrual cycle: Dysregulation in habitual abortion. *Mol Hum Reprod* 2000;6(7):627–34.
23. Vandermolen DT, Gu Y. Human endometrial interleukin-6 (IL-6): In vivo messenger ribonucleic acid expression, in vitro protein production, and stimulation thereof by IL-1 beta. *Fertil Steril* 1996;66(5):741–7.
24. Pellicer A, Ardiles G, Neuspiller F, Remohí J, Simón C, Bonilla-Musoles F. Evaluation of the ovarian reserve in young low responders with normal basal levels of follicle-stimulating hormone using three-dimensional ultrasonography. *Fertil Steril* 1998;70(4):671–5.
25. Dominguez F, Gadea B, Mercader A, Esteban FJ, Pellicer A, Simón C. Embryologic outcome and secretome profile of implanted blastocysts obtained after coculture in human endometrial epithelial cells versus the sequential system. *Fertil Steril* 2010;93(3):774–82.
26. Dimitriadis E, White CA, Jones RL, Salamonsen LA. Cytokines, chemokines and growth factors in endometrium related to implantation. *Hum Reprod Update* 2005;11(6):613–30.
27. Dimitriadis E, Salamonsen LA, Robb L. Expression of interleukin-11 during the human menstrual cycle: Coincidence with stromal cell decidualization and relationship to leukaemia inhibitory factor and prolactin. *Mol Hum Reprod* 2000;6(10):907–14.
28. Cork BA, Li TC, Warren MA, Laird SM. Interleukin-11 (IL-11) in human endometrium: Expression throughout the menstrual cycle and the effects of cytokines on endometrial IL-11 production in vitro. *J Reprod Immunol* 2001;50(1):3–17.
29. von Rango U, Alfer J, Kertschanska S et al. Interleukin-11 expression: Its significance in eutopic and ectopic human implantation. *Mol Hum Reprod* 2004;10(11):783–92.
30. Makrigiannakis A, Minas V, Kalantaridou SN, Nikas G, Chrousos GP. Hormonal and cytokine regulation of early implantation. *Trends Endocrinol Metab* 2006;17(5):178–85.
31. Linjawi S, Li TC, Tuckerman EM, Blakemore AIF, Laird SM. Expression of interleukin-11 receptor alpha and interleukin-11 protein in the endometrium of normal fertile women and women with recurrent miscarriage. *J Reprod Immunol* 2004;64(1–2):145–55.
32. Robertson SA, Seamark RF, Guilbert LJ, Wegmann TG. The role of cytokines in gestation. *Crit Rev Immunol* 1994;14(3–4):239–92.
33. Saeki Y, Wataya-Kaneda M, Tanaka K, Kaneda Y. Sustained transgene expression in vitro and in vivo using an Epstein-Barr virus replicon vector system combined with HVJ liposomes. *Gene Ther* 1998;5(8):1031–7.
34. Du M-R, Wang S-C, Li D-J. The integrative roles of chemokines at the maternal-fetal interface in early pregnancy. *Cell Mol Immunol* 2014;11(5):438–48.
35. Carvalho-Gaspar M, Billing JS, Spriewald BM, Wood KJ. Chemokine gene expression during allograft rejection: Comparison of two quantitative PCR techniques. *J Immunol Methods* 2005;301(1–2):41–52.
36. Dominguez F, Galan A, Martin JLL, Remohí J, Pellicer A, Simón C. Hormonal and embryonic regulation of chemokine receptors CXCR1, CXCR4, CCR5 and CCR2B in the human endometrium and the human blastocyst. *Mol Hum Reprod* 2003;9(4):189–98.
37. Caballero-Campo P, Dominguez F, Coloma J et al. Hormonal and embryonic regulation of chemokines IL-8, MCP-1 and RANTES in the human endometrium during the window of implantation. *Mol Hum Reprod* 2002;8(4):375–84.
38. Dey SK, Lim H, Das SK et al. Molecular cues to implantation. *Endocr Rev* 2004;25(3):341–73.
39. Teklenburg G, Salker M, Molokhia M et al. Natural selection of human embryos: Decidualizing endometrial stromal cells serve as sensors of embryo quality upon implantation. *PLoS One* 2010;5(4):e10258.
40. Sporn M, Roberts A, Wakefield L, Assoian R. Transforming growth factor-beta: Biological function and chemical structure. *Science* 1986;233(4763):532–4.
41. Giudice LC, Saleh W. Growth factors in reproduction. *Trends Endocrinol Metab* 1995;6(2):60–9.
42. Olayioye MA, Neve RM, Lane HA, Hynes NE. The ErbB signaling network: Receptor heterodimerization in development and cancer. *EMBO J* 2000;19(13):3159–67.

43. Bass KE, Morrish D, Roth I et al. Human cytotrophoblast invasion is up-regulated by epidermal growth factor: Evidence that paracrine factors modify this process. *Dev Biol* 1994;164(2):550–61.
44. Dakour J, Li H, Chen H, Morrish DW. EGF promotes development of a differentiated trophoblast phenotype having c-myc and junB proto-oncogene activation. *Placenta* 1999;20(1):119–26.
45. Li RH, Zhuang LZ. The effects of growth factors on human normal placental cytotrophoblast cell proliferation. *Hum Reprod* 1997;12(4):830–4.
46. Maruo T, Matsuo H, Otani T, Mochizuki M. Role of epidermal growth factor (EGF) and its receptor in the development of the human placenta. *Reprod Fertil Dev* 1995;7(6):1465–70.
47. Staun-Ram E, Goldman S, Gabarin D, Shalev E. Expression and importance of matrix metalloproteinase 2 and 9 (MMP-2 and -9) in human trophoblast invasion. *Reprod Biol Endocrinol* 2004;2:59.
48. Rathjen PD, Toth S, Willis A, Heath JK, Smith AG. Differentiation inhibiting activity is produced in matrix-associated and diffusible forms that are generated by alternate promoter usage. *Cell* 1990;62(6):1105–14.
49. Ozbilgin K, Karaca F, Turan A, Köse C, Vatansever S, OzcaKir T. The higher heparin-binding epidermal growth factor (HB-EGF) in missed abortion. *Taiwan J Obstet Gynecol* 2015;54(1):13–8.
50. Chobotova K, Spyropoulou I, Carver J et al. Heparin-binding epidermal growth factor and its receptor ErbB4 mediate implantation of the human blastocyst. *Mech Dev* 2002;119(2):137–44.
51. Paria BC, Elenius K, Klagsbrun M, Dey SK. Heparin-binding EGF-like growth factor interacts with mouse blastocysts independently of ErbB1: A possible role for heparan sulfate proteoglycans and ErbB4 in blastocyst implantation. *Development* 1999;126(9):1997–2005.
52. Lim H, Das SK, Dey SK. erbB genes in the mouse uterus: Cell-specific signaling by epidermal growth factor (EGF) family of growth factors during implantation. *Dev Biol* 1998;204(1):97–110.
53. Dunlap KA, Filant J, Hayashi K et al. Postnatal deletion of Wnt7a inhibits uterine gland morphogenesis and compromises adult fertility in mice. *Biol Reprod* 2011;85(2):386–96.
54. Bui TD, Zhang L, Rees MC, Bicknell R, Harris AL. Expression and hormone regulation of Wnt2, 3, 4, 5a, 7a, 7b and 10b in normal human endometrium and endometrial carcinoma. *Br J Cancer* 1997;75(8):1131–6.
55. Tulac S, Nayak NR, Kao LC et al. Identification, characterization, and regulation of the canonical Wnt signaling pathway in human endometrium. *J Clin Endocrinol Metab* 2003;88(8):3860–6.
56. Ben-Shlomo I. Sharing of unrelated receptors and ligands by cognate partners: Possible implications for ovarian and endometrial physiology. *Reprod Biomed Online* 2005;11(2):259–69.
57. Pavelock K, Braas K, Ouafik L, Osol G, May V. Differential expression and regulation of the vascular endothelial growth factor receptors neuropilin-1 and neuropilin-2 in rat uterus. *Endocrinology* 2001;142(2):613–22.
58. Bigsby RM, Bethin KE. Paracrine mediators of endometrial growth and differentiation. In: Aplin JD, Fazleabas AT, Glasser SR, Giudice LC, eds. *The Endometrium*. Second ed. Boca Raton, FL: CRC Press; 2008:319–30.
59. Hannan NJ, Paiva P, Meehan KL, Rombauts LJF, Gardner DK, Salamonsen LA. Analysis of fertility-related soluble mediators in human uterine fluid identifies VEGF as a key regulator of embryo implantation. *Endocrinology* 2011;152(12):4948–56.
60. Binder NK, Evans J, Gardner DK, Salamonsen LA, Hannan NJ. Endometrial signals improve embryo outcome: Functional role of vascular endothelial growth factor isoforms on embryo development and implantation in mice. *Hum Reprod* 2014;29(10):2278–86.
61. Kingsley DM. The TGF-beta superfamily: New members, new receptors, and new genetic tests of function in different organisms. *Genes Dev* 1994;8(2):133–46.
62. Piek E, Heldin CH, Dijke Ten P. Specificity, diversity, and regulation in TGF-beta superfamily signaling. *FASEB J* 1999;13(15):2105–24.
63. Chimote N, Chimote M, Mehta B, Nath N. Cytokines and growth factors in implantation. *J Reprod Biotechnol Fertil* 2010;1(2):219–43.
64. Jones RL, Stoikos C, Findlay JK, Salamonsen LA. TGF-beta superfamily expression and actions in the endometrium and placenta. *Reproduction* 2006;132(2):217–32.
65. Achache H, Revel A. Endometrial receptivity markers, the journey to successful embryo implantation. *Hum Reprod Update* 2006;12(6):731–46.
66. Aplin JD. Embryo implantation: The molecular mechanism remains elusive. *Reprod Biomed Online* 2006;13(6):833–9.
67. Hoozemans D, Schats R, Lambalk C, Hompes P. Human embryo implantation: Current knowledge and clinical implications in assisted reproductive technology. *Reprod Biomed Online* 2004;9(6):692–715.
68. Minas V, Loutradis D, Makrigiannakis A. Factors controlling blastocyst implantation. *Reprod Biomed Online* 2005;10(2):205–16.
69. Lessey BA, Castelbaum AJ. Integrins and implantation in the human. *Rev Endocr Metab Disord* 2002;3(2):107–17.
70. Fassler R, Meyer M. Consequences of lack of beta 1 integrin gene expression in mice. *Genes Dev* 1995;9(15):1896–908.
71. Surrey ES, Lietz AK, Gustofson RL, Minjarez DA. Does endometrial integrin expression in endometriosis patients predict enhanced in vitro fertilization cycle outcomes after prolonged GnRH agonist therapy? *Fertil Steril* 2010;93(2):645–51.

72. Torry DS, Leavenworth J, Chang M et al. Angiogenesis in implantation. *J Assist Reprod Genet* 2007;24(7):303–15.
73. Foulk RA, Zdravkovic T, Genbacev O, Prakobphol A. Expression of L-selectin ligand MECA-79 as a predictive marker of human uterine receptivity. *J Assist Reprod Genet* 2007;24(7):316–21.
74. Komatsu M, Carraway CA, Fregien NL, Carraway KL. Reversible disruption of cell-matrix and cell-cell interactions by overexpression of sialomucin complex. *J Biol Chem* 1997;272(52):33245–54.
75. Meseguer M. Human endometrial mucin MUC1 is up-regulated by progesterone and down-regulated in vitro by the human blastocyst. *Biol Reprod* 2001;64(2):590–601.
76. Salleh N. Diverse roles of prostaglandins in blastocyst implantation. *ScientificWorldJournal* 2014;2014:968141.
77. Irvine RF. How is the level of free arachidonic acid controlled in mammalian cells? *Biochem J* 1982;204(1):3–16.
78. Hara S, Kamei D, Sasaki Y, Tanemoto A, Nakatani Y, Murakami M. Prostaglandin E synthases: Understanding their pathophysiological roles through mouse genetic models. *Biochimie* 2010;92(6):651–9.
79. Vilella F, Ramirez L, Berlanga O et al. PGE2 and PGF2 concentrations in human endometrial fluid as biomarkers for embryonic implantation. *J Clin Endocrinol Metab* 2013;98(10):4123–32.
80. Gu G, Gao Q, Yuan X, Huang L, Ge L. Immunolocalization of adipocytes and prostaglandin E2 and its four receptor proteins EP1, EP2, EP3, and EP4 in the caprine cervix during spontaneous term labor. *Biol Reprod* 201286(5):159, 1–10.
81. Song H, Lim H, Paria BC et al. Cytosolic phospholipase A2alpha is crucial [correction of A2alpha deficiency is crucial] for “on-time” embryo implantation that directs subsequent development. *Development* 2002;129(12):2879–89.
82. Lim H, Paria BC, Das SK et al. Multiple female reproductive failures in cyclooxygenase 2-deficient mice. *Cell* 1997;91(2):197–208.
83. Tranguch S, Daikoku T, Guo Y, Wang H, Dey SK. Molecular complexity in establishing uterine receptivity and implantation. *Cell Mol Life Sci* 2005;62(17):1964–73.
84. Ambros V. MicroRNA pathways in flies and worms: Growth, death, fat, stress, and timing. *Cell* 2003;113(6):673–6.
85. Bartel DP. MicroRNAs: Genomics, biogenesis, mechanism, and function. *Cell* 2004;116(2):281–97.
86. Lai EC. microRNAs: Runts of the genome assert themselves. *Curr Biol* 2003;13(23):R925–36.
87. Lim LP, Lau NC, Garrett-Engle P et al. Microarray analysis shows that some microRNAs downregulate large numbers of target mRNAs. *Nat Cell Biol* 2005;433(7027):769–73.
88. Kuokkanen S, Chen B, Ojalvo L, Benard L, Santoro N, Pollard JW. Genomic profiling of microRNAs and messenger RNAs reveals hormonal regulation in microRNA expression in human endometrium. *Biol Reprod* 2010;82(4):791–801.
89. Revel A, Achache H, Stevens J, Smith Y, Reich R. MicroRNAs are associated with human embryo implantation defects. *Hum Reprod* 2011;26(10):2830–40.
90. Sha A-G, Liu J-L, Jiang X-M et al. Genome-wide identification of micro-ribonucleic acids associated with human endometrial receptivity in natural and stimulated cycles by deep sequencing. *Fertil Steril* 2011;96(1):150–5.
91. Altmäe S, Martínez-Conejero JA, Esteban FJ et al. MicroRNAs miR-30b, miR-30d, and miR-494 regulate human endometrial receptivity. *Reprod Sci* 2012;20(3):308–17.
92. Qian K, Hu L, Chen H et al. Hsa-miR-222 is involved in differentiation of endometrial stromal cells in vitro. *Endocrinology* 2009;150(10):4734–43.
93. Vilella F, Moreno-Moya JM, Balaguer N et al. Hsa-miR-30d, secreted by the human endometrium, is taken up by the pre-implantation embryo and might modify its transcriptome. *Development* 2015;142(18):3210–21.
94. Colombo M, Raposo G, Théry C. Biogenesis, secretion, and intercellular interactions of exosomes and other extracellular vesicles. *Annu Rev Cell Dev Biol* 2014;30(1):255–89.
95. Barkalina N, Jones C, Wood MJA, Coward K. Extracellular vesicle-mediated delivery of molecular compounds into gametes and embryos: Learning from nature. *Hum Reprod Update* 2015;21(5):627–39.
96. Théry C. Exosomes: Secreted vesicles and intercellular communications. *F1000 Biol Rep* 2011;3:15.
97. Lee Y, El Andaloussi S, Wood MJ. Exosomes and microvesicles: Extracellular vesicles for genetic information transfer and gene therapy. *Hum Mol Genet* 2012;21(R1):R125–34.
98. Valadi H, Ekström K, Bossios A, Sjöstrand M, Lee JJ, Lötvall JO. Exosome-mediated transfer of mRNAs and microRNAs is a novel mechanism of genetic exchange between cells. *Nat Cell Biol* 2007;9(6):654–9.
99. Thakur BK, Zhang H, Becker A et al. Double-stranded DNA in exosomes: A novel biomarker in cancer detection. *Cell Res* 2014;24(6):766–9.
100. Cai J, Han Y, Ren H et al. Extracellular vesicle-mediated transfer of donor genomic DNA to recipient cells is a novel mechanism for genetic influence between cells. *J Mol Cell Biol* 2013;5(4):227–38.
101. Kahlert C, Melo SA, Prottopov A et al. Identification of double-stranded genomic DNA spanning all chromosomes with mutated KRAS and p53 DNA in the serum exosomes of patients with pancreatic cancer. *J Biol Chem* 2014;289(7):3869–75.

102. Andaloussi El S, Mäger I, Breakefield XO, Wood MJA. Extracellular vesicles: Biology and emerging therapeutic opportunities. *Nat Rev Drug Discov* 2013;12(5):347–57.
103. Ng YH, Rome S, Jalabert A et al. Endometrial exosomes/microvesicles in the uterine microenvironment: A new paradigm for embryo-endometrial cross talk at implantation. *PLoS One* 2013;8(3):e58502.
104. Salomon C, Ryan J, Sobrevia L et al. Exosomal signaling during hypoxia mediates microvascular endothelial cell migration and vasculogenesis. *PLoS One* 2013;8(7):e68451.
105. Salomon C, Kobayashi M, Ashman K, Sobrevia L, Mitchell MD, Rice GE. Hypoxia-induced changes in the bioactivity of cytotrophoblast-derived exosomes. *PLoS One* 2013;8(11):e79636.
106. Salomon C, Yee S, Scholz-Romero K et al. Extravillous trophoblast cells-derived exosomes promote vascular smooth muscle cell migration. *Front Pharmacol* 2014;5:175.
107. Record M, Carayon K, Poirot M, Silvente-Poirot S. Exosomes as new vesicular lipid transporters involved in cell-cell communication and various pathophysiology. *Biochim Biophys Acta* 2014;1841(1):108–20.
108. Redman CWG, Tannetta DS, Dragovic RA et al. Review: Does size matter? Placental debris and the pathophysiology of pre-eclampsia. *Placenta* 2012;33(Suppl):S48–54.
109. Hedlund M, Stenqvist A-C, Nagaeva O et al. Human placenta expresses and secretes NKG2D ligands via exosomes that down-modulate the cognate receptor expression: Evidence for immunosuppressive function. *J Immunol* 2009;183(1):340–51.
110. Stenqvist A-C, Nagaeva O, Baranov V, Minchev-Nilsson L. Exosomes secreted by human placenta carry functional Fas ligand and TRAIL molecules and convey apoptosis in activated immune cells, suggesting exosome-mediated immune privilege of the fetus. *J Immunol* 2013;191(11):5515–23.
111. Saadeldin IM, Oh HJ, Lee BC. Embryonic-maternal cross-talk via exosomes: Potential implications. *Stem Cells Cloning* 2015;8:103–7.
112. Saadeldin IM, Kim SJ, Choi YB, Lee BC. Improvement of cloned embryos development by co-culturing with parthenotes: A possible role of exosomes/microvesicles for embryos paracrine communication. *Cell Reprogram* 2014;16(3):223–34.
113. Calkins K, Devaskar SU. Fetal origins of adult disease. *Curr Probl Pediatr Adolesc Health Care* 2011;41(6):158–76.
114. Barker DJP. The developmental origins of adult disease. *J Am Coll Nutr* 2004;23(6 Suppl):588S–95S.
115. Huang H-F, Sheng J-Z. *Gamete and Embryo-Fetal Origins of Adult Diseases*. Berlin: Springer Science & Business Media; 2013.
116. Wydooghe E, Vandaele I, Heras S et al. Autocrine embryotropins revisited: How do embryos communicate with each other in vitro when cultured in groups? *Biol Rev Camb Philos Soc* 2015. DOI: 10.1111/brv.12241.
117. Osterholm EA, Hostinar CE, Gunnar MR. Alterations in stress responses of the hypothalamic-pituitary-adrenal axis in small for gestational age infants. *Psychoneuroendocrinology* 2012;37(10):1719–25.
118. Lecoutre S, Breton C. Maternal nutritional manipulations program adipose tissue dysfunction in offspring. *Front Physiol* 2015;6:158.
119. Einstein F, Thompson RF, Bhagat TD et al. Cytosine methylation dysregulation in neonates following intrauterine growth restriction. *PLoS One* 2010;5(1):e8887.
120. Heijmans BT, Tobi EW, Stein AD et al. Persistent epigenetic differences associated with prenatal exposure to famine in humans. *Proc Natl Acad Sci USA* 2008;105(44):17046–9.
121. Jousse C, Parry L, Lambert-Langlais S et al. Perinatal undernutrition affects the methylation and expression of the leptin gene in adults: Implication for the understanding of metabolic syndrome. *FASEB J* 2011;25(9):3271–8.
122. Yang Q-Y, Liang J-F, Rogers CJ, Zhao J-X, Zhu M-J, Du M. Maternal obesity induces epigenetic modifications to facilitate Zfp423 expression and enhance adipogenic differentiation in fetal mice. *Diabetes* 2013;62(11):3727–35.
123. Borengasser SJ, Zhong Y, Kang P et al. Maternal obesity enhances white adipose tissue differentiation and alters genome-scale DNA methylation in male rat offspring. *Endocrinology* 2013;154(11):4113–25.
124. Masuyama H, Hiramatsu Y. Effects of a high-fat diet exposure in utero on the metabolic syndrome-like phenomenon in mouse offspring through epigenetic changes in adipocytokine gene expression. *Endocrinology* 2012;153(6):2823–30.
125. Stegeman R, Buchner DA. Transgenerational inheritance of metabolic disease. *Semin Cell Dev Biol* 2015;43:131–40.
126. Lalitkumar PGL, Sengupta J, Ghosh D. Endometrial tumor necrosis factor alpha (TNFalpha) is a likely mediator of early luteal phase mifepristone-mediated negative effector action on the preimplantation embryo. *Reproduction* 2005;129(3):323–35.
127. Godkin JD, Doré JJ. Transforming growth factor beta and the endometrium. *Rev Reprod* 1998;3(1):1–6.
128. Feinberg RF, Kliman HJ, Wang CL. Transforming growth factor-beta stimulates trophoblast oncofetal fibronectin synthesis in vitro: Implications for trophoblast implantation in vivo. *J Clin Endocrinol Metab* 1994;78(5):1241–8.

